

DESIGN AND DEVELOPMENT OF COMPACT COPLANAR WAVEGUIDE FED ANTENNAS FOR WIRELESS APPLICATIONS

A thesis submitted by

SUJITH R

*in partial fulfillment of the requirements
for the degree of*

DOCTOR OF PHILOSOPHY

Under the guidance of

Prof. P. MOHANAN

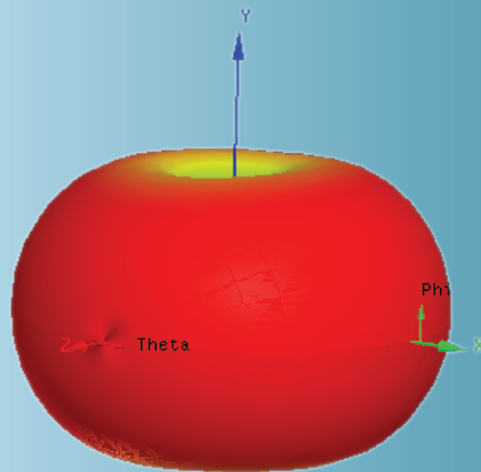


DEPARTMENT OF ELECTRONICS
FACULTY OF TECHNOLOGY
COCHIN UNIVERSITY OF SCIENCE AND TECHNOLOGY
KOCHI-22, INDIA

January 2012

DESIGN AND DEVELOPMENT OF COMPACT COPLANAR WAVEGUIDE FED ANTENNAS FOR WIRELESS APPLICATIONS

Ph.D Thesis
January 2012



A compact coplanar waveguide fed planar antenna is proposed by modifying the transmission line parameters. A quad band antenna suitable for wireless application is demonstrated. This uniplanar compact antenna is operating in GSM 900, DCS 1800, IEEE802.11.a, IEEE802.11.b and HiperLAN-2 bands with nearly omnidirectional radiation pattern. A harmonic suppressed antenna is also presented in this thesis. This antenna is operating in a single mode up to 10GHz. This may find good application in Wireless LAN.



CENTRE FOR RESEARCH IN ELECTROMAGNETICS AND ANTENNAS
DEPARTMENT OF ELECTRONICS
FACULTY OF TECHNOLOGY
COCHIN UNIVERSITY OF SCIENCE AND TECHNOLOGY
KOCHI-22, INDIA

Microwave Electronics

**DESIGN AND DEVELOPMENT OF COMPACT
COPLANAR WAVEGUIDE FED ANTENNAS FOR
WIRELESS APPLICATIONS**

A thesis submitted by

SUJITH R

in partial fulfillment of the requirements for the degree of

DOCTOR OF PHILOSOPHY

Under the guidance of

Prof. P. MOHANAN



**DEPARTMENT OF ELECTRONICS
FACULTY OF TECHNOLOGY
COCHIN UNIVERSITY OF SCIENCE AND TECHNOLOGY
KOCHI-22, INDIA**

January 2012

“Design and Development of Compact Coplanar Waveguide Fed Antennas for Wireless Applications

Ph.D. Thesis under the Faculty of Technology

Author

Sujith R

Research Scholar
Department of Electronics
Cochin University of Science and Technology
Kochi - 682022
Email: sujithrpkd@gmail.com

Supervising Guide

Dr. P. Mohanan

Professor
Department of Electronics
Cochin University of Science and Technology
Kochi - 682022
Email: drmohan@gmail.com

Department of Electronics
Cochin University of Science and Technology
Kochi - 682022

January 2012





**DEPARTMENT OF ELECTRONICS
COCHIN UNIVERSITY OF SCIENCE AND TECHNOLOGY,
KOCHI – 682 022**

Dr. P. Mohanan
Professor

Ph: 0484 2576418
E-mail: drmohan@cusat.ac.in

Certificate

This is to certify that this thesis entitled “**Design and Development of Compact Coplanar Waveguide Fed Antennas for Wireless Applications**” is a bonafide record of the research work carried out by Mr. SUJITH R under my supervision in the Department of Electronics, Cochin University of Science and Technology. The results embodied in this thesis or parts of it have not been presented for any other degree.

Cochin-22
4th January 2012

Dr. P. Mohanan
(Supervising Teacher)

Declaration

I hereby declare that the work presented in this thesis entitled “**Design and Development of Compact Coplanar Waveguide Fed Antennas for Wireless Applications**” is a bonafide record of the research work done by me under the supervision of Dr. P. Mohanan, Professor, Department of Electronics, Cochin University of Science and Technology, India and that no part thereof has been presented for the award of any other degree.

Cochin-22
4th January 2012

Sujith R
Research Scholar
Department of Electronics
Cochin University of Science
and Technology

Words of Gratitude...

I would like to express my sincere gratitude to my supervising guide, Dr. Mohanan Pezholil, Professor, Department of Electronics, Cochin University of Science and Technology, for his guidance, encouragement and the timely care that he rendered to me during my research period. His tremendous technical and mental support has been a steady state of inspiration to me. I shall forever cherish the exposure and facilities that he offered during period of my research under his guidance.

I am grateful to Dr. K. Vasudevan, Professor of the Department of Electronics for his constant encouragement and concern for my research. I also wish to thank him for his valuable personnel and professional suggestions throughout my research period.

My sincere acknowledgement goes to Dr. C. K. Aanandan, Professor, Department of Electronics, Cochin University of Science and Technology for his well-timed care in my research, valuable suggestions and constant encouragements to improve my work.

My sincere gratitude to Dr. K.G. Nair, Director, Centre for Science in Society, Cochin University of Science and Technology and former Head, Department of Electronics, Cochin University of Science and Technology for giving an opportunity to enter the field of research in electromagnetics and antennas by establishing Centre for Research in Electromagnetics and Antennas at Department of Electronics, Cochin University of Science and Technology.

Let me thank Prof. P.R.S. Pillai, Head, Department of Electronics, for extending the enormous facilities at Department of Electronics for my research work and Prof. K. T Mathew, Department of Electronics, for his whole hearted support and valuable suggestions.

My sincere thanks to Dr. Tessamma Thomas, Dr. M.H. Supriya, Dr. James Kurien, and all other faculty members of Department of Electronics for the help and assistance extended to me. My sincere thanks to all non teaching staff of Department of Electronics and Administrative office for their amicable relation, sincere cooperation and valuable helps.

I remember with appreciation Dr. Rohith K Raj, Dr. Manoj Joseph, Dr. Suma M.N and Dr. Deepu V about the supreme rapport we shared together. I also wish to acknowledge Dr. Gopikrishnan, Dr. Gijo Augustine, Dr. Jitha B, Dr. Bybi P.C, Mr. Ananthakrishnan and Dr. Deepti Das Krishna for their support.

Special thanks to Dr. Mridula S, Dr. Binu Paul and Mrs. Anju Pradeep, School of Engineering, CUSAT for their whole hearted support, helps and above all the association with me. My words are illimitable to thank Mr. Dinesh R, Mr. Nijas C.M, Mr. Tony D, Mr. Lindo A.O, Mr. Deepak U, Mr. Abdul Rasheed, Mr. Vinesh P V, Mr. Sreejith M. Nair, Mr. Ullas G. Kalapura, Mr. Paulbert Thomas, Mr. Cyriac M O, Mrs. Anju P Mathews, Mr. Sreenath S, Mr. Ashkar ali P, Mrs. Sarah Jacob, Ms. Sreekala, Mr. Sumesh and every member of Centre for Research in Electromagnetics and Antennas, CUSAT for their encouragement and help rendered to me.

My words are boundless to thank all my research and project colleagues in Centre for Ocean Electronics (CUCENTOL), Microwave Tomography and Material Research Laboratory (MTMR) and Audio and Image Research Lab (AIRL), Department of Electronics, Cochin University of Science and Technology.

Very special thanks to Sarin V.P, Laila D, Shameena V.A and Nishamol M.S for offering their immense care, technical and scientific talks shared together during my research period. I appreciate the shoulder to lean on.

I wish to acknowledge Department of Science and Technology (DST) and University Grants Commission (UGC) for providing financial assistance during my research period. I wish to place on record my gratitude to the great teachers, mentors, my intimate friends at all stages of my education.

I am really proud about the deep love and support which showered from my parents and family members that gave me the courage to complete this work. Moreover the unknown supreme power whose blessings and kindness which always guides me and helped me a lot to sail through.

Sujith R

CONTENTS

Chapter 1

Introduction 01 - 33

1.1. Introduction-----	01
1.2. The origin of Electromagnetic theory and the first Antennas –Glimpse through history -----	02
1.3. Important Milestones in Communication -----	06
1.4. Modern Wireless communication services-----	07
1.5. Present antenna types and design techniques -----	08
1.5.1. Microstrip antenna -----	09
1.5.2. Coplanar waveguide -----	12
1.5.3. DR loaded Antenna -----	15
1.5.4. PILA-PIFA based antenna-----	16
1.5.5. Metamaterial based Antenna -----	17
1.5.6. Photonic band gap structure based antenna -----	18
1.5.7. LTCC based antenna designs -----	18
1.6. Analysis of antennas -----	19
1.6.1. Transmission Line Matrix(TLM) method -----	20
1.6.2. Method of Moments (MoM) -----	21
1.6.3. Finite Element Method(FEM) -----	22
1.6.4. Finite Difference Time Domain (FDTD) method-----	23
1.7. Motivation of Present research -----	24
1.8. Thesis Organization -----	26

Chapter 2

Review of Literature and Methodology 35 - 87

2.1. Introduction-----	36
2.1.1. Planar Printed antennas -----	36
2.1.2. Coplanar Waveguide (CPW) fed Antennas -----	38
2.2. Antenna Fabrication and Experimental analysis -----	60
2.2.1. Selection of a dielectric substrate material -----	60
2.2.2. Photo Lithography-----	62
2.2.3. Antenna measurement facilities -----	63
2.2.3.1. HP8510C Vector Network Analyzer-----	64
2.2.3.2. E8362B Performance Network Analyzer (PNA) -----	65

2.2.3.3. Anechoic Chamber-----	66
2.2.3.4. Automated Turn table assembly for far field radiation pattern measurement-----	67
2.2.4. Measurement Procedure-----	67
2.2.4.1. Reflection coefficient, Resonant frequency and Impedance bandwidth-----	68
2.2.4.2. Far field radiation pattern-----	68
2.2.4.3. Antenna Gain -----	69
2.2.4.4. Efficiency measurement -----	69
2.2.5. Antenna Design and Optimisation using Ansoft HFSS-----	70

Chapter 3

Investigation on the Signal Strip modification of a Coplanar Waveguide

(CPW) transmission line..... 89 - 138

3.1. Introduction to Coplanar Waveguide (CPW) transmission line.--	90
3.2. Coplanar waveguide fed Monopole antenna-----	93
3.3. Top loaded monopole antenna -----	98
3.4. Dual band meandered monopole antenna-----	101
3.4.1. Effect of varying the strip length L_1 ($L_1+L_2+L_3$ is constant)---	104
3.4.2. Effect of varying the strip length L_1 ($L_1+L_2+L_3$ is not constant)-----	106
3.4.3. Effect of varying the strip length L_2 ($L_1+L_2+L_3$ is constant)---	107
3.4.4. Effect of varying the strip length L_2 ($L_1+L_2+L_3$ is not constant)-----	108
3.4.5. Effect of varying the strip length L_3 ($L_1+L_2+L_3$ is constant)---	108
3.4.6. Effect of varying the strip length L_3 ($L_1+L_2+L_3$ is not constant)-----	109
3.4.7. Variation on reflection characteristics with Ground plane length L_g -----	110
3.4.8. Variation on reflection characteristics with Ground plane width W_g -----	111
3.4.9. Radiation pattern-----	112
3.4.10. Gain and Efficiency -----	114
3.5. Design and Development of Quad band antenna-----	115
3.5.1. Measured Variation on reflection characteristics with strip length ($L_3 +L_4$) -----	121
3.5.2. Measured Variation on reflection characteristics with slot length CD -----	123
3.5.3. Measured Variation on reflection characteristics with right arm strip L_3 -----	124
3.5.4. Measured Variation on reflection characteristics with strip length L_1 -----	125

3.5.5. Measured Variation on reflection characteristics with Ground Length L_g -----	126
3.5.6. Measured Variation on reflection characteristics with Ground Width W_{gL} and W_{gR} -----	127
3.6. Important conclusions from this chapter-----	137

Chapter 4

Investigation on Ground plane modified

CPW fed planar antenna..... 139 - 181

4.1. Ground reduced CPW fed open ended Transmission line -----	140
4.2. Ground Meandered CPW fed antenna -----	144
4.2.1. Effect of varying the gap g -----	147
4.2.2. Effect of varying the meandering strip length L_g -----	148
4.2.3. Effect of varying the slot length (L_g - W_s) -----	149
4.2.4. Effect of slit gap 's' on reflection characteristics -----	150
4.2.5. Surface Current distribution -----	151
4.2.6. Radiation pattern -----	152
4.2.7. Reconfigurable ground meandered antenna using pin diodes -----	154
4.3. Ground plane increased Meandered CPW fed antenna-----	155
4.3.1. Effect of varying the meandering strip L_1 -----	157
4.3.2. Effect of increasing the signal strip length and ground plane length ($L_a=L_1+P+W_g$) -----	158
4.3.3. Variation in reflection characteristics with slit gap 's' -----	159
4.3.4. Effect of increasing the ground plane length L_g -----	160
4.3.5. Surface current distribution and Radiation pattern-----	161
4.3.6. Reconfigurable ground plane increased antenna using -----	165
4.4. Geometry of the proposed Compact CPW fed antenna-----	167
4.4.1. Effect of varying the Meandered length L_1 -----	168
4.4.2. Effect of varying the ground length L_g -----	169
4.4.3. Variation in reflection characteristics with strip gap 's' -----	170
4.4.4. Effect of varying the substrate height h -----	171
4.4.5. Effect of varying the Dielectric constant (ϵ_r) -----	172
4.4.6. Reflection characteristics of the ground modified planar antenna -----	174
4.4.7. Surface current distribution and Radiation pattern -----	176
4.4.8. Reconfigurable ground modified planar antenna using pin diodes -----	179
4.5. Conclusion of the ground optimized antenna-----	180

Chapter 5

Investigation on Signal strip and Ground

plane modified CPW fed planar antenna 183 - 221

5.1. Coplanar Waveguide Structure-----	184
5.2. Asymmetrically slotted CPW fed open ended transmission line-----	188
5.3. CPW fed open ended antenna with Symmetrical slots-----	192
5.3.1. Offset fed slot -----	193
5.3.2. Top loading the signal strip-----	197
5.3.3. Signal strip reduced coplanar waveguide feed-----	199
5.4. Symmetrically slotted antenna-----	205
5.5. Symmetrically slotted Reconfigurable antenna-----	209
5.6. H-shaped slot antenna with Harmonic Suppression-----	211
5.7. Conclusion-----	221

Chapter 6

Conclusion and Future Perspective..... 223 - 227

6.1. Thesis Highlights -----	224
6.2. Inferences from the investigations on signal strip modified Coplanar Waveguide antenna -----	224
6.3. Inferences from the investigations on ground plane modified antenna-----	225
6.4. Inferences from both ground and signal strip modified antenna -----	226
6.5. Suggestions for future work-----	227

Appendix

Coplanar Waveguide Fed Asymmetrically

Slotted Dual Band Antenna 229 - 242

List of Publication

Citations

Curriculum Vitae

Index

.....❧.....

<i>C o n t e n t s</i>	1.1 Introduction
	1.2 The origin of Electromagnetic theory and the first Antennas – A Glimpse through history
	1.3 Important Milestones in Communication
	1.4 Modern wireless communication services
	1.5 Present antenna types and design techniques – Planar Antennas
	1.6 Analysis of antennas
	1.7 Motivation of Present research
	1.8 Thesis Organization

This chapter highlights the historical events regarding the research and development of antenna with introductory notes on antenna. Antennas categorized for different applications according to frequency band are also discussed. Various types of antennas relevant to the present scenario and hence the importance of the thesis are also described.

1.1 Introduction

Antennas – The electronic eye and ear of all communication systems are unavoidable and inseparable part of modern gadgets. Knowingly or unknowingly every human is carrying atleast an antenna which makes it an important commodity ever made by human kind. The IEEE defines the antenna or aerial as “a means for radiating or receiving radio waves”. In general, an antenna is a transition device or a transducer, between guided wave and free space wave. The wide range of application of antennas is available in various regions of electromagnetic spectrum. The type and property of antenna depends on the frequency region at which it operates. The electrical and mechanical characteristics together with operating cost and environment will determine the design criterion for a particular antenna. Antennas are not only utilized for communication and broadcasting but also for the fascinating field of radio astronomy. Moreover, antennas are extensively used in various applications such as biomedicine, defence, radar, remote sensing, collision avoidance, air traffic control, GPS, WLAN’s etc. The antenna is an essential device in a communication system, but not an isolated device! This makes it an interesting and challenging subject.

1.2 The origin of Electromagnetic theory and the first Antennas – A Glimpse through history

Historical backgrounds are inevitable for the complete awareness of the present state of art in research activities and to generate scientific interest among students. Thales of Miletus, a Greek mathematician, astronomer and philosopher in 600BC noted that when amber is rubbed with silk it produces spark [1]. Thales was the pioneer in both electricity and magnetism but his

interest was philosophical rather than practical; hence it took centuries to investigate it in a serious experimental way.

William Gilbert of England in about A.D. 1600, conducted the first systematic experiments of electric and magnetic phenomena, by inventing the electroscope for measuring electrostatic effects. He was the first to recognize that earth itself is a huge magnet. American scientist, Benjamin Franklin in 1750 established the law of conservation of charges and established that there are both positive and negative charges. Charles Augustine de Coulomb of France measured electric and magnetic forces, and at the same time the German Scientist Karl Friedrich Gauss formulated divergence theorem relating volume and surface integrals. The investigation of Christian Oersted in 1819 that electricity could produce magnetism led Andre Marie Ampere to invent Solenoidal coil for producing magnetic field. In 1831, Michael Faraday discovered that magnetism could produce electricity. This is a remarkable invention in the history of science.

James Clerk Maxwell, a professor at Cambridge University, England, established the interdependency of electricity and magnetism in a profound and elegant manner. In his classic treatise of 1873, he published the first unified theory of electricity and magnetism and founds the science of electromagnetics. He postulated that light is electromagnetic in nature and that electromagnetic radiation of other wavelength should be possible.

Hertz in his classical experiment created spark at the center of the dipole and received a similar spark at a gap in the nearby loop in 1880's. The information in Hert'z experiment was actually in binary digital form, by tuning the spark on and off. This could be considered the very first digital wireless system, which consisted of two of the best-known antennas: the dipole and the

loop. Thus the dipole antenna is also called the Hertz antenna. This invention remained as a laboratory curiosity until 20 year old Marconi read his experiments. Young Marconi cut short his vacation and rushed home to test whether Hertzian waves could be used to send messages. In his spacious rooms at the upper floor of the Marconi mansion in Bologna, Marconi repeated Hertz's experiments. His happiness on success could not wait until next morning. So he woke up his mother and demonstrated his radio systems to her in the late night itself. Marconi quickly went on to add tuning, big antenna and ground systems for longer wavelengths and was able to signal over large distances. In 1901, he made his famous historical transatlantic communication. We now call it radio but then it was wireless: Marconi's Wireless. Monopole antennas (near quarter-wavelength) were widely used in Marconi's experiments; thus vertical monopole antennas are also called Marconi antennas [2].

Meanwhile, during 1894-1900 Jagadish Chandra Bose the famous, talented Indian scientist successfully generated and 60 GHz signals. Following the First World War, vacuum tubes became available for transmission; continuous waves replaced spark and radio broadcasting began in the 200 to 600 meter range. During World War II, battles were supposed to be won by the side that was first to spot enemy aeroplanes, ships or submarines. The British and American scientists developed radar technology to see targets from hundreds of miles away, even at night. This research resulted in the development of high-frequency radar antennas such as wire type antennas and aperture type (Reflector and Horn) antennas. Since antenna became an essential device in the radio broadcasting, communication and radar system. Broadband antennas, circularly polarized antennas, planar antennas and active antennas as well as much other type of antennas were subsequently developed for emerging applications and the opened new era in the development of antennas.

The Three dimensional huge antennas were replaced by planar antennas with the invention of microstrip antennas by Deschamps [3] in 1953. However, it took nearly 20 years to fabricate such an antenna. Their development was accelerated by the availability of good substrates with low loss tangent with attractive thermal and mechanical properties, improved photolithographic techniques, and better theoretical models. The development in wireless communication is rapid and highly progressive. The 1G analog systems of 1980's evolved into 2G digital technology in the 90's and to third generation of mobile communication which includes wireless multimedia services. The 3G mobile system evolved in 2002's eliminating previous incompatibilities and became a truly global system. The forthcoming 4G (fourth generation) mobile communication systems are projected to solve the still remaining problems of 3G systems and to provide a wide diversity of new services, from high quality voice to high definition video to high data rate wireless channels. A chronological overview of the development in wireless communication are summarized in Table 1.1

1.3 Important Milestones in Communication

Table 1.1 Milestones in Communication [4-7]

1837	Morse demonstration of telegraph
1865	Prediction of electromagnetic wave propagation by Maxwell
1876	Alexander Graham Bell invented the Telephone
1887	The existence of ElectroMagnetic waves is verified by Heinrich Rudolph Hertz.
1894	Wireless telegraphy by Marconi
1895	Jagadish Chandra Bose gave his first public demonstration of electromagnetic waves.
1901	First wireless transmission by Guglielmo Marconi with his transatlantic transmission.
1906	Lee de Forest's Radio Telephone company sold the first radio
1915	Direct telephone communications opened for service.
1921	Radio dispatch service initiated for police cars in Detroit, Michigan
1924	Directive Yagi-Uda antenna developed by Prof.Hidetsugu Yagi
1927	First television transmission.
1929	Microwave communication established by Andre G . Clavier
1933	Demonstration of Frequency Modulation by Armstrong
1934	AM(Amplitude Modulation)mobile communications systems used by state and municipal forces in the U.S
1935	RADAR by Watson Watt, Radio astronomy by Janskey
1943	The first telephone line from Calcutta, India to Kunming, China.
1944	Telephone cable laid across the English channel
1946	Radiotelephone connections made to PSTN(Public-switched telephone network),3.7-4.2 LOS link by AT&T
1947	First Mobile phone demonstration
1953	Deep space communication proposed by John Pierce.
1957	Soviet Union launches Sputnik, humanity's first artificial satellite.
1958	Invention of Integrated Circuit
1968	Development of the cellular telephony concept at Bell Laboratories.
1979	A 62,000 mile telecommunications system is implemented in Saudi Arabia
1980	1G first generation - only mobile voice service
1981	Beginning of first commercial cellular mobile communication
1982	Two way video teleconferencing service started
1986	Integrated Service Digital Network deployed
1990	2G-Second generation digital cellular deployed throughout the world.
1995	CDMA is introduced
2000	3G Standard is proposed.
2008	ITU-R organization specified the IMT-Advanced (International Mobile Telecommunications Advanced) requirements for 4G standards.

1.4 Modern wireless communication services

Antennas have wide range of application throughout the electromagnetic spectrum. In order to avoid the congestion during the communication process frequency bands are allocated for different applications. This frequency assignment will reduce the interference from multiple users. The different frequency band allocated by the governing council for smooth running of communication process is given in the table.1.2 with corresponding category of antenna.

Table 1.2. Wireless Communication [4-7]

Name of the Wireless Communication Service	Allocated frequency band	Commonly used Antenna
Digital Video Broadcasting (DVB-H)	470MHz-702MHz	Compact printed Antennas
Radio Frequency Identification (RFID)	865-868MHz, 2.446-2.454GHz	Loops, Folded-F, Patch and Monopole
Global System for Mobile (GSM 900)	890MHz-960MHz	Dipole, patch arrays and Monopoles.
Global Positioning System (GPS1400, GPS1575)	1227MHz -1575MHz, 1565MHz-1585MHz	Microstrip patch or bifilar helix
Digital Communication System (DCS 1800)	1710MHz-1880MHz	Dipole or patch arrays in base stations. Monopoles, sleeve dipoles and patch in mobile handset
Personal Communication System (PCS 1900)	1850MHz-1990MHz	
International Mobile Telecommunication-2000 (3G IMT-2000)	1885MHz-2200MHz	
Universal Mobile Telecommunication Systems (UMTS 2000)	1920MHz-2170MHz	
Industrial ,Scientific, Medical(ISM 2.4, ISM 5.2, ISM 5.8)	2400MHz-2484MHz, 5150MHz-5350MHz, 5725MHz-5825MHz	
Ultra Wide Band (UWB) communication	3.1GHz-10.6GHz	Planar printed antennas, Horn Antennas

The frequency range allotted for different band designation together with their usage is listed in the table.1.3. This table covers not only the mobile communication but from VHF to Ka band (3KHz-40GHz).

Table 1.3 Frequency range allotment for different communication[4-7]

Band Designation		Frequency range	Usage
VHF		3-30KHz	Long distance telegraphy and navigation
LF		30-300 KHz	Aeronautical navigation services, Radio broadcasting, Long distance communication,
MF		300-3000	Regional broadcasting, AM radio
HF		3-30MHz	Communications, broadcasting, surveillance, CB radio
VHF		30-300 MHz	Surveillance, TV broadcasting, FM radio
UHF		30-1000MHz	Cellular communications
Old	New	1-2 GHz	Long range surveillance, remote sensing
L	D		
S	E,F	2-4 GHz	Weather detection, Long range tracking
C	G,H	4-8 GHz	Weather detection, long-range tracking
X	I,J	8-12 GHz	Satellite communications, missile guidance, mapping
Ku	J	12-18 GHz	Satellite communications, altimetry, high resolution mapping
K	J	18-26 GHz	Very high resolution mapping
Ka	K	26-40 GHz	Air port surveillance

1.5 Present antenna types and design techniques – Planar Antennas

Why planar antennas – The 3-dimensional antennas used for communication purpose are huge and are not suitable for portable gadgets. Planar antennas can be directly printed onto a circuit board (Dielectric substrate), these are becoming popular within the wireless communication

market. Different types of planar antennas are discussed in the forthcoming sections. Among this microstrip antennas are very popular due to its excellent radiation characteristics and discussed in the next section.

1.5.1 Microstrip Antenna

The basic printed antenna, Microstrip antenna concept was first proposed in 1953 by Deschamps [3] of USA. Then Byron in 1970 proposed a strip radiator separated from a ground plane by a substrate for phased array application. He used a half wavelength wide strip, fed coaxially at the radiating edges, as the basic array element [8]. The microstrip element was patented by Munson [9] and design data about basic rectangular and circular patch antennas were published by Howell [10]. The simple fundamental configuration of microstrip antenna with radiating metallic patch on one side and a ground plane on other side of a substrate having uniform dielectric constant and thickness is shown in Figure 1.1. The patch conductors are normally of copper or gold and can assume any shape and its length is typically about one half of the dielectric wavelength corresponding to the resonant frequency [11-12].

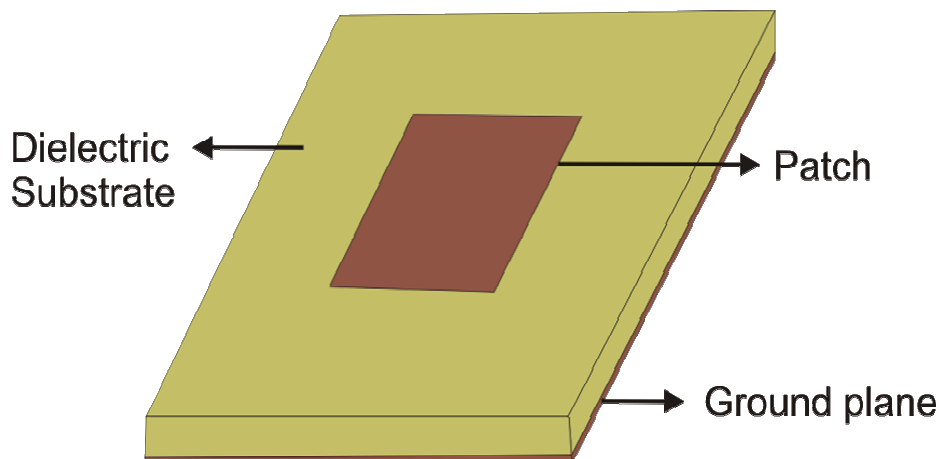


Figure 1.1 Geometry of Microstrip Antenna

The dielectric substrate material used will determine the size and radiation characteristics of the antenna. Increasing the dielectric constant can assure compactness but lowers the bandwidth and efficiency of the antenna and vice versa. The thickness of microstrip antenna is also important in determining the resonant characteristics. As the thickness increases the bandwidth increases at the risk of exciting surface waves and vice versa. The microstrip antenna can be fed in different ways

- **Coaxial Feed or Probe feed:**
Usually a microstrip antenna is fed by a coaxial probe. The inner conductor of the Sub Miniature Amphenol (SMA) connector is soldered to the patch metallization through a via hole and outer conductor is attached to the back side ground.
- **Microstrip Line Feed**
A Microstrip line on the same substrate appears to be a natural choice to feed a patch as the patch can be considered an extension of the Microstrip line, and both can be fabricated simultaneously.
- **Proximity Coupled Microstrip Feed**
Proximity feed uses a two layer substrate with a Microstrip line on the lower substrate, terminating in an opening below the patch which is printed on the upper substrate.
- **Aperture Coupled Microstrip Feed**
It consists of a Microstrip feed line on the bottom substrate coupled through a small aperture in the ground plane, to a Microstrip patch on the top substrate.

Microstrip antennas have several advantages compared to conventional microwave antennas, and therefore used for many applications covering the broad frequency range from 100MHz to 100GHz. Some of the principal advantages of microstrip antennas compared to conventional microwave antennas are[2,4,12]:

- Light weight, low volume and thin profile configuration suitable for modern wireless gadgets.
- Low fabrication cost
- Easy large scale fabrication.
- Suitable for integration with Monolithic Microwave Integrated Circuits (MMIC's).
- Compatible for producing linear and circular polarization with broadside radiation with simple feed.
- Feed lines and matching circuits can be simultaneously fabricated with antenna structure.
- Dual frequency or multi frequency operation can be possible with geometry modifications.
- Dual polarization antennas can be easily made.
- No cavity backing is required.

However microstrip antennas have some inherent disadvantages which limit the use in many wireless applications. These major demerits include

- Narrow band width and associated tolerance problems.
- Uniplanar radiation; Microstrip antennas radiate into half space.
- Lower power handling capacity and poor end fire radiation.

- Excitation of surface waves when thick substrates are used.
- Somewhat lower gain ($\sim 6\text{dBi}$).
- Large ohmic loss in the feed structure of arrays.

Even though microstrip antennas have some demerits, they are widely used for lot of applications. Several other types of antennas have emerged to cater to the new varieties of application and are discussed in detail in the forthcoming sections.

1.5.2 Coplanar Waveguide (CPW)

A conventional CPW on a dielectric substrate consists of a center strip conductor with semi-infinite ground planes on either side separated by a small gap. The three dimensional view of the open ended CPW transmission line is shown in figure.1.2.

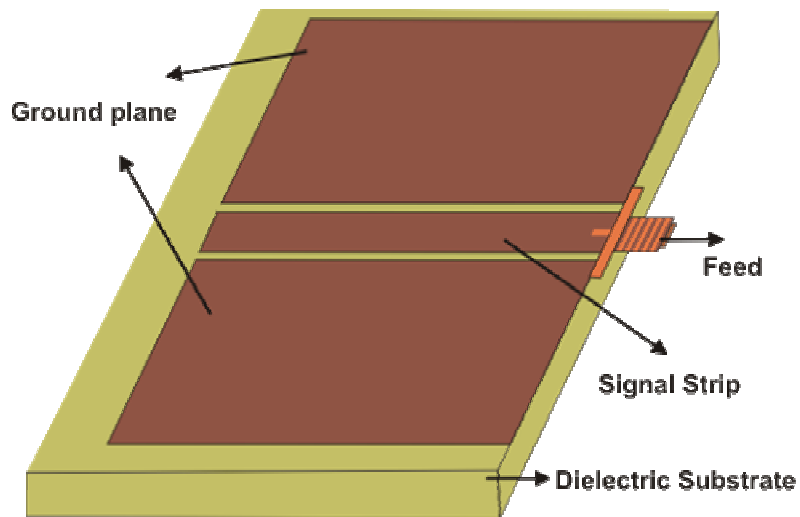


Figure 1.2 Geometry of Coplanar waveguide(CPW) Transmission line

This structure supports a quasi-TEM mode of propagation. The advantages of CPW transmission line over Microstrip are,

- Uniplanar structure
- Easy fabrication
- Active and Passive devices can be easily mounted on the surface.
- Eliminates the need for wraparound and via holes
- Less radiation loss
- Weak Cross talk between adjacent lines

Broadly coplanar waveguides can be classified into three types as follows

- **Conventional CPW**
Semi infinite ground planes on either side of the central line. But for practical purpose the ground planes are of finite extent.
- **Conductor backed CPW**
In this case there is an additional ground plane at the bottom surface of the substrate which not only gives mechanical support but also acts as a heat sink for active devices.
- **Micromachined CPW**
The micro machined CPWs are of two types, namely, the microshield line and the CPW suspended by a silicon dioxide membrane above a micromachined groove.

The CPW is excited by launching signal to the centre strip with respect to the ground strip. This produce a field distribution similar to the Odd mode distribution in coupled slot lines. The electric field is coupled out of phase in the two slots with magnetic field encircling each strip. In odd mode a magnetic wall is introduced at the plane passing though the centre of the signal strip. Here the field distributions in gaps are out of phase, and it cancels at the far field and hence less radiation loss.

The structural and radiation characteristics of CPW makes it suitable for almost all the fields of microwave engineering. CPW lines are commonly employed in Micro-Electro-Mechanical Systems (MEMS) Switches. MEMS are small integrated devices or systems that combine electrical and mechanical components. The rapid progress made in the area of semiconductor wafer processing has led to the successful development of MEMS based microwave circuits. The conductors located on the top surface of a substrate (uniplanar) makes it ideally suitable for fabricating metal membrane, capacitive, shunt-type switches etc [13]. MEMS shunt switches manufactured on CPW structures are found to have low insertion loss, low switching voltages, fast switching speed and excellent linearity. These switches offer the potential to build new generation low loss high linearity microwave circuits for phased array antennas and communication systems. Amplifiers, active combiners, frequency doublers, mixers, and switches have been realized using CPW. The CPW amplifier circuits include millimeter-wave amplifiers [14, 15 and 16] distributed amplifiers [17], cryogenically cooled amplifiers [18], cascade amplifiers [19], transimpedance amplifiers [20], dual gate HEMT amplifiers [21], and low-noise amplifiers [22].

Recent advances in the area of thin film deposition techniques, such as sputtering, laser ablation, chemical vapor deposition, and etching technologies, have resulted in the application of high temperature superconducting (HTS) materials to microwave circuits [23]. The HTS circuits have low microwave surface resistance over a wide range of frequencies. As a result signal propagation takes place along these transmission lines with negligible amount of attenuation. Furthermore the advantage of using CPW is that only one surface of the substrate needs to be coated with HTS material before patterning. Recently HTS low-pass and band-stop CPW filters have been demonstrated [24-25].

The CPW is invariably used in antenna designs as the feed of the radiating element and as radiating system. Coplanar Waveguide fed Patch Antennas are available in literature [26]. The feed system in these antennas is directly coupled, electromagnetically coupled, or aperture coupled to the patch.

1.5.3 DR Loaded Antenna

The radiating mechanism in a Dielectric Resonator Antenna (DRA) is the displacement current circulating in a dielectric medium, usually a ceramic pellet. That is the radiation characteristics are a function of the mode of operation excited in the DRA. These antennas give more degree of freedom since the user can choose the large variety of dielectric constant as per the user's requirement. Moreover, DRA's can decrease the size of antenna significantly by choosing high dielectric materials [27]. Geometry of DR antenna is shown in figure.1.3.

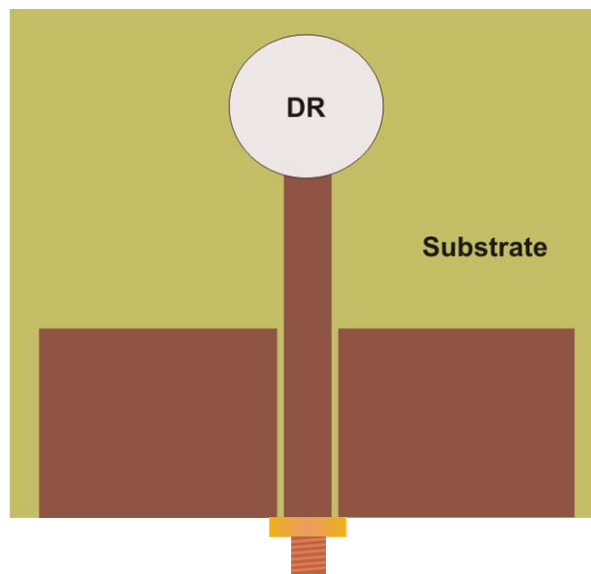


Figure 1.3 Geometry of Dielectric Resonator Antenna

DR antennas have high radiation efficiency since there is no inherent conductor loss in DR's and hence are highly attractive for millimeter wave

antennas, where the loss in metal fabricated antennas can be high. They are highly suitable for space application and in other compact wireless gadgets.

1.5.4 PILA and PIFA based Antenna

Planar Inverted L-Antenna (PILA) and Planar Inverted F-Antenna (PIFA) are the promising alternatives for external monopoles. The small size and low profile nature of the PIFA make it an excellent choice on portable equipment. Typical geometry of a PIFA is shown in figure.1.4.

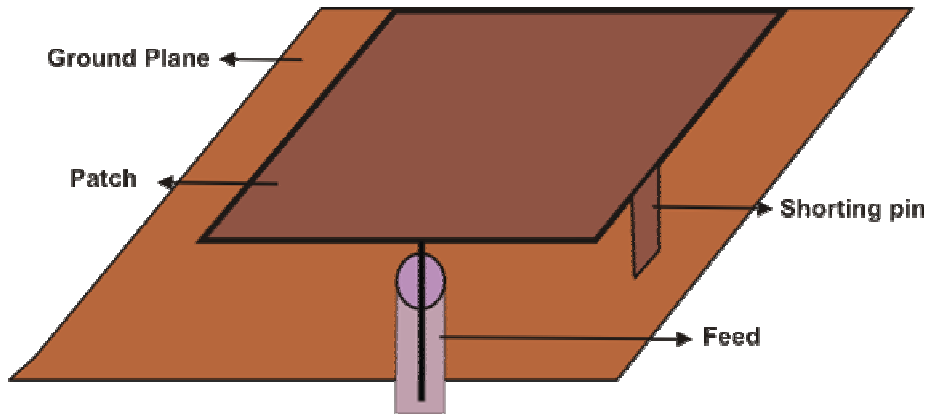


Figure 1.4 Geometry of Planar Inverted F-Antenna

The PILA/PIFA can be considered as a combination of the inverted-L/F (ILA/IFA) antenna and the short circuited rectangular microstrip antennas (SCMSA). The Inverted F Antenna and Microstrip Antenna have narrow bandwidth but their combinations resulting in PIFA have higher bandwidth to cover the popular communication bands. The basic PIFA consists of a ground plane, a top plate element, a feed wire feeding the resonating top plate, and a shorting plate that is connecting the ground and the top plate at one end of the resonating patch. Stacking and insertion of slits are included in PIFA's to create multiband operation [28-29].

1.5.5 Metamaterial based Antenna

Electromagnetic metamaterials (MTMs) are broadly defined as artificial effectively homogeneous electromagnetic structures with unusual properties not readily available in nature [30]. An effectively homogeneous structure is a structure whose structural average cell size (p) is much smaller than the guided wavelength (λ_g). Therefore, this average cell size should be at least smaller than a quarter of wavelength. The condition $p = \lambda_g/4$ is the effective homogeneity limit or effective homogeneity condition, to ensure that refractive phenomena will dominate over scattering/diffraction phenomena when a wave propagates inside the MTM medium. If the condition of effective homogeneity is satisfied, the structure behaves as a real material in the sense that electromagnetic waves are essentially myopic to the lattice and only probe the average, or effective, macroscopic and well defined constitutive parameters, which depend on the nature of the unit cell; the structure is thus electromagnetically uniform along the direction of propagation. The constitutive parameters are the permittivity ϵ and the permeability μ .

The urge of the antenna designers to reduce the size and to improve the radiation characteristics are satisfied by the introduction of metamaterials. The metamaterial, makes the antenna behave as if it were much larger than it really is, because the novel antenna structure stores energy, and re-radiates it. The radiated powers of an antenna can step-up by the introduction of metamaterials. Moreover, the efficiency-bandwidth limitations of conventional monopole antennas are overcome by using metamaterial.

Metamaterials employed in the ground planes surrounding antennas offers improved isolation between radio frequency, or microwave channels of MIMO antenna arrays. These high-impedance ground planes can also be used to improve

the radiation efficiency, and axial ratio performance of low-profile antennas located near the ground plane.

Nowadays a lot of researches have been carrying on metamaterial based antennas with plenty of applications in communication industry.

1.5.6 Photonic band gap structure based antenna designs

A Photonic Band Gap (PBG) material is a periodic dielectric, ferromagnetic, ferroelectric or metallic structure which is used to control and manipulate the propagation of electromagnetic waves. Initial PBG researches have been done on optical region but can be extended into a wide range of frequencies.

A standard antenna printed on a substrate radiates a fair amount of energy into the substrate. If one uses a substrate of PBG material whose stopband includes the operating frequency of the antenna, most of the energy radiated into the substrate is reflected back to the free space, and thus the radiation efficiency is improved. The PBG structures can be used to modify the radiation pattern of conventional Microstrip antennas. Recently there has been increasing interest in the microwave and millimeter wave application of Photonic Band Gap structures. Various designs of PBG structures for bandwidth enhancement, size reduction, suppression of unwanted harmonics, reduction of cross polarization etc can be found in literature [31-34].

1.5.7 LTCC based antenna designs

The Low Temperature Co-fired Ceramic (LTCC) technology can be defined as a way to produce multilayer circuits with the help of single tapes, which are to be used to apply conductive, dielectric and / or resistive pastes on. These different single sheets (50-250 μ m) have to be laminated together and fired in one step. This saves time, money and reduces circuits dimensions. An other great advantage is that

every single layer can be inspected (and in the case of inaccuracy or damage) and replaced before firing; this prevents the need of manufacturing a whole new circuit.

LTCC makes it possible to pack the filters and other components used in a mobile phone into a package having dimensions of few mm³. These LTCC technologies are viable alternative for miniaturization technique. Lot of ultra compact antennas are available in the literature utilizing this technology [35-37].

1.6 Analysis of antennas

Analysis of an antenna is essential in understanding the operating principle its design and enhancement. The radiation characteristic of the antenna both in near field and far field can be predicted using different analysis methods. These analysis methods are useful tools in predicting radiation characteristics of complex situations. The process is complicated by the presence of infinite radiation space, inevitable dielectric inhomogeneity, inhomogeneous boundary conditions, feed variation and geometry. Considering all these and depending up on the nature of problem the user can choose different analysis method available. The analysis of a microwave circuit can be considered as shown in figure.1.5.

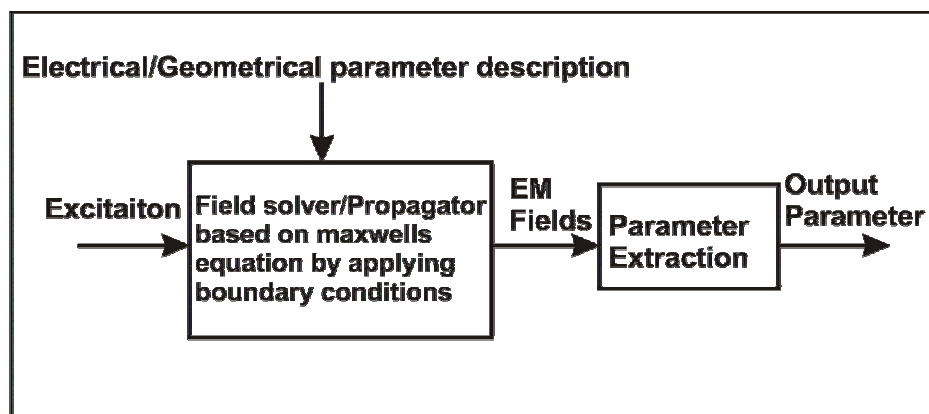


Figure 1.5. Schematic showing the modeling of an EM problem

Target geometry, electrical parameter and excitation used in the structure should be defined prior to the antenna analysis. Different methods for the analysis of antennas are described in the following sections,

Analytical model were developed for the analysis of microstrip antennas. Transmission line model, cavity model and multi port network model are used for the analysis. Full wave method for the analysis of an antenna, solves Maxwell's equation subject to boundary conditions at the interface. Accuracy, completeness and versatility are the key characteristics of this method. The numerical methods for the solution of Maxwell equation are shown in the table.1.4.

Table 1.4 Frequency and Time domain Solver [6,7]

Frequency domain: Field solver.		Time domain: Field Propagator.	
Requires Matrix inversion & system solution. Requires frequency samples across broad bandwidth, followed by a transform to obtain the result		Requires initial values & boundary values. Values updated in time. Ideal for massive parallel architecture. Wide band performance results in a single calculation	
Integral Equation	Differential method	Integral Equation	Differential method
Method of Moments: Electric Field integral Equation(EFIE) or mixed potential integral equation(MPIE)	Finite element method	Time domain Integral Equation(TDIE)	Transmission line matrix(TLM) Finite Difference Time Domain Method(FDTD)

1.6.1 Transmission Line Matrix (TLM) method

The transmission line matrix method was originally developed by Johns and Beurle[38]. It replaces the structure by a mesh, either 2D or 3D. The nodes

of the grid are interconnected by virtual transmission lines. Excitation at the source nodes propagate to adjacent nodes through those transmission lines at each time step. Generally, dielectric loading is accomplished by loading nodes with reactive stubs, whose characteristics impedance is appropriate for the amount of loading desired. Lossy media can be modeled by introducing loss into the transmission line equations or by loading the nodes with lossy stubs. Absorbing boundaries are constructed in TLM meshes by terminating each boundary node transmission line with its characteristics impedance. Analysis is performed in the time domain. Complex, nonlinear materials are readily modeled, impulse responses and time-domain behavior of the systems are determined explicitly, and the technique is suitable for implementation on massively parallel machines. But, voluminous problems using fine grids require excessive amounts of computation. TLM method shares the advantages and disadvantages of the FDTD method, and discussed later.

1.6.2 Method of Moments (MoM)

The use of MoM for solving electromagnetic structures became popular by the work of Richmond in 1965 and Harrington in 1967[39-40]. MoM is a method of solving a differential equation or an integral equation numerically by transforming the equation into simultaneous equations. Regarding antenna analysis integral equation for electric field on the surface of the conductor is usually used to obtain the surface current on the antenna. The substrate and ground plane are assumed to be infinite in lateral dimensions and formulation of the problem is based on rigorously enforcing the boundary condition. In Electric Field Integral Equation (EFIE) the boundary condition is applied to the total tangential electric field where as in Magnetic Field Integral Equation (MFIE) boundary condition is expressed in terms of magnetic field. Mixed Potential Integral Equations (MPIE) has both scalar and vector potentials in its

formulation [41]. The integral equation is then solved either in spectral domain or spatial domain by taking appropriate transformations. The procedure for applying MoM to solve an electromagnetic problem involves four steps:

- Derivation of the appropriate integral equation (IE)
- Conversion (discretization) of the IE into a matrix equation using basis (or expansions) functions and weighting (or testing) functions.
- Evaluation of the matrix elements
- Solving the matrix equation and obtaining the parameters of interest.

To solve Integral Equation it is discretised into set of linear equations by means of moment method. By solving the matrix equation the surface current on the patch conductor can be obtained which is then used for extracting the radiation pattern, polarization, directivity etc. MoM depends upon expanding the unknown quantity in the equation in terms of known entire domain or sub domain basis functions with unknown coefficients. The selection of basis function is a very important step in the numerical solution since they have the ability to accurately represent and resemble the anticipated unknown function while minimizing computational effort [42-44]. The popularly used basis functions are piece wise sinusoidal, pulse basis and roof top basis functions. A set of equations is generated by enforcing the boundary conditions with a suitable set of testing functions. This results in a matrix whose order is proportional to the number of segments on which the current distribution is represented. The solution to the problem is found by inverting this matrix.

1.6.3 Finite Element Method (FEM)

The finite element method is suitable for the solution of a wide class of partial differential or integral equations in almost all arbitrary geometries. FEM

uses a volumetric approach which requires the entire volume of the configuration to be meshed as opposed to surface integral techniques, which require only the surfaces to be meshed. The properties of the neighboring mesh elements are entirely different. In general, finite element techniques excel at modeling fine structural features in complex inhomogeneous configurations. However, unbounded radiation problems are not handled as effectively as MoM. It uses both tetrahedral and prismatic elements to mesh the structure.

The major weakness of FEM is that it is relatively difficult to model open configurations. However, in finite element methods, the electrical and geometric properties of each element can be defined independently. This permits the problem to be set up with a large number of small elements in regions of complex geometry and fewer but large elements in relatively open regions. Thus it is possible to model configurations that have complicated geometries and many arbitrarily shaped dielectric regions in a relatively efficient manner.

1.6.4 Finite Difference Time Domain (FDTD) method

The Finite Difference Time Domain (FDTD) method was first introduced by K.S.Yee in 1966 [45] and refined and reinvented by Taflove [46] in the 1970's. This very powerful electromagnetic tool is capable of addressing complex antenna structures by providing direct solutions to Maxwell's equations in differential form. This method permits the modelling of electromagnetic wave interactions with a level of detail as high as that of the Method of Moments. Unlike MoM, however, the FDTD does not lead to a system of linear equations defined over the entire problem space. Updating each field component requires knowledge of only the immediately adjacent field components calculated one-half time step earlier. Therefore, overall computer storage and running time requirements for FDTD are linearly proportional to

the number of field unknowns in the finite volume of space being modelled. Today FDTD method is well established in the field of Computational Electromagnetics. As the method is time domain based, it can reveal antenna characteristics over a wide frequency range with a single run. Due to the displacement between electric and magnetic field components in Yee's FDTD, Chen et al. [47] modified the FDTD and the new formulation is exactly equivalent to the symmetric condensed node model used in the TLM method. This implies that the TLM algorithm can be formulated in FDTD form and vice versa. However, both algorithms retain their unique advantages. FDTD has a simpler algorithm where constitutive parameters are directly introduced, while the TLM has certain advantages in the modeling of boundaries and the partitioning of the solution region. The selection of algorithm for numerical investigation is completely user dependent.

1.7 Motivation of Present research

The fundamental idea behind any antenna design is to radiate electromagnetic energy into free space through acceleration or deceleration of charges created by bent, curve, discontinuity and termination.

From the beginning itself Antenna designers have adopted different methodology to create radiation. Modification along the transmission lines is an interesting method of creating discontinuity and thereby enhancing radiation. It is worth noting that there are many antennas can be viewed as a modification of transmission lines For eg: the two wire transmission line is flared to form dipole antenna. Similarly the waveguide is flared to horn antennas to achieve effective radiation. If the transmission line is open or is opened by a discontinuity (a slot or hole), then the higher-order modes generated can radiate energy

Microstrip antenna - the pioneer of printed antenna technology that has gained the attention of mobile wireless system designers is an extension of the microstrip transmission lines. Similarly slot line transmission line is flared to form Vivaldi antenna. Thus all transmission lines can be easily transformed into an effective radiator.

The CPW structures are interesting candidates for microwave and millimeter wave application due to their useful design characteristics such as low radiation leakage, less dispersion, little dependence of the characteristic impedance on substrate height, uniplanar configuration and can be easily integrated into Monolithic Microwave Integrated Circuits (MMIC).

The CPW transmission line can also be converted to radiating structures by effectively modifying its parameters. The basic coplanar waveguide transmission line is interestingly modified [48] to an effective radiator by simply optimizing the dimensions and feed point. Thus other degree of freedom to effectively convert a CPW transmission line to a effective radiator is modifying the signal strip, ground plane etc. This is the fundamental concept behind this thesis work.

The signal strip is modified by changing it to two different unequal lengths [49], and a Coplanar Waveguide meandered feed line [50] is used to obtain broadband dual frequency operation on a planar monopole antenna, Modifying the signal strip is the main concentration of antenna researchers, and a lot of developments has been carried out during the last few decades. Some of these works are depicted on chapter 2 under the literature review.

It is reported that the ground plane modification of CPW structures, can also be used to convert it an efficient radiator. Introducing Defected ground structures (DGS), Photonic Band Gap (PBG) structures and various slots on the

ground plane can provide an efficient radiator. Among the slot antennas the inductive fed [52] and capacitive fed [52] antennas are very interesting. By introducing active components, the resonance of these slot antennas can be controlled. These antennas are highly compact with stable radiation characteristics.

Considering all the aforementioned works I am interested to modify the coplanar waveguide transmission line to an effective radiator. Among the available degrees of freedom, the first modification is on the signal strip to generate a quad band antenna. The ground plane of the antenna is also modified to make it a perfect radiator without altering the signal strip. Then both the ground plane and signal strip are modified simultaneously to get a compact antenna with excellent radiation characteristics.

1.8 Thesis Organization

Chapter 1 describes an overview of antenna research, state of the art technologies in antennas, coplanar waveguide, its applications and the motivation of present research.

Chapter 2 deals with the review of literature related to the present work. The chronology of antenna development exclusively from Coplanar Waveguide Transmission lines is presented. Various interesting design concepts of antenna research are explored in this chapter. Moreover, it also narrates the antenna fabrication method and the experimental facilities utilized. The measurement methods employed for characterizing the antenna presented in the thesis is also described.

The modification of an Open Ended Coplanar Waveguide Transmission line into an effective radiator is described and thoroughly investigated in Chapter 3. This chapter gives an insight into the radiation mechanism of the

signal strip modified antenna structure. The necessity to use multiband antennas instead of multiple antennas is demonstrated by the design of this quad band antenna. The design of a highly compact quad band antenna is discussed in detail. The antenna is highly suitable for all present day communication bands. The polarization of the antenna is same for all the four bands. The design criteria and parametric analysis is also presented.

Chapter 4 deals with the development of a compact antenna by modifying the ground plane of a Coplanar waveguide transmission line. The ground plane to signal strip gap is altered and the ground is meandered to get larger resonating length. The radiation of this antenna is mainly due to the vertical components and hence a good cross polarization level is obtained within this highly compact structure.

The radiation mechanism of a single band antenna derived from the open ended CPW fed transmission line is presented thoroughly in Chapter 5. In this chapter both the ground plane and signal strip are modified and studied in detail. A harmonic suppressed antenna is also presented by the modification of this structure. A tunable antenna is developed by incorporating a diode and giving proper bias. The physical dimensions of all these antennas are very small compared to the wavelength corresponding to the operating frequency. These compact antennas are good candidate for modern wireless gadgets.

Chapter 6 describes conclusions of this thesis. The scope for future works is also discussed.

A dual band antenna derived from the above structure is designed, developed and analyzed. This dual band antenna is presented as appendix A.

References

- [1] J.D. Kraus, “Antennas Since Hertz and Marconi”, IEEE Trans. Ants. Prop, AP-33, 131-137, 1985
- [2] Yi Huang, Kevin Boyle, “Antennas from Theory to Practice”, John Wiley and Sons
- [3] G.A. Deschamps, Microstrip Microwave Antennas, 3rd USAF symposium on Antennas, 1953
- [4] John D Kraus and Ronald J Marhefka, Antennas and Wave propagation, Tata McGraw hill, 2010
- [5] Tapan K Sarkar, “History of Wireless” , John Wiley and Sons
- [6] Binu Paul, “Development and Analysis of microstrip antennas for dual band microwave communication” Ph.D thesis, Cochin University of science and Technology.
- [7] Mridula S, “Investigations on a microstrip excited rectangular dielectric resonator antenna”, Ph.D thesis, Cochin University of science and Technology.
- [8] E.V. Byron, A New Flush Mounted Antenna Element for Phased Array Applications, Proceedings of Phased Array Antenna Symposium, 1970, pp. 187-192.
- [9] R.E Munson, Single Slot Cavity Antennas, US Patent no-3713162, January 22, 1973
- [10] J.Q. Howell, Microstrip Antennas, Dig. International symposium on Antennas Propagation Society, Williamsburg, VA, Dec 1972, pp 177-180
- [11] Constantine A Balanis “ Antenna theory analysis and design” John Wiley and Sons II nd edition
- [12] Pozar D.M., “The Analysis and Design of Microstrip Antennas and Arrays”, IEEE press, New York, 1995
- [13] M. Riaziat, E. Par, G. Zdasiuk, S. Bandy, and M. Glenn, “Monolithic Millimeter Wave CPW Circuits,” 1989 IEEE MTT-S Int. Microwave Symp. Dig., Vol. 2, pp. 525—528, Long Beach, CA, June 13—15, 1989.

- [14] G. S. Dow, T. N. Ton, and K. Nakano, "Q-Band Coplanar Waveguide Amplifier," *1989 IEEE MTT-S Int. Microwave Symp. Dig.* Vol. 2, pp. 809—812, Long Beach, California, June 13—15, 1989.
- [15] K. M. Strohm, J.-F. Luy, F. Schaffler, H. Jorke, H. Kibbel, C. Rheinfelder, R. Doerner, J. Gerdes, F. J. Schmuckle, and W. Heinrich, "Coplanar Ka-Band SiGe-MMIC Amplifier," *Electron. Lett.*, Vol. 31, No. 16, pp. 1353—1354, Aug. 1995.
- [16] M. Riaziat, S. Bandy, and G. Zdasiuk, "Coplanar Waveguides for MMICs," *Microwave J.*, Vol. 30, No. 6, pp. 125—131, June 1987.
- [17] R. Majidi-Ahy, M. Riaziat, C. Nishimoto, M. Glenn, S. Silverman, S. Weng, Y. C. Pao, G. Zdasiuk, S. Bandy, and Z. Tan, "94 GHz InP MMIC Five-Section Distributed Amplifier," *Electron. Lett.*, Vol. 26, No. 2, pp. 91—92, Jan. 1990.
- [18] A. Cappello and J. Pierro, "A 22-24-GHz Cryogenically Cooled GaAs FET Amplifier," *IEEE Trans. Microwave Theory Tech.*, Vol. 32, No. 3, pp. 226—230, March 1984.
- [19] R. Majidi-Ahy, C. Nishimoto, M. Riaziat, M. Glenn, S. Silverman, S.-L. Weng, Y.-C. Pao, G. Zdasiuk, S. Bandy, and Z. Tan, "100-GHz High-Gain InP MMIC Cascode Amplifier," *IEEE J. Solid-State Circuits*, Vol. 26, No. 10, pp. 1370—1378, Oct. 1991.
- [20] K. W. Kobayashi, L. T. Tran, M. D. Lammert, A. K. Oki, and D. C. Streit, "Transimpedance Bandwidth Performance of an HBT Loss-Compensated Coplanar Waveguide Distributed Amplifier," *Electron. Lett.*, Vol. 32, No. 24, pp. 2287—2288, Nov. 1996.
- [21] M. Schefer, H.-P. Meier, B.-U. Klepser, W. Patrick, and W. Bachtold, "Integrated Coplanar MM-Wave Amplifier With Gain Control Using a Dual-Gate InP HEMT," *IEEE Trans. Microwave Theory Tech.*, Vol. 44, No. 12, pp. 2379—2383, Dec. 1996.

- [22] D. Leistner, “Low Noise Amplifier at L- and Ku-Band for Space Applications in Coplanar Technology,” *23rd European Microwave Conf. Proc.*, pp. 823—827, Madrid, Spain, Sept. 6—9, 1993.
- [23] Nathan Newman and W. Gregory Lyons High-temperature superconducting microwave devices: Fundamental issues in materials, physics, and engineering, *Journal of Superconductivity*, Volume 6, Number 3, 119-160
- [24] Min Hwan Kwak , Kang-Yong Kang , Chun Kwon Choi, Sang Hyun Kim “High temperature superconducting low pass filter for suppressed harmonics” *Physica C Superconductivity*, Volumes 372-376, Part 1, August 2002, 532-535
- [25] Min Hwan Kwak, Seok Kil Han, Kwang Yong Kang and Dal Ahn, “Design of High-Temperature Superconducting Low-Pass Filter for Broad-Band Harmonic Rejection”, *IEEE Transactions on Antennas and Propagat.*, Vol. 11, No. 2, pp. 4023-4026, June 2001
- [26] Joom-Suk Suh, and Sang Hyun Kim J. W. Greiser, “Coplanar Stripline Antenna,” *Microwave J.*, Vol. 19, No. 10, pp. 47—49, October 1976.
- [27] A. Petosa, *Dielectric Resonator Antenna Handbook*. Boston, MA:Artech, 2007.
- [28] Benito sanz Izquierdo, John C.Batchelor, Richard J.Ingley and Mohammed I.Sobhy, “Single and Double layer planar multi band PIFAs”, *IEEE Transactions on Antennas and Propagat*, vol.54, no.5, pp 416-422, May 2006.
- [29] Dalia Mohammed Nashaat, Hala A. Elsadek and Hani Ghali, “ Single Feed Compact Quad band PIFA antenna for Wireless Communication Applications”, *IEEE Transactions on Antennas and Propagat*, vol.53, no.8, pp 2631-2635, August 2005.
- [30] Christophe caloz and Tatsuo Itoh, “Electromagnetic Metamaterials: Transmission line theory and Microwave Applications, The Engineering Approach” John Wiley and Sons
- [31] P.Salonen, M. Keskilammi, L. Sydanheimo, “A low cost 2.45GHz phtonic band gap patch antenna for wearable systems”, *IEEE international conference on Antennas and Propagation*, 77-80, April 2011.

- [32] Y.J. Sung and Y.S. Kim, “ An Improved Design of Microstrip Patch Antennas Using Photonic Band Gap structures”, IEEE Transactions on Antennas and Propagat, Vol.53, No.5,pp 1799-1802, May 2005.
- [33] Haiwen Liu, Zhengfan Li, Xiaowei Sun and Junfa Mao, “Harmonic Suppression With Photonic Bandgap and Defected Ground Structures”, IEEE Transactions on Antennas and Propagat, Vol.15, No.2,pp 55-56, February 2005.
- [34] Debatosh Guha, Manotosh Biswas and Yahia M.M Antar, “Microstrip patch antenna with defected ground structures for Cross Polarisation Suppression”, IEEE antennas and wireless propagation letters, vol.4,pp 455-458, 2005.
- [35] Gautier,W; Schoeninner B, Ziegler v, Prechtel U, Menzel W, “LTCC patch array for RF-MEMS based phased array antenna at 35GHz”, 38th European Microwave Conference, 27-31, pp: 151-154, Oc.2008.
- [36] Brezezina G, Roy L, MacEachern L, “Planar antennas in LTCC technology with transceiver integration capability for ultra-wideband applications” IEEE Trans. On Microwave Theory and Tech, Vol 54, Issue 6, Part 2,pp:2830-2839, June 2006.
- [37] RongLin Li, DeJean G, Moonkyun Maeng, Kyutae Lim, Pinel S, Tentzeris M.M, Laskar J, “Design of compact stacked patch antennas in LTCC multilayer packaging modules for wireless application”, IEEE Transactions on Advanced Packaging, Volume 27, Issue 4, Page(s): 581-589, Nov 2004.
- [38] P. B. Johns and R. L. Beurle, “Numerical solutions of 2-dimensional scattering problems using a transmission-line matrix,” *Proc. Inst. Elec.Eng.*, vol. 118, pp. 1203–1208, Sept. 1971.
- [39] J.H. Richmond, “Digital computer solutions of the rigorous equations for scattering problems,” *Proc. IEEE*, vol. 53, Aug. 1965, pp. 796–804.
- [40] Constantine A Balanis., “Advanced Engineering Electromagnetics,” John Wiley and Sons, USA,1989.

- [41] Mosig, J.R., “Arbitrarily shaped microstrip structures and their analysis with a mixed potential integral equation”, IEEE Trans., 1988, MTT-36, pp. 314-323.
- [42] R.Mitra and C.A Klein, “Stability and Convergence of Moment Method solutions”, in Numerical and Asymptotic Techniques in Electromagnetics, R.Mitra (Ed.),Springer Verlag, New York,1975,Chapter 5, pp 129-163
- [43] T.K Sarkar, “A Note on the choice of weighing functions in the Method of Moments”, IEEE Trans. Antennas and Propogat. ,vol AP-33,no.4,pp 436-441, April 1985.
- [44] T.K Sarkar, A.R Djordjevic and E.Arvas, “On the choice of expansion and weighing function in the solution of operator equations”, IEEE Trans. Antennas and Propogat. vol AP-33,no.9,pp 988-996,September 1985.
- [45] K.S.Yee, “Numerical solution of initial boundary value problems involving Maxwell’s equations in isotropic media,” IEEE Trans. Antennas Propagat., vol.14, no.4, pp.302-307, May 1966
- [46] Allen.Taflove, “Numerical issues regarding finite-difference time-domain modelling of Microwave structures,” Time-Domain Methods for Microwave structures – Analysis and Design, Ed.Tatsuo Itoh and Bijan Houshmand, IEEE Press..
- [47] X.Zhang,J.Fang,y.Liu and K.K Mei , “Calculation of dispersive characteristics of Microstrips by time domain finite difference method”, IEEE Trans.Mirowave theory and tech. vol 36,pp.263-267,1988.
- [48] Rohith K Raj,Manoj Joseph, C. K. Aanandan, K. Vasudevan and P. Mohanan, ‘A New Compact Microstrip-fed Dual-band Coplanar Antenna for WLAN application’, IEEE Trans. Antennas Propag., Vol. 54,No.12,pp 3755-3762, Dec 2006.
- [49] Horng-Dean Chen and Hong-Twu Chen, ‘A CPW-Fed Dual Frequency Monopole antenna’, IEEE Trans. Antennas Propag., Vol. 52,No.4,pp 978-982, April 2004.

- [50] W.-C. Liu, 'Broadband dual-frequency meandered CPW-fed monopole antenna', *Electron. Lett.*, Vol. 40, No.21, pp 1319-1320, oct. 2004.
- [51] Cheng-Chieh Yu and Xian-Chang Lin, 'A Wideband Single Chip Inductor-Loaded CPW-Fed Inductive Slot Antenna', *IEEE Trans. Antennas Propag.*, Vol. 56, No.5, pp 1498-1501, May 2008.
- [52] Y.-F. Lin, P.-C. Liao, P.-S. Cheng, H.-M. Chen, C.T.P. Song and P.S. Hall, 'CPW-fed capacitive H-shaped narrow slot antenna', *Electron. Lett.*, Vol. 41, No.17, pp 438-439, August. 2005.



REVIEW OF LITERATURE AND METHODOLOGY

<i>Contents</i>	2.1 Introduction
	2.2 Antenna Fabrication and Experimental analysis

This chapter presents different technologies proposed by various scientists and research groups for the development of compact planar Antennas. The main focus is on the development of Coplanar Waveguide Fed antennas in the last few decades. The recent advances in planar antennas are also addressed. The transformation of coplanar waveguides to an efficient radiator is properly investigated and presented in this chapter.

2.1 Introduction

The need of miniaturization in the present day communication industry is challenging. In the present scenario, printed antenna technology is highly suitable for wireless communication due to its low profile and other desirable radiation characteristics. Small monopole type antennas are overruled by compact small antennas for present day mobile communication applications.

Coplanar waveguides (CPW) are printed on one side of a dielectric substrate. CPW have attracted the attention of antenna designers due to their excellent properties like ease of integration with 'MMIC', low cost, wide bandwidth, flexibility towards multiband operation, low radiation leakage and less dispersion. The requirement of omnidirectional coverage, light weight and low cost made these CPW fed antennas a good candidate for wireless applications.

The main focus of the thesis is the study of coplanar waveguide transmission line. Rigorous investigations were performed on both the ground plane and signal strip of a coplanar waveguide transmission line to create effective radiation characteristics. Good amount of works have been done to transform CPW line to antenna suitable for mobile phone applications. References on the radiation properties of CPW transmission line have been included in this chapter

2.1.1 Planar Printed antennas

Printed antennas have a variety of attractive properties like compactness, mechanical durability, conformability, and cheap manufacturing costs. They have a range of applications in both the military and commercial sectors, and are often mounted on the exterior of aircraft and spacecraft, as well as in

mobile radio communication devices. Various challenges have to be faced by antenna designers for developing such devices. The chronological development in printed antenna technology is clearly illustrated in the following section.

The basic printed antenna, Microstrip antenna concept was first proposed in 1953 by Dechamps [1] of USA and by Gutton and Baissinot of France [2]. The realization of the microstrip antenna element patented by Munson[3] in 1970 gave a sudden boost to antenna industry.

The basic rectangular and circular microstrip patch antennas were proposed by Howell [4]. Later the transmission line model [5], the cavity model [6] and the spectral- domain method [7] were introduced for the analysis of microstrip antennas. The multi port network model generalizes the cavity model[8]. For very thin substrates the resonant frequency and input impedance have limited accuracy using these methods[9]. Moreover, they have limited capacity to handle problems such as mutual coupling, large arrays, surface wave effects and different substrate configuration.

The finite element approach[10] made possible to calculate the fields interior to the microstrip antenna with solutions closest to the true analytical solutions. The spectral domain full wave approach which uses the exact Green's function for the mixed dielectric nature of the microstrip antenna was proposed by Deshpande and Bailey[11]. Lot of analysis on patch geometries and feed structures were carried out using this technique.

The analysis of a rectangular patch and circular disc were studied using this method by Chew, Aberle and Bailey[12-14]. Studies on various modified

patch geometries were successfully carried out by lot of researchers all over the world for different applications.

John Q Howel [15] studied various types of microstrip antennas and has given design procedures for both linearly and circularly polarized antennas. Microstrip antennas having circular polarization operation have been studied and reported [16-18]. A circular polarized rectangular microstrip antenna with a single point feed was also designed by Haneishi and Yoshida [19].

The preliminary limitation of microstrip antennas was the narrow band width. This was overcome by modifying the patch geometries and also by using stacked patches as radiators [20]. Integral equation method [21-24], cavity model [25-27], transmission line model [28-29] and modal expansion method [30] are the techniques used to solve basic aperture coupled patch antenna geometries.

Y.J. Sung [31] introduced Defected Ground Structures (DGS) on microstrip patch antenna to suppress the higher order harmonics. W.C Liu [32] designed a dual-polarised single layer slotted patch antenna. Y. Qin [33] achieved broadband using an H-shaped patch coupled to a microstrip feed line via a ring slot in the ground plane. But still the enhancement in bandwidth is a serious issue in microstrip antenna designs.

2.1.2 Coplanar Waveguide (CPW) fed Antennas

The emergence of Coplanar Waveguide (CPW) fed antennas revolutionized the antenna industry in terms of cost, compactness, bandwidth etc. The uniplanar characteristics of CPW structures together with their attractive features like low radiation loss and less dispersion in comparison with a microstrip, little dependence of characteristic impedance on substrate parameters etc made them

popular. The development of the Coplanar Waveguide fed antennas from the beginning to recent years is detailed here.

Coplanar Waveguide (CPW) was invented by CPW (Cheng P. Wen) and is discussed in his manuscript entitled “Coplanar Waveguide: a surface strip transmission line suitable for nonreciprocal gyromagnetic device applications” published in 1969[34]. Practical applications of coplanar waveguide have been experimentally demonstrated by measurements on resonant isolators and differential phase shifters fabricated on low-loss dielectric substrates with high dielectric constants. Calculations have been made for the characteristic impedance, phase velocity, and upper bound of attenuation of a transmission line whose electrodes are all on one side of a dielectric substrate. This discovery enabled the microwave researchers to choose a good end transmission line for MMIC devices and for other compact microwave applications.

In 1970 Cheng P. Wen [35] reported the attenuation characteristics of coplanar waveguides. The Q measurements together with the loss characteristics of coplanar waveguides were presented and found to be in conjunction with microstrip lines of the same width and characteristic impedance.

H Matino[36] proposed the characteristic impedance measurement of coplanar waveguide. This letter presents experimental data, and theoretical equation including correction factors, for an effective relative permittivity concerning characteristic impedance. The next year the dependence of the characteristic impedance of a coplanar waveguide was measured as a function of slot width and substrate thickness by P.A.J.Dupuis and C.K. Campbell [37].

A theoretical method was presented by T. Kitazawa in 1976[38] for the analysis of a coplanar waveguide with thick metal-coating. It was shown that the metal coating thickness of the coplanar waveguide causes an increase in wavelength and a decrease in characteristic impedance. They also noted that the changes are about the same as those of a slot line.

E. Mueller [39] measured the effective relative permittivity of unshielded coplanar waveguides. The dependence of the effective relative permittivity of coplanar waveguides was measured as a function of frequency from 3-12 GHz and is compared with the computed values.

The transmission properties of a coplanar waveguide printed on conductor-backed substrates were analysed by Y.C. Shih and T. Itoh in 1982 [40] using the spectral-domain technique. They concluded that for a fixed substrate thickness, the characteristic impedance and the phase constant may be varied independently by simply adjusting the widths of the centre strip and the slots in the transmission line.

A new concept of exciting slotted antenna arrays was proposed by Aleksandar Nesic in 1982 [41] where both the slots and feeder are etched on the same side of the printed circuit board. A channel is cut perpendicular to the slots, and a coplanar waveguide for exciting the slots is inserted into the channel and the concept is experimentally verified on a model.

Analysis of slow wave phenomena in coplanar waveguide on a semiconductor substrate was proposed by Y. Fukuoka and T. Itoh [42] using mode-matching technique. This waveguide is suitable for monolithic microwave integrated circuits due to their coplanar configuration. After a lot of

study on the slow wave phenomena of coplanar waveguide was carried out by scientists and microwave researchers rigorously.

Anand Gopinath in 1982[43] investigated on the losses in Coplanar Waveguides elaborately. Conductor losses in coplanar waveguides have been calculated using a quasi-static Green's function approach. The conductor, dielectric and radiation losses are used to compute the quality factor of half wavelength resonators and compared with the measurement results.

A coplanar waveguide fed end-coupled resonator band pass filter was proposed and investigated by Dylan F. Williams in 1983[44]. Band pass filter design rules were developed for easy filter synthesis from "prototype" low-pass designs. Measurements of single section resonator Quality factors were used to predict filter insertion losses and verified with lot of examples.

A simplified method for evaluating the line parameters of a coplanar waveguide was presented by Kohji Koshiji[45] in 1983. The TEM mode of propagation was assumed and Laplace's equation is solved by means of the successive over relaxation method. Parameters such as potential distribution electric field, current distribution over conductor surface, characteristic impedance, dielectric loss and conductor loss are analyzed.

A new analytical expression for the impedance and the permittivity of coplanar waveguides with lower ground plane was presented by G. Ghione and C. Naldi[46] on the same year. These calculated expression shows very good agreement with the upper or lower bounds of the parameters, computed via a spectral-domain variational approach.

David A Rowe in 1983 [47] proposed a numerical method to calculate the impedance and the effective dielectric constant for a CPW with a ground plane

under a thin dielectric as a function of CPW parameters for different substrates. These results can be used to design the shielded coplanar waveguides.

The effect on characteristic impedance and line loss by inner conductor offset in a Coplanar Waveguide was reported by Kohji Koshiji and Eimei Shu in 1984 [48]. This effect can be an appreciable factor in designing highly precise circuits, such as MIC's using coplanar waveguide, or a coplanar-type standing-wave detector.

The influence of various structural parameters on the characteristics of the Metal-Insulator-Semiconductor Coplanar waveguide structure was investigated, together with the effect of the addition of a back conducting plane by Roberto Sorrentino in 1984[49]. They have developed the design criteria for low attenuation slow wave propagation.

Victor Fouad Hanna and Dominique Thebault[50] investigated theoretically and experimentally, the characteristic impedance and effective dielectric constant of an Asymmetric Coplanar Waveguide with infinite or finite dielectric thickness. It was observed that the line asymmetry decreases the characteristic impedance and increases its relative effective dielectric constant.

D. Bhattacharya in 1985 [51] proposed a simplified formula for the characteristic impedance of coplanar waveguide by determining the static capacitances between the parallel strips and is valid even up to zero gap width. On the same year C. Seguinot [52] suggested a time domain response of MIS Coplanar Waveguides for MMIC's.

The coplanar waveguides transmission line is compared with a microstrip line in terms of conductor loss, dispersion and radiation into parasitic modes. Robert W. Jackson [53] shows that for high frequency application CPW can be

chosen to give better results in terms of conductor loss and dispersion than microstrip.

K. Koshiji and E Shu [54] developed circulators using coplanar waveguides. One of the circulators designed in this way shows a maximum isolation of 19.1dB, insertion loss 0.8dB and VSWR 1.3 or less at a center frequency 9.56GHz.

D Mirshekar Syahkal in 1986[55] developed a full wave solution to investigate the dispersion in shielded coupled coplanar waveguides. The characteristics of even and odd modes of coplanar waveguide on semi-insulating GaAs substrate were investigated by R. Majidi Ahy in 1987[56]. The guide wavelength for each mode is directly obtained from standing wave measurements by electro-optic sampling, and compared to the theoretical values.

Parasitic effects occurring in actual realizations of coplanar waveguides (CPW) for microwave integrated circuits on GaAs substrates, such as the influence of an upper shield, conductor backing, finite-extent ground planes, and line-to-line coupling, were discussed and evaluated by Giovanni Ghione[57] in 1987.

Robert W. Jackson investigated the electromagnetic coupling possibility of Coplanar Waveguide in 1987 [58]. He proposed a transition which couples coplanar waveguide on one substrate surface (a motherboard) to coplanar waveguide on another substrate surface (a semiconductor chip) placed above the first without using any wire bonds. They also performed full wave analysis using coupled line theory.

A three-port magnetically-tunable ferrite resonator circuit which uses a ferrite resonator and coplanar waveguide on a dielectric substrate was proposed by Koichi Ohwi [59]. M. Riazat [60] and co-workers investigated the single-mode operation of coplanar waveguides. A grounded coplanar waveguide structure with finite-size ground planes is analysed as three coupled microstrip lines. The three normal propagation modes of this structure are examined for various geometries, and some physical layout guidelines are established.

A lumped equivalent circuit models for several coplanar waveguide discontinuities such as an open circuit, a series gap in the center conductor, and a symmetric step in the center conductor were investigated by Rainee N. Simons [61]. The element values are given as a function of the physical dimensions of the discontinuity. The model element values are de-embedded from measured S parameters. In addition, the effects of the center conductor width and the substrate thickness on the equivalent circuit element values are presented. The characteristics of a CPW right angle bend employing a novel compensation technique are also presented.

A coplanar waveguide array antenna which consists of a coplanar waveguide and wire loop antennas was proposed by K. Nakaoka [62]. The reported antenna has the advantages of wide bandwidth, lower losses in the transmission line and is independent of the thickness of copper clad dielectric.

Full-wave analysis of coplanar waveguide (CPW) and a slotline by the time-domain finite-difference method (TD-FD) was presented by Guo-Chun liang[63] in 1989. The transient propagating waveforms along the coplanar waveguide and slotline, which are excited by retarded Gaussian pulses, are found in the time domain. After the time-domain field distributions are obtained, frequency-domain

parameters such as the effective dielectric constant and the complex characteristic impedance are calculated using Fourier transformations.

John J. Burke [64] described a structure which forms a transition from coplanar waveguide on one substrate to microstrip on another. Energy is transferred via electromagnetic coupling rather than with wire bonds. A full-wave formulation along with the theory of asymmetrically coupled lines is used to analyze the two model transitions.

Robert W. Jackson [65] investigated the mode conversion at discontinuities in finite width conductor-backed coplanar waveguide. The moment method technique is used for CPW gap and shorted end studies. These studies are performed via a fully electromagnetic application of moment method technique and a significant conversion is found to occur at the gap end.

Majid Riaziat in 1990[66] investigated on the propagation modes and dispersion characteristics of coplanar waveguides. Radiation and guided modes are studied on the five subdivided class based on substrate thickness, backside metallization and ground plane width and their effect on loss and dispersion are also described.

Full-wave analysis of shielded coplanar waveguide short-end using transverse resonant method was presented by G.Bartolucci [67]. The resonant frequencies of the structure are computed by the full-wave electromagnetic field analysis. G.C Dalman[68] proposed a waveguide to coplanar waveguide adaptor with low transmission loss and high return loss free from strong resonances over a broadband width.

A method to couple microwave power from a coplanar waveguide to a microstrip line on opposite sides of a ground plane was demonstrated by R.N

Simons and R. Q Lee [69]. The coupler uses a metallic post which passes through an aperture on the ground plane connecting the strip conductor of the coplanar waveguide to the microstrip line.

Mohsen Naghed and Ingo Wolff[70] calculated the equivalent capacitances of coplanar waveguide discontinuities on multilayered substrates using a three-dimensional finite difference method. The application of the method was demonstrated for open ends and gaps in microstrip and coplanar waveguides as well as for more complicated structures such as interdigital capacitors.

An integral equation technique solved by the moment method associated with the single one-port model to analyze radiating end effects of coplanar waveguides (CPW's) was used by M'hamed Drissi[71]. They used series-gap-coupled straight CPW resonators to compare the theoretical results with the experimental ones.

A full-wave analysis of shielded coplanar waveguide two-port discontinuities based on the solution of an appropriate surface integral equation in the space domain was presented by Nihad I. Dib[72]. Equivalent circuit models and closed-form expressions to compute the circuit element values for these discontinuities are also presented.

Teek-Kyung Lee and group [73] characterized the quasi-static capacitance and inductance of the CPW using the Boundary Element Method (BEM). Mikio Tsuji [74] investigated the leakage behavior of coplanar wave guides of finite and infinite widths. They showed that above a critical frequency the dominant mode on coplanar waveguide leaks power in the form of a surface wave on the surrounding substrate, and that this leakage can cause undesirable cross talk and can produce unexpected package effects. Further studies then

revealed several new interesting behavioral features, such as unexpected sharp and deep minima (cancellation effects), various dimensional dependences, and the leakage behavior when the guide width changes from finite to infinite.

R.N Simons [75] demonstrated coplanar waveguide (CPW)/aperture coupled microstrip patch antennas constructed with ground coplanar waveguide (GCPW), finite coplanar waveguide (FCPW) and channelized coplanar waveguide (CCPW). The CCPW/Aperture coupled microstrip patch antenna has the largest bandwidth, whereas the GCPW/aperture coupled microstrip patch antenna has the best front-to-back ratio.

Aperture coupling was successfully employed with Coplanar Waveguide as the feed by Richard Q. Lee in 1992[76]. A grounded CPW with a series gap in the center strip conductor is used to couple microwave power to a microstrip patch antenna through an aperture in the common ground plane. This design permits the insertion of solid state devices in the series gap of the CPW feed and thus, is suitable for use in active antenna or quasi-optical combiner/mixer designs.

Jeng-Yi Ke[77] utilized the spectral domain approach to discuss the dispersion and leakage phenomenon in a coplanar waveguide structure caused by the substrate surface wave. The effective dielectric constant and the attenuation constant due to surface wave leakage are presented and discussed in detail.

Further the researchers elaborately used the coplanar waveguide as a feeding structure for patch antennas. R.L Smith [78] used a coplanar waveguide loop to feed a microstrip patch and E.T. Richardo[79] fabricated CPW on a

single layer substrate with various thickness and used to electromagnetically couple with planar antennas.

The CPW was conformally mapped by M.S. Islam [80] into a parallel plate configuration, where conductor loss is evaluated using a conductor surface impedance which is scaled by the conformal map.

Ming Yu [81] described a new quasi-static technique for the analysis of coplanar and microstrip transmission line discontinuities. The method is a variation of the Space-Spectral Domain Approach (SSDA) which represents a novel combination of the 1-D Method of Line (MOL) and the 1-D Spectral Domain Approach (SDA).

A novel coplanar waveguide fed coplanar strip dipole antenna was presented by K. Tilley [82]. They used a wideband balun to match the antenna. R.R.Kumar[83] reported the dispersion characteristics of conductor backed coplanar waveguide (CBCPW) in a metal enclosure. The higher order modes are also explained by means of an efficient numerical technique, namely the method of lines (MOL). Knowledge of higher order modes is essential for estimating 'singlemode' bandwidth and for characterising discontinuities.

A monopole strip antenna which consists of an open ended strip and a three-section coplanar waveguide feed is proposed and its attractive features are described by C. Isik[84] in 1995. He experimentally confirmed the dependence of the antenna on the width and length of the strip.

H.S. Tsai [85] developed CPW-fed multiple slot antennas for active arrays and integrated antennas. This also describes how the antenna can be engineered for a 50 ohm input impedance for a various substrate parameters,

and the concepts are verified using a three-slot antenna on $\epsilon_r = 2.2$ substrate and a five slot antenna on $\epsilon_r = 9.8$ substrate.

CPW fed slot antennas printed on multilayer dielectric substrates are numerically analyzed by Jean-Marc Laheurte [86] using a full-wave integral equation technique and the method of moments. The mutual coupling between slot antennas in an array environment is calculated for a three-layer high-low-high permittivity combination.

CPW-fed folded-slot antennas were analyzed using the finite-difference time-domain (FDTD) method by Huan Shang Tsai [87] et.al in 1996. The paper describes the problems encountered in the analysis, compares the theoretical results and measured data, and provides some design information for folded slots. In addition, the paper explores the manipulation of input impedance through the use of additional slots, yielding antennas with broadband 50Ω input impedance.

S. Matsuzawa and K. Ito [88] proposed a new structure of circularly polarised printed antenna fed by coplanar waveguide (CPW). FDTD analysis is performed and predicts the radiation of the circularly polarized wave from the antenna.

A microstrip antenna fed by a conductor backed coplanar waveguide was demonstrated by L. Giauffret and J.M. Laheurte in the same year [89]. The addition of a back-side metallic ground plane involves a possible power leakage owing to the excitation of parallel plate modes (PPMs). It is shown that the power leakage can be avoided by a proper choice of substrate characteristics.

The use of an elevated coplanar waveguide (CPW) to increase the bandwidth forced the researchers to theoretically analyze their performance. A full-wave analysis between 10 and 500 GHz of such an elevated CPW using 2-

D FDTD method is presented by S. Hofschen [90]. The influence of the elevation heights on the capacitance and the loss behavior of the transmission line are discussed in detail.

A circularly polarized patch antenna, fed by a coplanar waveguide was discussed by Y. Turki [91]. The antenna is excited by a couple of 100Ω slotlines which are combined to obtain a 50Ω coplanar waveguide. The axial ratio and the bandwidth of the antenna are similar to those obtained with other types of feeding.

I Linardou [92] described a twin Vivaldi antennas directly fed by coplanar waveguides. All the designs show a centred zero in the E plane with a low cross-polarisation. In the H plane they provide zeros for $\varphi = 90^\circ$ and 270° and are nondirectional for other values.

Erli Chen [93] expressed the analytical formulas using conformal mapping to explain the characteristics of coplanar transmission lines on multilayer substrates. Laurent Giauffret [94] investigated various shapes of excitation slots, such as open stubs, slot loops, and capacitively and inductively coupled slots in terms of return loss and front to back radiated power ratio on CPW fed aperture coupled microstrip antennas.

X.Din and A.F. Jacob[95] presented a new wide slot antenna with capacitively coupled CPW-feed and metallic strips in the apertures. A simplified formula to calculate the input impedance is also proposed by them.

A nonleaky conductor-backed coplanar waveguide (NL-CBCPW) was presented by D.R.Jahagirdar [96] for exciting microstrip patch antennas with emphasis on avoiding the leakage of power and allows easier integration with MMIC's.

A CPW-fed CPS dipole antenna was presented by AT. Kolsrud, Ming-Yi Li and Kai Chang [97] which operates at dual frequencies with a wideband CPW-to-CPS balun. Dual-frequency operation of the CPS dipole antenna was realised by introducing a small gap in the length of the dipole.

A coplanar waveguide (CPW) fed rectangular patch antenna excited by a rectangular slot-loop was designed for use in the 2.4GHz ISM band by Shih-Wen Lu in 1999 [98]. The size of the slot-loop was chosen to be as close to that of the patch, and the substrate cut is as narrow as possible.

W.S.T. Rowe and R.B. Waterhouse [99] presented a broadband CPW fed stacked patch antenna well suited for integration with monolithic and optical integrated circuits with a bandwidth of 40% on a high dielectric constant substrate.

A new concept for exciting slots with a CPW line based on inductive coupling was introduced by Santiago Sierra-Garcia [100]. He described how this coupling structure can be designed to tune the impedance of the antenna over a wide range. This new coupling topology was particularly suitable for series-fed array configurations and broad-band design.

Masashi Hotta, Yongxi Qian, and Tatsuo Itoh [101] analyzed the leakage loss of the conductor-backed coplanar waveguide (CBCPW) by using a novel hybrid two-dimensional finite difference time-domain/Marquardt curve-fitting technique. The validity and high accuracy of the method was confirmed by comparison with other experimental and theoretical results.

A novel coplanar waveguide fed quasi-Yagi antenna was proposed by J.Sor [102]. A wide bandwidth is achieved by using a broadband coplanar waveguide to a slotline balun. An X-band prototype has been realised which

demonstrates a broad bandwidth (30%), -19dB front to back ratio, and cross polarisation better than -17dB at 10GHz.

A.U Bhohe [103] presented a coplanar waveguide fed slot antenna for wideband operation. This antenna has an impedance bandwidth (for a VSWR < 2) of 49% and a radiation bandwidth of 42% at 4.8GHz, compared to the 12-20% impedance bandwidth of the standard CPW fed slot antenna.

The odd mode of a conductor backed CPW is successfully filtered by introducing a via-hole in one of the lateral ground plane by A. Mebarki[104]. The even mode propagates without being disturbed by the introduction of via hole.

Circularly polarized microstrip antenna with a coplanar waveguide feed was presented by Chih-Yu Huang[105] in 2000. This CP was achieved by inseting a slit to the boundary of the square microstrip patch, which makes possible the splitting of the dominant resonant mode into two near-degenerate orthogonal modes for CP radiation and introducing an inclined slot in the CPW feed line for coupling the electromagnetic (EM) energy to the square patch.

C.H.Cheng[106] proposed a broadband patch antenna fed by a coplanar waveguide based on stacked patch technique for aperture coupled patch antennas. Similarly M.S. Al Salameh[107] proposed a novel coupling scheme to rectangular dielectric resonator antennas. They used narrow coupling slot at the end of a coplanar waveguide (CPW) to couple the energy to a resonator.

Homg Dean Chen [108] proposed a novel compact dual-frequency monopole antenna by introducing an extended conductor line to a rectangular meander monopole. This antenna can operate in the 900 and 1800 MHz bands and provide sufficient bandwidths for the GSM and DCS systems.

Xian-Chang Lin and Ling Teng Wang [109] used photonic band gap structures with cross-shaped or square-shaped lattices on a broadband CPW fed loop slot antenna to achieve harmonic control. The compact PBG structures not only successfully get rid of the higher order modes but also facilitate the impedance matching of the antennas, leading to significant bandwidth augmentation.

A new design of a broadband circularly polarized square slot antenna fed by a single coplanar waveguide (CPW) is proposed by Jia Yi Sze [110] and verified experimentally. Broadband circular polarization (CP) operation is achieved by protruding a T-shaped metallic strip from the ground plane towards the slot center and feeding the square slot antenna using a 50- CPW with a protruded signal strip at 90 to the T-shaped strip.

Design of a coplanar waveguide (CPW) feed square microstrip antenna with circular polarisation (CP) radiation is described by Chih Yu Huang [111]. The CP is achieved by using an asymmetric inductively coupling slot in the ground plane of the CPW feed line.

Hornng Dean Chen [112] presented a CPW fed square slot antenna with widened tuning stub to achieve broadband operation. They experimentally showed that the impedance matching for the proposed antenna strongly depends on the location of the tuning stub in the square slot, and the impedance bandwidth is mainly determined by the width and length of the tuning stub.

A coplanar waveguide fed square slot antenna loaded with conducting strips was proposed and experimentally studied to provide broadband design by Jyh Ying Chiou [113]. By choosing a suitable length ratio (ratio of signal strip

in the slot to the loading metallic strip) the impedance bandwidth of the proposed antenna can be significantly increased.

G. Tzeremes[114] presented a quasi TEM equivalent circuit model for two optically driven coplanar waveguide (CPW)-fed slot antennas. This model takes into account both the electromagnetic fields in the CPW structure as well as the effects of the discontinuities of the antenna design.

CPW fed dual band antenna was demonstrated by W.C. Liu[115] in 2004 by inserting a meandering slit at the edge of a rectangular patch. The structure has uniplanar geometry and its compactness makes it suitable for portable mobile communication applications. A rectangular notch is introduced to obtain a broadband dualfrequency operation of a planar monopole antenna fed by a coplanar waveguide (CPW) by W.C. Liu and C.M.Wu[116]

A broadband dual-frequency planar monopole antenna with a coplanar waveguide meandered feed line was introduced by W.C. Liu [117]. This modified feeding technology offers good impedance match for a wide dual-band covering 2.4/5.2 GHz WLAN operations. S.Y.Chen and P.Hsu[118] presented a coplanar waveguide fed capacitive folded-slot antenna for the radio frequency identification application at 5.8GHz.

A rectangular slot antenna with U-shaped tuning stub was proposed by R.Chair[119]. The antenna is excited by a 50Ω CPW to achieve ultra wide bandwidth. A CPW-fed planar ultra-wideband antenna with hexagonal radiating elements is presented by Y Kim [120] in 2004. The frequency band notch characteristic is attained very close to the desired frequency by inserting a V-shaped thin slot on the hexagonal radiating element.

The design procedure of a wideband CPW fed hybrid slot antennas and CPW fed log-periodic slot antennas was presented by Alpesh U. Bhobe[121]. They have studied the impedance matching and the radiation characteristics of these structures using method of moments.

K. Chung, T. Yun and J. Choi [122] presented a CPW fed monopole antenna with parasitic elements and slots to attain wideband characteristics. They introduced the parasitic elements and three slots to increase the impedance bandwidth.

Sierpinski fractal monopole antenna with a CPW feed was presented by M. Kitlinski and R. Kieda[123] for multiband applications. Fourth iteration of the Sierpinski gasket with scale factor $\delta=1.5$ is used as the radiating element. A novel broadband, dual-polarised coplanar-waveguide-fed T-shaped uniplanar antenna was presented by R.B. Hwang [124]. Full wave numerical analysis with experimental results are presented in detail.

J. Yeo, Y. Lee and R. Mittra [125] presented a planar volcano-smoke slot antenna (PVSA) useful for wideband wireless communication applications. The antenna is a planar slot – with an appearance reminiscent of a volcanic crater and a puff of smoke – and is fed by a coplanar waveguide (CPW) to achieve the wide bandwidth. A coax-to-CPW transition, which is crucial for achieving wide bandwidth performance, is also modelled and introduced into the antenna.

A patch monopole antenna for radio frequency identification (RFID) applications using a coplanar waveguide feed with folded slots to expand the impedance bandwidth was presented by W.C. Liu and Z.K Hu[126]. By properly selecting a folded slot on a rectangular patch, compact antenna size, broad impedance bandwidth and good radiation characteristics suitable for the RFID application at 5.8 GHz could be achieved.

A CPW fed right-angled dual tapered notch antenna for ultrawideband (UWB) communication was demonstrated by Y.Kim[127]. The antenna has two tapered notches, which are located at a right-angled corner of a dielectric substrate. The combination of two proposed antennas can be used to eliminate the null areas in the wide-angle direction of the devices.

Shih Yuan Chen [128] presented a broad band radial slot antenna fed by a coplanar waveguide for dual frequency operation. Various frequency ratios for the two operating frequencies can be obtained by varying the included angle between the radial slots and/or by varying the length of the central slot pair. Radiation patterns are broadside and bidirectional.

A new type of CPW-fed dual-annular-slot antenna operating at 5.8 GHz band was introduced by S.-H. Hsu and K. Chang [129]. The authors studied the inductive and capacitive configurations separately and verified the results with measurement.

X.C. Lin and C.C Yu [130] investigated a CPW-fed hybrid antenna consisting of a CPW fed inductive slot and a dual inverted-F monopole antenna. This hybrid antenna exhibits dual-band behaviour with sufficient bandwidths to meet the system requirements of Wireless Local Area Network (WLAN), IEEE 802.11a (5725–5825 MHz), HIPERLAN/2(5470–5725 MHz) and IEEE 802.11 b/g (2400–2483 MHz).

A coplanar waveguide fed monopole antenna with a planar patch element embedded with a cross slot was presented by C.M.Wu [131] which was capable of generating two separate resonant modes with good impedance match. The authors discussed the design considerations for achieving dual-band operation of the proposed antenna.

A slotted bow-tie antenna with pattern reconfigurability was proposed by Sung-Jung Wu [132] which consists of a coplanar waveguide (CPW) input, a pair of reconfigurable CPW-to-slotline transitions, a pair of Vivaldi-shaped radiating tapered slots, and four PIN diodes. With suitable arrangement of the bias network, the proposed antenna demonstrates reconfigurable radiation patterns in the frequency range from 3.5 to 6.5 GHz.

A low-profile, planar, circularly polarised monopole antenna with a shorting sleeve strip using a coplanar-waveguide transmission line for wireless communication in digital communication system and the global positioning system bands was studied by C.J. Wang [133]. The coupling effect between the monopole antenna and sleeve is utilized properly to excite the two resonant modes.

M.E. Chen [134] presented a CPW fed Ultra Wide Band antenna with an open annulus strip as a ground plane and an open crescent patch in the inner space of the annulus as a radiating element. The radius of the inner crescent patch and the inner radius of the outer annulus should be adjusted carefully to obtain optimal impedance bandwidth.

A uniplanar aperture-coupled slot dipole antenna capable of tri-band operation was presented by Shih-Yuan Chen [135]. By varying the length of the protruded slots the three resonances can be tuned and adjusted. A dipole like radiation pattern with low cross polarized radiation is obtained in all the three bands.

Cheng-Chieh Yu [136] presented a wideband single chip inductor loaded CPW fed inductive slot antenna. An inductor with optimum value is shunt at one

end of the inductive slot antenna to excite additional lower resonance. Moreover, the bandwidth is further widened by enlarging the over the slot ground height.

A coplanar waveguide-fed inductively coupled stepped impedance slot antenna was proposed by Wen-Hua Tu[137] which have a size reduction of 32% compared to a conventional uniform slot antenna.

An UWB printed slot antenna, suitable for integration with the printed circuit board (PCB) of a wireless universal serial-bus (WUSB) dongle was presented by D.D. Krishna [138]. In addition to compact size, the antenna was insensitive to ground plane length variations, making it suitable for WUSB dongle and mobile UWB applications.

P.C. Bybi[139] presented a compact, planar, wideband antenna designed by modifying the coplanar waveguide with a wideband performance. Wide bandwidth >75% centered at 2.50 GHz, quasi omnidirectional radiation coverage, moderate gain and efficiency are the salient features of the antenna.

A dual-band coplanar waveguide (CPW)-fed hybrid antenna consisting of a 5.4 GHz high-band CPW-fed inductive slot antenna and a 2.4 GHz low-band bifurcated F-shaped monopole antenna was proposed and investigated experimentally by Xiang-Chang Lin and Cheng-Chieh Yu [140]. A coplanar-waveguide (CPW)-fed circularly polarized slot antenna with a bandwidth of 31.2% was proposed by Chien-Jen Wang [141].

A triple-band coplanar waveguide (CPW) fed LI-shaped monopole antenna was proposed by Y. Jee and Y.M. Seo[142]. The antenna is composed of an I shaped monopole and a meandered L shaped. These can be independently optimized for particular operating frequency.

D.-O. Kim and C.-Y. Kim [143] proposed the design strategy for the triple-band notched ultra-wideband (UWB) antenna emphasising the rejection characteristic at 3.5/5.5/8.2 GHz bands. They embedded the notching elements onto the primitive antenna to serve as respective stop band filters.

A coplanar waveguide (CPW) antenna was proposed for dual-band WLAN applications by K.G.Thomas and M. Sreenivasan[144]. The antenna comprises of a rectangular patch and rectangular notch, both together providing impedance matching for the lower and upper resonance.

Y.S.Li[145] presented a coplanar-waveguide (CPW)-fed ultra-wideband antenna with dual band-notch characteristics. By cutting two U-shaped slots in the radiation patch and an H-shaped slot in the CPW ground, two band-notched frequencies will appear which reduce the potential interference between UWB systems and narrow band systems.

An endfire directional tapered slot antenna with ultra-wideband characteristic using CPW to wideslot transition was presented by H. Kim [146]. By widening the slot width in the transition, ultra wideband characteristic with enhanced directivity is obtained.

K.P Ray and S.Tiwari [147] presented a coplanar waveguide fed printed hexagonal monopole antenna with ultra wideband application. A parametric study of hexagonal configurations with two different feed arrangements (vertices and side feed) has been carried out to study the effect of feed gap on bandwidth.

Taehee Jang [148] presented the design and analysis of compact coplanar waveguide(CPW)-fed zeroth-order resonant(ZOR) antennas. The CPW geometry provides reduction in antenna size since vias are not required and will provide more design freedom.

2.2 Antenna Fabrication and Experimental analysis

The antenna for a particular application must be fabricated and tested. The various steps employed in the fabrication of a coplanar waveguide fed antenna are listed below.

2.2.1 Selection of a dielectric substrate material

The first important procedure for an antenna designer is to select a suitable dielectric substrate. The electrical and material properties of the selected substrate should match with the required application. The stability of substrate material parameters like dielectric constant and loss tangent with temperature and frequency are important. Since the antenna is coplanar waveguide fed which is uniplanar in nature, single sided substrates are chosen for fabrication.

High performance microwave materials for substrates and packaging industry are in great demand for microelectronic industry. Such materials should possess important properties like low dielectric constant and low dielectric loss to reduce the propagation delay and to increase the signal speed. High Dielectric constant substrates causes surface wave excitation and low bandwidth performance. High loss tangent substrate adversely affects the efficiency of the antenna especially at high frequencies. In addition the material should have high thermal conductivity for dissipating heat. The other important substrate characteristics include the thickness, homogeneity, isotropicity and physical strength of the substrate [149-153]. Increasing the thickness of the substrate will increase the bandwidth at the expense of efficiency owing to the generation of surface waves. There is no ideal substrate; the choice depends on the application of the fabricating device.

Dielectric constant, loss tangent and thickness of the material are important factors to be considered for fabrication. The relative permittivity and loss tangent of a substrate can be measured using various methods [154-155]. In the present study the dielectric constant of the material is measured using Cavity perturbation method. This technique is highly suitable for low loss and low or medium dielectric constant. By using very thin substrates (small volume), it is possible to measure high dielectric constant materials also.

A rectangular waveguide operating in the S or X-band with a slot at the top is used for the measurement. The waveguide is transformed into a cavity by placing two irises at the beginning of the waveguides. Depending on the dimension of the cavity, various modes will develop inside the cavity with various Q and loss. Initially the frequency, bandwidth and quality factor of different modes are measured for the empty cavity. Depending up on the type of the cavity more than five modes can be obtained in a particular waveguide. The sample whose properties to be measured should be extremely small. This sample is inserted into the waveguide cavity through the slots created at the top. The sample should be placed in such a way to perturb the field to a maximum level. After inserting the material the shift in frequency, bandwidth and quality factor are again measured. The complex dielectric constant can be calculated using the following equation,

$$\epsilon_r' = \frac{V_c (f_c - f_s)}{2V_s f_s} + 1$$

$$\epsilon_r'' = \frac{(V_c) (Q_c - Q_s)}{4V_s Q_c Q_s}$$

$$\tan \delta = \frac{\epsilon_r'}{\epsilon_r''}$$

Where f_c = Resonant frequency of the empty cavity

f_s = Resonant frequency of the cavity with sample

V_c = Volume of the cavity

V_s = Volume of the sample

Q_c = Quality factor of the empty cavity

Q_s = Quality factor of the cavity with sample

Thus the dielectric constant of the selected substrate is measured. Next step is to etch the required pattern on this substrate.

2.2.2 Photo Lithography

Photolithography or Optical lithography is the process of transferring geometric shapes from a photo-mask to the surface of a substrate. The design of the optimized antenna should be printed on the selected single side substrate. The geometry is drawn using any of the CAD software with high precision. This is printed on a butter paper or transparent OHP sheet. Here a negative photo resist is used for photolithography; therefore an inverse of the pattern is used for making the mask. The substrate with copper on one side is rubbed with metal cloth to remove any of the imperfection and cleaned with acetone to remove impurities on the metal surface. Any disparity in the etched structure will shift the resonant frequency from the predicted values, especially when the operating frequency is very high. A thin layer of photo resist mixed with thinner with 1:2 ratio is coated on the surface of the substrate and dried. Then the mask is placed above the photo resist and is exposed to UV light for a specific time. During this time the UV light is exposed to the portions where the material is required and the photo resist become hard. Then the developer solution removes the resist from unexposed portions. Then the

substrate is applied with suitable dye to have clear visibility for the developed structure. Then it is washed in the running water. The unwanted metallic structure can be removed by etching it in ferric chloride. FeCl_3 dissolves the copper parts except underneath the hardened photo resist layer. The laminate is then cleaned carefully to remove the hardened photo resist using acetone solution. Different steps involved in the fabrication procedure are shown in the figure.2.1.

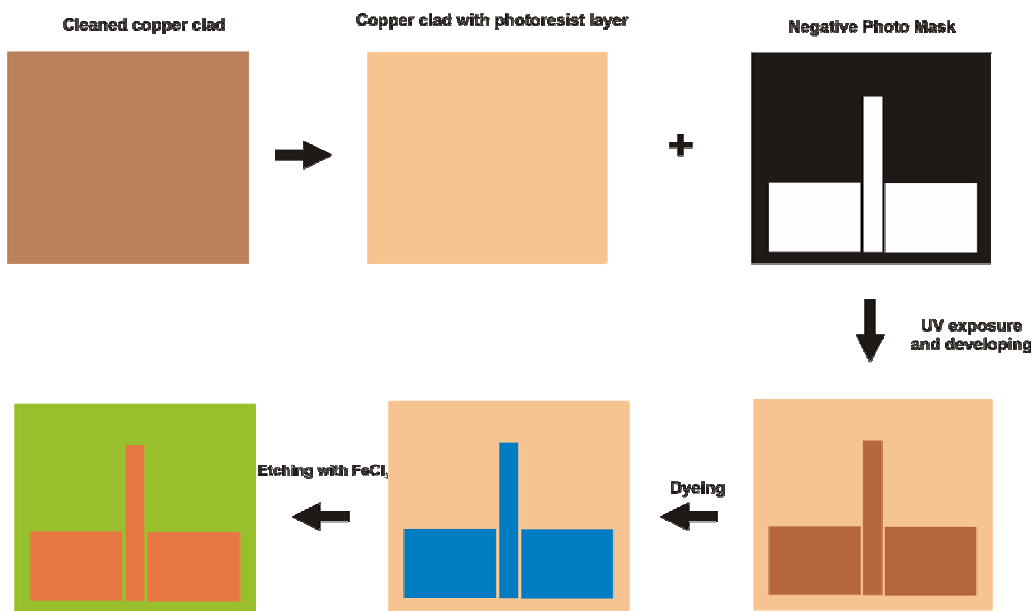


Figure 2.1 Photolithographic process

2.2.3 Antenna Measurement Facilities

Antenna characteristics such as reflection and radiation characteristics are measured using HP8510C vector Network Analyzer, PNAE8362B analyzer and allied setup. The indigenously developed CREMA SOFT is used for the automation and synchronization of all the measurements. In this section a brief description of the basic facilities used for the antenna measurements are presented,

2.2.3.1 HP8510C Vector Network Analyzer

The 8510C series microwave vector network analyzers provide a complete solution for characterizing the linear behavior of either active or passive networks over the 45 MHz to 50 GHz frequency range. The 8510C network analyzer measures the magnitude, phase, and group delay of two-port networks to characterize their linear behavior. Optionally, the network analyzer is also capable of displaying a network's time domain response to an impulse or a step waveform by computing the inverse Fourier transform of the frequency domain response [156].

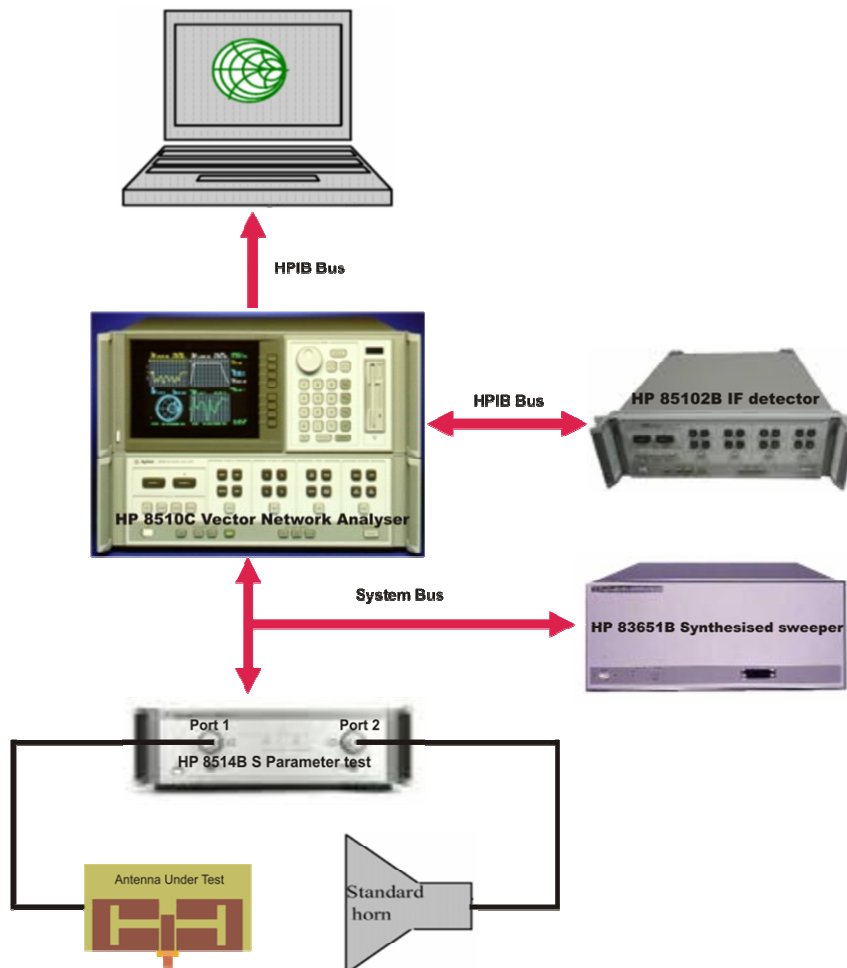


Figure 2.2 Vector Network Analyser based measurement system

32bit microcontroller MC68000 based system can measure two port network parameters such as S_{11} , S_{12} , S_{22} , S_{21} and it's built in signal processor analyses the transmit and receive data and displays the results in many plot formats. The NWA consists of source, S parameter test set, signal processor and display unit. The schematic of the Vector Network Analyzer based measurement set up is shown in figure.2.2.

The synthesized sweep generator HP 83651B uses an open loop YIG tuned oscillator to generate the RF stimulus. It can synthesize frequencies from 10 MHz to 50 GHz. The frequencies can be set in step mode or ramp mode depending on the required measurement accuracy.

The antenna under test (AUT) is connected to one of the port of the S-parameter test set (HP8514B) and the forward and reflected power at the measurement points are separated and down converted to 20MHz using frequency down converter. It is again down converted to 20KHz and processed in the HP8510C processing unit. All the systems discussed above are interconnected using GPIB bus. A computer interfaced to the system is used for coordinating the whole operation remotely. An indigenously developed software CREMA SOFT is used to retrieve and store the measurement data. The data stored is saved in .csv format and can be easily plotted and interpreted using commercially available software's.

2.2.3.2 E8362B Performance Network Analyzer (PNA)

The Agilent E8362B PNA (Performance Network Analyzer) provides excellent performance, advanced automation features, flexible connectivity and is easy to use. Designers and engineers prefer the Agilent E8362B for fast sweep speed, wide dynamic range, low trace noise and its flexible connectivity options for testing high performance components.

Other features and specifications include:

- The operation range is from 10 MHz to 20 GHz
- 123 dB dynamic range and <0.006 dB trace noise
- 26 μ s/point measurement speed, 32 channels, 16,001 points
- TRL/LRM calibration, on-wafer, in-fixture, waveguide, and antenna measurements
- Mixer conversion loss, return loss, isolation, and absolute group delay
- Amplifier gain compression, harmonic, IMD, and pulsed-RF

Windows operating system and user interface mouse makes measurement procedure much easier. In thesis, this instrument is used to measure the dielectric constant using cavity perturbation and other reflection characteristics studies.

2.2.3.3 Anechoic Chamber

The free space environment required for antenna pattern measurements is realized by the use of an anechoic chamber. The anechoic chamber provides a 'quiet zone', free from all types of Electro-Magnetic interferences [157]. All the antenna characterizations are done in an anechoic chamber to avoid reflections from nearby objects. The absorbers used for building the chamber are made with high quality low foam impregnated with dielectrically / magnetically lossy medium. The walls are covered with carbon black impregnated polyurethane foam based pyramidal and flat absorbers of appropriate sizes. The tapered pyramidal shapes provide good impedance matching for the microwave power impinges upon it. The chamber is covered with an aluminum sheet on all the

sides to prevent external interferences. The polyurethane foam structure gives the geometrical impedance matching, while the dispersed carbon provides the required attenuation, for a wide frequency range of 1GHz to 18GHz.

2.2.3.4 Automated Turn table assembly for far field radiation pattern measurement

The turn table assembly arranged at the far field region consists of a stepper motor driven rotating platform for mounting the Antenna Under Test (AUT). The in-house developed microcontroller based antenna positioner STIC 310C is used for radiation pattern measurement. The main lobe tracking for gain measurement and radiation pattern measurement is done using this setup. A standard wideband horn (1-18GHz) is used as receiving antenna for radiation pattern measurements. The in-house developed automation software ‘*Crema Soft*’ built in the Matlab environment coordinates all the measurements.

2.2.4 Measurement Procedure

The experimental procedures followed to determine the antenna characteristics are discussed below. The network analyzer in real practice is connected to large cables and connectors. At higher frequencies the connector and cables have their losses, it should be avoided. Thus the instrument should be calibrated with known standards of open, short and matched loads to get accurate scattering parameters. There are many calibration procedures available in the network analyzer. Single port, full two port and TRL calibration methods are usually used. The two port passive or active device scattering parameters can be accurately measured using TRL calibration method. Proper phase delay is introduced while calibrating, to ensure that the reference plane for all measurements in the desired band is actually at 0^0 , thus taking care of probable

cable length variations. Using single port calibration method we can measure reflection coefficient, VSWR, input impedance etc.

2.2.4.1 Reflection coefficient, Resonant frequency and Impedance bandwidth

By choosing the single port calibration standard we can perform all these kind of measurements. The reflection characteristics of the antenna are measured by connecting the Antenna Under Test (AUT) to any one of the two ports of VNA and operating the analyzer in S_{11}/S_{22} mode. The NWA is calibrated for the required frequency band and stored in the CALSET. The AUT is connected to the calibrated port. The frequency vs reflection parameter (S_{11}/S_{22}) values are then stored in a computer in comma separated variable (.CSV) format using the 'Crema Soft'.

The frequency for which the return loss value is minimum is taken as resonant frequency of the antenna. The range of frequencies for which the return loss value is within the -10dB points is usually treated as the bandwidth of the antenna. Then the percentage of bandwidth of the antenna can be calculated using,

$$\%Bandwidth = \frac{bandwidth}{centrefrequency} * 100$$

2.2.4.2 Far field radiation pattern

The measurement of far field radiation pattern is conducted in an anechoic chamber. The AUT is placed in the quiet zone of the chamber on a turn table and connected to one port of the network analyzer. A wideband horn is used as a transmitter and connected to the other port of the network analyzer. The turn table is controlled by a STIC positioner controller. The automated radiation pattern measurement process is coordinated by the 'Crema Soft' software.

In order to measure the radiation pattern, the network analyzer is kept in S_{21}/S_{12} mode with the frequency range within the -10dB return loss bandwidth. The number of frequency points are set according to the convenience. The start angle, stop angle and step angle of the motor is also configured in the '*Crema Soft*'. The antenna positioner is boresighted manually. Now the THRU calibration is performed for the frequency band specified and saved in the CAL set. Suitable gate parameters are provided in the time domain to avoid spurious reflections if any. The *Crema Soft* will automatically perform the radiation pattern measurement and store it as a file in comma separated variable (.CSV).

2.2.4.3 Antenna Gain

The gain of the antenna under test is measured along the bore sight direction, where the radiation is found to be maximum. The gain transfer method using a standard gain antenna is employed to determine the absolute gain of the AUT [158-159]. The experimental setup is similar to the radiation pattern measurement setup. An antenna with known gain is first placed in the antenna positioner and the THRU calibration is done along the boresight direction for the frequency range of interest. Standard antenna is then replaced by the AUT and the change in S_{21} along the boresight direction is noted. Note that the AUT should be aligned so that the gain in the main beam direction is measured. This is the relative gain of the antenna with respect to the reference antenna. The absolute gain of the antenna is obtained by adding this relative gain to the original gain of the standard antenna.

2.2.4.4 Efficiency Measurement

The antenna efficiency is estimated using wheeler cap method [160] by making two impedance measurements. The antenna impedance with metallic cap and without metallic cap are measured. Since the test antenna behaves like

a series RLC circuit near its resonance, then the input resistance R should decrease after applying the cap, and the efficiency is calculated by the following expression.

$$\text{Efficiency, } \eta = \frac{R_{\text{nocap}} - R_{\text{cap}}}{R_{\text{nocap}}}$$

Where R_{nocap} and R_{cap} are the measured resistance of the antenna without the metallic cap and with the metallic cap respectively.

2.2.5 Antenna Design and Optimization using Ansoft HFSS

Preliminary investigation and optimization in antenna design are done by commercially available electromagnetic simulation software's. The simulation studies in the thesis are done using Ansoft's High Frequency Structure Simulator (HFSS).

HFSS (High frequency Structure Simulator) is a 3D electromagnetic field simulator based on Finite Element Method for modeling arbitrary volumetric structures [161]. It integrates simulation, modeling, visualization and automation in an easy to learn environment. With adaptive meshing and brilliant graphics the HFSS gives an unparalleled performance and complete insight to the actual radiation phenomenon in the antenna. With HFSS one can extract the parameters such as S, Y, Z, visualize 3D electromagnetic fields (near- and far-field), and optimize design performance. An important and useful feature of this simulation engine is the availability of different kinds of port schemes. It provides lumped port, wave port, incident wave scheme etc. The accurate simulation of coplanar waveguides and microstrip lines can be done using wave port. The parametric set up available with HFSS is highly suitable for Antenna engineer to optimize the desired dimensions. The first step in

simulating a system in HFSS is to define the geometry of the system by giving the material properties and boundaries for 3D or 2D elements available in HFSS window. The suitable port excitation scheme is then given. A radiation boundary filled with air is then defined surrounding the structure to be simulated. Now, the simulation engine can be invoked by giving the proper frequency of operations and the number of frequency points. Finally the simulation results such as scattering parameters, current distributions and far field radiation pattern can be displayed. The vector as well as scalar representation of E, H, and J values of the device under simulation gives a good insight into the antenna under analysis.

References

- [1] G.A. Deschamps, Microstrip Microwave Antennas, 3rd USAF symposium on Antennas, 1953
- [2] H. Gutton and G. Bassinot, Flat Aerial for Ultra high Frequencies, French Patent No. 703113, 1955
- [3] R.E Munson, Single Slot Cavity Antennas, US patent no-3713162, January 22, 1973
- [4] J.Q Howell, Microstrip Antennas, Dig. International symposium Antennas Propagation Society, Williamsburg, VA, Dec 192, pp. 177-180
- [5] A. G. Derneryd, “ Linear Polarized Microstrip Antennas,” IEEE Trans. On Antennas and propagat., vol. 30, pp. 846-850, 1976
- [6] Y. T. Lo, D. Solomon and W. F. Richards, “ Theory and Experiment on Microstrip Antennas,” IEEE Trans. on Antennas and Propagat., vol. 27, pp. 137-145, 1979
- [7] M. D. Deshpande and M. C. Bailey, “Input impedance of Microstrip antennas,” IEEE Trans. on Antennas and Propagat., vol. 30, pp. 645-650, 1982

- [8] J.R. James and P.S. Hall, Handbook of Microstrip Antennas, Peter Peregrines, 1989
- [9] D.H. Schaubert, D.M. Pozar, A. Adrian, Effect of Microstrip antenna Substrate thickness and permittivity, IEEE transactions on Antennas and Propagation, vol-AP-3,1989, pp. 677-682
- [10] K.R. Carver and E.L. Coffey, Theoretical investigation of the Microstrip Antenna, Physic. And Sci.Lab., Tech. Memo., PT-00929, New Mexico State University, 1976
- [11] M.D. Deshpande and M.C. Bailey, Input impedance of microstrip antennas, IEEE transactions on Antennas and Propagation, vol-AP-30, 1982, pp.645-660
- [12] W.C. Chew and J. A. Kong, Analysis of circular microstrip Disc Antenna with a Thick Dielectric substrate, IEEE Transactions on Antennas and Propagation, vol-AP-29,1981,pp. 68-76
- [13] J.T. Aberle and D.M. Pozar, Analysis of infinite arrays of One and two probe fed circular patches, IEEE transactions on Antennas and Propagation, vol-AP-38, 1990, pp. 421-432
- [14] M.C. Bailey and M.D. Deshpande, Analysis of Elliptical and circular Microstrip Antennas Using Moment Method, IEEE transactions on Antennas and Propagation, vol-AP-33, 1985, pp. 954-959
- [15] John Q Howel, Microstrip antennas, IEEE transactions on Antennas and Propagation, January 1975
- [16] M.Haneishi and Y. Suzuki, Circular polarization and Bandwidth in Handbook of Microstrip antennas, vol-1, J.R. James and P.S. Hall, Peter Peregrinus, London, 1989
- [17] Y. Suzuki, N. Miyano and T.Chiba, Circularly Polarized Radiation from singly fed Equilaterally Triangular Microstrip antenna, IEE Proceedings of Microwaves, Antennas and Propagation, Vol.134, Issue.2, pp.194-198

- [18] K.K. Tsang and R.J. Langley, Design of circular patch Antennas on Ferrite substrate, IEE Proceedings of Microwave Antennas and Propagation, Vol-145, no-1, 1998, pp.49-55
- [19] M. Haneshi and S. Yoshida, A Design Method of circularly Polarized Rectangular Microstrip Antenna by one point feed, in K.C. Gupta and A. Benalla, Artech House, 1988, pp.313-323
- [20] Jashwant S. Dahele, Kai-fong Lee and D.P. wong, Dual-frequency stacked annular-Ring microstrip Antenna, IEEE transactions on Antennas and Propagation, Vol. AP-35, No.11, 1987, pp. 1281-1285
- [21] P.L. Sullivan and D. H. Schaubert, Analysis of an Aperture Coupled Microstrip Antenna, IEEE transactions on Antennas and Propagation, Vol. AP-34, 1986, pp. 977-984
- [22] D.M. Pozar, A reciprocity method of analysis for Printed Slot and Slot Coupled Microstrip Antennas, IEEE transactions on Antennas and Propagation, Vol. AP-34, 1986, pp.1439-1445
- [23] D.M. Pozar and S.M. Voda, A Rigorous Analysis of a Microstrip Line fed Patch Antenna, IEEE transactions on Antennas and Propagation, Vol. AP-35, 1987, pp.1343-1350
- [24] S.D. Targonski and D. M. Pozar, Design of Wide Band Circularly polarized Aperture Coupled Microstrip Antennas, , IEEE transactions on Antennas and Propagation, Vol. AP-41, 1993, pp.214-220
- [25] M.Himidi, J.P. Daniel and C Terret, Analysis of Aperture coupled microstrip antenna using Cavity Method, Electronics Letters, vol-25, 1989, pp. 391-392
- [26] M.A. Saed, Efficient Method for Analysis and Design of aperture Coupled Rectangular Microstrip Antennas, IEEE transactions on Antennas and Propagation, Vol. AP-41, 1993, pp.986-988
- [27] M.Yazidi, H.Himidi and J.P. Daniel, Aperture Coupled Microstrip Antenna for Dual Frequency Operation, Electronics Letters, vol-29, 1993, pp.1506-1508

- [28] M. Himdi, J.P. Daniel and C Terret, Transmission Line Analysis of Aperture Coupled Microstrip Antenna, Electronics Letters, vol-25, 1989, pp.1229-1230
- [29] M. Yazidi, H.Himidi and J.P. Daniel, Transmission line analysis of Non Linear Slot coupled Microstrip Antenna, , Electronics Letters, vol-28, 1992, pp.1406-1408
- [30] A.Ittipiboon et al, A Modal Expansion Method of Analysis and Measurement on Aperture Coupled Microstrip Antenna, IEEE Transactions on Antennas and Propagation, Vol-AP-39, 1991,pp. 1567-1574
- [31] Y. J. Sung, M. Kim, and Y.-S. Kim, “Harmonics Reduction With Defected Ground Structure for a Microstrip Patch Antenna,” IEEE Trans. on Antennas and Propagat., vol. 2, 2003, pp. 111-113
- [32] W.-C. Liu, C.-C. Huang and C.-M. Wu, “Dual-polarised single-layer slotted patch antenna,” Electronics Lett., vol. 4, no. 12, 2004
- [33] Y. Qin, S. Gao, A. Sambell, E. Korolkiewicz and M. Elsdon, “Broadband patch antenna with ring slot coupling,” Electronics Lett., vol. 40, no. 1, 2004
- [34] Cheng P. Wen, Coplanar Waveguide: A Surface Strip Transmission Line Suitable for Nonreciprocal Gyromagnetic Device Applications, IEEE transactions on Microwave Theory and Techniques, Vol. MTT-17, No. 12, December 1969
- [35] Cheng P. Wen, Attenuation Characteristics of Coplanar Waveguides, Proceedings of the IEEE, January 1970
- [36] H. Matino, Characteristic Impedance Measurements of a Coplanar Waveguide, Electronics Letters, Vol.7, No. 23, November 1977
- [37] P.A.J. Dupuis, C.K. Campbell, Characteristic impedance of surface-strip coplanar waveguides, Electronics Letters, Vol.9, No. 16, November 1973
- [38] T. Kitazawa, Y. Hayashi and M. Suzuki, A Coplanar waveguide with Thick metal-Coating, IEEE transactions on Microwave Theory and Techniques, September 1976

- [39] E.Mueller, Measurement of the Effective relative permittivity of unshielded coplanar waveguides, *Electronics Letters*, Vol.13, No. 24, November 1977
- [40] Y.C. Shih, T. Itoh, Analysis of Conductor backed Coplanar waveguides, *Electronics Letters*, Vol.18, No. 12, June 1982
- [41] Aleksandar Nestic, Slotted Antenna array excited by a Coplanar Waveguide, *Electronics Letters*, Vol. 18, No.6, March 1982
- [42] Y. Fukuoka and T. Itoh, Analysis of slow-wave phenomena in coplanar waveguide on a semiconductor substrate, *Electronics Letters*, Vol. 18, No.14, July 1982
- [43] A. Gopinath, Losses in coplanar waveguides, *IEEE Transactions on Microwave Theory and Techniques*, Vol-MTT-30, No. 7,September 1976
- [44] Dylan F. Williams and S E Schwarz, Design and performance of Coplanar Waveguide Bandpass filter, *IEEE Transactions on Microwave Theory and Techniques*, Vol-MTT-31, No. 7,July 1983
- [45] Kohji Koshiji, Eimei Shu and Shichiro Miki, Simplified computation of coplanar waveguide with finite conductor thickness, *IEE Proceedings* , Vol 130, No. 5, August 1983
- [46] G. Ghione and C. Naldi, Parameters of coplanar waveguides with lower ground plane, *Electronics Letters*, Vol. 19, No.18, July 1983
- [47] David A. Rowe and Binng Y. Lao, Numerical analysis of Shielded Coplanar waveguides, *IEEE Transactions on Microwave Theory and Techniques* , Vol-MTT-31, No. 11,November 1983
- [48] Kohji Koshiji and Eimei Shu, Effect of inner conductor Offset in a Coplanar waveguide,*IEEE Transactions on Microwave Theory and Techniques*, Vol. MTT-32, No. 10, October 1984
- [49] Roberto Sorrento, Giorgio Leuzzi and Agnes Silbermann, Characteristics of Metal-Insulator Semiconductor coplanar Waveguides for Monolithic Microwave circuits, *IEEE Transactions on Microwave Theory and Techniques*, Vol. 32, No. 4, April 1984

- [50] Victor Fouad Hanna and Dominique thebault, Theoretical and Experimental Investigation of Asymmetric Coplanar Wave, IEEE Transactions on Microwave Theory and Techniques, Vol. MTT-32, No. 12, December 1984
- [51] D. Bhattacharya, Characteristic Impedance of coplanar waveguide, Electronics Letters, Vol. 21, No.13, June 1985
- [52] C. Seguinot, M. El Kadiri, P. Kennis, P. Pribetich and J.P. Villotte, Time domain response of MIS Coplanar Waveguides for MMICS, Electronics Letters, Vol. 21, No.25/26, December 1985
- [53] Robert W. Jackson , Considerations in the Use of Coplanar Waveguide For Millimeter-Wave Integrated Circuits, IEEE Transactions on Microwave Theory and Techniques, Vol. MTT- 32, No.12, December 1986
- [54] K. Koshiji and E. Shu, Circulators using coplanar waveguide, Electronics Letters, Vol. 21, No.25/26, December 1985
- [55] D. Mirshekar-Syahkal, Dispersion in Shielded coupled coplanar waveguides, Electronics Letters, Vol. 22, No.7, March 1986
- [56] R. Majidi-Ahy ,K. J. Weingarten, M. Riaziat, B. A. Auld and D. M. Bloom, Electro-optic sampling measurement of coplanar waveguide(Coupled slot line) modes, Electronics Letters, Vol. 23, No.24, November 1987
- [57] Giovanni Ghione and Carlo U. Naldi, Coplanar Waveguides for MMIC Applications: Effect of Upper Shielding, Conductor Backing, Finite-Extent Ground Planes, and Line-to-Line Coupling, IEEE Transactions on Microwave Theory and Techniques, Vol.MTT-35, No.3, March 1987
- [58] Robert W. Jackson and David W. Matolak, Surface to surface Transition via Electromagnetic coupling of Coplanar Waveguides, IEEE Transactions on Microwave Theory and Techniques, Vol.MTT-35, No.11, November 1987
- [59] Koichi Ohwi and Fumiaki Okada, A three-port Ferrite resonator circuit using coplanar waveguide, IEEE transactions on Magnetics, Vol.MAG-23, No.5, September 1987.

- [60] M.Riazat, I.J.Feng, R.Majidi-ahy and B.A.Auld, Single mode operation of Coplanar Waveguides, *Electronics Letters*, Vol. 23, No.24, November 1987, pp. 1281-1283
- [61] Rainee N.Simons and George E. Ponchak, Modelling of some coplanar waveguide discontinuities, *IEEE Transactions on Microwave Theory and Techniques*, Vol. 36, No.12, December 1988, pp. 1796-1803
- [62] K. Nakaoka, Coplanar waveguide array antenna, *Electronics Letters*, Vol. 24, No.7, March 1988, pp. 413-415
- [63] Guo-chun Liang, Yao-Wu Liu and Kenneth K. Mei, Full-Wave Analysis of Coplanar Waveguide and Slotline Using the Time-Domain Finite-Difference Method, *IEEE Transactions on Microwave Theory and Techniques*, Vol. 37, No.12, December 1989, pp. 1949-1957
- [64] John J Burke and Robert W. Jackson, Surface-to-Surface Transition via Electromagnetic Coupling of Microstrip and Coplanar Waveguide, *IEEE Transactions on Microwave Theory and Techniques*, Vol. 37, No.3, March 1989, pp. 519-525
- [65] Robert W. Jackson, Mode Conversion at Discontinuities in Finite- Width Conduct or- Backed Coplanar Waveguide, *IEEE Transactions on Microwave Theory and Techniques*, Vol. 37, No.10, October 1989, pp. 1582-1589
- [66] M.Riazat, R.Majidi-ahy, and I.J.Feng, Propagation Modes and Dispersion Characteristics of Coplanar Waveguides, *IEEE Transactions on Microwave Theory and Techniques*, Vol. 38, No.3, March 1990, pp. 245-251
- [67] G. Bartolucci and J. Piotrowski, Full wave analysis of shielded coplanar waveguide short-end, *Electronics Letters*, Vol. 26, No.19, September 1990, pp. 1615-1616
- [68] G.C. Dalman, New Waveguide to Coplanar waveguide transition for centimeter and millimeter wave applications, *Electronics Letters*, Vol. 26, No.13, June 1990, pp. 830-831

- [69] R.N. Simons and R.Q.Lee, Coplanar-Waveguide/Microstrip probe coupler and applications to antennas, *Electronics Letters*, Vol. 26, No.24, November 1990, pp. 1998-2000
- [70] Mohsen Naghed and Ingo wolff, Equivalent Capacitances of Coplanar Waveguide Discontinuities and Interdigitated Capacitors Using a Three-Dimensional Finite Difference Method, *IEEE Transactions on Microwave Theory and Techniques*, Vol. 38, No.12, December 1990,pp. 1808-1815
- [71] M'hamed Drissi, Victor Fouad Hanna, and Jacques Citerne, Analysis of Coplanar Waveguide Radiating End Effects Using the Integral Equation Technique, *IEEE Transactions on Microwave Theory and Techniques*, Vol. 39, No.1, January 1991,pp. 112-116
- [72] Nihad I. Dib, Linda P. B. Katehi, George E. Ponchak, and Rainee N. Simons, Theoretical and Experimental Characterization of Coplanar Waveguide Discontinuities for Filter Applications, *IEEE Transactions on Microwave Theory and Techniques*, Vol. 39, No.5, May 1991,pp. 873-882
- [73] Taek-Kyung Lee, Hao Ling, and Tatsuo Itoh, Boundary Element Characterization of Coplanar Waveguides, *IEEE Microwave and Guided wave Letters*, Vol.1, No.12, December 1991 pp. 385-387
- [74] Mikio Tsuji, Hiroshi Shigesawa, and Arthur A. Oliner, New Interesting Leakage Behavior on Coplanar Waveguides of Finite and Infinite Widths, *IEEE Transactions on Microwave Theory and Techniques*, Vol. 39, No.12, December 1991,pp. 2130-2137
- [75] R. N. Simons and R. Q. Lee, Coplanar Waveguide aperture coupled patch antennas with ground plane/substrate of finite extent, *Electronics Letters*, Vol. 28, No.1, January 1992, pp. 75-76
- [76] Richard Q. Lee, and Rainee N. Simons, Coplanar Waveguide Aperture-Coupled Microstrip Patch Antenna, *IEEE Microwave and Guided wave letters* , Vol.2, No. 4, April 1992,pp. 138-139

- [77] Jeng-Yi Ke, I-Sheng Tsai, and Chun Hsiung Chen, Dispersion and Leakage Characteristics of Coplanar Waveguides, *IEEE Transactions on Microwave Theory and Techniques*, Vol. 40, No.10, October 1992, pp. 1970-1973
- [78] R. L. Smith and J. T. Williams, Coplanar waveguide feed for microstrip patch antennas, *Electronics Letters*, Vol. 28, No.26, December 1992, pp. 2272-2274
- [79] E. T. Rahardjo, S. Kitao and M. Haneishi, Planar antenna excited by electromagnetically coupled coplanar waveguides, *Electronics Letters*, Vol. 29, No.10, May 1993, pp. 870-872
- [80] M. S. Islam, E. Tuncer and D. P. Neikirk, Calculation of conductor loss in coplanar waveguide using conformal mapping, *Electronics Letters*, Vol. 29, No.13, June 1993, pp. 1189-1191
- [81] Ming Yu, Riidiger Vahldieck, and Ke Wu, Theoretical and Experimental Characterization of Coplanar Waveguide Discontinuities, *IEEE Transactions on Microwave Theory and Techniques*, Vol. 41, No.9, September 1993, pp.1638-1640
- [82] K. Tilley, X.-D. Wu and K. Chang, Coplanar waveguide fed coplanar strip dipole antenna, *Electronics Letters*, Vol. 30, No.3, February 1994, pp. 176-177
- [83] R.R. Kumar, S. Aditya and D. Chadha, Modes of a shielded conductor-backed coplanar waveguide, *Electronics Letters*, Vol. 30, No.2, January 1994, pp. 146-148
- [84] C. ISik, Monopole strip antenna excited by coplanar waveguide, *Electronics Letters*, Vol. 31, No.20, September 1995, pp. 1709-1710
- [85] H. S. Tsai and R. A. York, Multi-Slot 50-0 Antennas for Quasi-Optical Circuits, *IEEE Microwave and Guided wave letters* , Vol.5, No. 6, June 1995, pp. 180-182
- [86] Jean-Marc Laheurte, Linda P. B. Katehi, and Gabriel M. Rebeiz, CPW-Fed Slot Antennas on Multilayer Dielectric Substrates, *IEEE Transactions on Antennas and propagation*, Vol.44, No. 8, August 1996, pp. 1102-1111

- [87] Huan-Shang Tsai, and Robert A. York, FDTD Analysis of CPW-Fed Folded-Slot and Multiple-Slot Antennas on Thin Substrates, IEEE Transactions on Antennas and Propagation, Vol.44, No. 2, February 1996, pp. 217-226
- [88] S. Matsuzawa and IC. Ito, Circularly polarised printed antenna fed by coplanar waveguide, Electronics Letters, Vol. 32, No.22, October 1996, pp. 2035-2036
- [89] L. Giauffret and J.M. Laheurte, Microstrip antennas fed by conductor backed coplanar waveguides, Electronics Letters, Vol. 32, No.13, June 1996, pp. 1149-1150
- [90] S. Hofschien and I. Wolff, Simulation of an Elevated Coplanar waveguide Using 2-D FDTD, IEEE Microwave and Guided wave letters , Vol.6, No. 1, January 1996,pp. 28-30
- [91] Y. Turki, C. Migliaccio and J.M. Laheurte, Circularly polarised square patch antenna fed by coplanar waveguide, Electronics Letters, Vol. 33, No.15, July 1997, pp. 1322-1323
- [92] I. Linardou, C. Migliaccio, J.M. Laheurte and A. Papiernik, Twin Vivaldi antenna fed by coplanar waveguide, Electronics Letters, Vol. 33, No.22, October 1997, pp. 1835-1837
- [93] Erli Chen and Stephen Y. Chou, Characteristics of Coplanar Transmission Lines on Multilayer Substrates: Modeling and Experiments, IEEE Transactions on Microwave Theory and Techniques, Vol. 45, No.6, June 1997,pp.939-945
- [94] Laurent Giauffret, Jean-Marc Laheurte, and A. Papiernik, Study of Various Shapes of the Coupling Slot in CPW-Fed Microstrip Antennas, IEEE Transactions on Antennas and Propagation, Vol.45, No. 4, April 1997, pp. 642-647
- [95] X. Ding and A.F. Jacob, CPW fed slot antenna with wide radiating apertures, IEE Proc.-Microw. Antennas Propag., Vol. 145, No. 1, February 1998,pp. 104-108

- [96] D. R. Jahagirdar, and R. D. Stewart, Nonleaky Conductor-Backed Coplanar Waveguide-Fed Rectangular Microstrip Patch Antenna, *IEEE Microwave and Guided wave letters* , Vol.8, No. 3, March 1998,pp. 115-117
- [97] AT. Kolsrud, Ming-Yi Li and Kai Chang, Dual-frequency electronically tunable CPWfed CPS dipole antenna, *Electronics Letters*, Vol. 34, No.7, April 1998, pp. 609-611
- [98] Shih-Wen Lu, Tsung-Fang Huang and Powen Hsu, CPW-fed slot-loop coupled patch antenna on narrow substrate, *Electronics Letters*, Vol. 35, No.9, April 1999, pp. 682-683
- [99] W.S.T. Rowe and R.B. Waterhouse, Broadband CPW fed stacked patch antenna, *Electronics Letters*, Vol. 35, No.9, April 1999, pp. 681-682
- [100] Santiago Sierra-Garcia and Jean-Jacques Laurin, Study of a CPW Inductively Coupled Slot Antenna, *IEEE Transactions on Antennas and propagation*, Vol.47, No. 1, January 1999, pp. 58-64
- [101] Masashi Hotta, Yongxi Qian, and Tatsuo Itoh, Efficient FDTD Analysis of Conductor-Backed CPW's with Reduced Leakage Loss, *IEEE Transactions on Microwave Theory and Techniques*, Vol. 47, No.8, August 1999,pp.1585-1587
- [102] J. Sor, Yongxi Qian and T. Itoh, Coplanar waveguide fed quasi-Yagi antenna , *Electronics Letters*, Vol. 36, No.1, January 2000, pp. 1-2
- [103] A.U. Bhohe, C.L. Holloway, M. Picket-May and R. Hall, Coplanar waveguide fed wideband slot antenna, *Electronics Letters*, Vol. 36, No.16, august 2000, pp. 1340-1342
- [104] A. Mebarki and H. Baudrand, Odd-mode filtering by asymmetrical via-hole in coplanar waveguide, *Electronics Letters*, Vol. 36, No.17, august 2000, pp. 1467-1468
- [105] Chih-Yu Huang and Kin-Lu Wong, Coplanar Waveguide-Fed Circularly Polarized Microstrip Antenna, *IEEE Transactions on Antennas and propagation*, Vol.48, No. 2, February 2000, pp. 328-329

- [106] C.H. Cheng, K. Li and T. Matsui , Stacked patch antenna fed by a coplanar waveguide, *Electronics Letters*, Vol. 38, No.25, December 2002, pp. 1630-1631
- [107] M. S. Al Salameh, Yahia M. M. Antar, and Guy Séguin, Coplanar-Waveguide-Fed Slot-Coupled Rectangular Dielectric Resonator Antenna, *IEEE Transactions on Antennas and propagation*, Vol.50, No. 10, October 2002, pp. 1415-1419
- [108] Homg-Dean Chen, Compact CPW-fed dual-frequency monopole antenna, *Electronics Letters*, Vol. 38, No.25, December 2002, pp. 1622-1624
- [109] Xian-Chang Lin and Ling-Teng Wang, A Broadband CPW-Fed Loop Slot Antenna With Harmonic Control, *IEEE Transactions on Wireless propagation letters*, Vol.2, 2003, pp. 323-325
- [110] Jia-Yi Sze, Kin-Lu Wong, and Chieh-Chin Huang, Coplanar Waveguide-Fed Square Slot Antenna for Broadband Circularly Polarized Radiation, *IEEE Transactions on Antennas and propagation*, Vol.51, No. 8, August 2003, pp. 2141-2144
- [111] Chih-Yu Huang and Ching-Wei Ling, CPW feed circularly polarised microstrip antenna using asymmetric coupling slot, *Electronics Letters*, Vol. 39, No.23, November 2003, pp. 1627-1628
- [112] Horng-Dean Chen, Broadband CPW-Fed Square Slot Antennas With a Widened Tuning Stub, *IEEE Transactions on Antennas and propagation*, Vol.51, No. 8, August 2003, pp.1982-1986
- [113] Jyh-Ying Chiou, Jia-Yi Sze, and Kin-Lu Wong, A Broad-Band CPW-Fed Strip-Loaded Square Slot Antenna, *IEEE Transactions on Antennas and propagation*, Vol.51, No. 4, April 2003, pp. 719-721
- [114] G. Tzeremes, Tsai S. Liao, Paul K. L. Yu, and C. G. Christodoulou, Computation of Equivalent Circuit Models of Optically Driven CPW-Fed Slot Antennas for Wireless Communications, *IEEE Transactions on Wireless propagation letters*, Vol.2, 2003, pp. 140-142

- [115] W.C. Liu and W.R. Chen, CPW-fed compact meandered patch antenna for dual-band operation, *Electronics Letters*, Vol. 40, No.18, September 2004, pp. 1094-1095
- [116] W.-C. Liu and C.-M. Wu, Broadband dual-frequency CPW-fed planar monopole antenna with rectangular notch, *Electronics Letters*, Vol. 40, No.11, May 2004, pp. 642-643
- [117] W.-C. Liu, Broadband dual-frequency meandered CPW-fed monopole antenna, *Electronics Letters*, Vol. 40, No.21, October 2004, pp. 1319-1321
- [118] S.-Y. Chen and P. Hsu, CPW-fed folded-slot antenna for 5.8 GHz RFID tags, *Electronics Letters*, Vol. 40, No.24, November 2004, pp. 1516-1517
- [119] R. Chair, A. A. Kishk and K. F. Lee, Ultrawide-band Coplanar Waveguide-Fed Rectangular Slot Antenna, *IEEE Transactions on Wireless propagation letters*, Vol.3, 2004, pp. 227-229
- [120] Y. Kim and D.-H. Kwon, CPW-fed planar ultra wideband antenna having a frequency band notch function, *Electronics Letters*, Vol. 40, No.7, April 2004, pp. 403-405
- [121] Alpesh U. Bhoje, Christopher L. Holloway, Melinda Picket-May and Richard Hall, Wide-Band Slot Antennas With CPW Feed Lines: Hybrid and Log-Periodic Designs, *IEEE Transactions on Antennas and propagation*, Vol.52, No. 10, October 2004, pp. 2545-2554
- [122] K. Chung, T. Yun and J. Choi, Wideband CPW-fed monopole antenna with parasitic elements and slots, *Electronics Letters*, Vol. 40, No.17, August 2004, pp. 1038-1040
- [123] M. Kitlinski and R. Kieda, Compact CPW-fed Sierpinski fractal monopole antenna, *Electronics Letters*, Vol. 40, No.22, October 2004, pp. 1387-1388
- [124] R.B. Hwang, A broadband CPW-fed T-shaped antenna for wireless communications, *IEE Proc.-Microw. Antennas Propag.*, Vol. 151, No. 6, December 2004, pp. 537-543

- [125] J. Yeo, Y. Lee and R. Mittra, Wideband slot antennas for wireless communications, IEE Proc.-Microw. Antennas Propag., Vol. 151, No. 4, August 2004, pp. 351-355
- [126] W.-C. Liu and Z.-K. Hu, Broadband CPW-fed folded-slot monopole antenna for 5.8 GHz RFID application, Electronics Letters, Vol. 41, No.17, August 2005, pp. 937-939
- [127] Y. Kim and D.-H. Kwon, CPW-fed right-angled dual tapered notch antenna for ultra-wideband communication, Electronics Letters, Vol. 41, No.12 , June 2005, pp. 674-675
- [128] Shih-Yuan Chen and Powen Hsu, Broad-Band Radial Slot Antenna Fed by Coplanar Waveguide for Dual-Frequency Operation, IEEE Transactions on Antennas and propagation, Vol.53, No. 11, November 2005, pp. 3448-3452
- [129] S.-H. Hsu and K. Chang, CPW-fed dual-annular-ring slot antennas, Electronics Letters, Vol. 43, No.21 , October 2007, pp. 1125
- [130] X.-C. Lin and C.-C. Yu, Dual-band CPW-fed hybrid antenna, Electronics Letters, Vol. 43, No.11 , May 2007, pp. 599-600
- [131] C.-M. Wu, Dual-band CPW-fed cross-slot monopole antenna for WLAN operation, IET Microw. Antennas Propag., 2007, pp. 542–546
- [132] Sung-Jung Wu and Tzyh-Ghuang Ma, A Wideband Slotted Bow-Tie Antenna With Reconfigurable CPW-to-Slotline Transition for Pattern Diversity, IEEE Transactions on Antennas and propagation, Vol.56, No. 2, February 2008, pp. 327-334
- [133] C.-J. Wang Y.-C. Lin, New CPW-fed monopole antennas with both linear and circular polarizations, IET Microw. Antennas Propag., 2008, Vol. 2, No. 5, pp. 466–472
- [134] M.-E. Chen and J.-H. Wang, CPW-fed crescent patch antenna for UWB applications, Electronics Letters, Vol. 44, No.10 , May 2008, pp. 613-614

- [135] Shih-Yuan Chen, You-Chieh Chen, and Powen Hsu, CPW-Fed Aperture-Coupled Slot Dipole Antenna for Tri-Band Operation, *IEEE Antennas and wireless propagation letters*, vol.7,2008, 535-537.
- [136] Cheng-Chieh Yu and Xian-Chang Lin, A Wideband Single Chip Inductor-Loaded CPW-Fed Inductive Slot Antenna, *IEEE Transactions on Antennas and propagation*, Vol.56, No. 5, May 2008, pp. 1498-1501
- [137] Wen-Hua Tu, Compact Harmonic-Suppressed Coplanar Waveguide-Fed Inductively Coupled Slot Antenna, *IEEE Antennas and wireless propagation letters*, vol.7,2008, 543-545.
- [138] D.D. Krishna, M. Gopikrishna, C.K. Aanandan, P. Mohanan and K. Vasudevan, Ultra-wideband slot antenna for wireless USB dongle applications, *Electronics Letters*, Vol. 44, No.18 , August 2008, pp. 1057-1058
- [139] P. C. Bybi, Gijo Augustin, B. Jitha, C. K. Aanandan, K. Vasudevan and P. Mohanan, Quasi-Omnidirectional Antenna for Modern Wireless Communication Gadgets, *IEEE Antennas and wireless propagation letters*, vol.7, 2008, 505-508.
- [140] Xian-Chang Lin and Cheng-Chieh Yu, A Dual-Band CPW-Fed Inductive Slot-Monopole Hybrid Antenna, *IEEE Transactions on Antennas and propagation*, Vol.56, No. 1, January 2008, pp. 282-285
- [141] Chien-Jen Wang and Chih-Hsing Chen, CPW-Fed Stair-Shaped Slot Antennas With Circular Polarization, *IEEE Transactions on Antennas and propagation*, Vol.57, No.8, August 2009, pp. 2483-2486
- [142] Y. Jee and Y.-M. Seo, Triple-band CPW-fed compact monopole antennas for GSM/PCS/DCS/WCDMA applications, *Electronics Letters*, Vol. 45, No.9 , April 2009, pp. 446-448
- [143] D.-O. Kim and C.-Y. Kim, CPW-fed ultra-wideband antenna with triple-band notch function, *Electronics Letters*, Vol. 46, No.18 , September 2010, pp. 1246-1248

- [144] K.G. Thomas and M. Sreenivasan, Compact CPW-fed dual-band antenna, *Electronics Letters*, Vol. 46, No.1 ,January 2010, pp. 13-14
- [145] Y.S. Li, X.D. Yang, C.Y. Liu and T. Jiang, Compact CPW-fed ultra-wideband antenna with dual band-notched characteristics, *Electronics Letters*, Vol. 46, No.14 ,July 2010, pp. 967-968
- [146] H. Kim and C.W. Jung, Ultra-wideband endfire directional tapered slot antenna using CPW to wide-slot transition, *Electronics Letters*, Vol. 46, No.17 ,August 2010, pp. 1183-1185
- [147] K.P. Ray S. Tiwari, Ultra wideband printed hexagonal monopole antennas, *IET Microw. Antennas Propag.*, 2010, Vol. 4, Iss. 4, pp. 437–445
- [148] Taehee Jang, Jaehyuk Choi, and Sungjoon Lim, Compact Coplanar Waveguide (CPW)-Fed Zeroth-Order Resonant Antennas With Extended Bandwidth and High Efficiency on Vialess Single Layer, *IEEE Transactions on Antennas and propagation*, Vol.59, No.2, February 2011, pp. 363-372.
- [149] J Youngs, G. C. Stevens and A. S. Voughan, “Trends in dielectric research: an international review from 1980-2004,” *J.Phys. D: Appl. Phys*, 2006, pp 1267-1276
- [150] M.G.Pecht, G.R. Agarwal, P.McCluskey, T.Dishongh, S. Javadpour and R.Mahajan, “Electronic Packaging Materials and their properties”, CRC Press, London, 1999.
- [151] T.Hu, J. Juuti, H. Jantunen and T. Vilkmann, “Dielectric properties of BST/Polymer composites”, *J.Eur.Ceram.Soc.*, 2007, pp 3997-4001.
- [152] D.D.L.Chung, “Materials for Electronic Packaging,” Butterworth Heinemann, Washington, 1995.
- [153] M.T. Sebastian, “Dielectric materials for wireless communications”, Elsevier publishers., UK, 2008.
- [154] Rao Y, Qu J, Marinis T, Wong C P, “A precise numerical prediction of effective dielectric constant for polymer ceramic composites based on effective medium theory” *IEEE Trans. Compon. Packag. Tech* 2000, pp. 680-683.

- [155] Prakash A, Vaid J K Mansingh A, “Measurement of dielectric parameters at microwave frequencies by cavity perturbation technique”, IEEE Trans. Microwave Theory and Techniques, vol.27 , 1979, pp. 791-795
- [156] HP8510C Network Analyzer operating and programming manual, Hewlett Packard, 1988.
- [157] Design, Development and Performance Evaluation of an Anechoic Chamber for Microwave Antennas Studies, E. J. Zachariah, K. Vasudevan, P. A. Praveen Kumar, P. Mohanan and K. G. Nair, Indian Journal of Radio and Space Physics, Vo. 13, February 1984, pp. 29-31
- [158] C. A. Balanis, Antenna Theory: Analysis and Design, Second Edition, John Wiley & Sons Inc. 1982
- [159] John D. Kraus, Antennas Mc. Graw Hill International, second edition, 1988
- [160] Cellular Handset Antenna Efficiency Measurement Using the Wheeler Cap, Skyworks Solutions, Inc
- [161] HFSS User’s manual, version 10, Ansoft Corporation, July 2005

.....❧.....

INVESTIGATION ON THE SIGNAL STRIP MODIFICATION OF A COPLANAR WAVEGUIDE (CPW) TRANSMISSION LINE

Contents	3.1 Introduction to Coplanar Waveguide (CPW) transmission line.
	3.2 Coplanar waveguide fed Monopole antenna
	3.3 Top loaded monopole antenna
	3.4 Dual band meandered monopole antenna
	3.5 Design and Development of Quad band antenna

This chapter deals with the design and development of a Co-Planar Waveguide (CPW) fed planar antenna. The chapter begins with an elaborative study on open ended Coplanar Waveguide transmission line. A thorough parametric analysis of a CPW is presented to understand the radiation mechanism and radiation performance. From the analysis and detailed study it is found that, the open ended CPW fed transmission line can be transformed into a radiating structure by suitably modifying the signal strip. This modified CPW fed antenna operates in quad bands with omnidirectional radiation pattern with reasonable gain.

3.1 Introduction to Coplanar Waveguide (CPW) transmission line

A conventional Coplanar Waveguide (CPW) on a dielectric substrate consists of a center strip conductor with semi-infinite ground planes on either side separated by a small gap. CPW structures supporting quasi TEM mode have gained great attention in microwave and millimeter wave applications due to uniplanar structure. They are commonly used in Monolithic Microwave Integrated Circuits (MMIC). The CPW transmission lines have lower radiation loss and less dispersion than microstrip lines. Moreover, the characteristic impedance and phase velocity of CPW are less dependent on the substrate height and more dependent on the dimensions in the plane of the conducting surface [1]. Due to this exceptional behavior, CPW structures have been explored a lot for compatible modern wireless communication gadgets.

When a finite length open ended CPW is excited, a standing wave pattern is formed with the reflection coefficient nearly equal to one. The structure is not radiating electromagnetic energy. This is not the case for all frequencies. The device exhibit low values of reflection coefficient and matched at higher frequencies. Thus a particular Finite Ground Coplanar Waveguide (FGCPW) will not radiate electromagnetic energy at lower frequency band.

A conventional 50Ω coplanar waveguide transmission line with ground plane width $W_g = 20\text{mm}$, ground plane length $L_g = 20\text{mm}$, signal strip width $W = 3\text{mm}$ and gap $g = 0.35\text{mm}$ is designed. The front view of such a FGCPW printed on a substrate of dielectric constant (ϵ_r) 4.4 and thickness (h) 1.6mm is shown in figure.3.1 (a). The side view and 3-dimensional view is also shown in figure.3.1 (b) and 3.1(c) respectively.

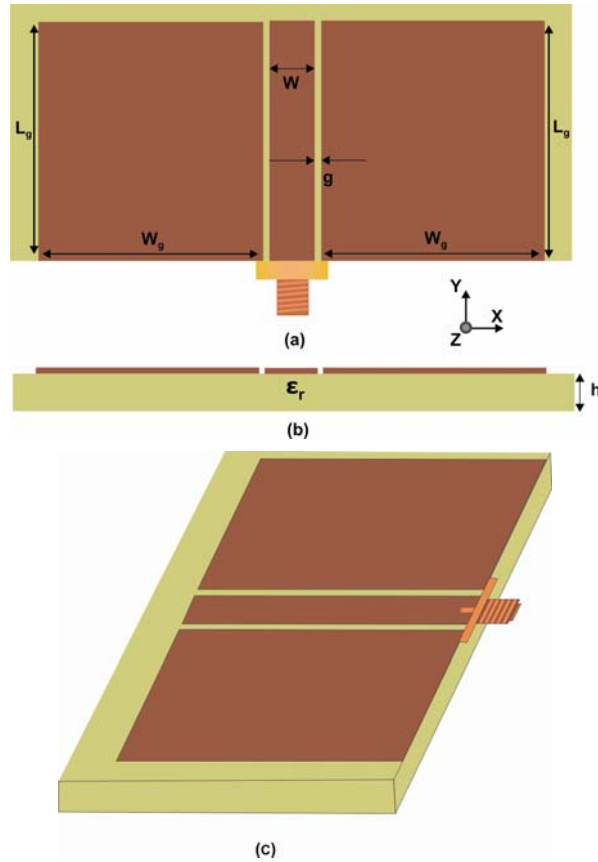
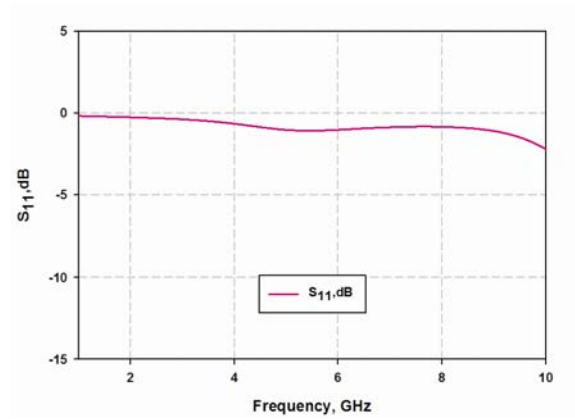
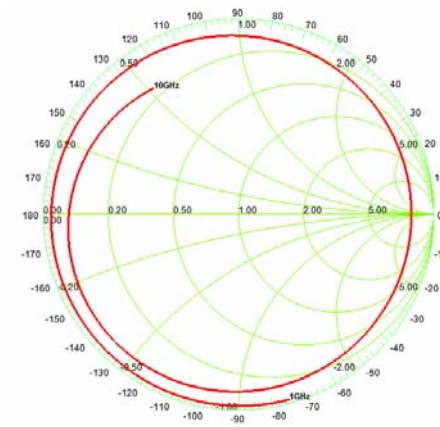


Figure 3.1 Finite Ground Coplanar Waveguide (FGCPW) (a) Front view (b) Side view(c)3D view ($W_g=20\text{mm}$, $L_g=20\text{mm}$, $W=3\text{mm}$, $g=0.35\text{mm}$, $h=1.6\text{mm}$ and $\epsilon_r=4.4$)

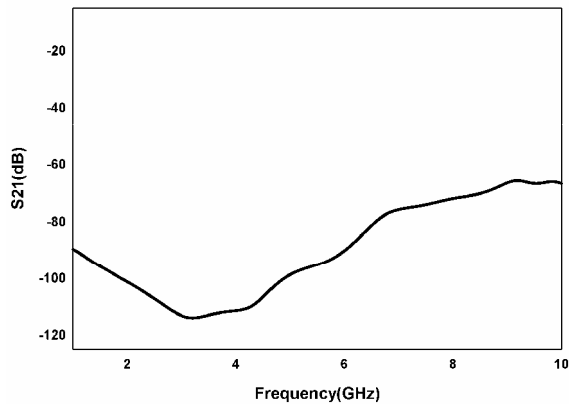
The measured reflection characteristic and impedance characteristics of this CPW structure is shown in figure.3.2 (a) and (b) respectively. From the figure it is found that the reflection coefficient is very high in the band and is behaving as an open ended transmission line with low radiation. The smith chart gives a clear picture on the impedance characteristics of this structure from 1GHz to 10GHz. From the figure it is evident that for all frequencies the locus of impedance curve is on the outer region of the smith chart. Thus this open ended structure is unmatched at these frequency regions with very low radiation. This is confirmed with the transmission characteristics shown in figure 3.2(c).



(a)



(b)



(c)

Figure 3.2 (a) Reflection characteristics of a FGCPW (b) Impedance Diagram (c) Transmission characteristics (W_g=20mm, L_g=20mm, W=3mm, g=0.35mm, h=1.6mm and $\epsilon_r=4.4$)

It is reported that a transmission line can be converted to a radiating structure by creating discontinuity [2]. This possibility is explored in this thesis. An open ended CPW transmission line can be converted into an efficient radiator by improving the matching at the desired frequency. Matching and hence radiation can be achieved by introducing discontinuity on the structure. In a normal CPW, discontinuity can be created in three different ways.

- a) Modifying the signal strip.
- b) Modify the ground plane.
- c) Modify the signal strip and ground plane simultaneously so that both will contribute to impedance match and effective radiation.

In this chapter a quad band antenna designed by modifying the signal strip is discussed elaborately. The other two modification techniques are discussed in later chapters.

3.2 Coplanar waveguide fed Monopole antenna

Design and Development of a coplanar waveguide fed monopole antenna with modified signal strip is the main theme of the present chapter. Initially the coplanar waveguide transmission line is modified to fundamental quarter wavelength monopole [2] by increasing the signal strip length L_1 as shown in figure.3.3.

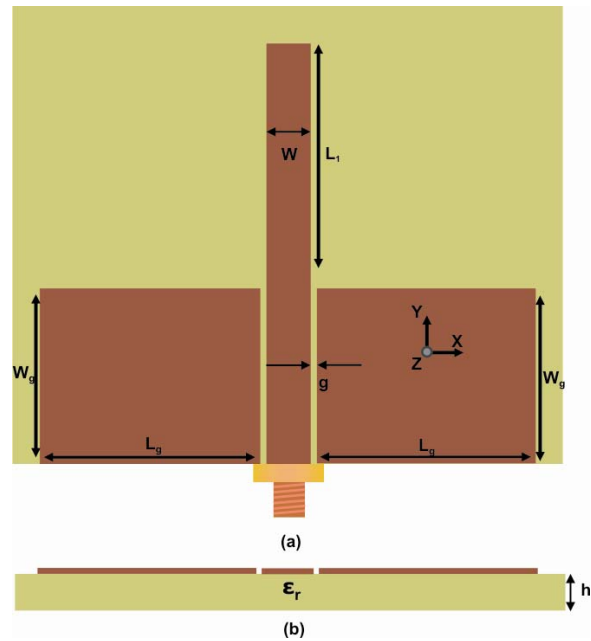


Figure 3.3 Finite Ground Coplanar Waveguide monopole antenna
(a) Front view (b) side view
**($W_g=20\text{mm}$, $L_g=20\text{mm}$, $L_1=18\text{mm}$, $W=3\text{mm}$, $g=0.35\text{mm}$, $h=1.6\text{mm}$
 and $\epsilon_r=4.4$)**

The antenna is printed on a substrate of dielectric constant $\epsilon_r=4.4$ and height $h=1.6\text{mm}$. The signal strip width (w) and signal to ground gap (g) are selected for 50Ω impedance match. The effect of signal strip length (L_1) on the resonant frequency of the monopole antenna is shown in figure.3.4. The signal strip length is arbitrarily varied from 14mm to 22mm in this study. It is evident from the reflection characteristics that as the length increases the frequency shifts to lower side. The variation in resonant frequency, bandwidth and quality factor of the antenna is shown in table 3.1. At $L_1=14\text{mm}$ the antenna is operating at 3.8625GHz with a 10dB bandwidth of 730MHz . This means the Q of the system is 5.2838 . Moreover, the quality factor of this resonating system remains almost constant with strip length.

Table 3.1 Variation in resonant frequency, band width and quality factor with monopole length L1

Monopole Length (L ₁)mm	Resonant Frequency (GHz)	10 dB bandwidth	Quality factor	Guided wavelength (λ _g)
14	3.8625	0.731	5.2838	0.26
16	3.5625	0.6813	5.2289	0.27
18	3.2875	0.6062	5.425	0.28
20	3.05	0.5563	5.482	0.29
22	2.8687	0.525	5.464	0.30

This monopole antenna of signal strip length L₁=18mm is resonating at 3.2875GHz. From the experiment it is found that this occurs when L₁ is quarter wavelength. The transmission characteristic of the antenna is shown in figure.3.5. For all cases it is found that maximum transmission occurs at the resonance. This confirms that this is working as a λ/4 monopole antenna.

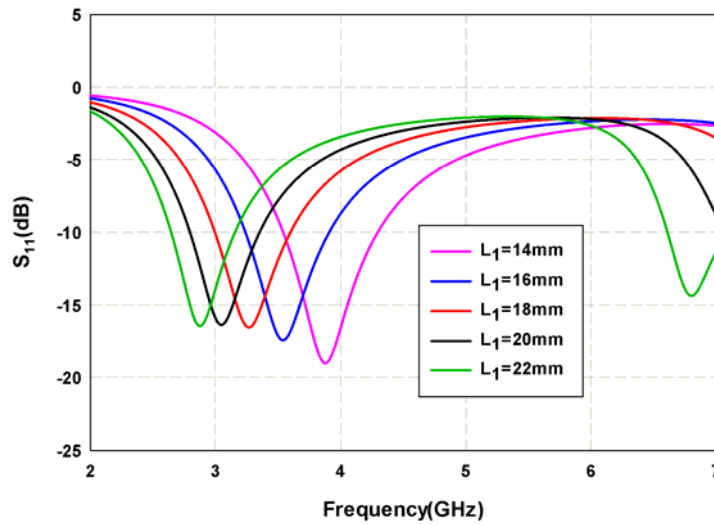


Figure 3.4 Variation of Reflection(S₁₁) Characteristics of FGCPW monopole antenna with monopole length L₁ (W_g=20mm, L_g=20mm, W=3mm, g=0.35mm, h=1.6mm and ε_r=4.4)

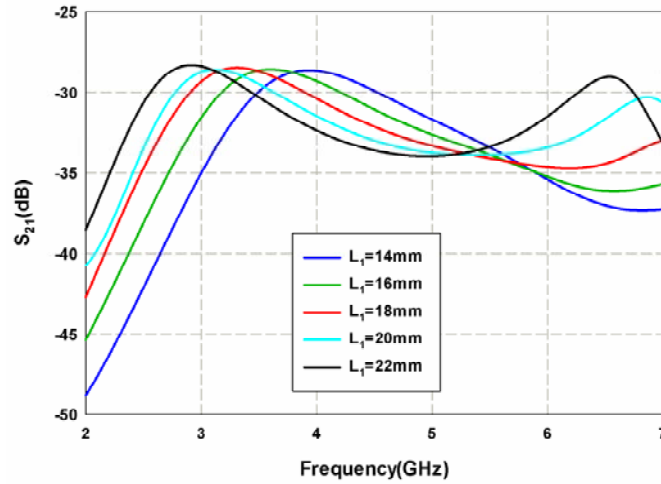


Figure 3.5 Variation of Transmission(S_{21}) Characteristics of FGCPW monopole antenna with monopole length L_1 ($W_g=20\text{mm}$, $L_g=20\text{mm}$, $W=3\text{mm}$, $g=0.35\text{mm}$, $h=1.6\text{mm}$ and $\epsilon_r=4.4$)

The variation in resonant frequency with dielectric constant and height of the substrate is shown in Table 3.2. While varying the dielectric constant the height of the substrate is taken as 1.6mm and while varying the height of the substrate dielectric constant is taken as 4.4. As the dielectric constant and height increases the resonant frequency shift to lower region and vice versa.

Table 3.2 Variation in resonant frequency with dielectric constant and height of the substrate ($W_g=20\text{mm}$, $L_g=20\text{mm}$, $L_1=18\text{mm}$, $W=3\text{mm}$, $g=0.35\text{mm}$, $h=1.6\text{mm}$ and $\epsilon_r=4.4$)

Dielectric Constant	Obtained Resonant frequency(GHz)	Height of substrate (mm)	Obtained Resonant frequency(GHz)
2	3.8625	1.2	3.3688
3	3.5812	1.4	3.3188
4	3.3625	1.6	3.2563
5	3.1563	1.8	3.225
6	3.0063	2	3.1688

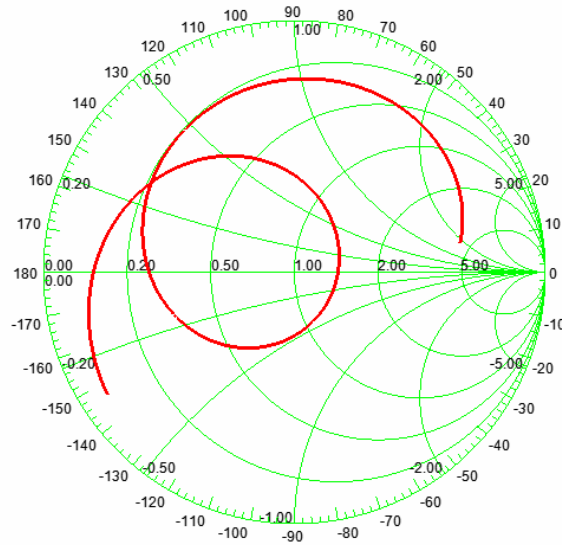


Figure 3.6 Smith chart showing the impedance characteristics of the FGCPW Antenna
($W_g=20\text{mm}$, $L_g=20\text{mm}$, $L_1=18\text{mm}$, $W=3\text{mm}$, $g=0.35\text{mm}$, $h=1.6\text{mm}$ and $\epsilon_r=4.4$)

The impedance characteristic of the coplanar waveguide fed monopole antenna is shown in figure.3.6. From the Smith chart it is evident that the real part of impedance is nearly equal to 60Ω at the resonant frequency. Moreover, the reactance is found to be nearly equal to zero and becomes inductive or capacitive as we move away from resonance. From the experimental and simulation studies it is confirmed that the resonance occurs when the monopole length is almost equal to $\lambda_g/4$, where $\lambda_g = \frac{\lambda}{\sqrt{\epsilon_{re}}}$ is the wavelength in the substrate

with ϵ_{re} as the effective dielectric constant in the substrate = $\frac{(\epsilon_r + 1)}{2}$

The simulated surface current distribution of the antenna at resonance is shown in the figure.3.7. It is obviously noticeable that there is a quarter wavelength variation of field along the signal strip length L_1 . The current is maximum near the ground plane and minimum at the tip of the monopole. It is also noted that there is

no significant current variation on the finite ground plane at the resonant frequency. Nevertheless there is a very small current variation at the edges along the width of the ground plane which varies with the ground plane dimension.

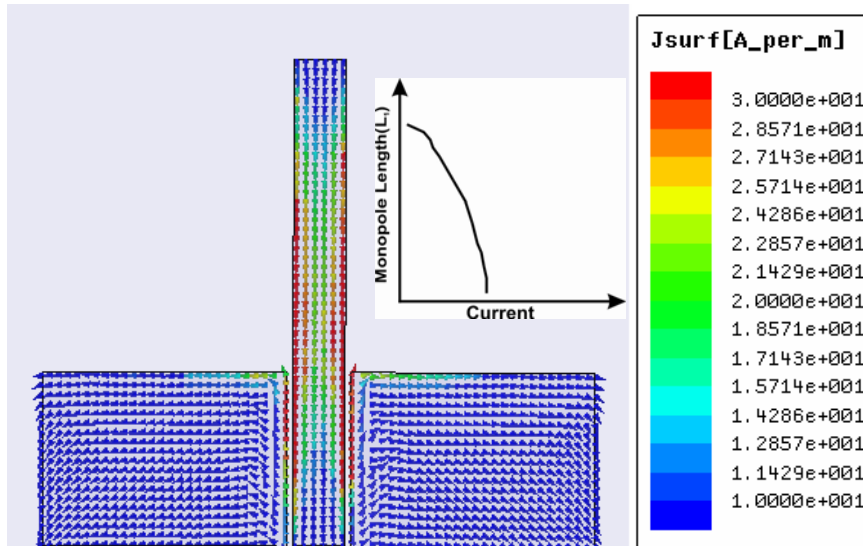


Figure 3.7 Current distribution of FGCPW monopole antenna ($W_g=20\text{mm}$, $L_g=20\text{mm}$, $L_1=18\text{mm}$, $W=3\text{mm}$, $g=0.35\text{mm}$, $h=1.6\text{mm}$ and $\epsilon_r=4.4$)

3.3 Top loaded monopole antenna

Increasing the ground plane dimension and signal strip dimension will affect the overall compactness of the antenna. As we already discussed that by increasing the monopole length will decrease the resonant frequency but the overall size increases. In order to bring the resonance to lower frequency without altering the size, the signal strip is meandered. A strip of length L_2 is added to the monopole antenna resulting a structure as shown in figure.3.8 (a). The bending will provide additional resonating length in the given area. With bending the unutilized area in the substrate is made available for the radiation phenomenon. Conventional monopole antenna is resonating at 3.26GHz. Bending the monopole to one side will shift the resonant frequency from 3.26GHz to 2.14GHz as in figure.3.9 (a).

Moreover there is a possibility for resonance at higher frequency. The impedance characteristic of the antenna is shown in figure.3.9 (b). The impedance is found to be matched at lower frequency. But at higher frequency the imaginary part is found to be inductive and hence it is not matched at that frequency as in the figure. Here the overall dimension of the antenna remains unchanged.

Again another strip of same length L_2 is added to the other side to make it a symmetrically meandered (T-shaped) antenna as shown in figure.3.8 (b). The unused space in the substrate is effectively made use in this design. The reflection characteristic of the antenna with symmetric bend is shown in figure.3.9. By symmetrically extending the strip L_2 as in the figure will not affect earlier resonance much. There is no considerable improvement in the reflection characteristics for the symmetrically meandered structure rather than a small frequency shift to lower value which provide a further compactness. But while looking to the impedance characteristics it is found that at higher frequency the imaginary part is nearly zero hence, the higher resonance is made visible and is found to be matched in this case.

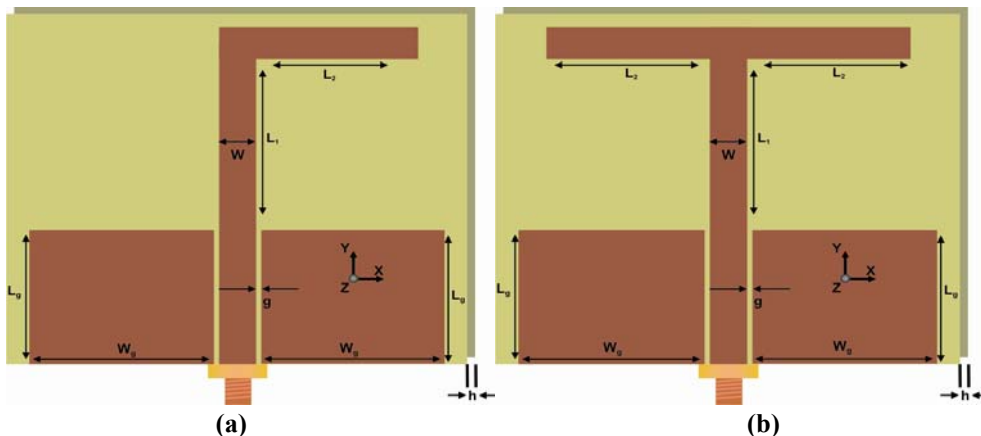
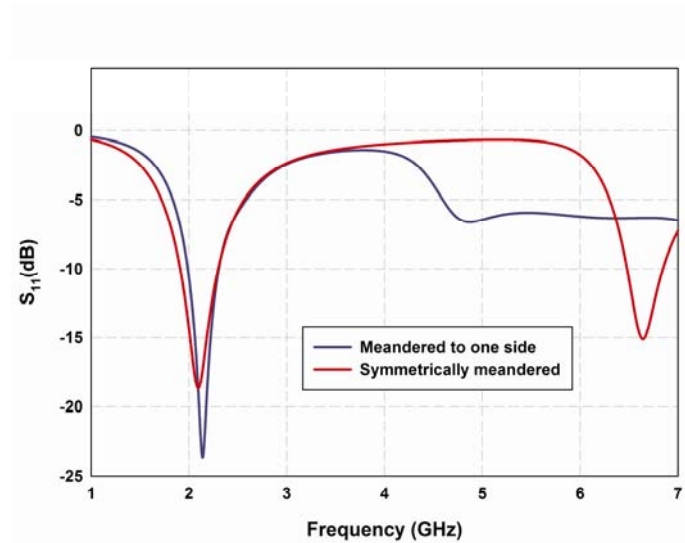
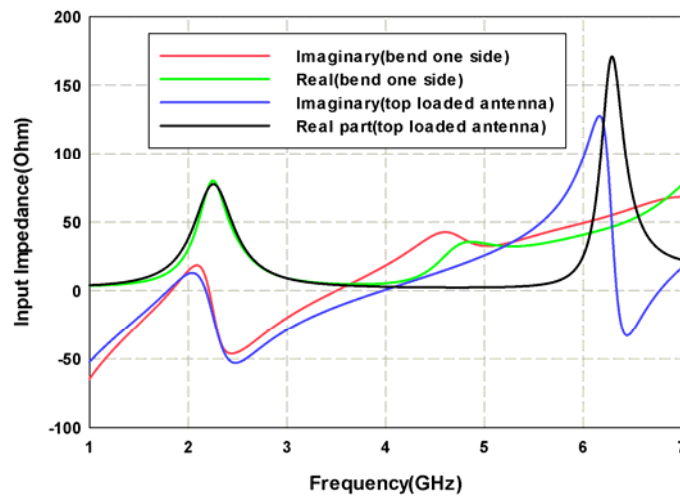


Figure 3.8 Finite Ground plane monopole antenna with (a) Meandered to one side (b) Symmetrical meandered
 ($W_g=20\text{mm}$, $L_g=20\text{mm}$, $L_1=18\text{mm}$, $L_2=10\text{mm}$, $W=3\text{mm}$, $g=0.35\text{mm}$, $h=1.6\text{mm}$ and $\epsilon_r=4.4$)



(a)



(b)

Figure 3.9 (a) Reflection Characteristics (b) Input Impedance of Finite Ground plane monopole antenna with Meandered to one side and Symmetrical meandered
 $(W_g=20\text{mm}, L_g=20\text{mm}, L_1=18\text{mm}, L_2=10\text{mm}, W=3\text{mm}, g=0.35\text{mm}, h=1.6\text{mm}$ and $\epsilon_r=4.4)$

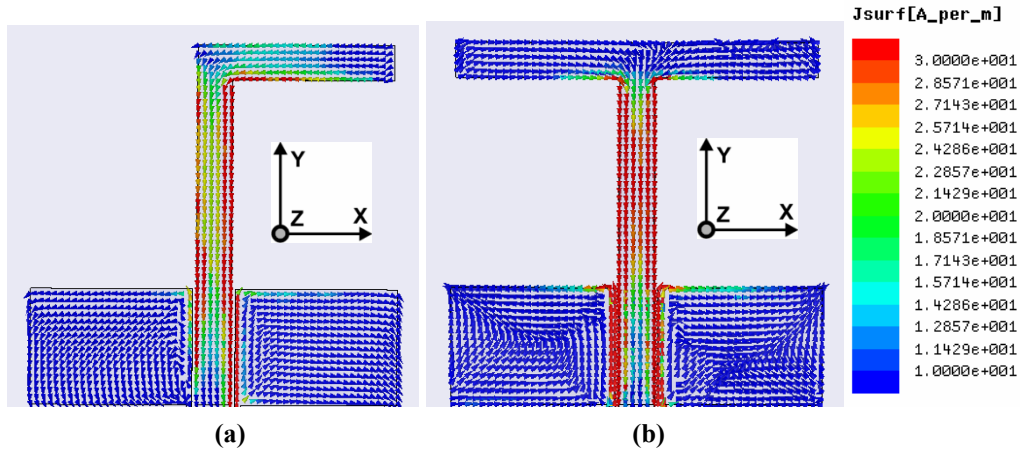


Figure.3.10 Current distribution of Finite Ground plane monopole antenna with (a) Meandered to one side (b) Symmetrical meandered ($W_g=20\text{mm}$, $L_g=20\text{mm}$, $L_1=18\text{mm}$, $L_2=10\text{mm}$, $W=3\text{mm}$, $g=0.35\text{mm}$, $h=1.6\text{mm}$ and $\epsilon_r=4.4$)

The current distribution of the antenna which is meandered to one side at 2.14GHz is shown in figure.3.10 (a). Like a monopole antenna discussed before there is a quarter wavelength variations in current along the length. Moreover, the intensity of current is found to be higher on the lower edge of the bend structure compared to the upper edge. The current distribution of the symmetrically bend structure is shown in figure.3.10 (b). Here the directions of current in the two horizontal arms are opposite. But it is found that the current distribution is much more uniform on both the signal strip and ground plane for a symmetrically bended antenna. In both cases (Meandered to one side and symmetrically bend) there is a quarter wavelength variation of current along the monopole. The total area of the antenna remains intact in both the cases.

3.4 Dual band meandered monopole antenna

Without altering the overall compactness, the frequency can be further decreased by folding the signal strip as shown in figure.3.11. The antenna consists of a T-shaped monopole with symmetrical vertical strips (L_3) on both sides. These

two symmetrical vertical strips each of length L_3 is used to increase the current path without affecting the overall compactness and other desirable radiation characteristics. The bending should be done in such a way that the effective reactive coupling should not affect the overall impedance match. This bending in a given area will increase the resonating length (since the physical length increases) and shift the frequency downwards, and hence provide compactness.

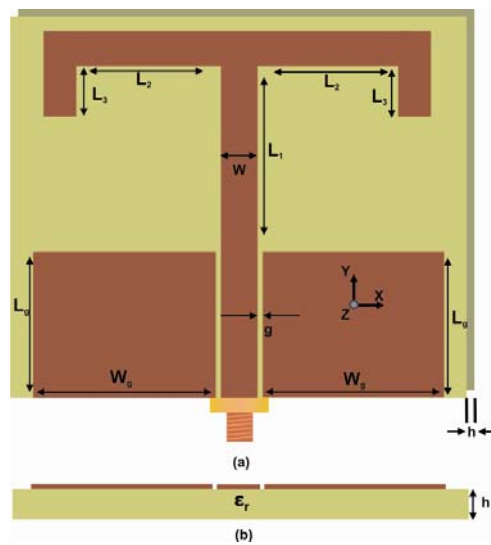


Figure.3.11 Geometry of the symmetrical meandered dual band antenna
(a) Front View (b) Side view
**($L_1=18\text{mm}$, $L_2=11.5\text{mm}$, $L_3=7\text{mm}$, $W=3\text{mm}$, $W_g=14\text{mm}$, $L_g=10\text{mm}$,
 $h=1.6\text{mm}$, $\epsilon_r=4.4$ and $g=0.35\text{mm}$)**

Thus top loading a monopole antenna make the higher resonance visible in the frequency region. Thus we can say that top loading can excite additional resonance. The addition of stubs L_2 and L_3 will give desired response for the antenna at the resonant frequency. The increased length L_3 causes a corresponding shift in the resonance towards the lower frequency. Simulated and experimental return loss of the antenna is shown in figure.3.12.

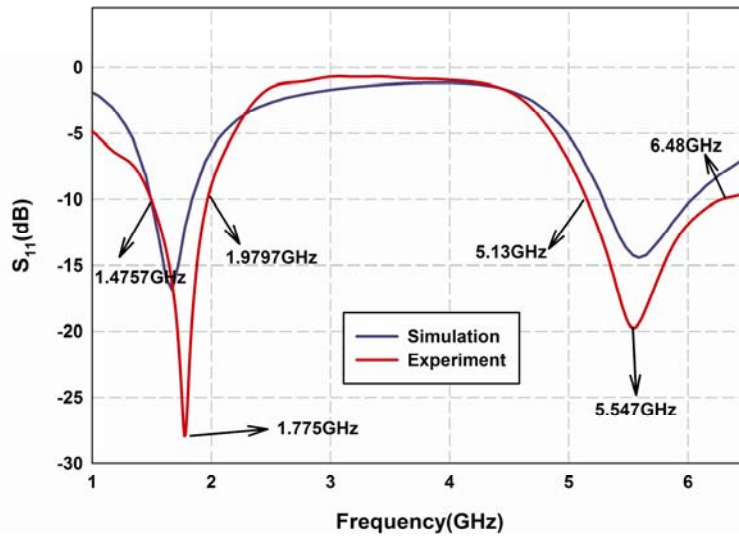
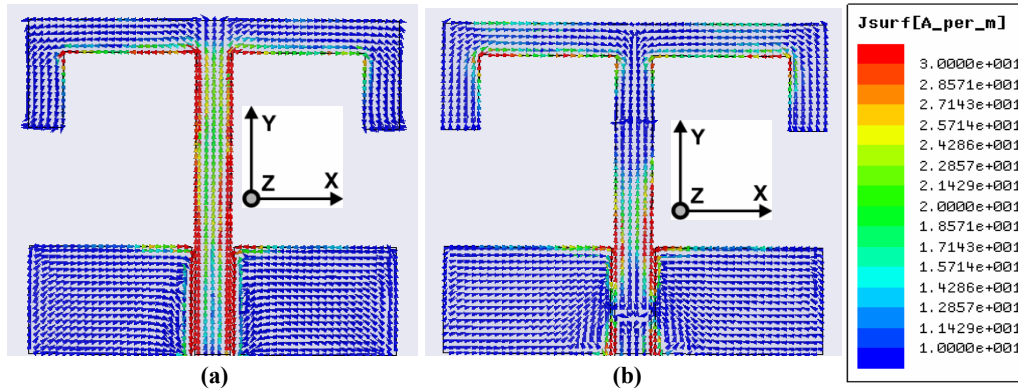


Figure.3.12 Measured and Simulated reflection characteristics of the dual band antenna
 ($L_1=18\text{mm}$, $L_2=11.5\text{mm}$, $L_3=7\text{mm}$, $W=3\text{mm}$, $W_g=14\text{mm}$, $L_g=10\text{mm}$, $h=1.6\text{mm}$, $\epsilon_r=4.4$ and $g=0.35\text{mm}$)

The lower band centered at 1.77GHz has a wide bandwidth from 1.47GHz-1.97GHz with a percentage bandwidth of about 34% covering DCS 1800 and DCS 1900/PCS. The measured impedance bandwidth of the upper band centered at 5.54GHz determined by 10-dB return loss, is good enough to cover the HIPERLAN (5150-5350MHz) band and ISM WLAN 5.8(5.725-5.875GHz) band, with wide bandwidth from 5.13GHz-6.48GHz.

The current distributions at the two resonant frequencies of the designed antenna are shown in figure.3.13. The current distributions on the horizontal arms (which provide the required resonating physical length) are equal and opposite and hence the radiated field due to this cancels at the far field. So the radiation is primarily due to the y-component and hence it is polarized along y-direction in the two bands. Moreover, the current distribution on the lateral ground planes is found to be symmetrical and as shown in the figure. It is also noted that the fundamental mode at 1.77GHz is due to the lengths $L_1+L_2+L_3$ which is nearly equal to $\lambda_g/4$.



**Figure.3.13 Current distribution of the Dual band antenna (a)1.77GHz
(b) 5.55GHz
($L_1=18\text{mm}$, $L_2=11.5\text{mm}$, $L_3=7\text{mm}$, $W=3\text{mm}$, $W_g=14\text{mm}$, $L_g=10\text{mm}$,
 $h=1.6\text{mm}$, $\epsilon_r=4.4$)**

This aspect is reconfirmed by conducting experiments with different parametric lengths. The analyses of dual band antenna with different antenna parameters are discussed in the next sections.

3.4.1 Effect of varying the strip length L_1 ($L_1+L_2+L_3$ is constant)

The distance between the top load and the ground plane is crucial in providing the impedance match. Since the length L_1 determines the distance between the top load and ground plane, it is important and should be optimized for providing better impedance matching at the resonant frequencies. The variation of the reflection characteristics of the antenna with the strip length L_1 by keeping the total length ($L_1+L_2+L_3$) constant is investigated initially. The reflection characteristic of the antenna is shown in figure.3.14. The first resonance frequency is not affected by the length L_1 since the total resonant length ($L_1+L_2+L_3$) remains constant, but the impedance matching gets affected. It is also noted that the higher resonance is very much affected by the strip length. As the length increases the higher frequency decreases and vice versa. From the impedance characteristics

shown in figure it is found that for lower frequency the impedance become more capacitive and the impedance loci is found to shrink as L_1 increased. For higher frequency the impedance loci is found to expand as L_1 is increased.

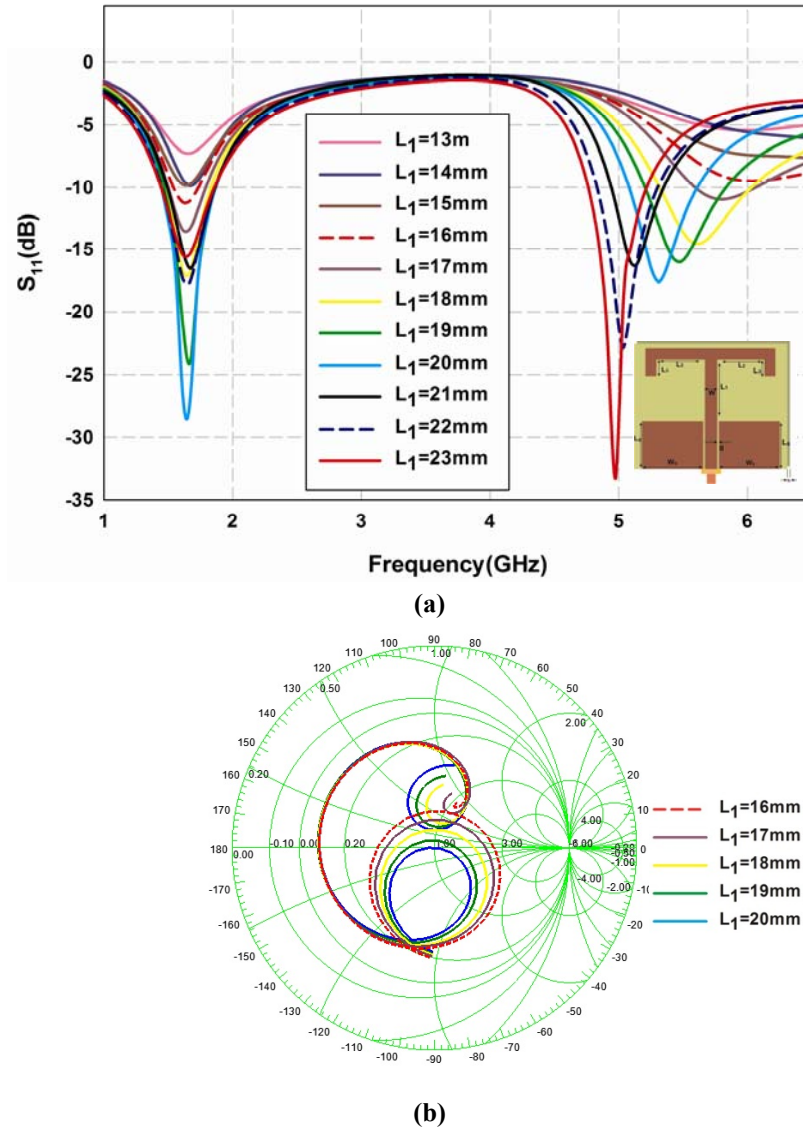


Figure 3.14 Variation of a) reflection characteristics b) impedance characteristics with strip length L_1 and by keeping the total length $L_1+L_2+L_3$ constant ($L_1=18\text{mm}$, $L_2=11.5\text{mm}$, $L_3=7\text{mm}$, $W=3\text{mm}$, $W_g=14\text{mm}$, $L_g=10\text{mm}$, $h=1.6\text{mm}$, $\epsilon_r=4.4$)

3.4.2 Effect of varying the strip length L_1 ($L_1+L_2+L_3$ is not a constant)

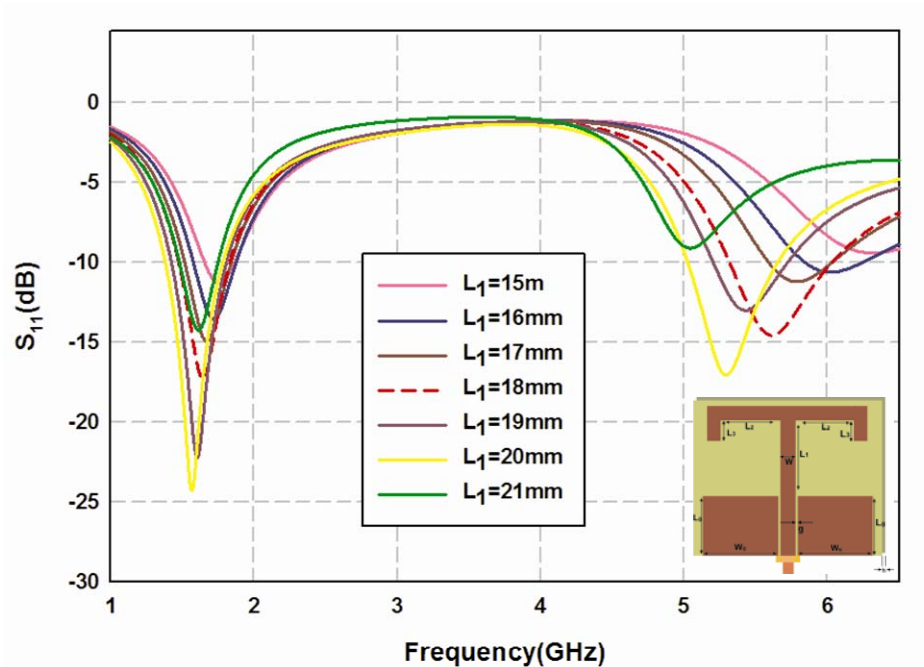


Figure 3.15 Variation of reflection characteristics with strip length L_1 and total length $L_1+L_2+L_3$ is not constant ($L_2=11.5\text{mm}, L_3=7\text{mm}, W=3\text{mm}, W_g=14\text{mm}, L_g=10\text{mm}, h=1.6\text{mm}, \epsilon_r=4.4$)

The variation of reflection coefficient with strip length L_1 without keeping the total length constant ($L_1+L_2+L_3 \neq \text{not constant}$) is also studied. Here the length L_2 and L_3 are constant throughout the variation. The corresponding reflection characteristic is shown in figure.3.15. Both the resonances are affected in this case. From the reflection characteristics it is found that as the length increases both the resonances decrease and vice versa. But the percentage shift in the higher frequency is larger as compared to the lower frequency.

The top loaded strips L_2 and L_3 is a part of radiating structure for lower frequency, but for higher frequencies these act as an open ended stubs whose length can affect the resonant frequency. Thus by varying the open ended stubs the higher frequency can be tuned.

From the above studies it is clear that the lower resonance is fully depending on the total length of the strip $L_1+L_2+L_3$ because it remains constant when total length is constant. But a thorough analysis should be performed to analyze the reason for each resonance.

3.4.3 Effect of varying the strip length L_2 ($L_1+L_2+L_3$ is a constant)

The variation in the reflection characteristics of the antenna with the strip length L_2 by keeping the total length constant is studied and its response is shown in the figure.3.16. As the length L_2 increases keeping the total length constant, both the resonant frequencies will almost tend to remain in the same position as their resonating length constant. But the separating distance between L_1 and L_3 will vary as L_2 changes. This change in stub length L_2 causes a corresponding change in reactance of the antenna and hence the resonant frequency changes as in the figure.

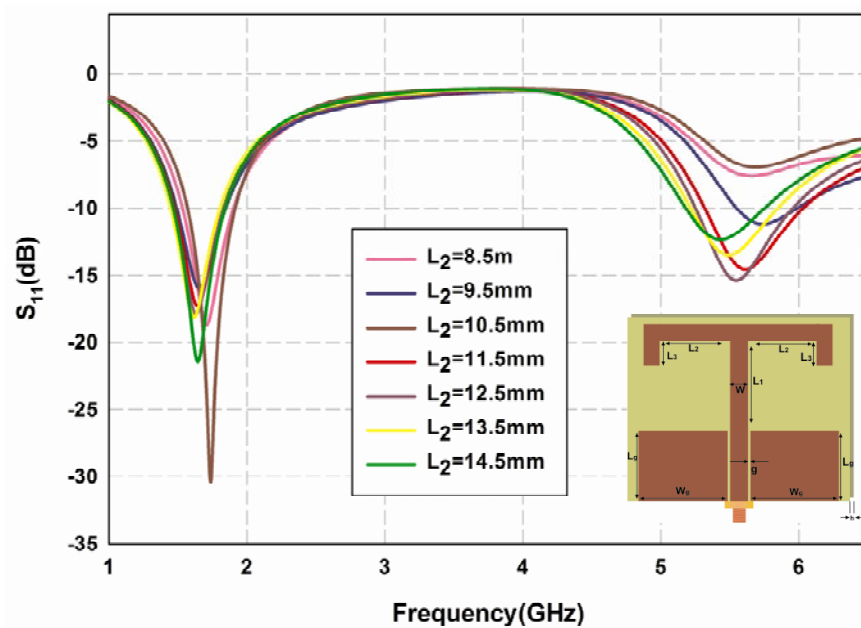


Figure.3.16 Variation of reflection characteristics with strip length L_2 and by keeping total length $L_1+L_2+L_3$ is constant ($L_1=18\text{mm}$, $L_3=7\text{mm}$, $W=3\text{mm}$, $W_g=14\text{mm}$, $L_g=10\text{mm}$, $h=1.6\text{mm}$, $\epsilon_r=4.4$)

3.4.4 Effect of varying the strip length L_2 ($L_1+L_2+L_3$ is not a constant)

The variation in the reflection characteristics of the antenna with the strip L_2 without keeping the total length constant is studied and its response is shown in the figure.3.17. As the stub length L_2 varies the distance between the vertical strips (L_1 and L_3) changes. As mentioned in the previous section the length of this open ended stub can be used to tune the resonant frequency. As L_2 increases both resonating bands shifts to lower frequency value and vice versa. A length of $L_2=11.5\text{mm}$ is chosen as optimum by considering the impedance match.

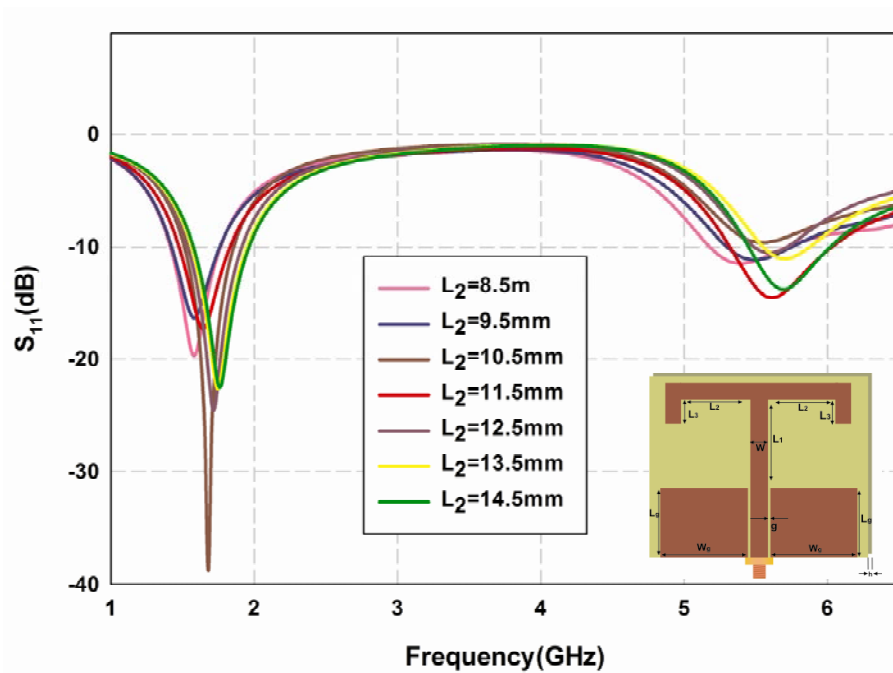


Figure.3.17 Variation of reflection characteristics with strip length L_2 and total length $L_1+L_2+L_3$ is not constant ($L_1=18\text{mm}$, $L_3=7\text{mm}$, $W=3\text{mm}$, $W_g=14\text{mm}$, $L_g=10\text{mm}$, $h=1.6\text{mm}$, $\epsilon_r=4.4$)

3.4.5 Effect of varying the strip length L_3 ($L_1+L_2+L_3$ is a constant)

The variation of reflection characteristics with strip length L_3 by keeping $L_1+L_2+L_3$ as constant is analyzed and shown in figure.3.18. Thus the lower

resonant frequency is not affected by its variation but the impedance matching is deeply affected. Thus it should be taken into consideration while optimizing the final design; that the total length is the main factor in determining the lower resonance. The higher resonance is fundamentally contributed by the total length but the interaction between strips L_1 and L_3 will also contribute towards this resonant frequency.

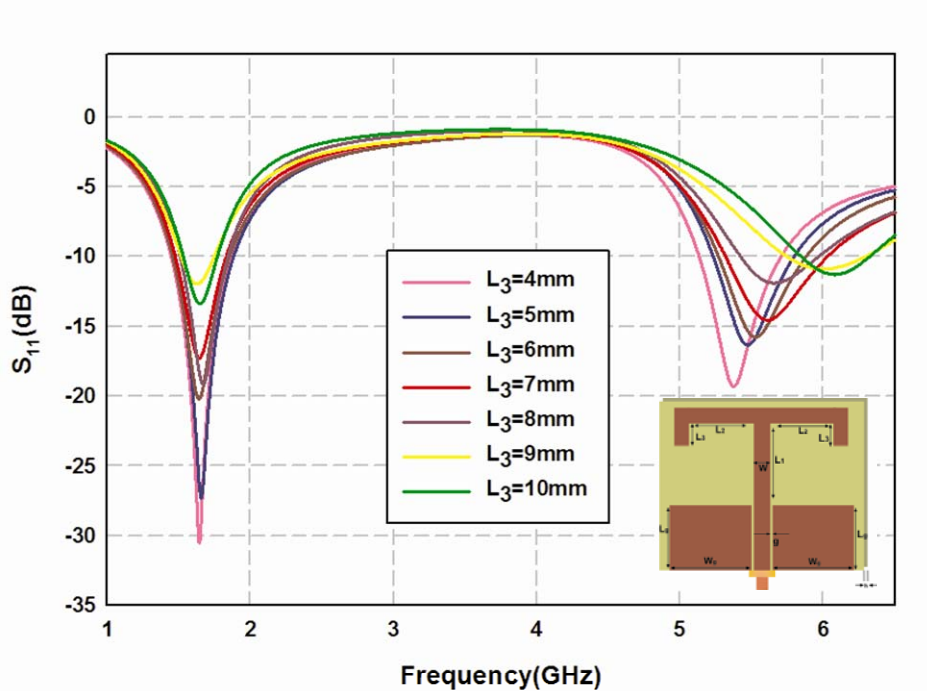


Figure 3.18 Variation of reflection characteristics with strip length L_3 by keeping total length $L_1+L_2+L_3$ as constant ($W=3\text{mm}$, $W_g=14\text{mm}$, $L_g=10\text{mm}$, $h=1.6\text{mm}$, $\epsilon_r=4.4$)

3.4.6 Effect of varying the strip length L_3 ($L_1+L_2+L_3$ is not a constant)

The effect of the vertical strip L_3 on the reflection characteristics is studied and is shown in figure.3.19. As L_3 increases the resonant length corresponding to the lower frequency increases and the frequency shift towards the lower region and vice versa. There is a small effect on the resonant

frequency of the upper band and the impedance matching deteriorates as seen in the figure. As L_3 increases its coupling with strip L_1 and ground plane varies which affects the impedance characteristics. Thus the first resonance is mainly due to the total length $L_1+L_2+L_3$ and the second resonance is primarily due to the monopole length L_1 .

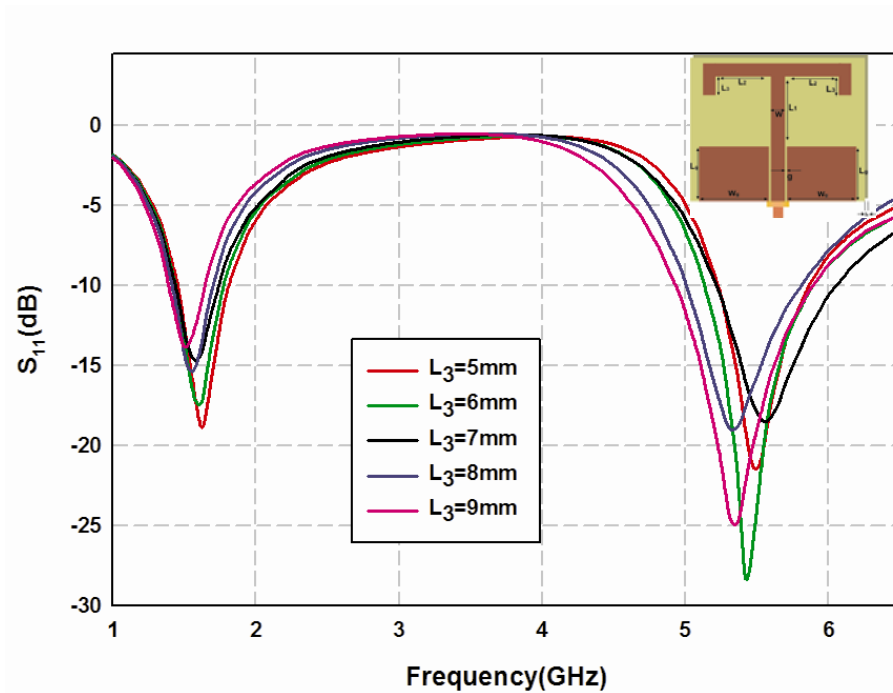


Figure 3.19 Variation of reflection characteristics with strip length L_3 and total length $L_1+L_2+L_3$ is not constant ($L_1=18\text{mm}$, $L_2=11.5\text{mm}$, $W=3\text{mm}$, $W_g=14\text{mm}$, $L_g=10\text{mm}$, $h=1.6\text{mm}$, $\epsilon_r=4.4$)

3.4.7 Variation on reflection characteristics with Ground plane length L_g

The ground plane parameters like length L_g and width W_g should be optimized properly. The effect of ground plane length on the radiation and impedance characteristics of the antenna is studied and its variation is shown in figure.3.20. It is found that there is not much variation in the resonant frequency with the ground plane length L_g . However, the impedance match and hence the

antenna performance is affected slightly as in the figure. Thus the length of ground plane is chosen as $L_g=0.1\lambda_g$ by considering the compactness and impedance match at the resonant frequency.

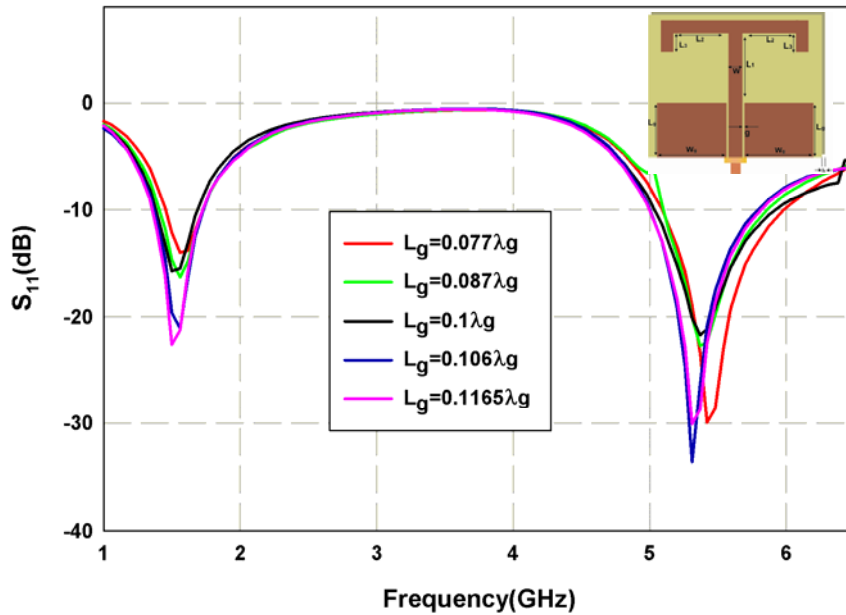


Figure 3.20 Variation of reflection characteristics with ground plane lenth L_g
 ($L_1=18\text{mm}$, $L_2=11.5\text{mm}$, $L_3=7\text{mm}$, $W=3\text{mm}$, $W_g=14\text{mm}$, $h=1.6\text{mm}$, $\epsilon_r=4.4$)

3.4.8 Variation on reflection characteristics with Ground plane width W_g

There should be a compromise between compactness and performance of any antenna. The width W_g of the ground plane is varied and its effects on reflection characteristics are also studied. Here, as the width increases the resonance shift to lower frequency and vice versa. But it should be noted that when W_g is decreased beyond $0.1\lambda_g$ the resonance frequency is severely affected as shown in figure.3.21. Moreover, it is meaningless to put a very large ground plane for a compact wireless device, if small ground plane itself is providing better performance. The radiation characteristics of a finite ground CPW should be analyzed to confirm the antenna performance.

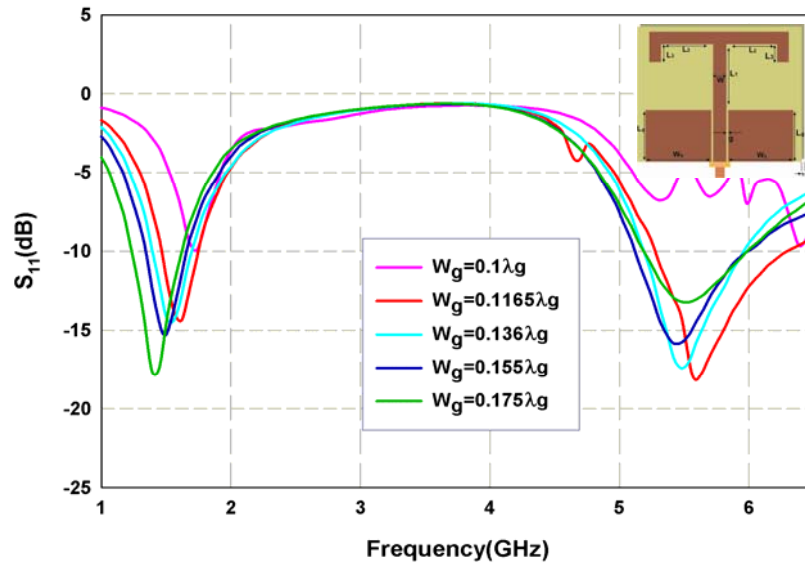


Figure 3.21 Variation of reflection characteristics with ground plane Length W_g
 $(L_1=18\text{mm}, L_2=11.5\text{mm}, L_3=7\text{mm}, W=3\text{mm}, L_g=10\text{mm}, h=1.6\text{mm}, \epsilon_r=4.4)$

3.4.9 Radiation pattern

The polarization of the antenna is along the Y-direction (Vertical) for both the resonant frequencies. From the current distribution shown in figure.3.13 it is clear that the field component along the strip L_1 is y-directed while that of L_2 is along +x and -x direction. Thus the x-directed component gets cancelled at the far field resulting the polarization along the y-direction for both the resonant frequencies.

The measured co-polar and cross-polar radiation pattern of the antenna at resonance for both E and H planes are shown in figure.3.22. The pattern is found to be omnidirectional. A constant gain pattern is obtained along the H-plane and along E-plane a pattern with two nulls at 90° and 270° degrees is obtained. The nulls are found to be above and below the lateral ground planes i.e. above the horizontal arm L_2 and on the connector side. The antenna shows good cross polarization level of nearly 15dB along the boresight direction for both the frequencies along the principal planes.

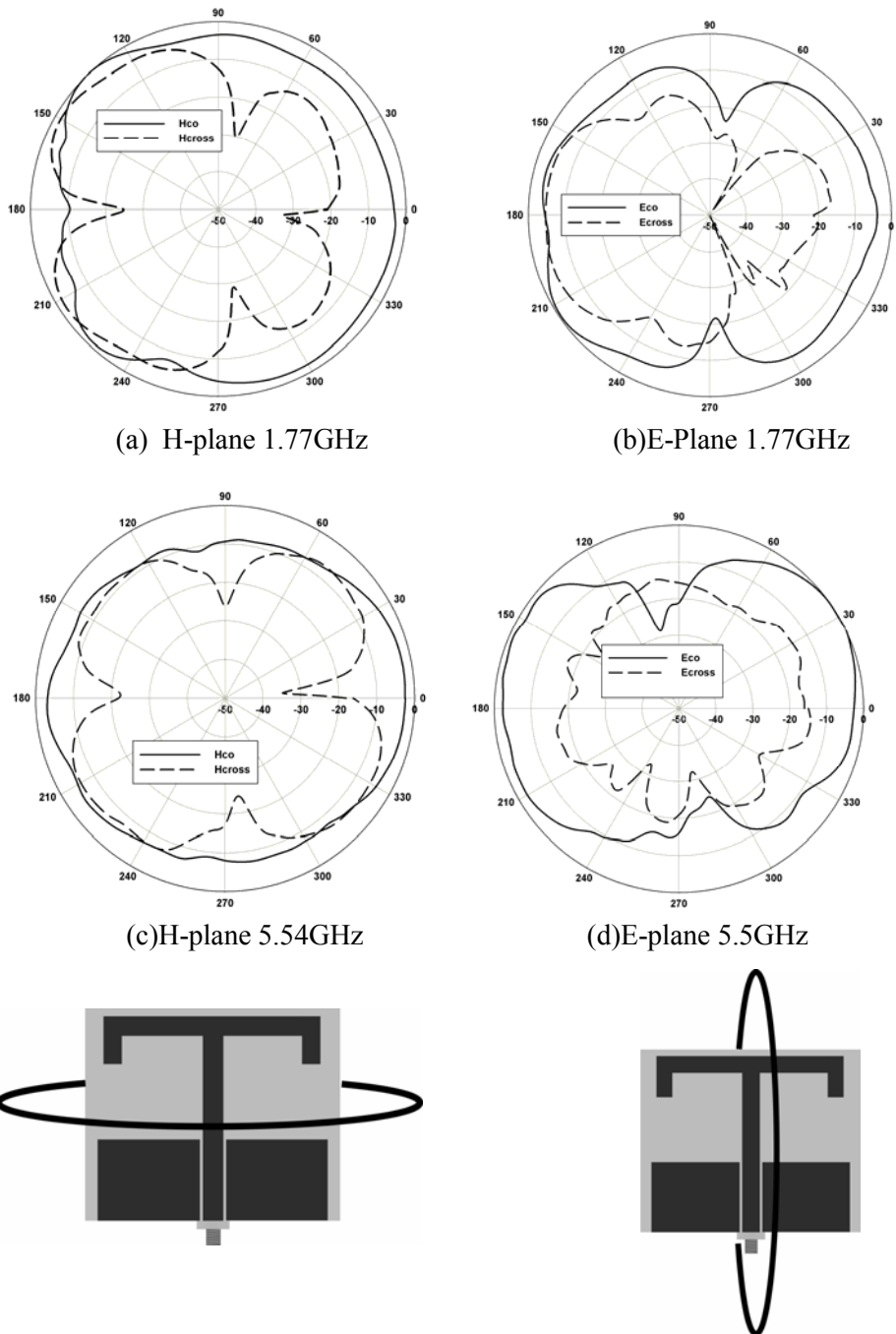
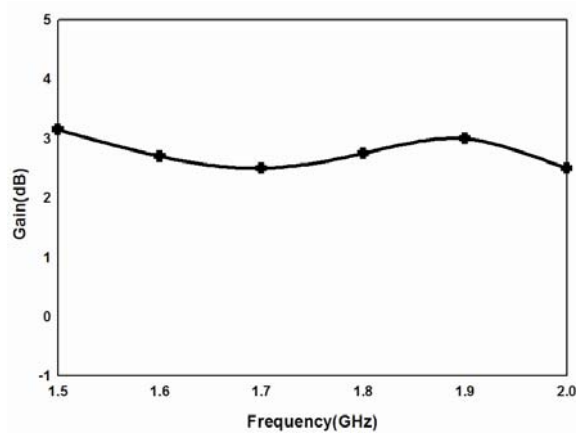


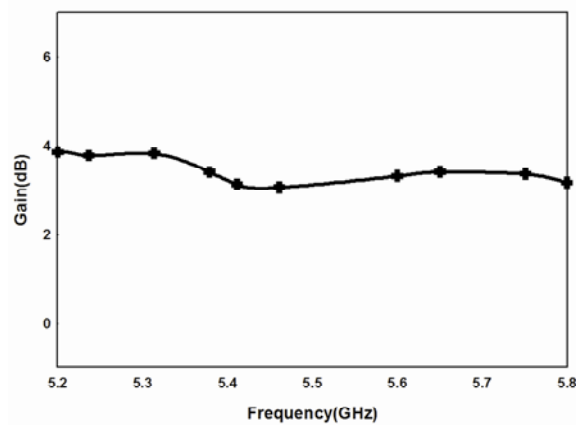
Figure 3.22 Measured Radiation pattern of the dual band antenna at
 (a)H-plane 1.77GHz (b)E-plane 1.77GHz (c) H-plane 5.5GHz
 (d) E-plane 5.5GHz
 ($L_1=18\text{mm}$, $L_2=11.5\text{mm}$, $L_3=7\text{mm}$, $W=3\text{mm}$, $W_g=14\text{mm}$, $L_g=10\text{mm}$,
 $h=1.6\text{mm}$, $\epsilon_r=4.4$)

3.4.10 Gain and Efficiency

The Measured gains of the antenna at two bands are shown in figure.3.23. The antenna shows an average gain of 3dBi in the lower band and 3.5dBi in the upper band. The measured efficiency of the antenna using wheeler cap method is also shown in figure.3.24. The antenna is showing an average efficiency greater than 80% in both the bands.



(a) 1.77GHz band



(b) 5.5GHz band

Figure 3.23 Measured gain of the dual band antenna at (a) 1.77GHz (b) 5.55GHz
 $(L_1=18\text{mm}, L_2=11.5\text{mm}, L_3=7\text{mm}, W=3\text{mm}, W_g=14\text{mm}, L_g=10\text{mm},$
 $h=1.6\text{mm}, \epsilon_r=4.4)$

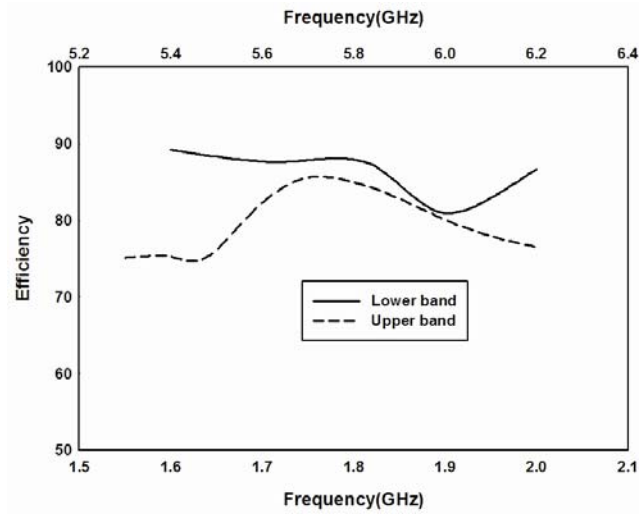


Figure.3.24 Measured efficiency of the dual band antenna
($L_1=18\text{mm}$, $L_2=11.5\text{mm}$, $L_3=7\text{mm}$, $W=3\text{mm}$, $W_g=14\text{mm}$, $L_g=10\text{mm}$,
 $h=1.6\text{mm}$, $\epsilon_r=4.4$)

3.5 Design and Development of Quad band antenna

The signal strip of the Dual band antenna presented in the above section can be modified to resonate in additional application bands. Antenna resonating in four different frequency bands are discussed in this.

From the studies explained in the section above section, it is clear that in order to excite an additional resonance it is necessary to create an additional resonating path or to excite the higher harmonics. It is better to create additional resonating path for the new resonance because it is difficult to independently control the higher harmonic radiation with the fundamental one. Thus the top loaded signal strip (L_3) is modified by increasing the length (L_3+L_4) on one side of the top load and thereby creating asymmetry in the structures as shown in figure.3.25. This asymmetry can generate a resonance in addition to the existing two resonances. Now the resonances are centered at 1.61GHz, 2.4GHz and

5.8GHz respectively. The comparison of resonant frequencies of the monopole antenna, symmetrically meandered antenna and asymmetrically loaded antenna are shown in figure.3.26.

Thus the simple monopole antenna is resonating at 3.286GHz. There is only one resonance in the entire band. This curve is marked as 'a'. When the antenna is symmetrically top loaded, it resonates at two frequencies (b). It resonates at 1.77GHz and 5.54GHz respectively. However when it is asymmetrically loaded it resonates a three frequencies (c). The three modes are at 1.61GHz, 2.4GHz and 5.8GHz respectively.

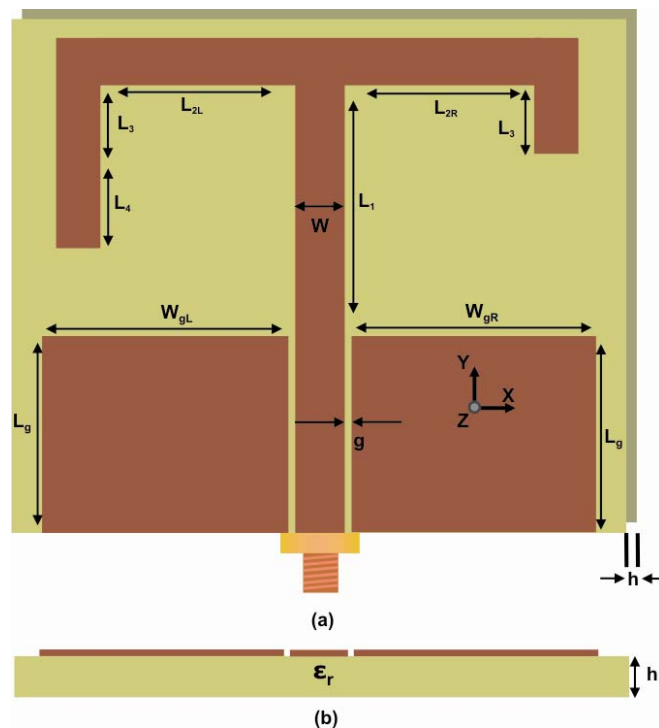


Figure 3.25 Geometry of the unsymmetrical triple band antenna (a) Front view (b) side view

$(L_1=18\text{mm}, L_{2R}=L_{2L}=11.5\text{mm}, L_3=4\text{mm}, L_4=8\text{mm}, W=3\text{mm}, L_g=10\text{mm}, W_{gR}=W_{gL}=14\text{mm}, g=0.35\text{mm}, h=1.6\text{mm}, \epsilon_r=4.4)$

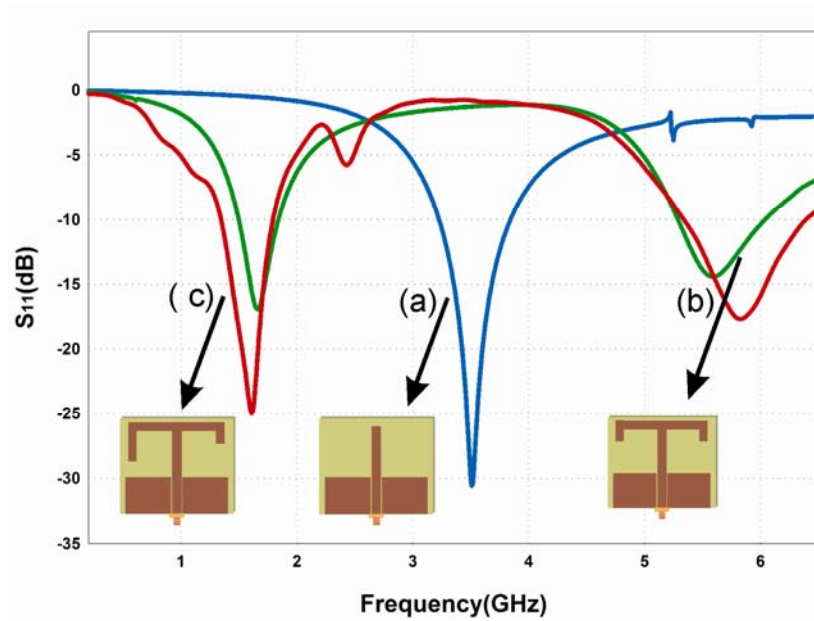


Figure 3.26 Reflection characteristics comparison of single band, dual band and triple antenna
 $(L_1=18\text{mm}, L_{2R}=L_{2L}=11.5\text{mm}, L_3=4\text{mm}, L_4=8\text{mm}, W=3\text{mm}, L_g=10\text{mm}, W_{gR}=W_{gL}=14\text{mm}, g=0.35\text{mm}, h=1.6\text{mm}, \epsilon_r=4.4)$

By the addition of the strip L_4 the resonance at 1.77GHz of the dual band antenna explained in the earlier section due to the length $(L_1+L_{2L}+L_3)$ is now shifted down to 1.61GHz, corresponding to a resonant length $(L_1+L_{2L}+L_3+L_4)$. It is noted that this total length is nearly equal to the quarter wavelength corresponding to 1.61GHz.

By the addition of this strip another resonance is excited at 2.4GHz. The frequency corresponding to the resonance is in the application region (ISM 2.4) but is poorly matched. This resonance is nearly equal to half wavelength corresponding to the resonant length $(L_1+L_{2R}+L_3)$.

The higher resonance at 5.54GHz is also shifted to 5.8GHz as shown in the figure which is corresponding to a length $(L_1+L_{2R}+L_3)$ of $0.9\lambda_g$. Thus further design

should carry out by taking at most care to keep the existing matched resonances as such and to provide impedance matching for the resonance at 2.4GHz.

In order to provide better insight to the antenna performance the current distribution on the antenna should be analyzed. The current distribution of the triple band antenna is shown in figure.3.27.

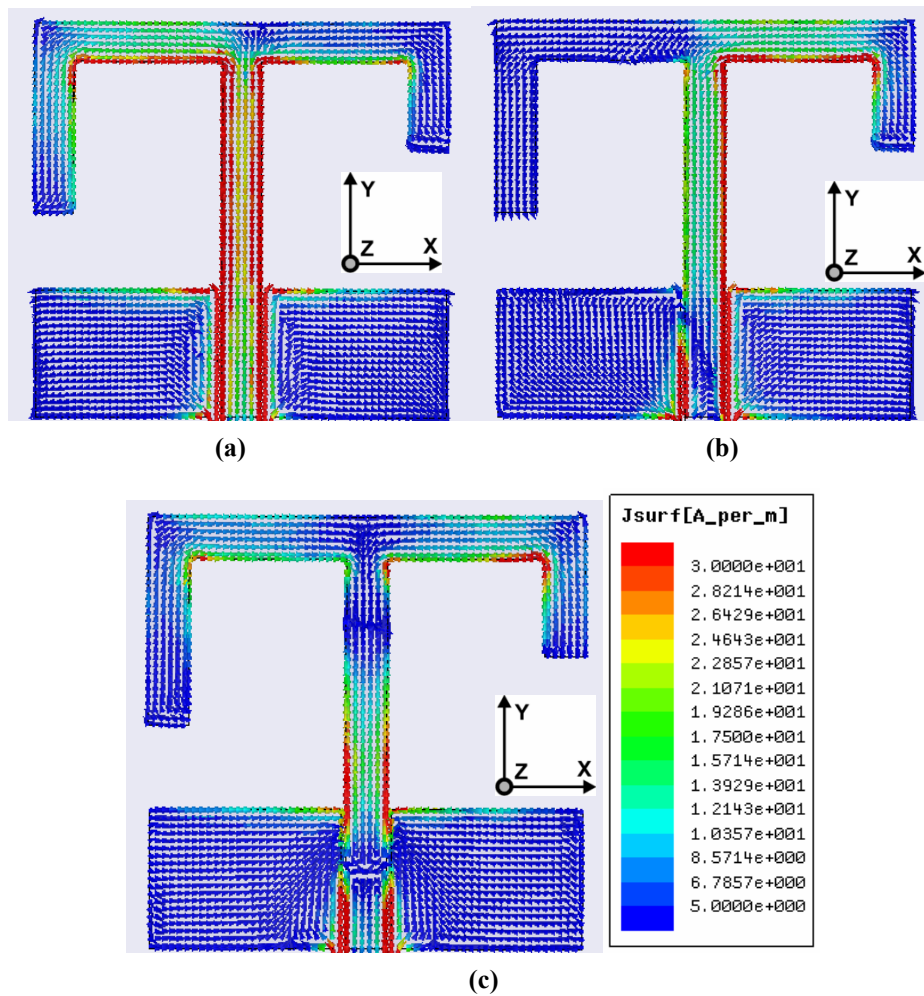


Figure.3.27 Current distribution of the Dual band antenna (a) 1.61GHz (b) 2.4GHz (c) 5.8GHz
 $(L_1=18\text{mm}, L_{2R}=L_{2L}=11.5\text{mm}, L_3=4\text{mm}, L_4=8\text{mm}, W=3\text{mm}, L_g=10\text{mm}, W_{gR}=W_{gL}=14\text{mm}, g=0.35\text{mm}, h=1.6\text{mm}, \epsilon_r=4.4)$

A quarter wavelength variations are found along the resonating length for the first two resonances as in the figure. The first resonant path is due to the longer asymmetrical path and the second is due to smaller path. A three quarter variation of current is observed along the shorter asymmetrical path and larger asymmetrical path. Since these two resonances are close to each other they merge together to give a wide bandwidth corresponding to the third resonance as in figure.3.27 (C).

In addition to the three resonances of the antenna the next aim is to generate an additional resonance at 900MHz together with better match for the present bands; preserving the compactness. It is really challenging to excite a lower frequency without trading the compactness of the antenna.

Keeping the overall area intact a slit 'ABCDEFGH' is introduced in the antenna as shown in figure.3.28. It should be noted that the present modification is made without altering the already existing three resonant paths. That is the existing resonant paths are there and a new discontinuity is created. This forces the current to flow through a longer path around the slit (Through ABCDEFGH) and produce an additional lower resonance at 900MHz as shown in figure.3.29. The subsequent resonances are at 1.74GHz, 2.44GHz and 5.5GHz. It is interesting to note that in addition to the excitation at 900MHz the structure provides a well matched resonances at the existing resonant frequencies centered at 1.74GHz, 2.44GHz and 5.5GHz.

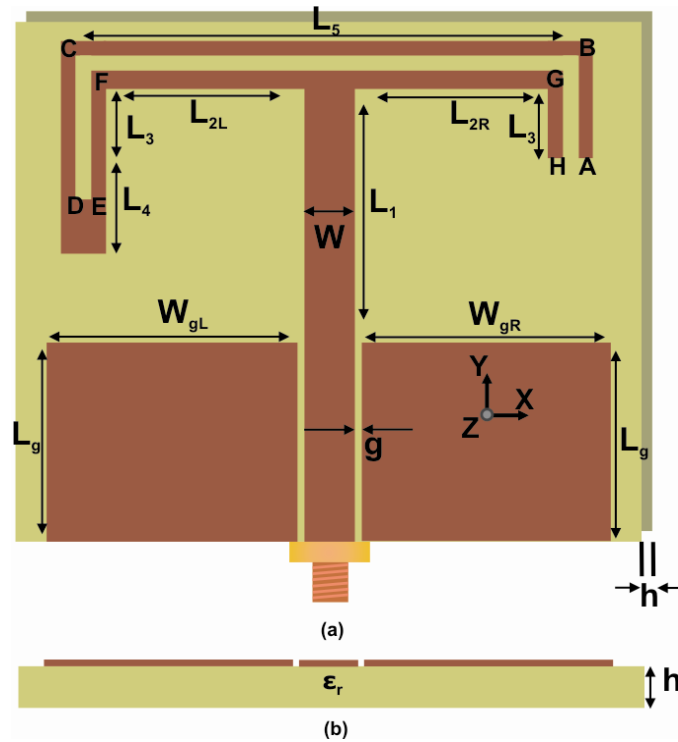


Figure 3.28 Geometry of the Quad band antenna (a) front view (b) side view ($L_1=18\text{mm}$, $L_{2R}=L_{2L}=11\text{mm}$, $L_3=4\text{mm}$, $L_4=8\text{mm}$, $L_5=31\text{mm}$, $L_g=10\text{mm}$, $W_{gR}=W_{gL}=14\text{mm}$, $W_s=3\text{mm}$, $CD=10\text{mm}$, $BC=29\text{mm}$, $DE=ha=1\text{mm}$, $h=1.6\text{mm}$, $\epsilon_r=4.4$ and $g=0.35\text{mm}$)

The GSM900 band (850MHz-960MHz) exhibits 2:1 VSWR impedance bandwidth and is wide enough to cover the GSM application band. The resonance at 1.61GHz of the triple band antenna is now shifted to 1.74GHz with a 2:1 VSWR band width from 1.56GHz-1.92GHz covering the DCS-1800 application band. The resonance at 2.4GHz of the triple band antenna is matched by adding the slit. The antenna offers a 2:1 VSWR band width from 2.39GHz to 2.49GHz which is wide enough to cover the ISM-2.4 band. Moreover, this antenna covers the 5.2/5.8GHz WLAN band with 2:1 VSWR bandwidth from 5.07GHz-6.23GHz. The measured and simulated reflection characteristics and of the antenna are shown in figure.3.29.

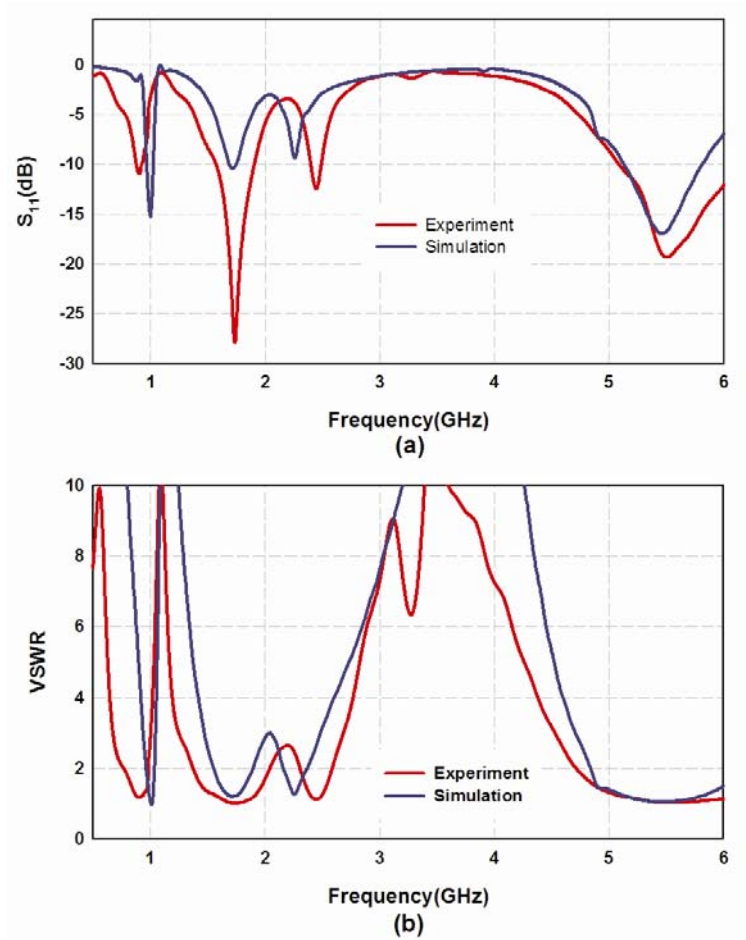


Figure 3.29 Experimental and Simulation results of the quad band antenna (a) Reflection characteristics and (b) VSWR ($L_1=18\text{mm}$, $L_{2R}=L_{2L}=11\text{mm}$, $L_3=4\text{mm}$, $L_4=8\text{mm}$, $L_5=31\text{mm}$, $L_g=10\text{mm}$, $W_{gR}=W_{gL}=14\text{mm}$, $W_s=3\text{mm}$, $CD=10\text{mm}$, $BC=29\text{mm}$, $DE=ha=1\text{mm}$, $h=1.6\text{mm}$, $\epsilon_r=4.4$ and $g=0.35\text{mm}$)

3.5.1 Measured Variation on reflection characteristics with strip length ($L_3 + L_4$)

An exhaustive parametric study has been performed to investigate the effect of various parameters on antenna performance. The variation in reflection characteristics with strip length $L_3 + L_4$ (on the Left arm – with L_3 as constant) is shown in figure.3.30. It is found that by increasing the strip length the second

resonance frequency is mainly affected and shifts towards the lower frequency region and vice versa. Similarly as the length increases the inductive reactance corresponding to the third resonance increases, affecting the overall impedance match. By considering the radiation and impedance characteristics corresponding to the DCS-1800 application band the strip length is optimized at 12mm. From the studies it is confirmed that the second resonance frequency can be easily tuned by adjusting L_3+L_4 .

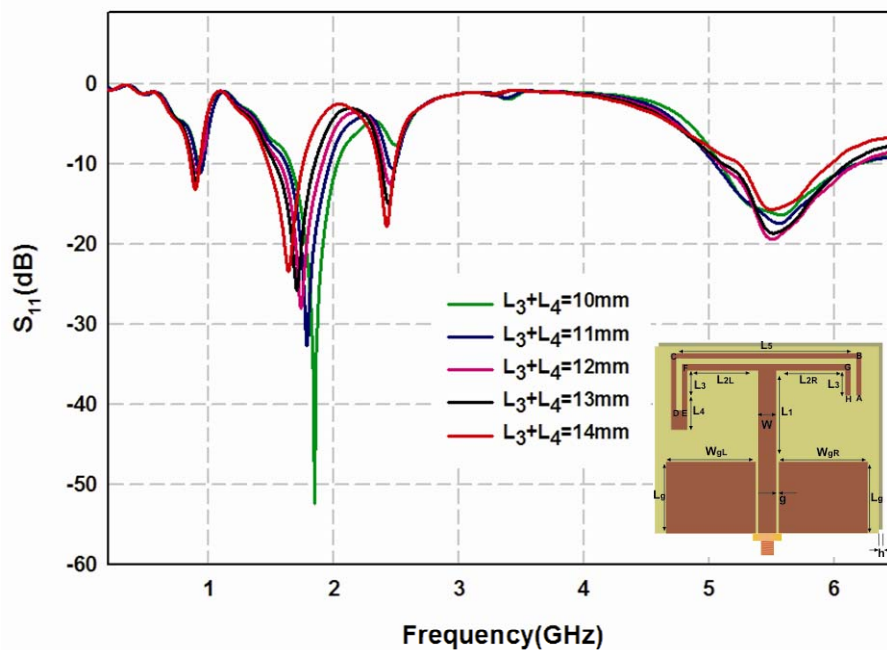


Figure 3.30 Variation in reflection characteristics of the antenna with variation in L_3+L_4
 ($L_1=18\text{mm}$, $L_{2R}=L_{2L}=11\text{mm}$, $L_5=31\text{mm}$, $L_g=10\text{mm}$, $W_{gR}=W_{gL}=14\text{mm}$, $W_s=3\text{mm}$, $CD=10\text{mm}$, $BC=29\text{mm}$, $DE=HA=1\text{mm}$, $h=1.6\text{mm}$, $\epsilon_r=4.4$ and $g=0.35\text{mm}$)

3.5.2 Measured Variation on reflection characteristics with slot length CD

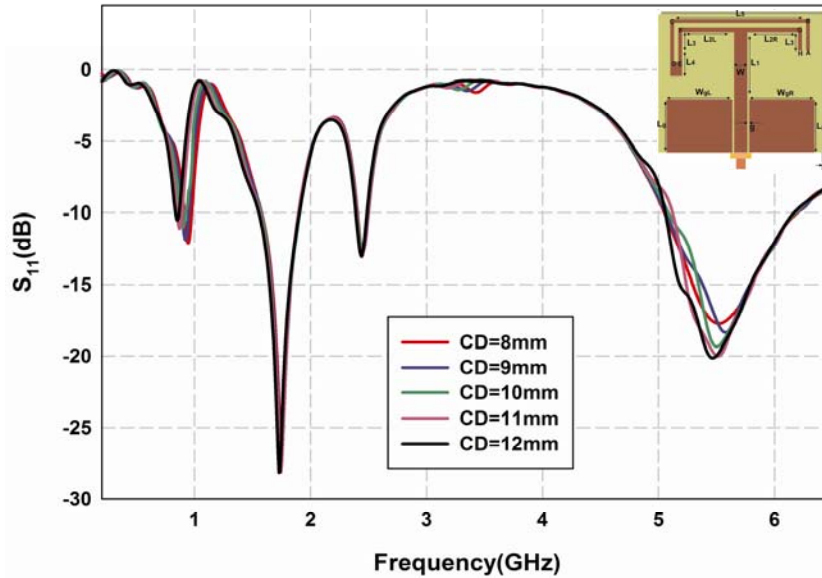


Figure 3.31 Variation in reflection characteristics of the antenna with slit length CD
 ($L_1=18\text{mm}$, $L_{2R}=L_{2L}=11\text{mm}$, $L_3=4\text{mm}$, $L_4=8\text{mm}$, $L_5=31\text{mm}$,
 $L_g=10\text{mm}$, $W_{gR}=W_{gL}=14\text{mm}$, $W_s=3\text{mm}$, $BC=29\text{mm}$, $DE=HA=1\text{mm}$,
 $h=1.6\text{mm}$, $\epsilon_r=4.4$ and $g=0.35\text{mm}$)

The measured variation in the return loss characteristics of the antenna with respect to the slit perimeter ‘ABCDEFGH’ (by varying length CD) is shown in figure.3.31. In this the length of slot perimeter varies and all other parameters remain unaffected. As slit perimeter increases, the lower resonance at 900MHz shifts down, worsening the impedance match. All other resonances remain unaltered as their resonating lengths are unaffected. Thus by adjusting the slit length we can tune the lower resonant mode. The width of the slot is selected as 1mm throughout the study. If the slit is opened or closed at both ends the resonating length will get halved and there will not be any resonance at lower frequency. So it is very important to keep the ends of the slits complimentary to each other, that is while one end is opened the other end should be closed (so that the total perimeter of the slot is constant)

3.5.3 Measured Variation on reflection characteristics with right arm strip L_3

Variation on reflection characteristics with strip length L_3 (on the right arm) is studied and is shown in figure.3.32. From the figure it is clear that the strip length affects the third and fourth resonances significantly. As the length increases the third and fourth resonance centered at 2.44GHz and 5.5GHz are shifted to lower resonant frequencies and vice versa. Since variation in L_3 results in variation of the effective slit length; the lower resonance at 900MHz is also affected slightly. The second resonance is not affected since the total length $L_1+L_{2L}+L_3+L_4$ remains constant.

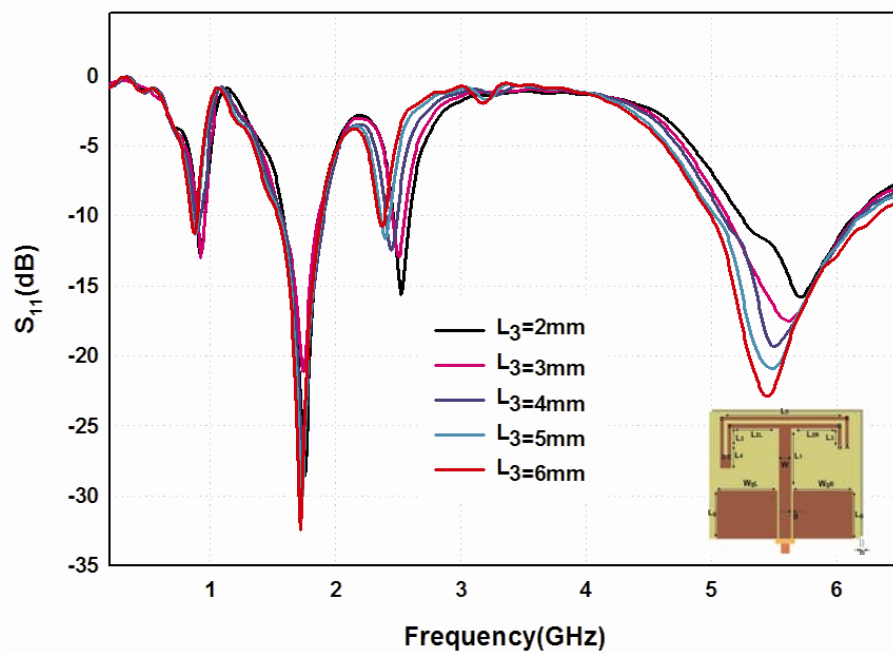


Figure 3.32 Variation in reflection characteristics of the antenna with strip length L_3
 $(L_1=18\text{mm}, L_{2R}=L_{2L}=11\text{mm}, L_4=8\text{mm}, L_5=31\text{mm},$
 $L_g=10\text{mm}, W_{gR}=W_{gL}=14\text{mm}, W_s=3\text{mm}, CD=10\text{mm}, BC=29\text{mm},$
 $DE=HA=1\text{mm}, h=1.6\text{mm}, \epsilon_r=4.4 \text{ and } g=0.35\text{mm})$

3.5.4 Measured Variation on reflection characteristics with strip length L_1

The variation in the reflection characteristics of the antenna with respect to the strip length L_1 is shown in figure.3.33. It is found that the strip length affects the fourth resonance significantly. For a small change of strip length L_1 can contribute to a larger shift in resonant frequency for the fourth resonance. The impedance matching of the third resonance is also affected by the length. The first two resonant frequencies are found to remain almost constant.

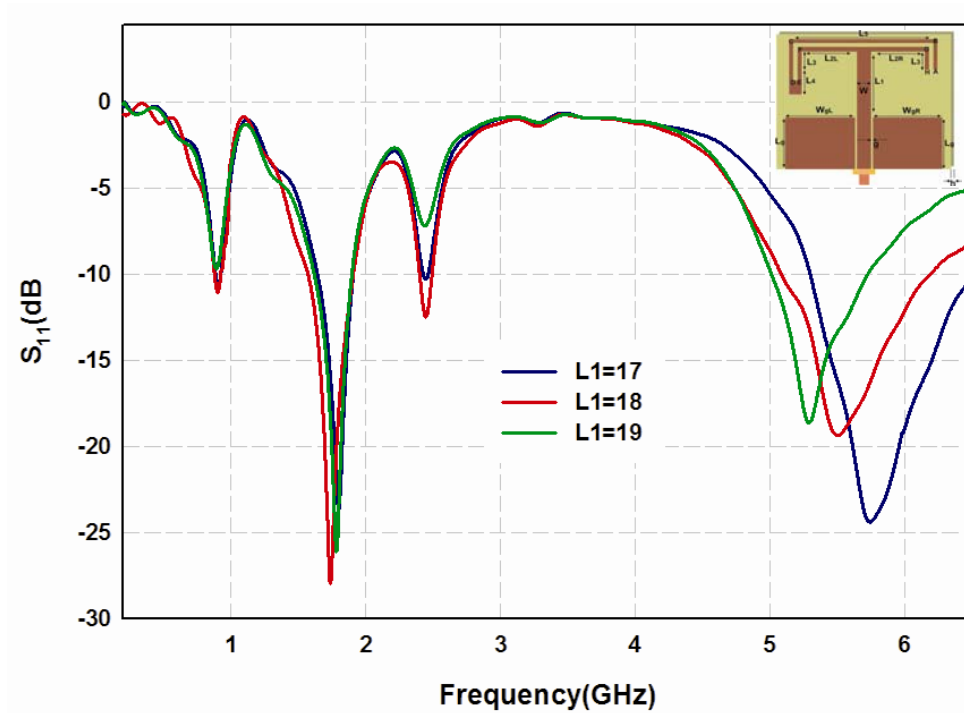


Figure 3.33 Variation in reflection characteristics of the antenna with strip length L_1
 $(L_{2R}=L_{2L}=11\text{mm}, L_3=4\text{mm}, L_4=8\text{mm}, L_5=31\text{mm},$
 $L_g=10\text{mm}, W_{gR}=W_{gL}=14\text{mm}, W_s=3\text{mm}, CD=10\text{mm},$
 $BC=29\text{mm}, DE=HA=1\text{mm}, h=1.6\text{mm}, \epsilon_r=4.4$ and $g=0.35\text{mm})$

3.5.5 Measured Variation on reflection characteristics with Ground Length L_g

In the performance of compact antennas the effect of ground plane is also very crucial. The variation on reflection characteristics with ground length is shown in figure.3.34. There is a considerable change in the return loss characteristics of the antenna with ground length. As L_g changes the coupling between signal strip and ground plane varies which results a corresponding change in the resonant frequency. Considering the application band and compactness of the antenna, the length of the ground plane is optimized as $0.27\lambda_g$. Where λ_g is the dielectric wavelength corresponding to lowest frequency.

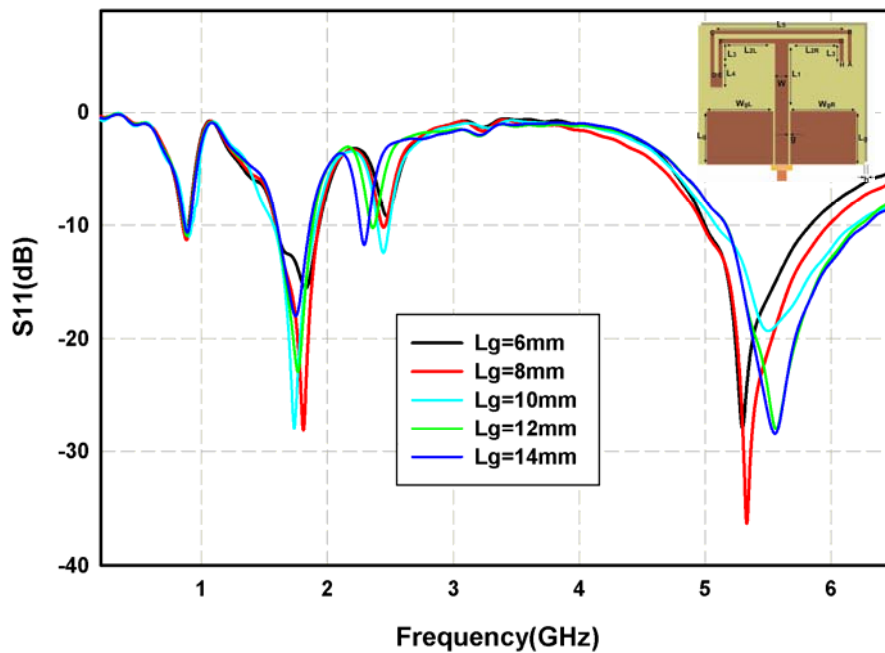


Figure 3.34 Variation in reflection characteristics of the antenna with ground length L_g

($L_1=18\text{mm}$, $L_{2R}=L_{2L}=11\text{mm}$, $L_3=4\text{mm}$, $L_4=8\text{mm}$, $L_5=31\text{mm}$,
 $W_{gR}=W_{gL}=14\text{mm}$, $W_s=3\text{mm}$, $CD=10\text{mm}$, $BC=29\text{mm}$,
 $DE=HA=1\text{mm}$, $h=1.6\text{mm}$, $\epsilon_r=4.4$ and $g=0.35\text{mm}$)

3.5.6 Measured Variation on reflection characteristics with Ground Width W_{gL} and W_{gR}

The variation in reflection characteristics with Ground width W_{gL} and W_{gR} are studied and is shown in figure.3.35. The lower resonance at 900MHz is not at all affected by ground widths. The impedance matching at third resonance is severely affected but there is not much variation in the second resonant frequency. The fourth resonant frequency shows drastic variation with the ground width. As the ground width increases the frequency shift towards lower band with a corresponding deterioration in the impedance matching. Considering all the aforementioned observation the ground plane width is optimized at $0.38\lambda_g=14\text{mm}$.

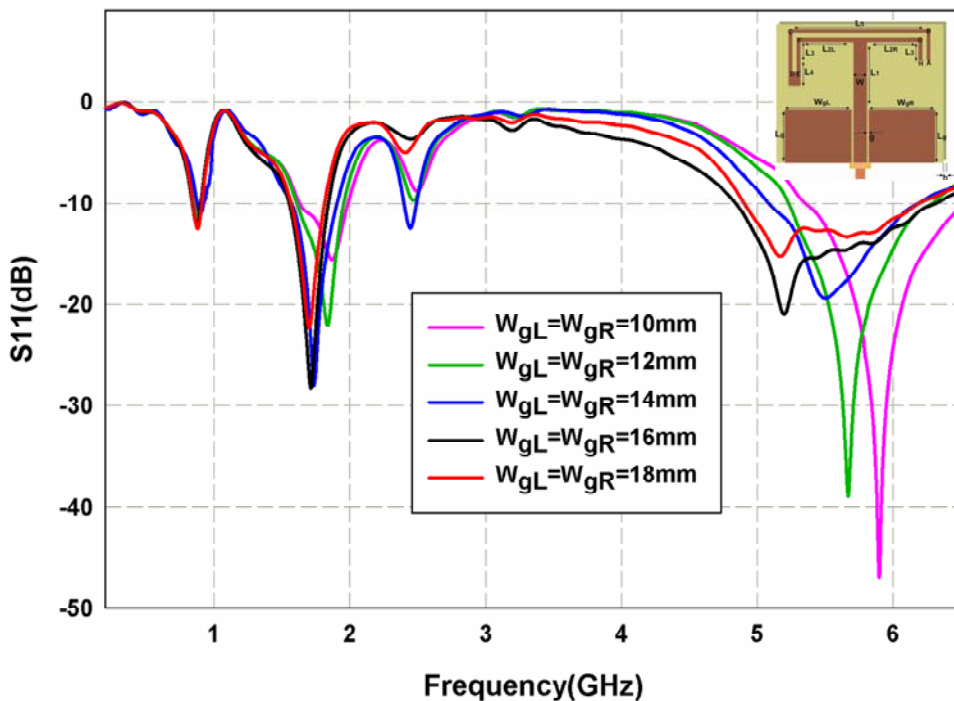


Figure 3.35 Variation in reflection characteristics of the antenna with ground width W_{gL} and W_{gR}
 ($L_1=18\text{mm}$, $L_{2R}=L_{2L}=11\text{mm}$, $L_3=4\text{mm}$, $L_4=8\text{mm}$, $L_5=31\text{mm}$, $L_g=10\text{mm}$, $W_s=3\text{mm}$, $CD=10\text{mm}$, $BC=29\text{mm}$, $DE=HA=1\text{mm}$, $h=1.6\text{mm}$, $\epsilon_r=4.4$ and $g=0.35\text{mm}$)

From the exhaustive parametric analysis performed above the working principle of the antenna at four frequency bands are analyzed. The design criterion for the quad band antenna based on the above observations is explained in this section. The first resonance centered at 900MHz is due to the total perimeter of slit. Slit perimeter can be calculated as,

$$\text{Slit perimeter} = (0.4 * \lambda_1) / \sqrt{\epsilon_{\text{reff}}} \text{ ----- (1)}$$

Where, $\epsilon_{\text{reff}} = (1 + \epsilon_r + 1) / 3$ is the effective dielectric constant of substrate, and λ_1 is the wavelength corresponding to the first resonant frequency. It is presumed that the capacitive coupling between the strips (ABCD & EFGH) across the slit effectively increases the overall length of the antenna, thereby reducing the physical length to 0.4 times the guided wavelength.

The second resonance centered at 1.74GHz occurs due to the combined effect of the length ($L_1 + L_{2L} + L_3 + L_4$) and strip length ABCD (Fig.3.28). The strip length ABCD will adjust in accordance with $L_1 + L_{2L} + L_3 + L_4$ because L_{2L} is equal to L_{2R} and width W_s of the signal strip is constant. and therefore it can be calculated as below.

$$L_1 + L_{2L} + L_3 + L_4 = (0.35 * \lambda_2) / \sqrt{\epsilon_{\text{reff}}} \text{ ----- (2)}$$

Where $L_{2L} = 2.75 L_3$ is chosen for minimum capacitive coupling between L_1 and L_3 . The additional capacitive coupling contributed by top loading results in increasing the physical length, hence assuring compactness.

The third resonance is due to $L_1 + L_{2R} + L_3$ (Fig.3.32). It is interesting to note that the matching is severely affected by L_1 (Fig.3.33) and $L_3 + L_4$ (Fig.3.30) without affecting the resonant frequency. On increasing L_1 the real part of impedance is decreased causing a corresponding deterioration in

impedance match. As L_3+L_4 increases the inductive reactance increases with corresponding increase in the imaginary part of impedance contributing to better impedance matching. The design criterion for the third resonance is,

$$L_1+L_{2R}+L_3 = (0.4*\lambda_3)/\sqrt{\epsilon_{\text{reff}}} \text{-----} (3)$$

The fourth resonance centered at 5.5GHz is affected by the variation in L_1 (Fig.7), L_3 (Fig.6) and L_3+L_4 (Fig.5). A significant change in resonance with ground dimensions is also observed (Fig.8-9). The shift in resonance is due to the change in reactance, resulting from a change in the coupling between the ground and the signal strip. Hence the fourth resonance is due to two parallel symmetrical paths $L_1+L_{2R}+L_3$ and $L_1+L_{2L}+L_3+L_4$. These two resonances merge to give a broad band at 5.5GHz. The path lengths are found to be equal to three quarter wavelengths at the corresponding resonant frequency. Since a significant variation is only due to L_1 , the length should be selected in such a way so as to cover the application band as given below.

$$L_1 = (0.49*\lambda_4)/\sqrt{\epsilon_{\text{reff}}} \text{-----} (4)$$

The decrease in the physical lengths of the antenna at the different resonant frequencies is due to the top loading effect, by virtue of which the antenna appears electrically larger [3].

From the parametric studies, it is inferred that the ground plane affects the impedance matching of the resonant modes. By considering the compactness and antenna performance the ground plane length and width are optimized as follows.

$$L_g = (0.27*\lambda_4)/\sqrt{\epsilon_{\text{reff}}} \text{-----} (5)$$

$$W_{gL} = W_{gR} = (0.38 * \lambda_4) / \sqrt{\epsilon_{\text{reff}}} \text{-----} (6)$$

To validate the design equations for various quad band antennas are designed for different dielectric substrates. The above equations are validated by characterizing antenna characteristics. The predicted antenna resonances are reasonably good agreement with the obtained results as shown in Table 3.3.

Table 3.3 % error in resonant frequency of the antenna for different dielectric substrate at 0.9, 1.8, 2.4 and 5.2 GHz

Substrate (Dielectric constant)	Obtained Simulated Frequency(GHz)				% Error			
	F ₁	F ₂	F ₃	F ₄	F ₁	F ₂	F ₃	F ₄
Rogers RT/duroid 5880 (2.2)	0.95	1.70	2.30	5.42	5.55	5.55	4.34	4.23
Taconic RF-35 (3.5)	0.92	1.76	2.42	5.12	2.22	2.22	0.83	1.53
Alumina (9.4)	0.98	1.94	2.36	5.78	8.88	7.77	1.66	11.15
Rogers RO6010 (10.2)	0.98	1.93	2.39	5.77	8.88	7.2	0.41	10.96

The measured co and cross polarized received power of the antenna along with return loss is shown in Figure.3.36. Since the Y-component dominates over the X-component for all the four bands, the antenna is polarized along the Y direction. The antenna shows good polarization purity in the first and fourth band. The polarization is moderate on the second and third band. The first resonance at 900 MHz is due to the perimeter of the slit *ABCDEFGH*. Since the direction of current is opposite in its parallel arms it is seen that the X-component gets cancelled in the far field resulting the polarization along Y direction. In the second band centered at 1.74GHz, the Y-component dominates the X-component resulting in polarization along Y-direction.

But for the third band centered at 2.44GHz, the polarization purity is poor, because here the X (due to L_{2R}) and Y (due to L₁+L₃) components have

approximately equal contribution. At 5.54GHz the symmetrical contribution from both horizontal strips makes the X-component cancel in the far field resulting in polarization along the Y-direction.

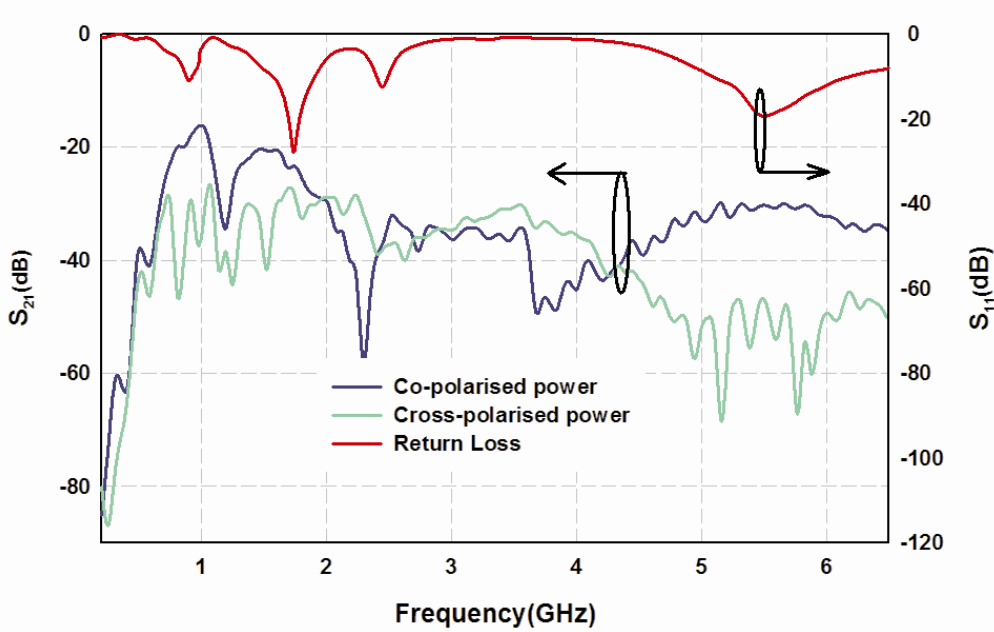
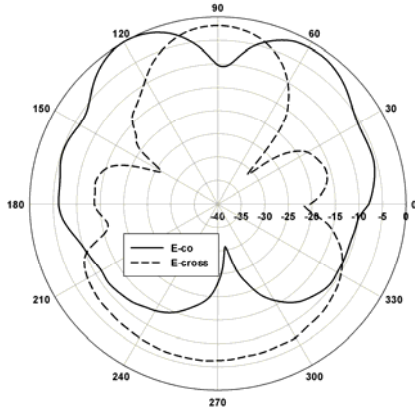
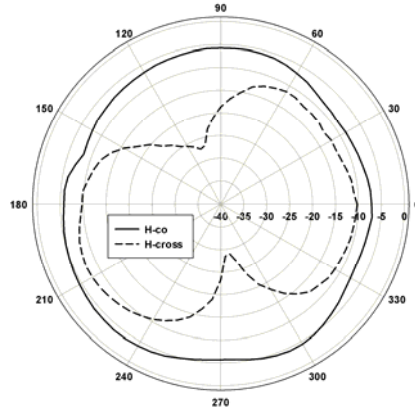


Figure 3.36 Comparison of co polar and cross polar level of quad band antenna with reflection characteristics
 ($L_1=18\text{mm}$, $L_{2R}=L_{2L}=11\text{mm}$, $L_3=4\text{mm}$, $L_4=8\text{mm}$, $L_5=31\text{mm}$, $L_g=10\text{mm}$, $W_{gR}=W_{gL}=14\text{mm}$, $W_s=3\text{mm}$, $CD=10\text{mm}$, $BC=29\text{mm}$, $DE=HA=1\text{mm}$, $h=1.6\text{mm}$, $\epsilon_r=4.4$ and $g=0.35\text{mm}$)

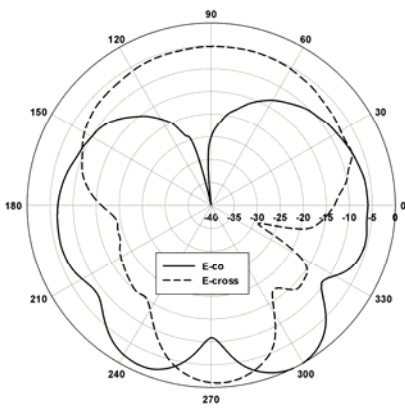
The measured 2D radiation patterns of the antenna in the four resonant bands are shown in Figure.3.37. The antenna shows good radiation characteristics in the entire band of operation. The antenna gives good polarization purity in all the operating bands. The pattern is non-directional in H-plane and directional in E-plane.



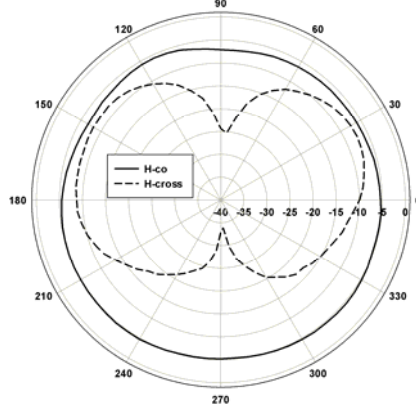
(a) E-plane 900MHz



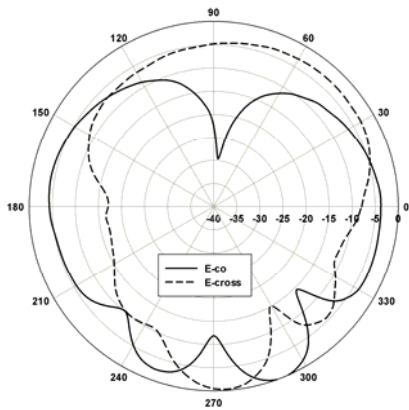
(b) H-plane 900MHz



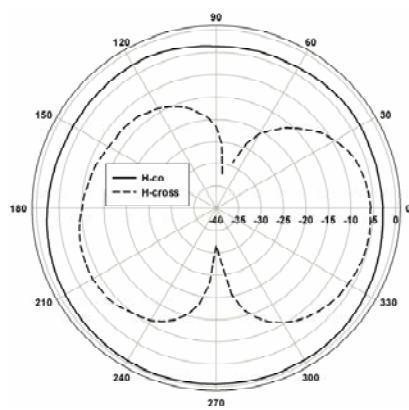
(c) E-plane 1.77GHz



(d) H-plane 1.77GHz



(e) E-plane 2.4GHz



(f) H-plane 2.4GHz

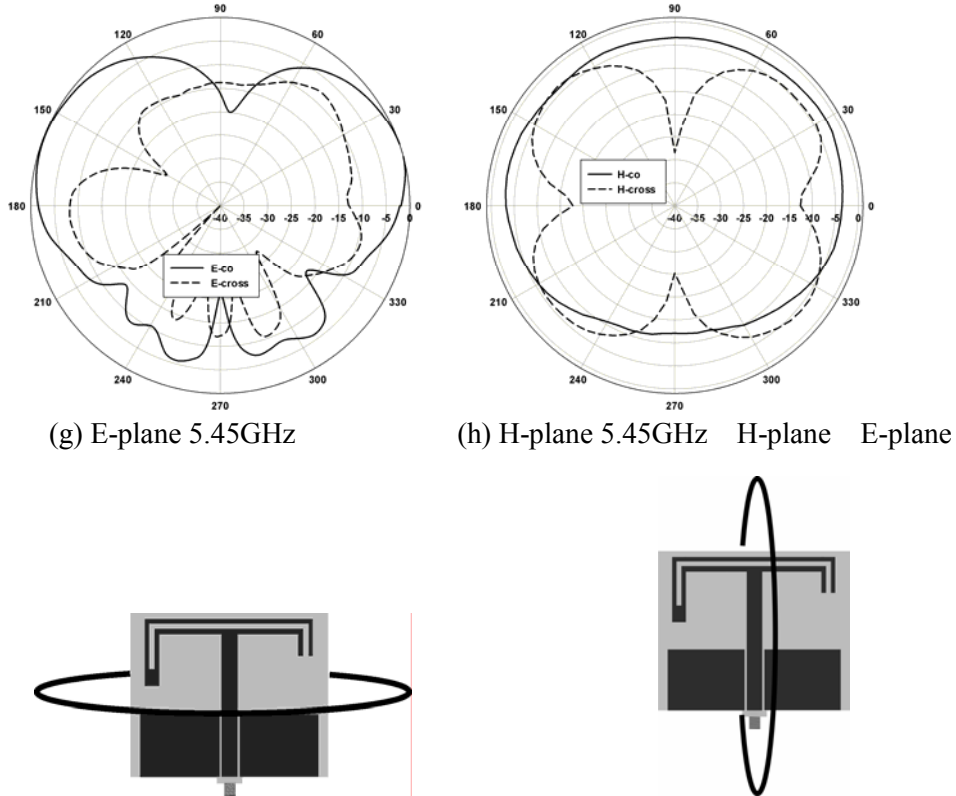


Figure3.37 Measured radiation pattern of the quad band antenna (a) E-plane 900MHz (b) H-plane 900MHz (c) E-plane 1.77GHz (d) H-plane 1.77GHz (e) E-plane 2.4GHz (f) H-plane 2.4GHz (g) E-plane 5.45GHz (h) H-plane 5.45GHz
 $(L_1=18\text{mm}, L_{2R}=L_{2L}=11\text{mm}, L_3=4\text{mm}, L_4=8\text{mm}, L_5=31\text{mm}, L_g=10\text{mm}, W_{gR}=W_{gL}=14\text{mm}, W_s=3\text{mm}, CD=10\text{mm}, BC=29\text{mm}, DE=HA=1\text{mm}, h=1.6\text{mm}, \epsilon_r=4.4 \text{ and } g=0.35\text{mm})$

The simulated 3D radiation pattern of the antenna is shown in figure.3.38. A good omnidirectional radiation pattern is obtained at 900MHz and 1.77GHz band. From the pattern it is clear that the antenna has a constant gain along the XZ plane and null along the positive and negative Y-direction. The pattern is somewhat disturbed in the higher frequencies at 2.4GHz and 5.45GHz.

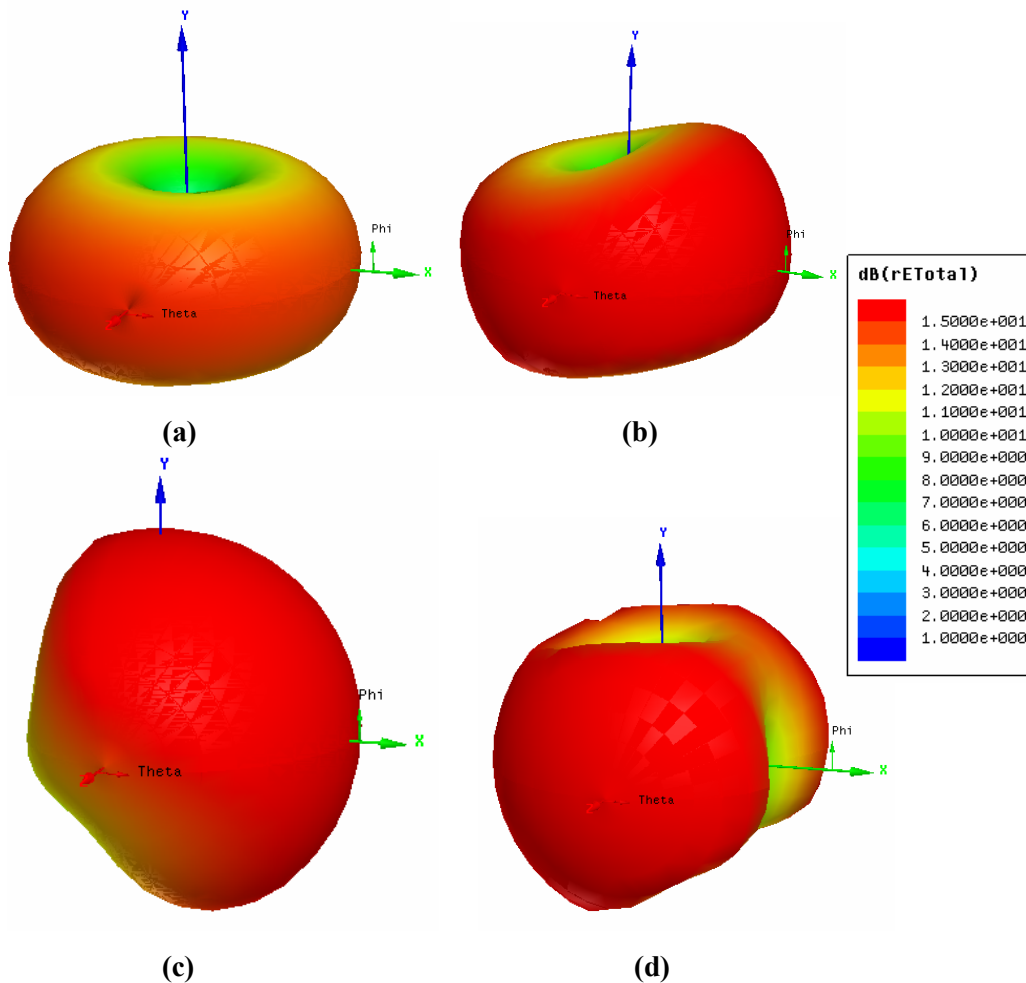


Figure 3.38 Simulated 3D radiation pattern of the quad band antenna (a) 900MHz (b) 1.77GHz (c) 2.4GHz (d) 5.45GHz
 $(L_1=18\text{mm}, L_{2R}=L_{2L}=11\text{mm}, L_3=4\text{mm}, L_4=8\text{mm}, L_5=31\text{mm},$
 $L_g=10\text{mm}, W_{gR}=W_{gL}=14\text{mm}, W_s=3\text{mm}, CD=10\text{mm}, BC=29\text{mm},$
 $DE=HA=1\text{mm}, h=1.6\text{mm}, \epsilon_r=4.4 \text{ and } g=0.35\text{mm})$

The current distributions on the quad-band antenna at different bands are shown in fig.3.39. These current distributions again confirm our earlier arguments about the different resonances. The current distribution in lower resonance (900MHz) is shown in fig.3.39 (a). It is obvious that the intensity of current is found to be maximum around the slit perimeter. The direction of

current is found to be opposite in both the parallel arms and it re-confirms the resonating current path described in earlier section. From fig.3.39 (b) it is found that the current distribution is maximum in the main arm (L_1) together with the lateral strip ($L_{2L}+L_3+L_4$). Similarly the intensity of current distribution for third frequency is found to be in the other arm ($L_1+L_{2R}+L_3$) as shown in fig.3.39(c). The current distribution for the fourth resonance shown in fig.3.39 (d) is found to be a variation through both the parallel opposite arms ($L_1+L_{2R}+L_3$ and $L_1+L_{2L}+L_3+L_4$). Since the arms are nearly equal in length the two resonances will come close and merge together to give a wideband response.

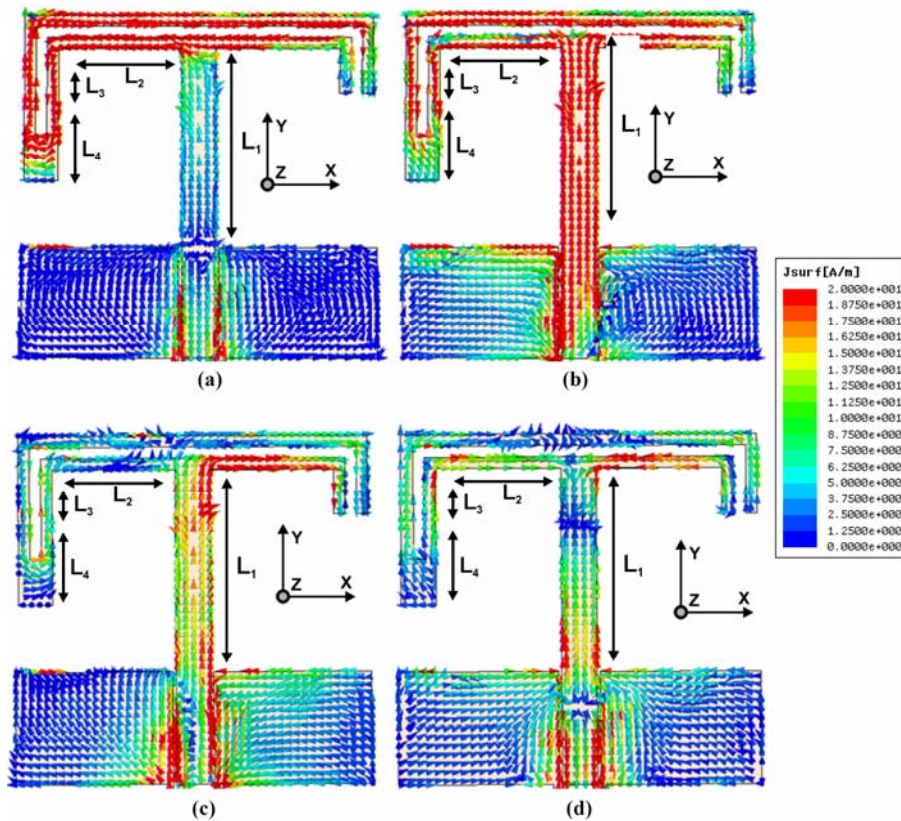


Figure 3.39 Simulated current distribution of the quad band antenna
 (a) 900MHz (b) 1.77GHz (c) 2.4GHz (d) 5.45GHz
 ($L_1=18\text{mm}$, $L_{2R}=L_{2L}=11\text{mm}$, $L_3=4\text{mm}$, $L_4=8\text{mm}$, $L_5=31\text{mm}$,
 $L_g=10\text{mm}$, $W_{gR}=W_{gL}=14\text{mm}$, $W_s=3\text{mm}$, $cd=10\text{mm}$, $bc=29\text{mm}$,
 $de=ha=1\text{mm}$, $H=1.6\text{mm}$, $\epsilon_r=4.4$ and $g=0.35\text{mm}$)

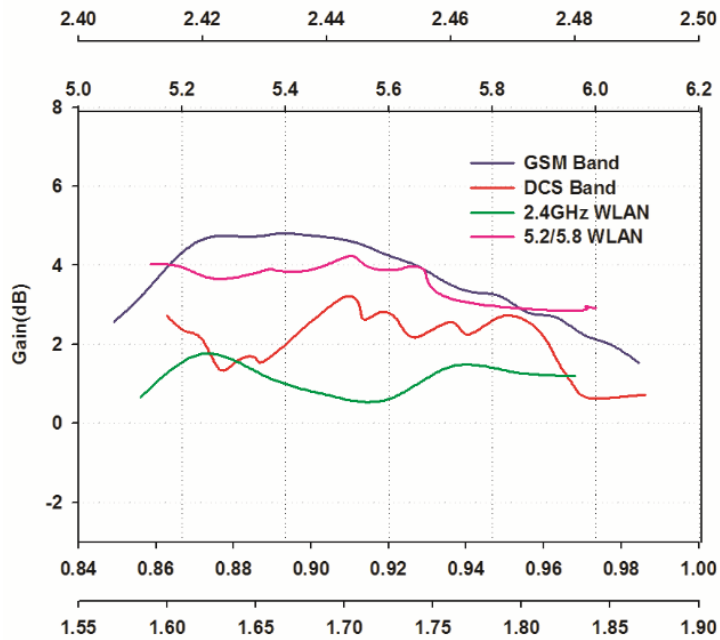


Figure 3.40 Measured Gain of the quad band antenna in four bands
 $(L_1=18\text{mm}, L_{2R}=L_{2L}=11\text{mm}, L_3=4\text{mm}, L_4=8\text{mm}, L_5=31\text{mm},$
 $L_g=10\text{mm}, W_{gR}=W_{gL}=14\text{mm}, W_s=3\text{mm}, cd=10\text{mm}, bc=29\text{mm},$
 $de=ha=1\text{mm}, H=1.6\text{mm}, \epsilon_r=4.4 \text{ and } g=0.35\text{mm})$

Gain of the antenna is measured using gain transfer method and is shown in figure.3.40. The peak gains of the antenna in the four bands are 1.25dBi, 1.94dBi, 1.11dBi and 3.71dBi respectively. The gain is considerably constant in the H-plane and hence is useful for omni-directional communication.

The comparison on the radiation characteristics of the dual band monopole antenna and Quad band monopole antenna is shown in Table 3.4.

Table 3.4. Comparison of Dual and Quad band monopole

Sl. No	Antenna	Resonant Frequency	Band Width	Application Band	Area	Polarization	Gain
1	Dual band monopole Antenna	1.77GHz	1.47-1.97	DCS 1800/1900	32x31x1.6 cubic cm	Linear	3dBi
		5.54GHz	5.13-6.48	HIPERLAN ISM WLAN 5.8		Linear	3.5dBi
2	Quad band monopole Antenna	900MHz	840-970MHz	GSM 900	32x31x1.6 cubic cm	Linear	1.25dBi
		1.74GHz	1.56-1.92GHz	DCS-1800		Linear	1.94dBi
		2.44GHz	2.39-2.49GHz	ISM 2.4		Linear	1.11dBi
		5.5GHz	5.07-6.23GHz	5.2/5.8GHz WLAN		Linear	3.71dBi

3.6 Important conclusions from this chapter

- The signal strip of a coplanar waveguide transmission line can be effectively modified to act as a radiator.
- An additional resonance in a CPW fed monopole antenna can be generated by suitably top loading it.
- Folding technique can be effectively used to make the antenna more compact.
- Asymmetric loaded CPW antenna can be used for triple band operation.
- The introduction of slit will generate an additional lower resonance without increasing the overall compactness of the antenna.
- The presented quad band antenna is providing good impedance matching with independent control on resonances.
- Design equations are developed and are validated on different dielectric substrates.

References

- [1] Brian K. Kormanyos, William Harokopus, Linda P. B. Katehi and Gabriel M. Rebeiz, CPW-Fed Active Slot Antennas ,IEEE Trans on Microwave Theory and Technique, Vol.42, No.4, April 1994.
- [2] Suma M.N, Investigations on broadband planar monopole antennas with truncated ground plane, Ph.D Thesis, Cochin University of Science and Technology, January 2008.
- [3] Jeremy.K.Raines, 2007, Folded Unipolar antennas Theory and applications, New York, McGraw Hill.

.....❧.....

INVESTIGATION ON GROUND PLANE MODIFIED CPW FED PLANAR ANTENNA

Contents	4.1	Ground reduced CPW fed open ended Transmission line
	4.2	Ground Meandered CPW fed antenna
	4.3	Ground plane increased Meandered CPW fed antenna
	4.4	Geometry of the proposed Compact CPW fed antenna
	4.5	Conclusion of the ground optimized antenna

This chapter deals with the evolution of a coplanar waveguide fed antenna, with modified ground plane. An interesting method to convert coplanar waveguide transmission line to an antenna by modifying the ground plane is elaborately discussed in this chapter. A method to reconfigure the antenna using PIN diode is also discussed.

4.1 Ground reduced CPW fed open ended Transmission line

An open ended coplanar waveguide fed transmission line with lateral ground plane dimension ($L_g \times W_g$) is shown in figure.4.1. As explained in the previous chapter this structure behaves as a normal transmission line. The structure will not radiate electromagnetic energy at lower frequencies but have some leaky radiation at higher frequencies.

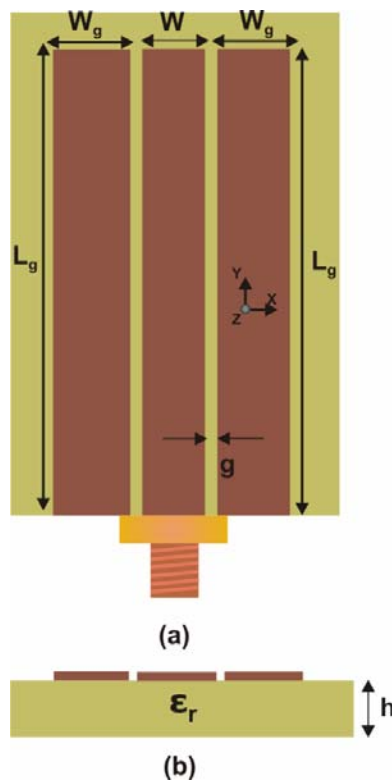


Figure 4.1 Geometry of the coplanar waveguide fed reduced ground antenna (a) Front view (b) Side view
($L_g=20\text{mm}$ $W_g=3\text{mm}$ $W=3\text{mm}$ $g=1.2\text{mm}$ $h=1.6\text{mm}$ $\epsilon_r=4.4$)

The gap 'g' between the signal strip and ground plane is the primary factor determining the impedance of this structure. Increasing or decreasing the gap will definitely alter the impedance and radiation characteristics. Physical constraints limit the decrease in gap, but we can increase the gap without any

constraints. The reflection characteristics of the antenna for different gap ‘g’ are shown in figure 4.2 (a) & (b).

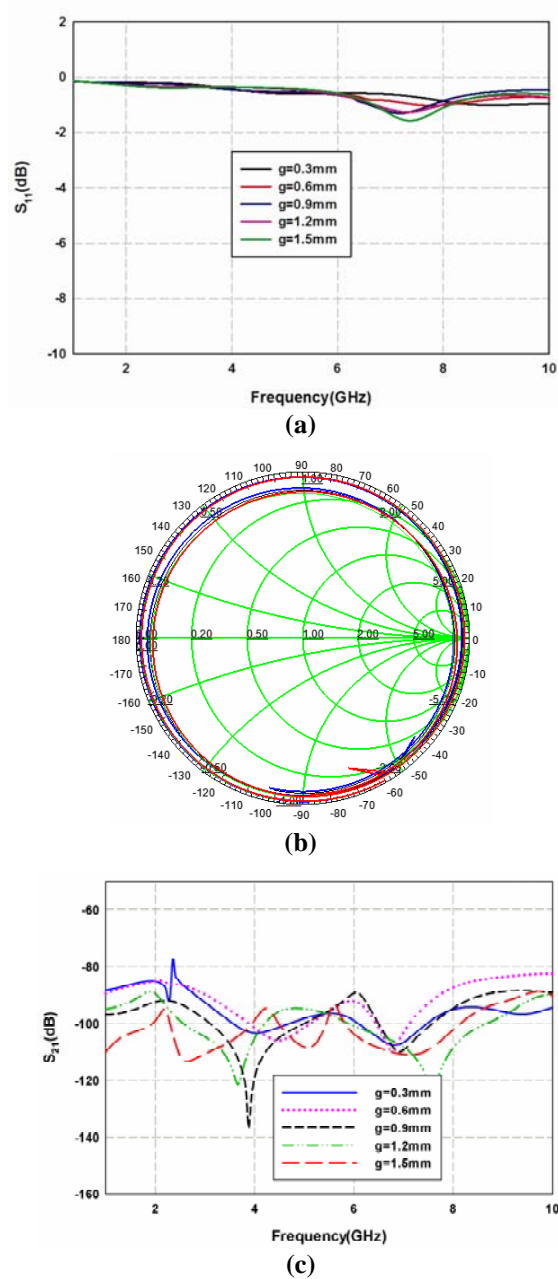


Figure 4.2 (a) Reflection Characteristics of Reduced Ground Plane Coplanar Waveguide (RGPCW) (b) Impedance characteristics of RGPCW ($L_g=20\text{mm}$, $W_g=3\text{mm}$, $W=3\text{mm}$, $h=1.6\text{mm}$ and $\epsilon_r=4.4$)

From the figure it is evident that for a gap width (g) of 0.3mm the structure behaves as a normal transmission line. As the gap increases the transmission line property of the structure deteriorates and starts to radiate from the discontinuity. The impedance characteristics of the structure are also shown in figure 4.2(b) with different gap width. From the smith chart it is found that the real part of the impedance is very low for all the values of 'g'. The transmission characteristics of the structure are also shown in figure.4.2.c. The structure is not radiating in the entire radiating frequency bands. In order to have a good radiation, the structure should be properly matched to the input impedance at the required resonating frequency.

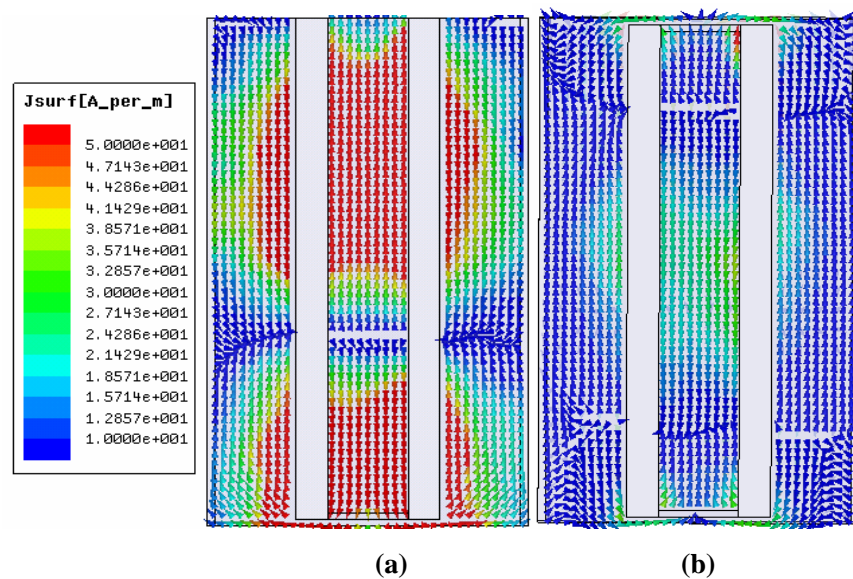


Figure 4.3 Current distribution of (a) Gap optimized CPW fed Antenna at 7.34GHz b) Gap optimized CPW fed Antenna with matched load at 7.34GHz ($L_g=20\text{mm}$, $W_g=3\text{mm}$, $W=3\text{mm}$, $g=1.2\text{mm}$, $h=1.6\text{mm}$ and $\epsilon_r=4.4$)

The surface current distribution of the gap optimized antenna at 7.34GHz is shown in figure.4.3 (a). From figure it is clear that due to reflection from open end of the transmission line a standing wave is formed along the

transmission line. It is strongly evident from the surface current distribution that the currents existing on either side of the feed are equal in amplitude and opposite in phase. This strongly indicates that there is negligible radiation from the feed and the propagation mode remains unaltered. It is also seen that there is some leaky radiation along the transmission line at higher frequencies (7.34GHz). The surface current distribution of the same structure with matched load at the farther end is shown in figure.4.3 (b). The structure behaves as a normal transmission line and the total energy is transferred from one end to the other end without any reflection. The simulated 3-Dimensional radiation pattern of the gap optimized antenna at 7.34GHz is shown in figure.4.4. From the figure it is clear that there is radiation along XZ plane with null along the Y-direction. Even though there is radiation, the amount of total radiated power is very little and the present antenna is inefficient. So it is necessary to improve the radiation characteristics without increasing the compactness.

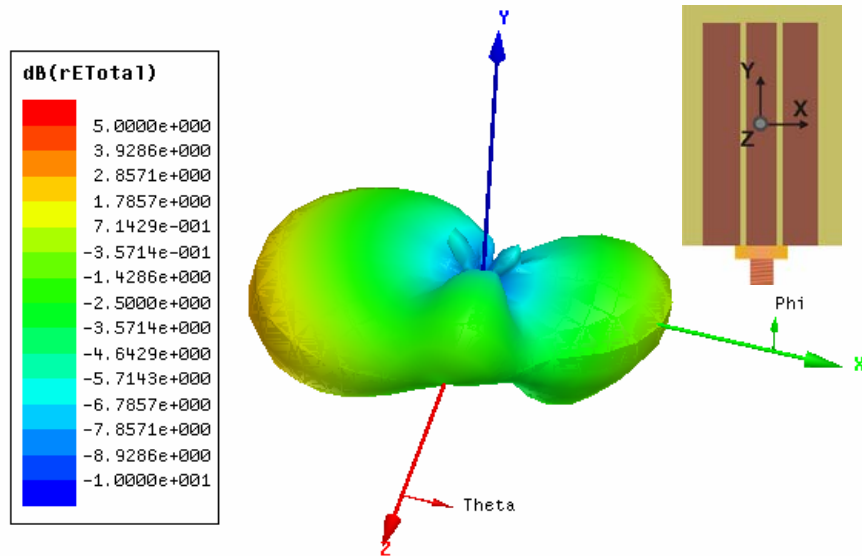


Figure 4.4 Radiation pattern of gap optimized CPW fed antenna at 7.34GHz
 ($L_g=20\text{mm}$, $W_g=3\text{mm}$, $W=3\text{mm}$, $g=1.2\text{mm}$, $h=1.6\text{mm}$ and $\epsilon_r=4.4$)

From the initial analysis it can be concluded that the ground plane can be properly tailored to excite the resonance in an open ended CPW. The optimum ground plane dimension and the ground to signal gap to fix the resonance at a particular frequency is also derived and optimized. The detailed discussion on the ground plane variation is included in the following sections.

4.2 Ground Meandered CPW fed antenna

Thus the initial investigation on the ground plane modification reveals that by judiciously modifying the ground plane parameters a resonant mode can be excited. This means a CPW transmission line can be effectively converted to a radiator by ground modification. Now it is proposed to increase the current path along the ground plane. The ground plane of the antenna is modified as shown in Figure.4.5. A slit of width 'S' is inserted on both the lateral ground planes of length L_g . The slit is placed in such a way that its one end is open and other end is short to give a meandered path along the ground plane. The signal strip of the antenna remains unaltered. It is also noted that the total dimension of the structure described in the previous section remains unchanged while meandering the ground plane strip. Moreover, meandering is done in such a way that the symmetrical nature of the structure remains intact.

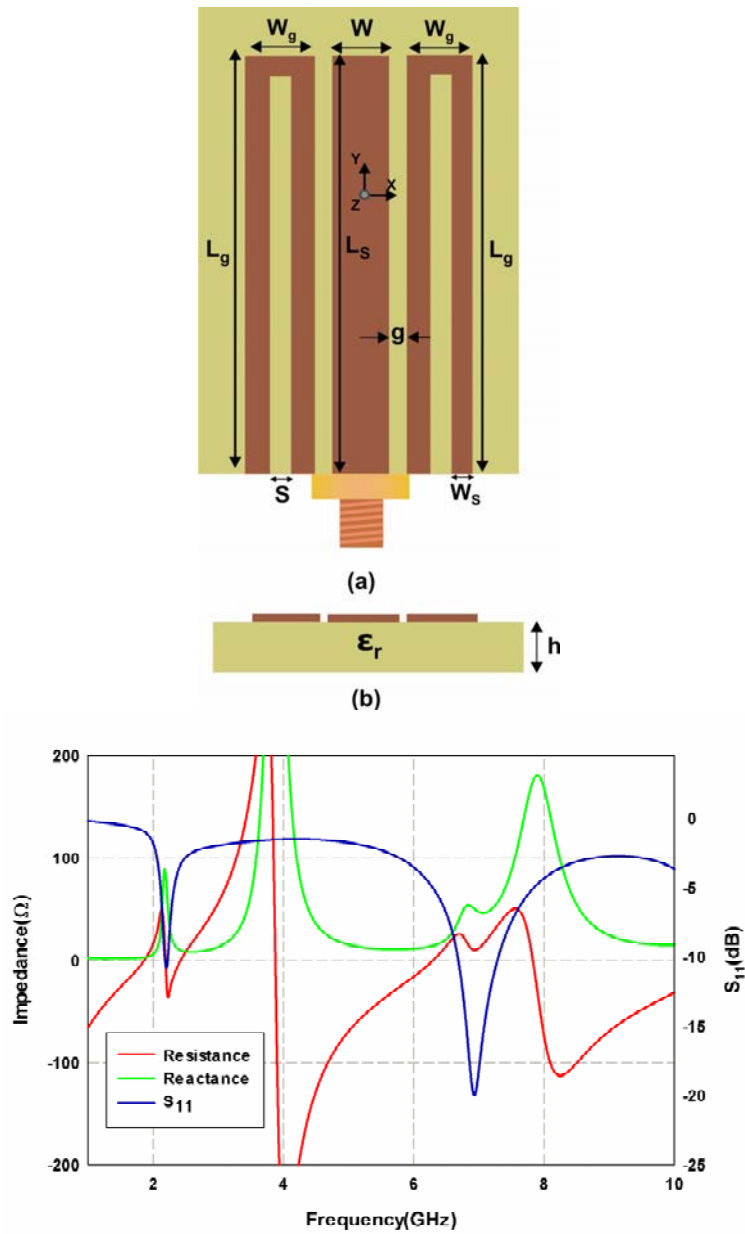


Figure 4.5 Geometry of the ground meandered CPW fed antenna (a) Front view (b) Side view (c) Reflection and impedance characteristics ($L_g=20\text{mm}$, $L_S=20\text{mm}$, $W_g =2.5\text{mm}$, $W_s=1\text{mm}$, $W=3\text{mm}$, $g=1\text{mm}$, $S=0.5\text{mm}$, $h=1.6\text{mm}$ and $\epsilon_r=4.4$)

The reflection characteristic of the antenna is shown in figure.4.5(c). The antenna exhibits a resonance at 2.21GHz with improved impedance match (-10.6dB) than the structure explained in the previous section. It is well understood that the lower resonance is due to the increased current path through the ground plane. A higher resonance at around 6.94GHz is also obtained with good impedance match. We are interested only in the fundamental mode resonating at 2.21GHz, with good impedance match.

The Smith chart showing the impedance characteristics of the ground meandered antenna is shown in figure.4.6. It is noted from Smith chart that the impedance is slightly capacitive at the fundamental resonant frequency. From the smith chart it is found that at 2.21GHz the real part of the impedance is very high. In order to achieve good radiation behavior this should be matched to 50Ω .

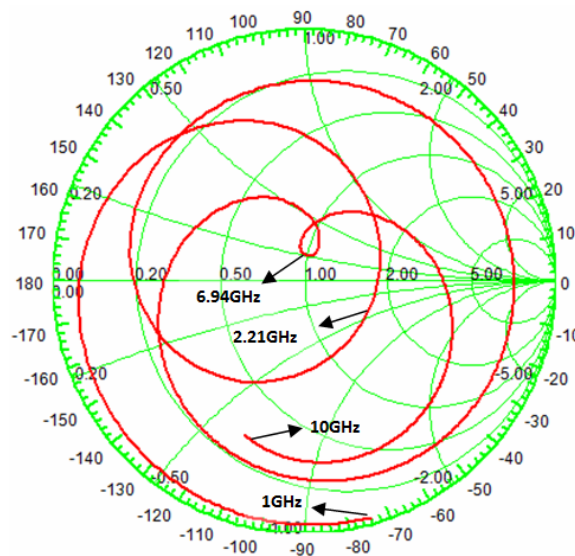


Figure 4.6 Impedance characteristics of the ground meandered antenna
 $(L_g=20\text{mm}, W_g=2.5\text{mm}, L_s=20\text{mm}, W_s=1\text{mm}, W=3\text{mm}, g=1\text{mm}, S=0.5\text{mm}, h=1.6\text{mm}$ and $\epsilon_r=4.4$)

4.2.1 Effect of varying the gap g

The investigation on the planar CPW fed transmission line in the previous section shows that there is a possibility of resonance while changing the signal to ground gap (g). The effect on reflection characteristics with ' g ' is shown in figure.4.7. It is found that there is some small changes in the resonant frequency as well as on the input impedance for small variation in the signal to ground gap. Thus the ground to signal gap can play an important role in providing impedance matching performance at the fundamental mode. Hence, here the gap width is arbitrarily chosen as 1mm, considering the compactness and radiation properties.

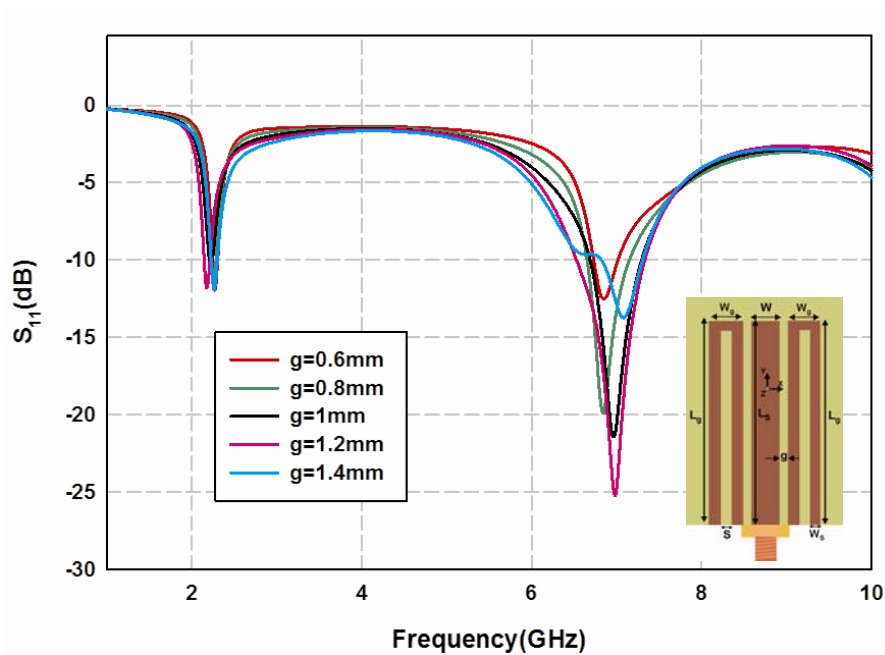


Figure 4.7 Variation in reflection characteristics of ground meandered antenna with variation in gap (g)
 ($L_g=20\text{mm}$, $W_s=1\text{mm}$, $W_g=2.5\text{mm}$, $L_s=20\text{mm}$, $W=3\text{mm}$, $S=0.5\text{mm}$, $h=1.6\text{mm}$ and $\epsilon_r=4.4$)

4.2.2 Effect of varying the meandering ground strip length L_g

The variation of reflection characteristics with strip length L_g is shown in figure.4.8. As the strip length decreases the resonance shift to higher frequency as expected. It is also noted that the impedance match become poor as the length is below 14mm. Thus the resonance can be tuned by changing the ground strip length L_g from 14mm to 20mm for a constant signal strip length of L_s . The maximum attainable length by considering the physical constraints for a perfectly matched resonance is 20mm for which is nearly equal to $0.215\lambda_g$ at 2.21GHz; λ_g is the guided wavelength at resonant frequency, where $\lambda_g = \frac{\lambda}{\sqrt{\epsilon_{\text{reff}}}}$; $\epsilon_{\text{reff}} = \frac{\epsilon_r + 1 + 1}{3}$ is the effective dielectric constant.

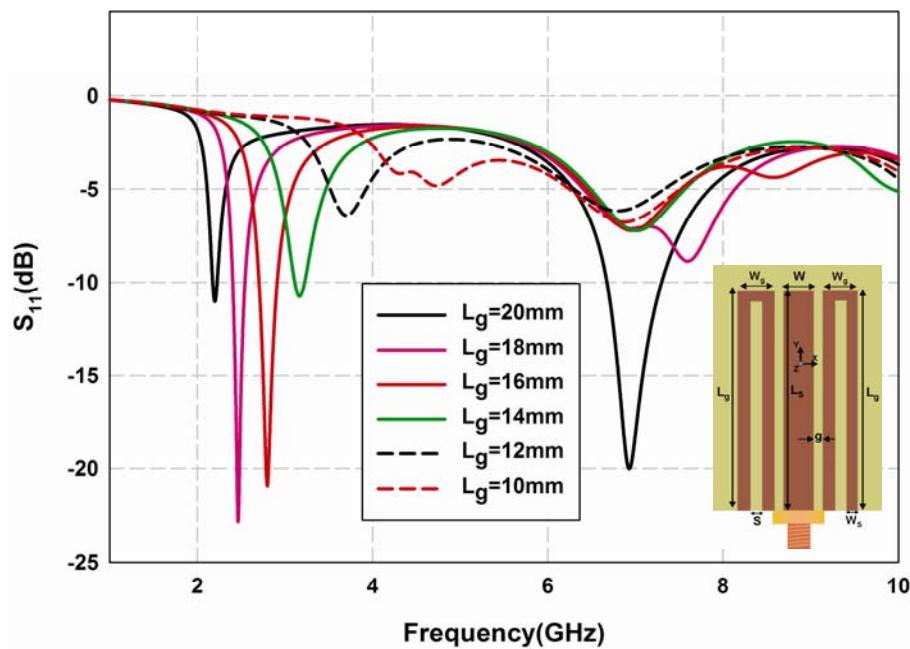


Figure 4.8 Variation in reflection characteristics of ground meandered antenna with meandered ground strip (L_g) ($W_s=1\text{mm}$, $W=3\text{mm}$, $W_g=2.5\text{mm}$, $g=1\text{mm}$, $S=0.5\text{mm}$, $h=1.6\text{mm}$ and $\epsilon_r=4.4$)

4.2.3 Effect of varying the slot length (L_g - W_s)

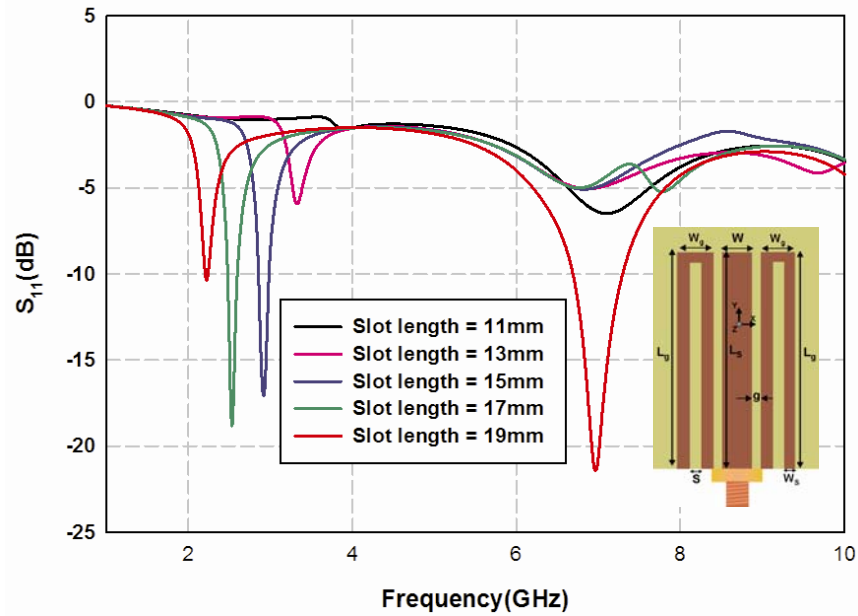


Figure 4.9 Variation in reflection characteristics of ground meandered antenna with slot length by keeping L_g constant ($L_g=20\text{mm}$, $W_g=2.5\text{mm}$, $W_s=1\text{mm}$, $W=3\text{mm}$, $g=1\text{mm}$, $S=0.5\text{mm}$, $h=1.6\text{mm}$ and $\epsilon_r=4.4$)

From the studies discussed in previous sections it is clear that the resonance has a little dependence on the signal to ground gap 'g' and is varying significantly with the strip length L_g . The effect of slot length (L_g - W_s) is shown in figure 4.9. As the slot length decreases the resonant frequency shift to higher region and viceversa. Further decrease in slot length will make the structure behave like a normal gap increased transmission line with radiation at higher frequency as described in the previous sections. Thus it is concluded from the above studies that the radiation is strongly due to the perimeter of the slot. It is possible to tune the resonance by simply changing the slot length and hence the perimeter of the slot. The maximum attainable slot length for a constant strip length $L_g=0.215\lambda_g$ is $0.20\lambda_g$.

4.2.4 Effect of varying the slot gap 's' on reflection characteristics

The variation in reflection characteristics with slot gap 's' is shown in figure.4.10. By varying the slot gap 's' the strip width 'Ws' also varies since the total width 'W' remains constant. By increasing 's' the strip width Ws decreases and vice versa. It is found that any variation in slot gap 's' is only affecting the impedance matching of the antenna. By increasing gap 's', the distance between the two vertical strips increases and the capacitance decreases hence the effective reactance changes. The real part of the impedance remains almost unaffected with the variation in gap. Thus the reactance of the antenna can be tuned by changing the slot gap 's' without changing the resonance frequency.

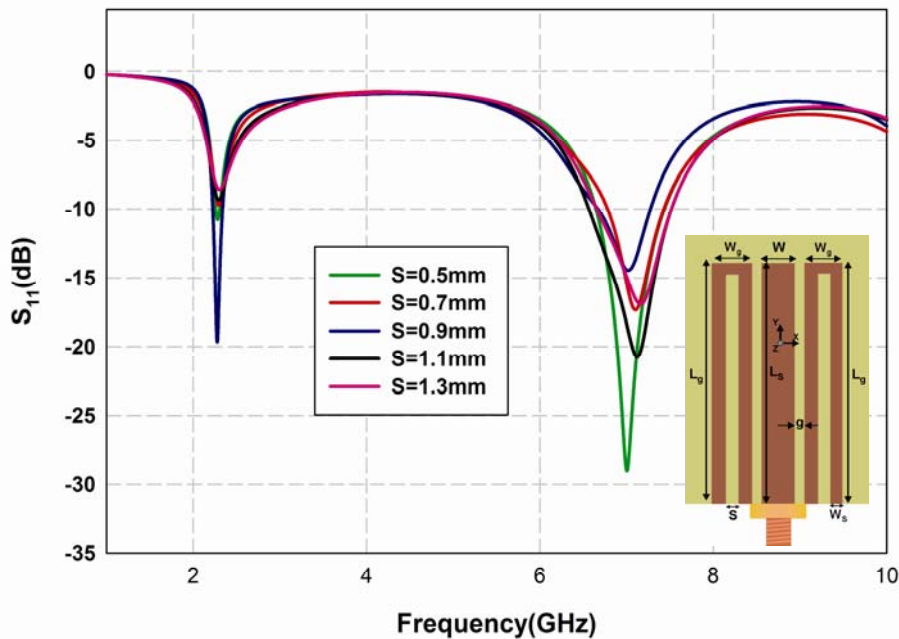


Figure 4.10 Variation in reflection characteristics of ground meandered antenna with slot gap 's'
 ($L_g=20\text{mm}$, $W_g=2.5\text{mm}$, $W_s=1\text{mm}$, $W=3\text{mm}$, $g=1\text{mm}$, $h=1.6\text{mm}$ and $\epsilon_r=4.4$)

4.2.5 Surface Current distribution

The radiation characteristics can be explained from the simulated surface current distribution on the antenna structure. The surface current distribution of the optimized antenna at 2.21GHz is shown in figure.4.11. The electric field along the signal strip and the two lateral ground planes are in opposite direction. Thus the structure is still resonating at the fundamental odd mode as in the case of a normal coplanar waveguide transmission line. There is an almost quarter wavelength variation of current along the meandered path. Moreover, the electric fields are aligned along the Y-direction and there is only feeble X-component. Thus the antenna is linearly polarized along the Y-direction.

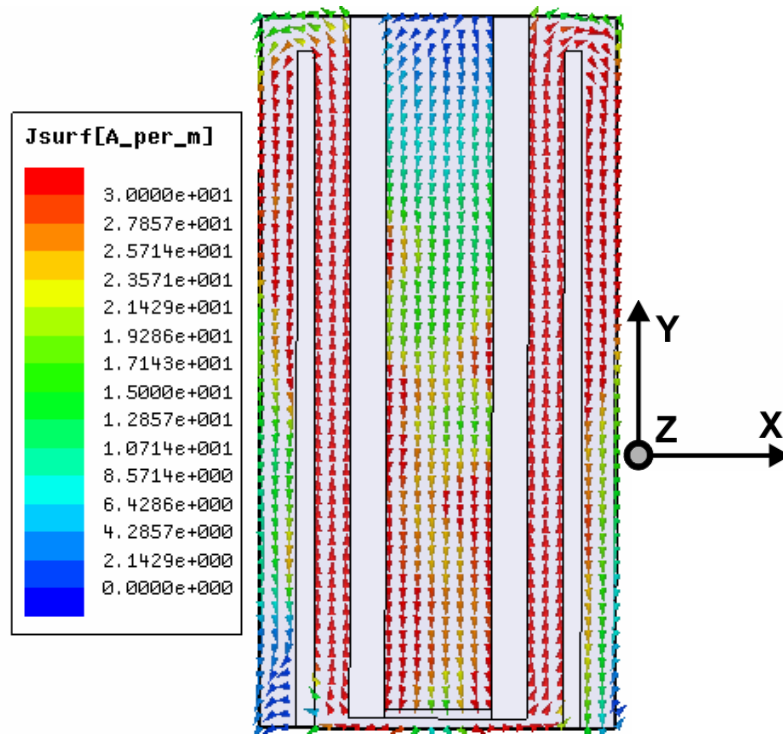


Figure 4.11 Current distribution of the ground meandered antenna ($L_g=20\text{mm}$, $W_g=2.5\text{mm}$, $W_s=1\text{mm}$, $W=3\text{mm}$, $g=1\text{mm}$, $S=0.5\text{mm}$, $h=1.6\text{mm}$ and $\epsilon_r=4.4$)

4.2.6 Radiation pattern

The simulated 3-Dimensional radiation pattern of the antenna at 2.21GHz is shown in figure.4.12. A good non-directional radiation pattern along the XZ plane with nulls along the positive and negative Y-direction is obtained. From the current distribution it is found that the fields are in the vertical direction causing a field addition in the far field along the XZ plane. Thus the antenna is polarized along the Y-direction. Thus a non-radiating structure with less radiation (Fig 4.1) is converted to an effective radiator with an omnidirectional radiation pattern (fig.4.4).

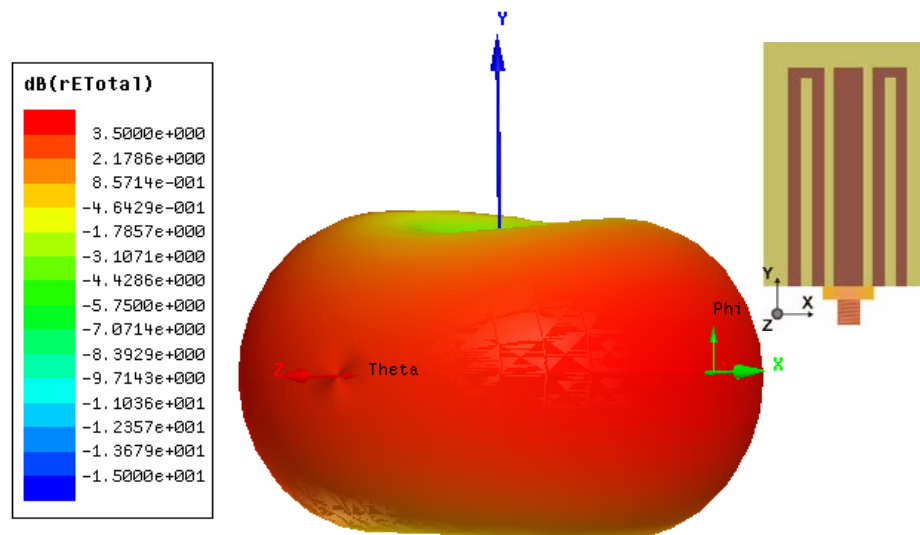


Figure 4.12 3D radiation pattern of the ground meandered antenna
 $(L_g=20\text{mm}, W_g=2.5\text{mm}, W_s=1\text{mm}, W=3\text{mm}, g=1\text{mm}, S=0.5\text{mm},$
 $h=1.6\text{mm}$ and $\epsilon_r=4.4)$

In order to have a better understanding of the cross polar isolation of the antenna it is better to look at the two dimensional radiation patterns. The simulated 2D radiation pattern of the antenna is shown in figure.4.13. The antenna shows a non-directional radiation pattern in the H-plane and figure of eight pattern in the E-

plane. The maximum deviation of the received power in the H-plane is only 1dB. In both the planes the cross polar discrimination is better than 20dB.

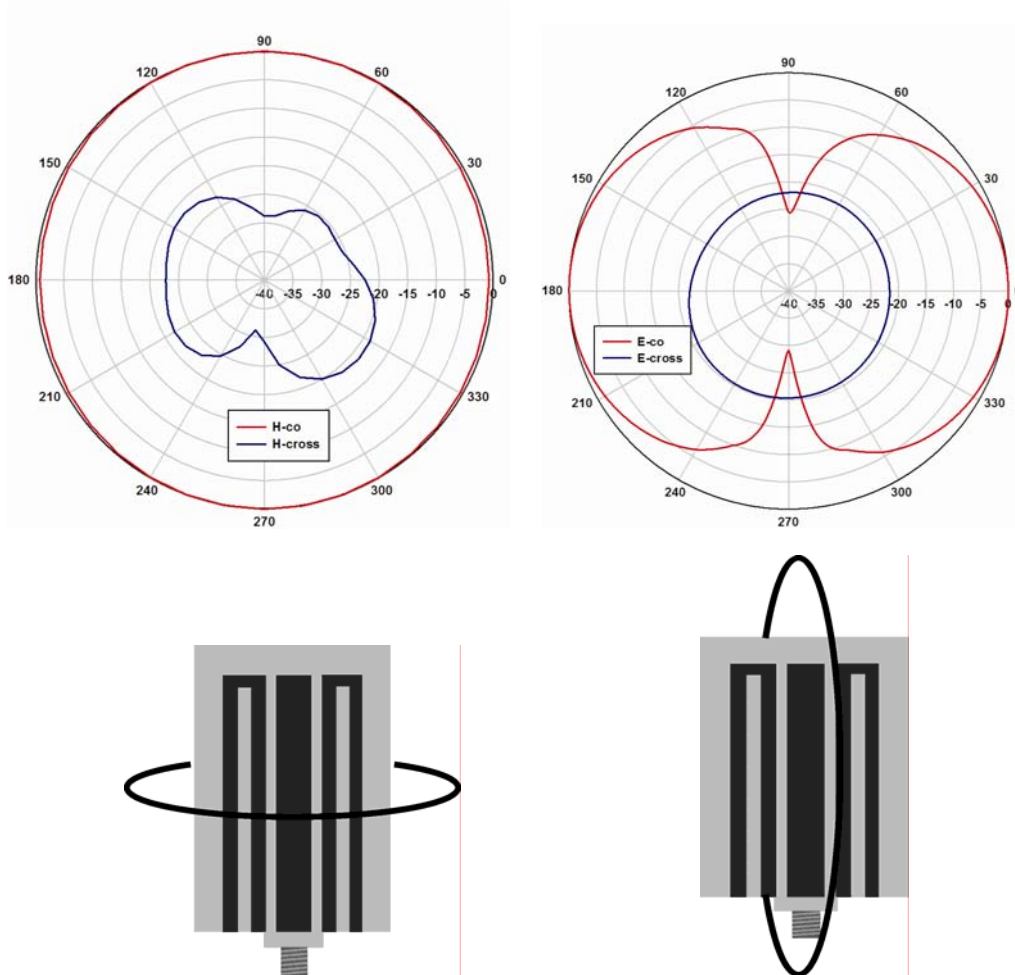


Figure 4.13 Simulated 2D radiation pattern of the ground meandered antenna ($L_g=20\text{mm}$, $W_g=2.5\text{mm}$, $W_s=1\text{mm}$, $W=3\text{mm}$, $g=1\text{mm}$, $S=0.5\text{mm}$, $h=1.6\text{mm}$ and $\epsilon_r=4.4$)

Even though the antenna provides good radiation characteristics, the resonance is not properly matched to provide the required impedance characteristics over the frequency bands. Therefore the next aim is to enhance the matching to increase the efficiency.

4.2.7 Reconfigurable Ground meandered antenna with pin diodes

The possibility of tuning the antenna is investigated here. The geometry of the antenna with switching device is shown in figure.4.14. A pin diode is placed at a distance S_L from the open end of the slot as shown in the figure. The variation in reflection characteristics with pin diode at different locations in the slot is shown in figure.4.15. With the forward biased diode placed at different positions, the current flow around the slot perimeter is modified. The current is found to flow through the diode during forward bias and hence the total resonating length gets altered. Thus by changing the diode position we can easily change the total slot perimeter and hence the resonance frequency. Switching to higher frequencies is possible by adding more PIN diodes. The frequency to which the antenna to be designed is determined by the diode position. This experiment again confirms that the resonance is due to the slot length.

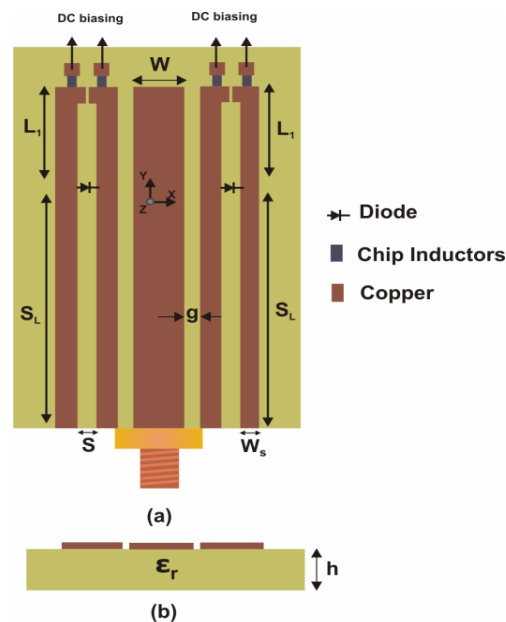


Figure 4.14 Geometry of the ground meandered antenna with pin diodes at different positions ($S_L+L_1=20\text{mm}$, $W_g=2.5\text{mm}$, $W_s=1\text{mm}$, $W=3\text{mm}$, $g=1\text{mm}$, $S=0.5\text{mm}$, $h=1.6\text{mm}$ and $\epsilon_r=4.4$)

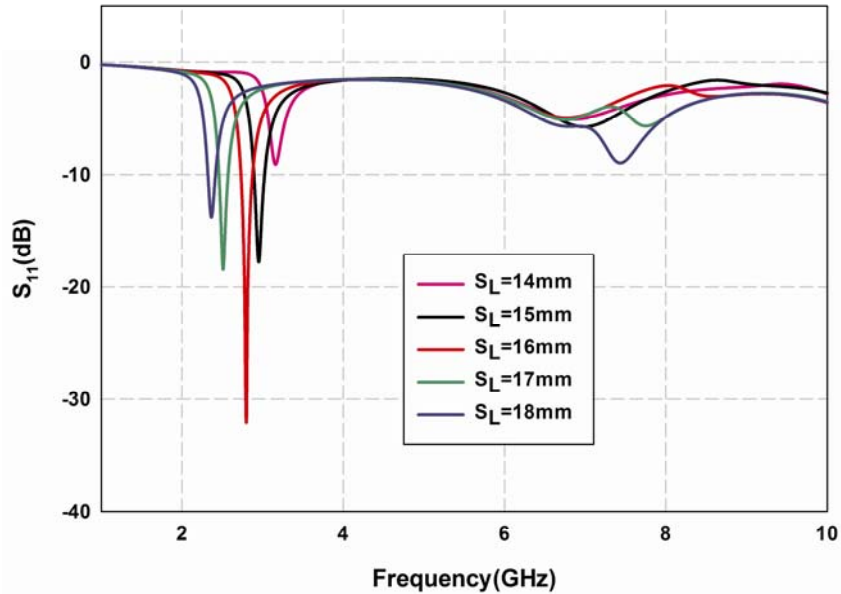


Figure 4.15 Variation in reflection characteristics of ground meandered antenna with pin diodes at different positions ($S_L+L_1=20$ mm, $W_g=2.5$ mm, $W_s=1$ mm, $W=3$ mm, $g=1$ mm, $S=0.5$ mm, $h=1.6$ mm and $\epsilon_r=4.4$)

4.3 Ground plane increased Meandered CPW fed antenna

A small ground plane of $L_g \times W_g$ mm² is introduced in the new design to increase the matching. A constant slot width of S is introduced inside the meandering structure. The open end of meandering should have a separation of 'p' from the ground plane. Thus the total length of both the meandered symmetrical ground becomes $(2 * L_1 + W_g + S)$ which primarily contribute for the resonance. The signal to ground plane gap 'g' remains unaltered in the present study.

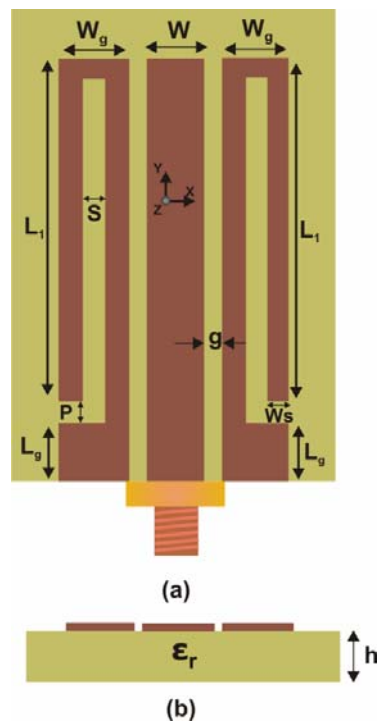


Figure 4.16 Geometry of the ground plane increased meandered antenna (a) Front view (b) Side view
 ($W_g=2.5\text{mm}$, $W_s=1\text{mm}$, $W=3\text{mm}$, $L_1=18\text{mm}$, $L_g=2.5\text{mm}$, $g=1\text{mm}$, $S=0.5\text{mm}$, $P=1\text{mm}$, $h=1.6\text{mm}$ and $\epsilon_r=4.4$)

The reflection and transmission characteristic of the antenna is shown in figure.4.17. The antenna resonates at 2.44GHz with good impedance match. It offers a 2:1 VSWR bandwidth from 2.33GHz-2.53GHz covering the 2.4GHz WLAN application band.

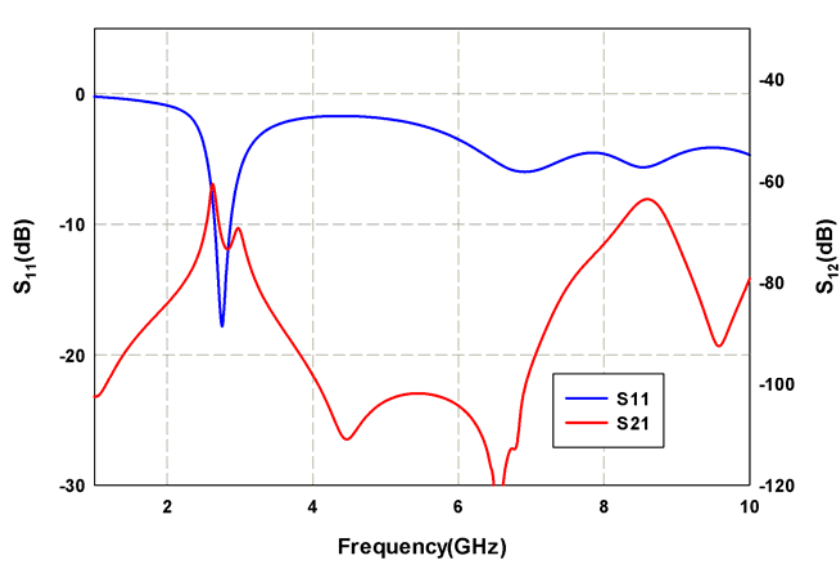


Figure 4.17 Reflection and transmission characteristics of the ground plane increased meandered antenna
 $(W_g=2.5\text{mm}, W_s=1\text{mm}, W=3\text{mm}, L_1=18\text{mm}, L_g=3\text{mm}, g=1\text{mm}, S=0.5\text{mm}, P=1\text{mm}, h=1.6\text{mm}$ and $\epsilon_r=4.4$)

4.3.1 Effect of varying the meandering strip L_1

The length of the meandered strip L_1 is varied and its effect on the reflection characteristics is discussed in this section. The variation of reflection coefficient with L_1 is shown in figure.4.18. As the strip length decreases the resonance shift to higher frequency with a corresponding deterioration in the impedance match. It is observed that as the length increases the reactive part becomes highly inductive. Moreover, while decreasing the length, the real part of impedance moves towards high value. Due to this the matching deteriorates. This antenna is scalable for all frequencies. In this present dimension the tuning is possible only for small frequency range ie by changing the length L_1 from 18mm to 14mm because of the constant signal strip length L_s .

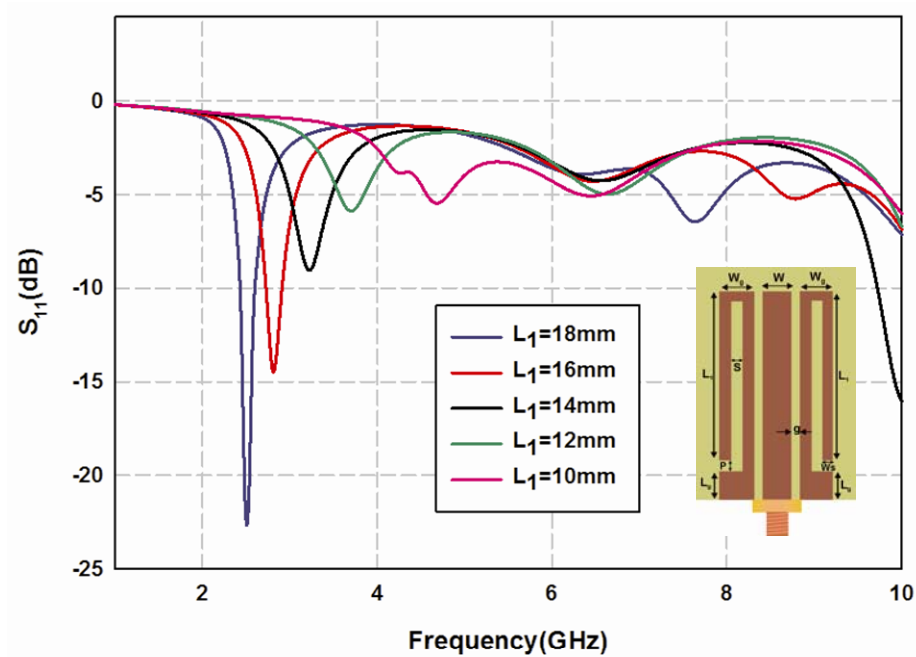


Figure 4.18 Variation in Reflection characteristics of the ground plane increased meandered antenna with strip length L_1 ($W_g=2.5\text{mm}$, $W_s=1\text{mm}$, $W=3\text{mm}$, $L_g=3\text{mm}$, $g=1\text{mm}$, $S=0.5\text{mm}$, $P=1\text{mm}$, $h=1.6\text{mm}$ and $\epsilon_r=4.4$)

4.3.2 Effect of increasing the signal strip length and ground plane length ($L_a = L_s - (L_1 + P + L_g)$)

It is necessary to confirm that the radiation characteristic is mainly due to the slot perimeter. The variation of reflection characteristics with L_a is shown in figure.4.19. From the figure it is clear that the first resonance is not varying with signal strip length, but its impedance matching is deeply affected. Since the slot length remains constant throughout, the resonance remains the same. Thus it is clearly confirmed from this variation study that the resonance is only due to slot perimeter. In order to attain constant meandered width W_s and to achieve impedance matching the length L_a is limited to 1mm.

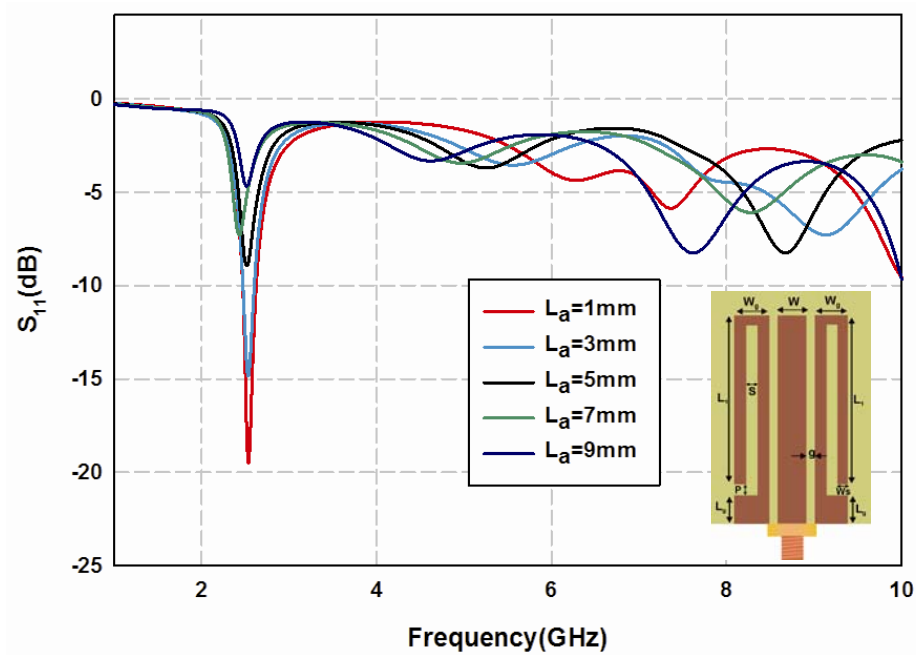


Figure 4.19 Variation in Reflection characteristics with signal strip and ground plane length of the ground plane increased meandered antenna by keeping the slot length constant ($W_g=2.5\text{mm}$, $W_s=1\text{mm}$, $W=3\text{mm}$, $L_g=3\text{mm}$, $L_1=18\text{mm}$ $g=1\text{mm}$, $S=0.5\text{mm}$, $P=1\text{mm}$, $h=1.6\text{mm}$ and $\epsilon_r=4.4$)

4.3.3 Variation in reflection characteristics with slot gap 's'

The variation in reflection characteristics of the antenna with slot gap 's' is shown in figure.4.20. It is noted that the gap 's' is not affecting the resonant frequency. By changing the gap the effective reactance and resistance remains almost unaltered hence there is not much change in the resonant frequency. Thus from the studies it is concluded that small variation in the slot gap is not much affecting the resonance frequency of the antenna.

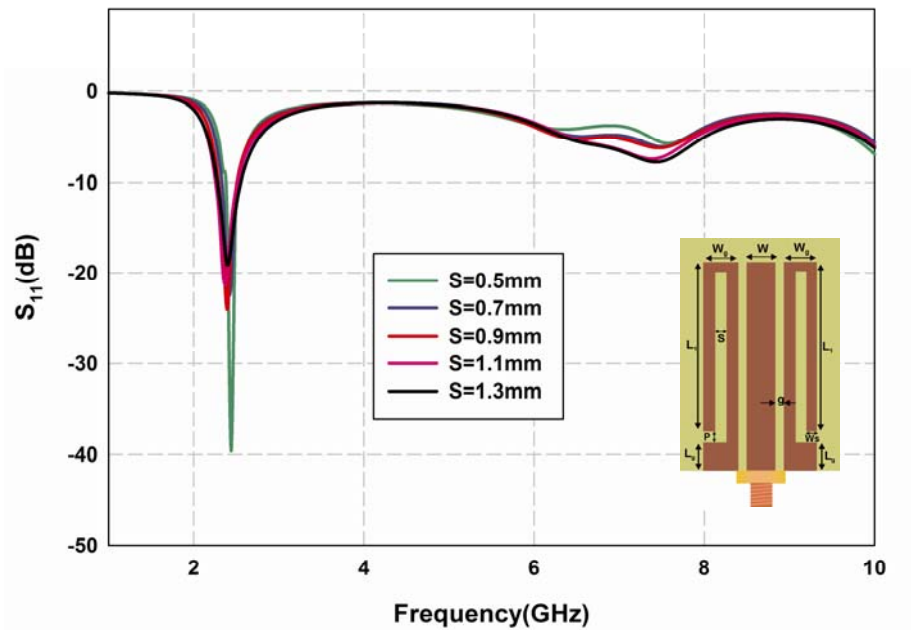


Figure 4.20 Variation in Reflection characteristics with slot gap 's' of the ground plane increased meandered antenna ($W_g=2.5\text{mm}$, $W_s=1\text{mm}$, $W=3\text{mm}$, $L_g=3\text{mm}$, $L_1=18\text{mm}$, $g=1\text{mm}$, $S=0.5\text{mm}$, $P=1\text{mm}$, $h=1.6\text{mm}$ and $\epsilon_r=4.4$)

4.3.4 Effect of increasing the ground plane length (L_g)

The variation of reflection characteristics with the ground plane length is discussed in this section. The length of the ground plane should not determine the resonant characteristics of the antenna ideally, since the antenna should be mounted on different environment. The variation of reflection characteristics of the antenna with feed length is shown in figure 4.21. It is clearly observed from the figure that the feed length is highly critical. Matching of the antenna is severely affected by the ground length. As the length of the feed increases the matching becomes poor. This should not happen in real time environment where large feed lengths should be used. It is also noted that the resonant frequency is independent of the ground plane length since the slot perimeter

which primarily constitutes for the resonance. Thus the ground is not playing as a good transmission line for larger ground lengths. As the length increases the impedance matching degrades and hence deteriorates the radiation characteristics. The variation in impedance performance with ground plane length should be minimized for real time application. This main hurdle is investigated in the next phase.

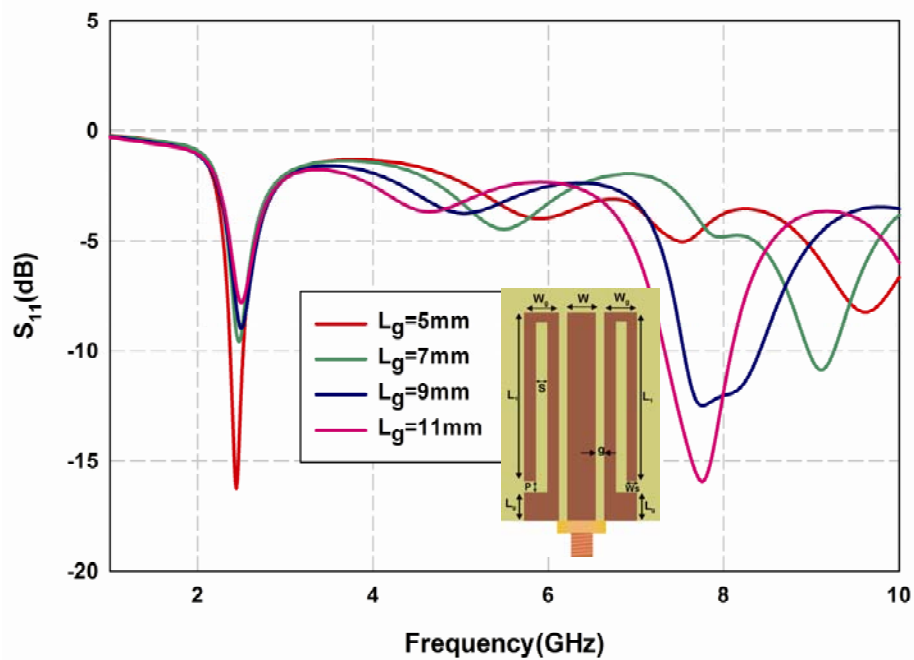


Figure 4.21 Variation of Reflection characteristics with ground plane length (feed length) of the ground plane increased meandered antenna by keeping all other parameters constant ($W_g=2.5\text{mm}$, $W_s=1\text{mm}$, $W=3\text{mm}$, $L_g=3\text{mm}$, $L_1=18\text{mm}$ $g=1\text{mm}$, $S=0.5\text{mm}$, $P=1\text{mm}$, $h=1.6\text{mm}$ and $\epsilon_r=4.4$)

4.3.5 Surface current distribution and Radiation pattern

To understand the radiation characteristics of the antenna the surface current distribution is presented. The surface current distribution of the antenna at resonant frequency is shown in figure.4.22. A symmetrical variation of

surface current in the two meandered arms is clearly seen in the figure.4.22. Moreover, the variation is continuous in the ground rectangle also. Thus any change in the ground dimension can affect the results significantly. This feature is also observed in the ground length extension study shown earlier. This should be avoided and the feed should remain as independent entity in a specific design for better performance. In this structure also the electric field vectors are aligned in the Y-direction causing the effective polarization along the Y- direction.

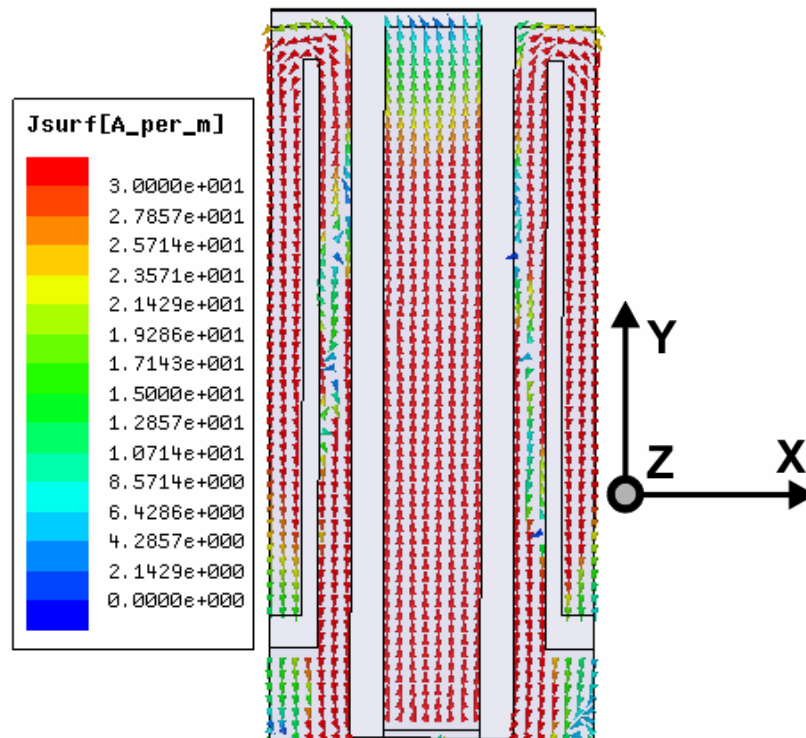


Figure 4.22 Current distribution of the ground plane increased meandered antenna
 $(W_g=2.5\text{mm}, W_s=1\text{mm}, W=3\text{mm}, L_1=18\text{mm}, L_g=3\text{mm}, g=1\text{mm}, S=0.5\text{mm}, P=1\text{mm}, h=1.6\text{mm}$ and $\epsilon_r=4.4$)

The 3-Dimensional and 2-Dimensional radiation patterns of the antenna at the resonance are shown in figure.4.23 and figure.4.24 respectively. The

antenna is giving a non-directional radiation pattern along the XZ plane and null along the Y-direction like a monopole antenna. Due to the symmetrical structure of the antenna, the radiation pattern is also symmetric. The antenna has non-directional radiation pattern in the H-plane and figure of eight radiation pattern in the E-plane with a beam width of more than 90° . The structure exhibits a cross polar discrimination of more than 25dB in both the planes. The radiation pattern shows the same characteristics throughout the band starting from 2.2GHz to 2.65GHz.

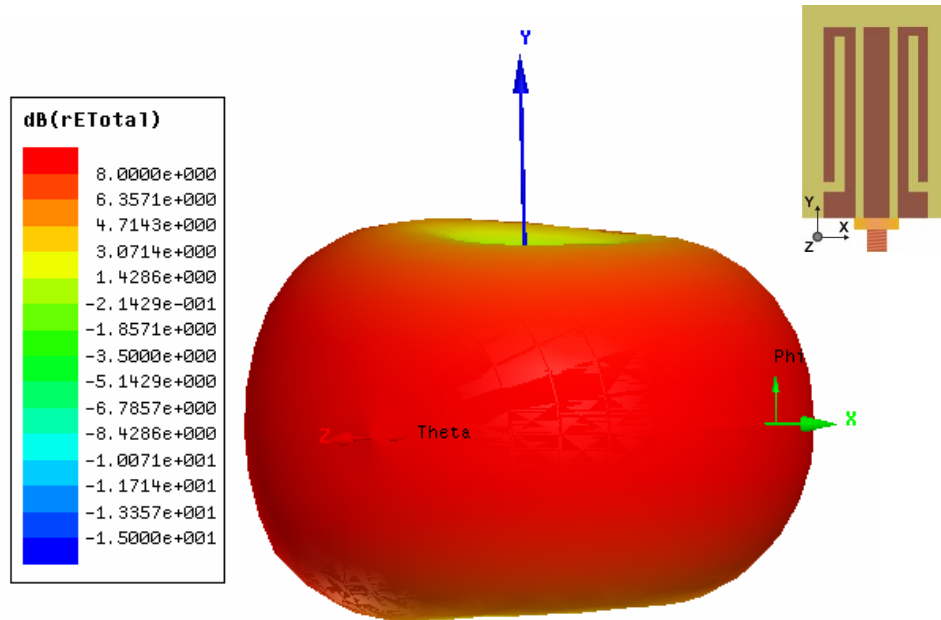


Figure 4.23 3D radiation pattern of the ground plane increased meandered antenna
($W_g=2.5\text{mm}$, $W_s=1\text{mm}$, $W=3\text{mm}$, $L_1=18\text{mm}$, $L_g=3\text{mm}$, $g=1\text{mm}$, $S=0.5\text{mm}$, $P=1\text{mm}$, $h=1.6\text{mm}$ and $\epsilon_r=4.4$)

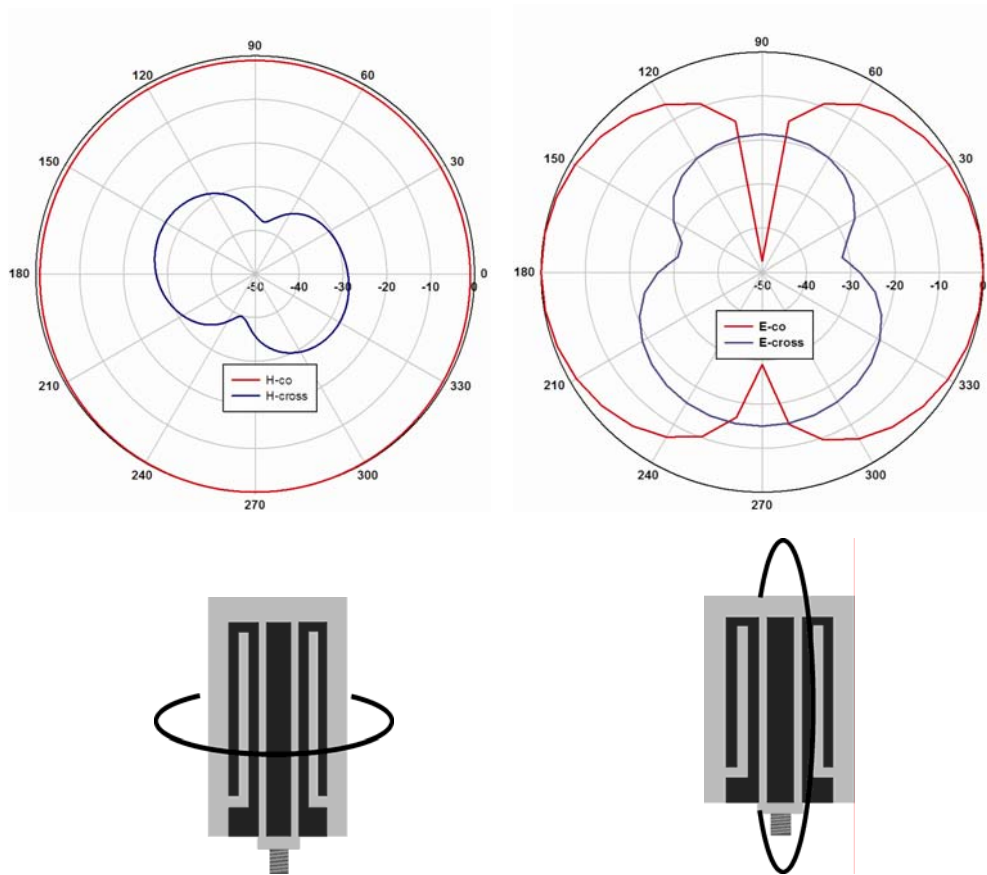


Figure 4.24 2D radiation pattern of the ground plane increased meandered antenna ($W_g=2.5\text{mm}$, $W_s=1\text{mm}$, $W=3\text{mm}$, $L_1=18\text{mm}$, $L_g=3\text{mm}$, $g=1\text{mm}$, $S=0.5\text{mm}$, $P=1\text{mm}$, $h=1.6\text{mm}$ and $\epsilon_r=4.4$)

The antenna shows good radiation characteristics, but the ground plane length is a mammoth factor which affects the matching. If the antenna is to be connected to an external circuit using coaxial cable or other transmission line, the ground plane length may alter, which may change the radiation characteristics. It is also shown in the previous section that ground length is also affecting the impedance match of the antenna. This should be avoided and impedance characteristics should be independent of transmission line length. Thus the impedance of the antenna should be properly matched to 50Ω to improve the performance of the antenna with variation in ground plane length.

Thus the main focus in next section is to tackle the effect of ground plane length and to develop a new design.

4.3.6 Reconfigurable ground plane increased antenna

A frequency reconfigurable ground plane increased antenna is shown in figure 4.25. As in the previous section BAR-64 pindiodes are connected at a distance S_L from the meandered strip end. Two chip inductors are connected as in figure to avoid the RF interference towards the external DC biasing circuit.

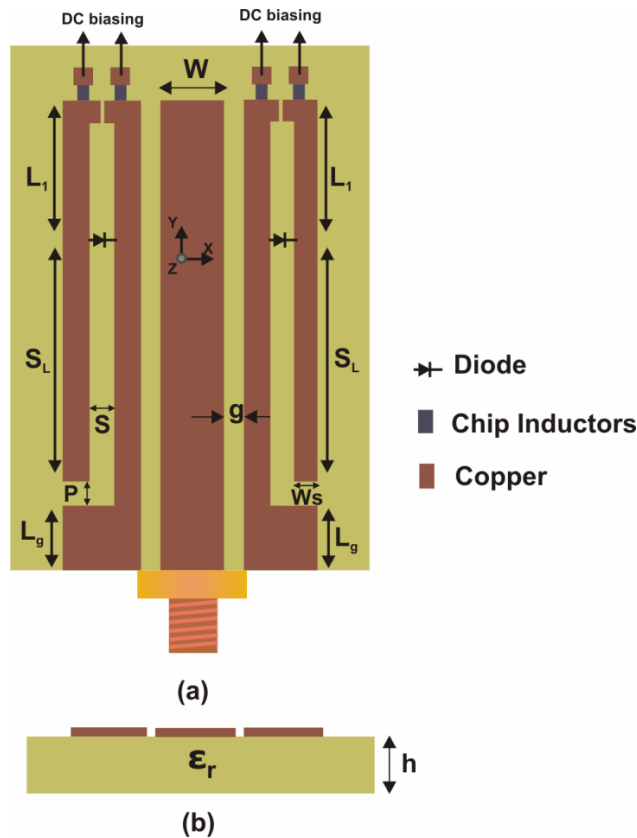


Figure 4.25 Geometry of the Reconfigurable ground plane increased meandered antenna using pin diodes
 $(W_g=2.5\text{mm}, W_s=1\text{mm}, W=3\text{mm}, S_L+L_1=18\text{mm}, L_g=3\text{mm}, g=1\text{mm}, S=0.5\text{mm}, P=1\text{mm}, h=1.6\text{mm}$ and $\epsilon_r=4.4$)

Variation studies have been performed by changing the pin diode position and its reflection characteristics are shown in figure.4.26. During the forward bias, the pin diodes act as a short circuit to RF and modify the current path. Thus the meandering path length will reduce and the frequency of the antenna will be shifted to higher regions. This method can be easily used for reconfigurable configurations. It is found from the observation that the tuning ratio is 1.35, ie we can tune the antenna from 2.6GHz to 3.5GHz conveniently by properly selecting the diode location.

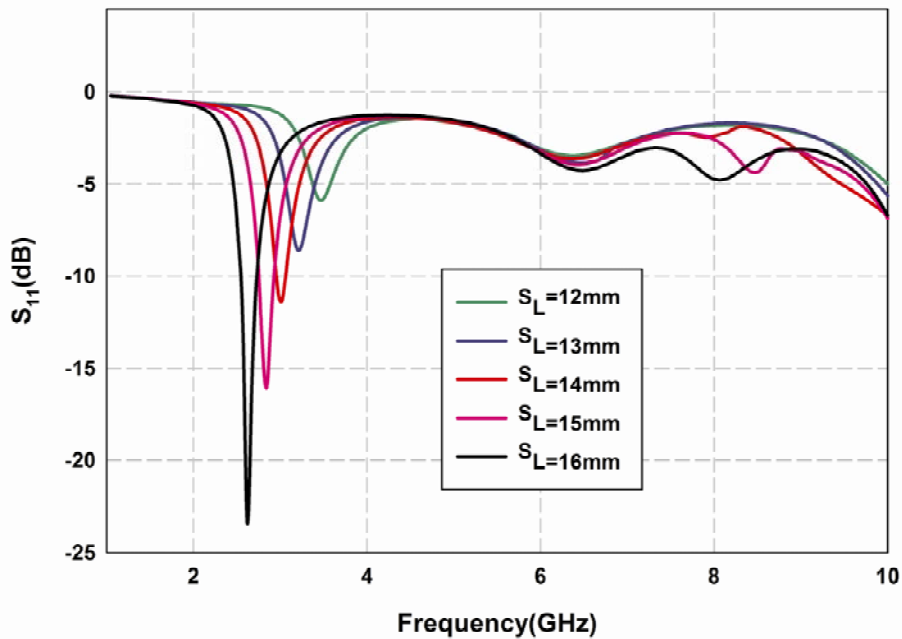


Figure 4.26 Variation of reflection characteristics of the antenna with diode position S_L
 ($W_g=2.5\text{mm}$, $W_s=1\text{mm}$, $W=3\text{mm}$, $L_1=18\text{mm}$, $L_g=3\text{mm}$, $g=1\text{mm}$, $S=0.5\text{mm}$, $P=1\text{mm}$, $h=1.6\text{mm}$ and $\epsilon_r=4.4$)

The main conclusions from the above section are,

- The antenna is resonating with the resonant length corresponding to the meandered strip length, ie the perimeter of the slot.

- By varying the perimeter of the slot the resonance of the antenna can be tuned to required frequency.
- The radiation pattern is highly symmetrical due to the symmetrical nature of the antenna structure.
- The impedance match of the antenna is found to vary with ground plane or the feed length.
- Radiation properties need to be improved further for using this antenna in real time applications.

4.4 Geometry of the proposed Compact CPW fed antenna

An antenna is supposed to connect to the internal electronic circuits through a transmission line. Thus the length of the transmission line must not affect its performance. Even though the increased ground area can improve the radiation characteristics, the reflection characteristic is not stable with ground plane length as shown in figure.4.21. Hence the electrical property of this antenna varies slightly with the connector dimensions. It is because the input impedance of the antenna is not perfectly matched to 50Ω . As per the design equation of coplanar waveguide feed, the gap, 'g' and signal strip width 'W' should be optimized for 50Ω . As such the gap g is calculated as 0.35mm, for a signal strip width $W=3\text{mm}$ when printed on a substrate of dielectric constant 4.4 and thickness 1.6mm. The geometry of the compact ground modified antenna is shown in figure.4.27.

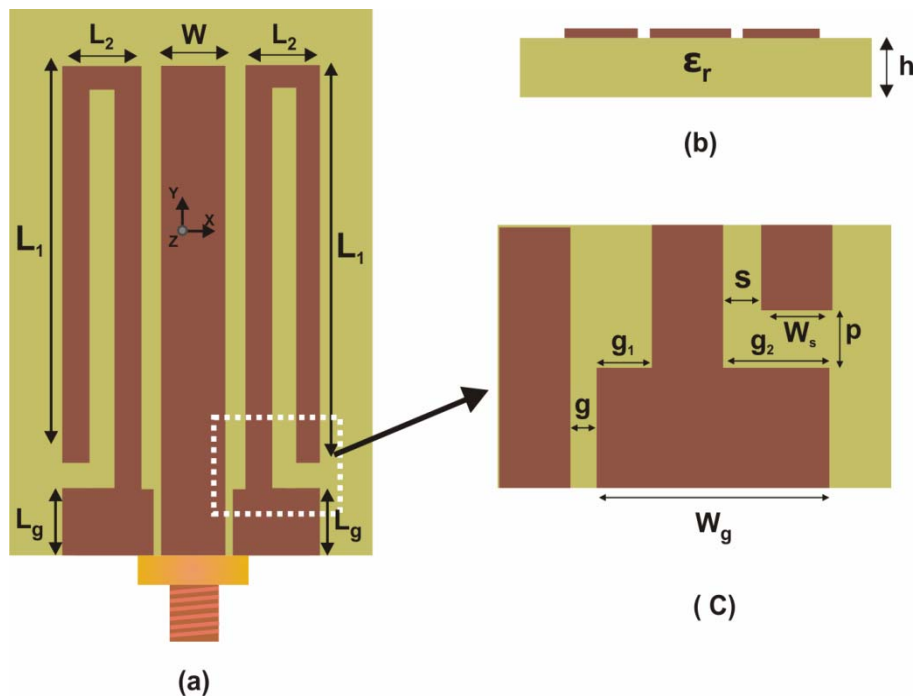


Figure 4.27 Geometry of the ground modified meandered antenna

It is necessary to reconfirm that this structure have the same characteristics of the earlier antenna discussed in the previous section. The mode of propagation on the antenna should not vary with change in any of the antenna parameters. To understand the effect of various parameters on antenna performance, exhaustive parametric analysis are performed and are discussed in the following sections.

4.4.1 Effect of varying the Meandered length L_1

The effect on the radiation characteristics of the antenna with meandering strip length L_1 is discussed in this section. The variation of reflection coefficient with the signal strip length L_1 is shown in figure.4.28. It is clear that the resonant frequency is depending on this length. As the length decreases the resonant frequency shift to higher frequency region as shown in the figure.

Thus frequency can be tuned by varying the strip length. There are physical constraints to increase the strip length beyond 64% of the total y-dimension, and hence it is the maximum length attainable without altering the overall compactness.

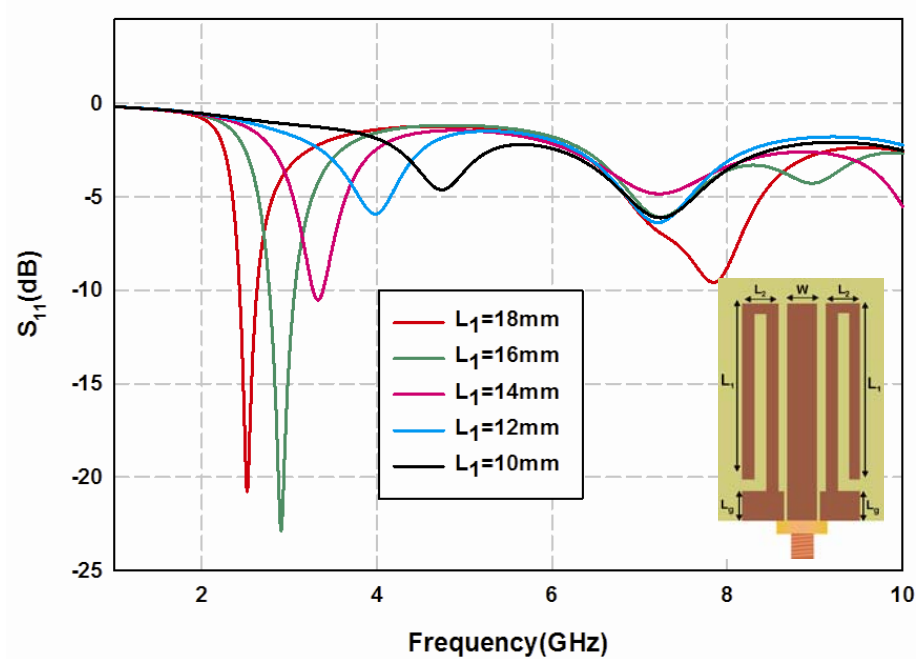


Figure 4.28 Variation in reflection characteristics with Meandered strip (L_1) of the ground modified planar antenna ($W_g=3.15\text{mm}$, $L_g=3\text{mm}$, $L_2=2.5\text{mm}$, $W_s=1\text{mm}$, $W=3\text{mm}$, $g=0.35\text{mm}$, $g_1=0.65\text{mm}$, $g_2=1.5\text{mm}$, $P=1\text{mm}$, $S=0.5\text{mm}$, $h=1.6\text{mm}$ and $\epsilon_r=4.4$)

4.4.2 Effect of varying the ground length L_g

The other important factor to be characterized for good antenna performance is the ground plane length L_g . If the antenna is connected by an external coaxial or other transmission line its performance should not change. The variation of reflection coefficient with the ground plane length of the antenna is shown in figure.4.29. The resonance of the antenna remains

unaltered with the ground length as it is perfectly behaving as a normal transmission line. Moreover, it is found that there is not much variation in the impedance match with the transmission line length. Thus it is confirmed in the present design that the effect of ground plane is not critical and is more stable than the unmodified antenna discussed earlier. Hence the problem of ground plane extension is prevailed by introducing the 50Ω balanced feed.

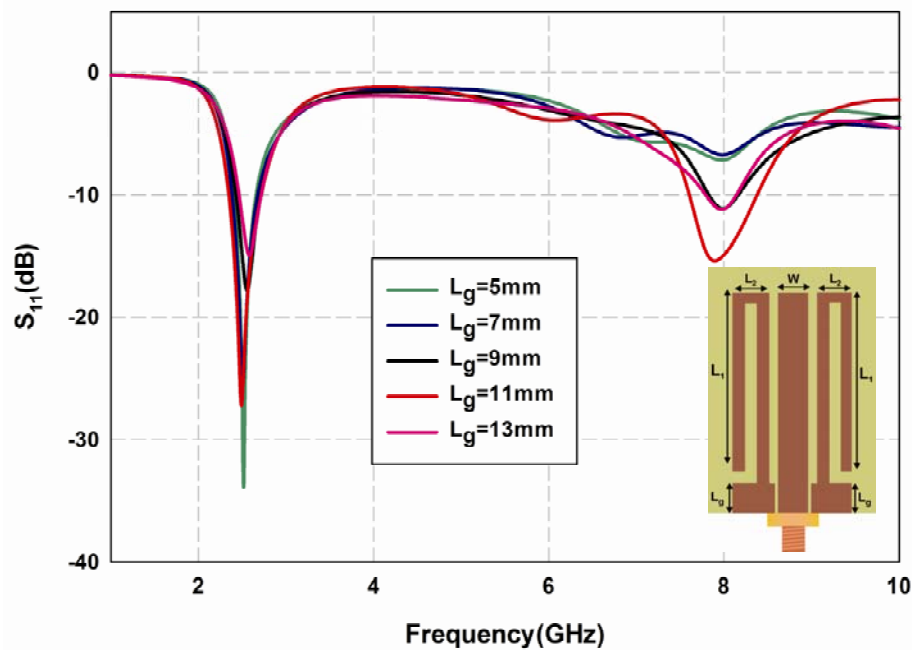


Figure 4.29 Variation in reflection characteristics with Ground plane length L_g of the ground modified planar antenna ($L_1=18\text{mm}$, $W_g=3.15\text{mm}$, $L_2=2.5\text{mm}$, $W_s=1\text{mm}$, $W=3\text{mm}$, $g=0.35\text{mm}$, $g_1=0.65\text{mm}$, $g_2=1.5\text{mm}$, $P=1\text{mm}$, $S=0.5\text{mm}$, $h=1.6\text{mm}$ and $\epsilon_r=4.4$)

4.4.3 Variation in reflection characteristics with slot gap 's'

The variation in reflection characteristics with slot gap 's' of the ground modified coplanar waveguide fed antenna is shown in figure.4.30. As explained in the previous sections the gap is not much affecting the impedance match and resonant frequency of the antenna. As the strip gap

increases the perimeter of the slot causing the resonance is increased slightly causing a very minute shift in the resonant frequency. There is some physical constraints for increasing the slot gap beyond or equal to the ground plane width. Since the variation is not critical the user has the liberty to choose the antenna parameters without much design constraints. Moreover, there is not much effect on increasing the gap on the impedance characteristics and hence it can be fixed at any arbitrary value. The gap width is chosen as 0.5mm in this thesis.

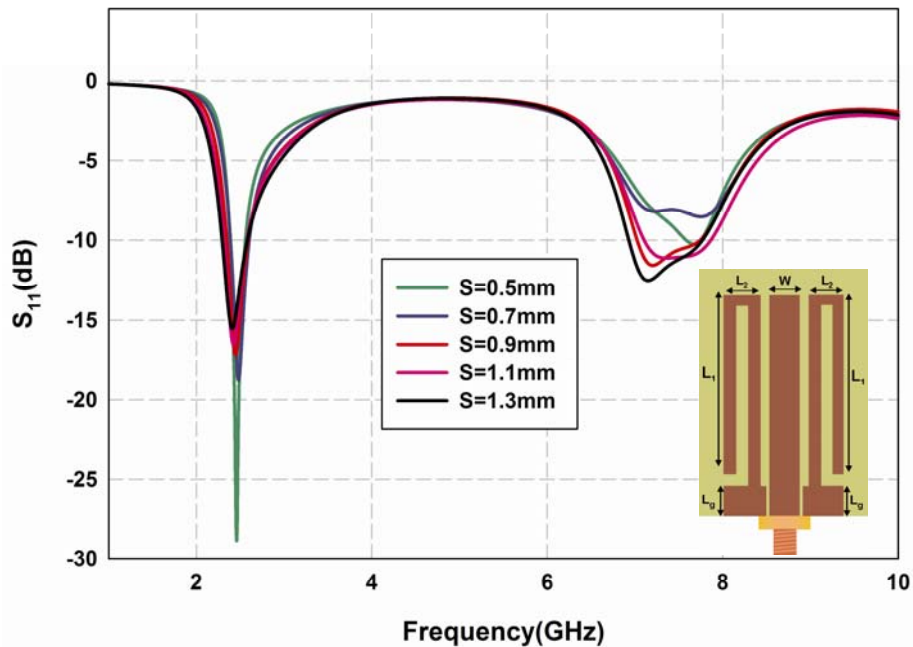


Figure 4.30 Variation in reflection characteristics of the ground modified planar antenna with slot gap's'
 ($L_1=18\text{mm}$, $W_g=3.15\text{mm}$, $L_2=2.5\text{mm}$, $W_s=1\text{mm}$, $W=3\text{mm}$, $g=0.35\text{mm}$, $g_1=0.65\text{mm}$, $g_2=1.5\text{mm}$, $P=1\text{mm}$, $S=0.5\text{mm}$, $h=1.6\text{mm}$ and $\epsilon_r=4.4$)

4.4.4 Effect of varying the substrate height h

The variation in the resonant characteristics of the antenna with respect to the height of the substrate is shown in the figure.4.31. From the figure it is clear

that there is not much variation in resonance frequency with height of the substrate. Moreover, the fringing fields are from the signal strip to ground plane which are placed on the same side of the substrate (uniplanar) and hence there is not much field inside the substrate. This gives an independent privilege for the designer in choosing the substrate height.

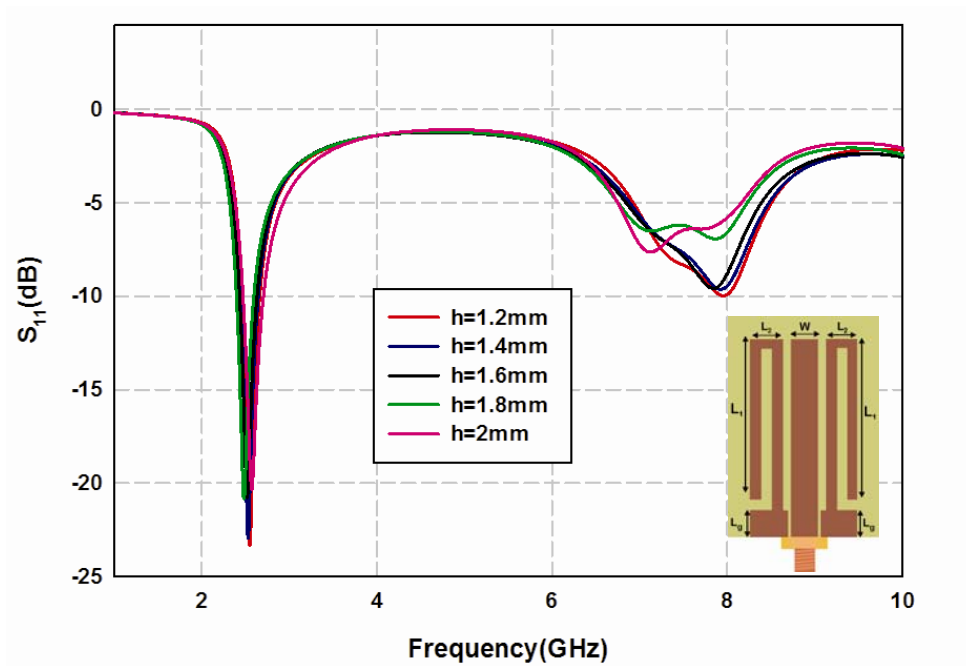


Figure 4.31 Variation in reflection characteristics with substrate height h of the ground modified planar antenna ($L_1=18$ mm, $W_g=3.15$ mm, $L_g=3$ mm, $L_2=2.5$ mm, $W_s=1$ mm, $W=3$ mm, $g=0.35$ mm, $g_1=0.65$ mm, $g_2=1.5$ mm, $P=1$ mm, $S=0.5$ mm and $\epsilon_r=4.4$)

4.4.5 Effect of varying the Dielectric constant (ϵ_r)

The dielectric constant of the antenna is varied by keeping the impedance 50 Ω . While varying the dielectric constant of the substrate the impedance match of the antenna remains unaltered but the resonant frequency shifts. Since the antenna is uniplanar in nature, its dependency on the substrate is negligible. The variation in resonant frequency with the dielectric constant

of the substrate is shown in the figure.4.32. As the dielectric constant increases the resonant frequency decreases with a corresponding increase in quality factor because the fringing fields are more confined with increasing the dielectric constant.

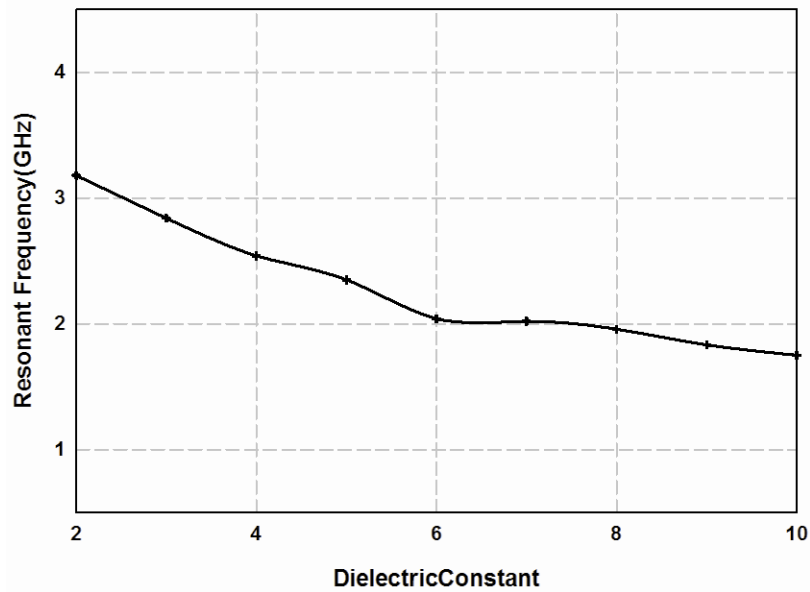


Figure 4.32 Variation in reflection characteristics with substrate Dielectric constant of the ground modified planar antenna ($L_1=18\text{mm}$, $L_g=3\text{mm}$, $W_g=3.15\text{mm}$, $W_s=1\text{mm}$, $W=3\text{mm}$, $g=0.35\text{mm}$, $g_1=0.65\text{mm}$, $g_2=1.5\text{mm}$, $P=1\text{mm}$, $S=0.5\text{mm}$ and $h=1.6\text{mm}$)

Thus from the above parametric analysis the geometry of the antenna is optimized for good radiation and impedance characteristics. The final parameters of the compact ground modified CPW fed antenna is shown in the table 4.1.

Table.4.1 Antenna parameters of the ground modified CPW fed planar antenna

Sl. No	Antenna parameter	Optimized value
1	L_g	$0.035 \lambda_g$
2	L_1	$0.21 \lambda_g$
3	L_2	$0.0296 \lambda_g$
4	W_g	$0.0374 \lambda_g$
5	W_s	$0.0118 \lambda_g$
6	W	$0.035 \lambda_g$
7	g	$0.004 \lambda_g$
8	g_1	$0.0077 \lambda_g$
9	g_2	$0.0178 \lambda_g$
10	P	$0.0118 \lambda_g$
11	S	$0.0059 \lambda_g$
12	h	$0.019 \lambda_g$
13	ϵ_r	4.4

4.4.6 Reflection characteristics of the Ground modified planar antenna

The simulated and measured reflection characteristic of the proposed antenna is shown in figure 4.33. The simulation is carried out using Ansoft HFSS and measurement using HP8510C Vector Network Analyser. The result shows good agreement between the simulation and experiment. The 2:1 VSWR bandwidth of the antenna is from 2.38GHz-2.68GHz with 12% impedance bandwidth. This measured 300MHz bandwidth is wide enough to cover the 2.4GHz WLAN application band. The impedance characteristic of the optimized antenna is shown in figure.4.34.

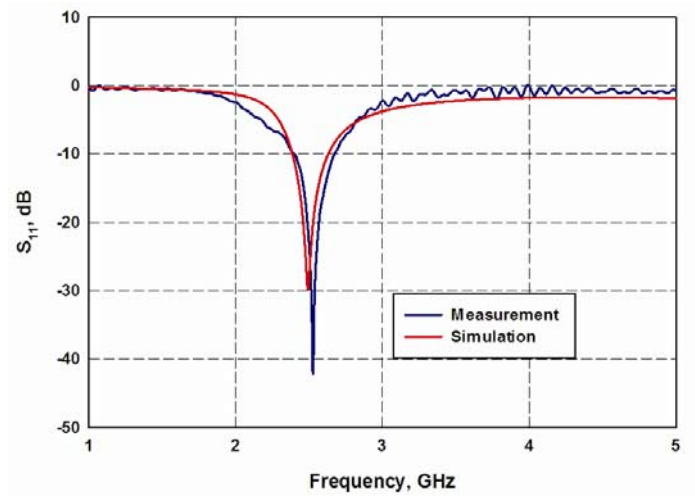


Figure 4.33 Reflection characteristics of the optimized antenna ($W_g=3.15\text{mm}$, $L_1=18\text{mm}$, $L_g=3\text{mm}$, $W_s=1\text{mm}$, $W=3\text{mm}$, $g=0.35\text{mm}$, $g_1=0.65\text{mm}$, $g_2=1.5\text{mm}$, $P=1\text{mm}$, $S=0.5\text{mm}$, $h=1.6\text{mm}$ and $\epsilon_r=4.4$)

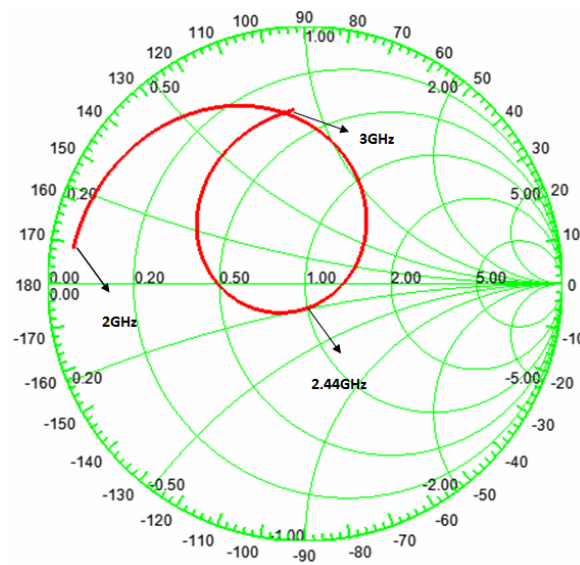


Figure 4.34 Impedance characteristics of the optimized ground modified planar antenna ($W_g=3.15\text{mm}$, $L_1=18\text{mm}$, $L_g=3\text{mm}$, $W_s=1\text{mm}$, $W=3\text{mm}$, $g=0.35\text{mm}$, $g_1=0.65\text{mm}$, $g_2=1.5\text{mm}$, $P=1\text{mm}$, $S=0.5\text{mm}$, $h=1.6\text{mm}$ and $\epsilon_r=4.4$)

The impedance characteristic of the antenna from 2GHz to 3GHz is shown in figure.4.34. A matched resonance centered at 2.44GHz is clearly observed in the figure.

4.4.7 Surface current distribution and Radiation pattern

The simulated surface current distribution of the antenna is shown in figure.4.35. There is a symmetrical variation of current along the symmetrical meandered path. At resonance, a quarter wave variation of the current along the length is noticed. The electric field components are aligned along Y-direction as observed in the current distribution. Since the major contributions are from the Y-component, the polarization of the antenna is also along Y-direction. It is also to be noted that the radiation is entirely due to the meandered symmetrical strips. The photograph of the fabricated antenna is shown in figure.4.36. The antenna has an overall dimension of 22mmX10mmX1.6mm, which is highly compact to be mounted on small electronic gadgets.

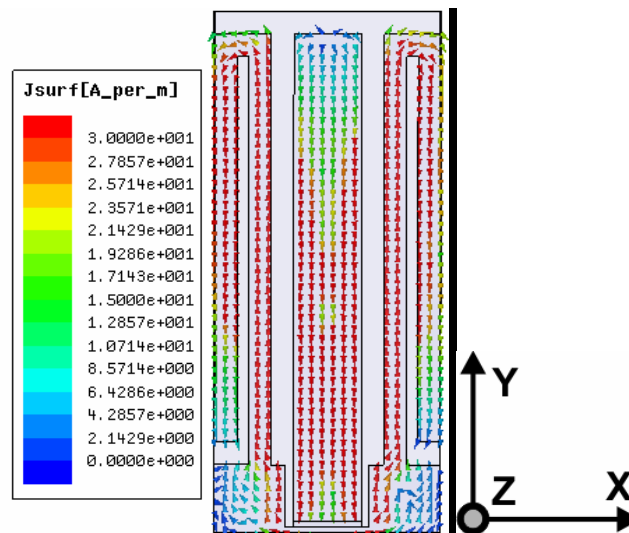


Figure 4.35 Simulated Current distribution of the optimized ground modified planar antenna
 $(L_1=18\text{mm}, L_g=2.5\text{mm}, W_g=3.15\text{mm}, W_s=1\text{mm}, W=3\text{mm}, g=0.35\text{mm}, g_1=0.65\text{mm}, g_2=1.5\text{mm}, P=1\text{mm}, S=0.5\text{mm}, h=1.6\text{mm}$ and $\epsilon_r=4.4)$

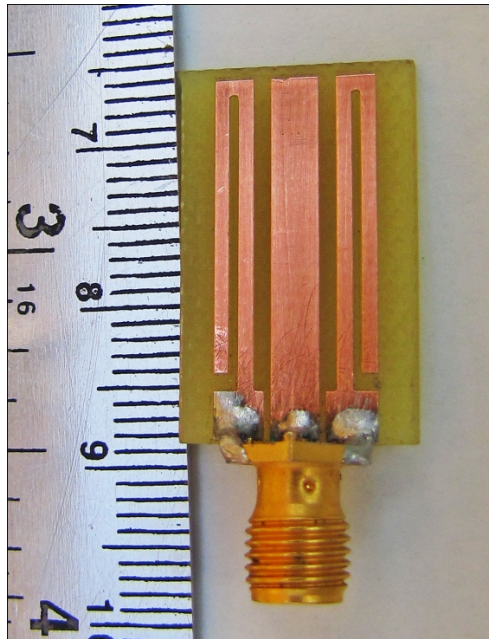


Figure 4.36 Photograph of the optimized ground modified planar antenna ($L_1=18\text{mm}$, $L_g=2.5\text{mm}$, $W_g=3.15\text{mm}$, $W_s=1\text{mm}$, $W=3\text{mm}$, $g=0.35\text{mm}$, $g_1=0.65\text{mm}$, $g_2=1.5\text{mm}$, $P=1\text{mm}$, $S=0.5\text{mm}$, $h=1.6\text{mm}$ and $\epsilon_r=4.4$)

The 3D radiation pattern of the antenna at 2.44GHz is shown in figure.4.37. The pattern is highly symmetric and omnidirectional in nature. Since the structure is highly symmetrical with respect to the signal strip there is no tilt in the radiation pattern.

The 2D radiation pattern of the antenna is shown in figure.4.38 (a) & (b). From the figure it is clear that the antenna has a non directional radiation pattern in the XZ-plane and figure of eight radiation pattern in the YZ-plane. The cross polar isolation of the antenna is found to be better than 15dB on both the planes. The antenna offers a size reduction of more than 85% compared to a standard CPW fed quarter wavelength monopole antenna. Moreover, the antenna provides an average gain of 1.3dBi and an efficiency of 75%.

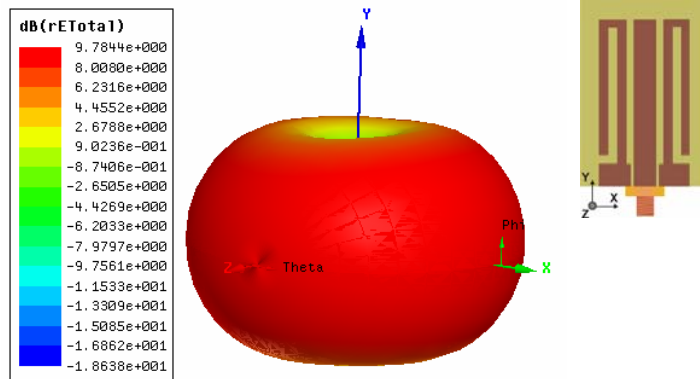


Figure 4.37 Simulated 3D radiation pattern of the ground modified planar antenna ($L_1=18\text{mm}$, $L_g=2.5\text{mm}$, $W_g=3.15\text{mm}$, $W_s=1\text{mm}$, $W=3\text{mm}$, $g=0.35\text{mm}$, $g_1=0.65\text{mm}$, $g_2=1.5\text{mm}$, $P=1\text{mm}$, $S=0.5\text{mm}$, $h=1.6\text{mm}$ and $\epsilon_r=4.4$)

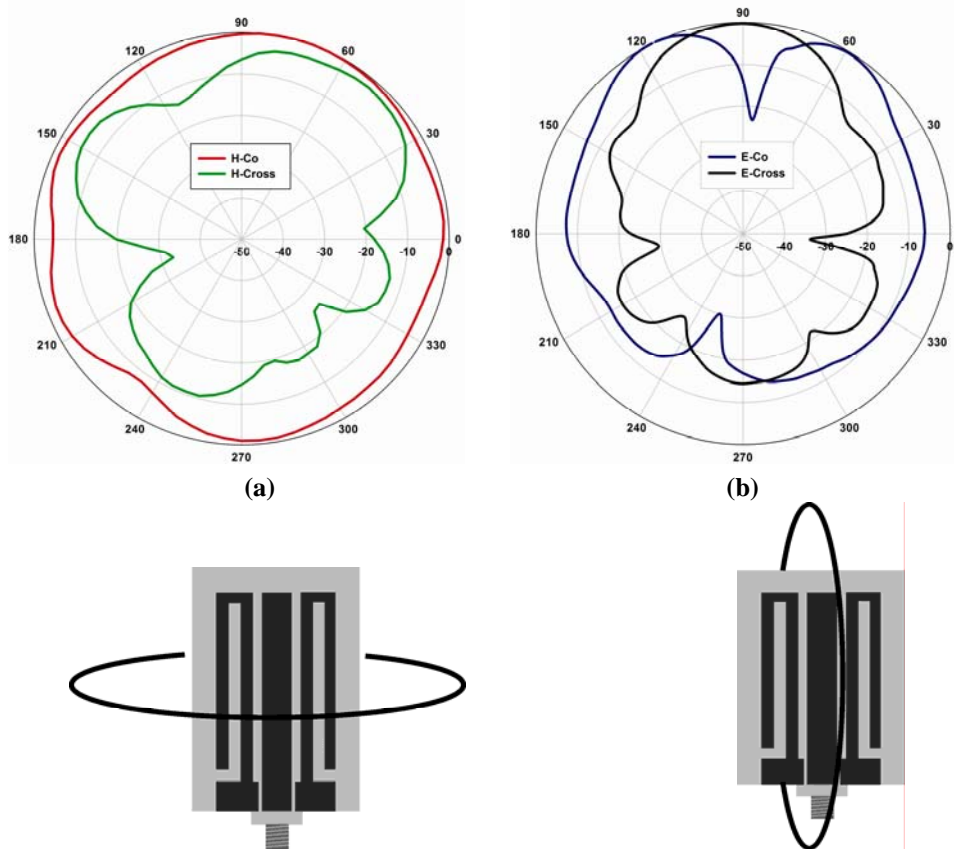


Figure 4.38 Measured 2-Dimensional radiation pattern of the optimized ground modified planar antenna ($L_1=18\text{mm}$, $L_g=2.5\text{mm}$, $W_g=3.15\text{mm}$, $W_s=1\text{mm}$, $W=3\text{mm}$, $g=0.35\text{mm}$, $g_1=0.65\text{mm}$, $g_2=1.5\text{mm}$, $P=1\text{mm}$, $S=0.5\text{mm}$, $h=1.6\text{mm}$ and $\epsilon_r=4.4$)

4.4.8 Reconfigurable ground modified planar antenna using pin diodes

The possibilities of tuning the antenna for reconfigurable applications are presented here. Two diodes are connected at a distance S_L from the open end of the slot as shown in figure.4.33. A small gap is created and a chip inductor is also connected in the structure for providing better DC and RF isolation as shown in the figure. The reconfiguration is possible from the fundamental lower frequency to higher frequency.

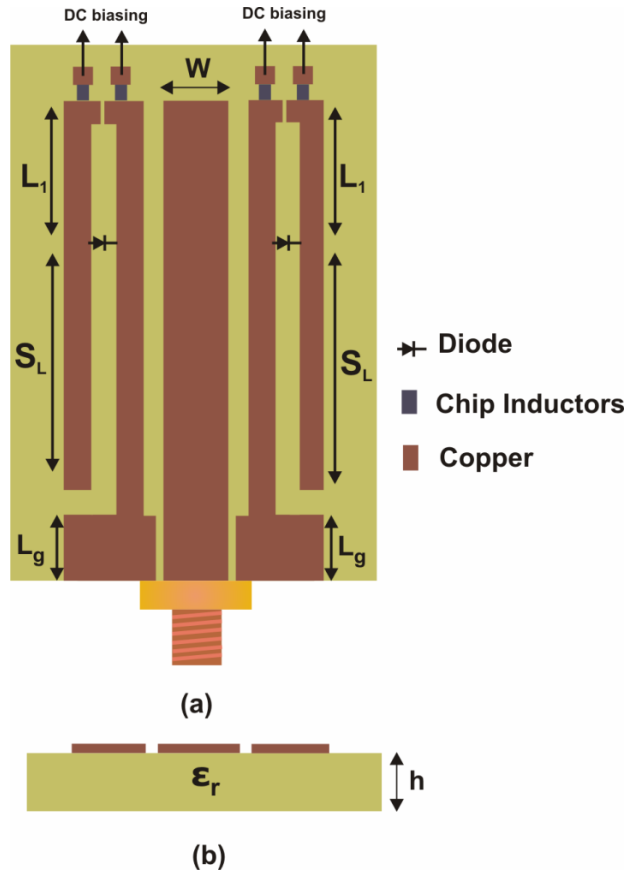


Figure 4.39 Geometry of the reconfigurable ground modified planar antenna using pin diodes
 $(W_g=2.5\text{mm}, W_s=1\text{mm}, W=3\text{mm}, L_1=18\text{mm}, L_g=3\text{mm}, g=1\text{mm}, S=0.5\text{mm}, P=1\text{mm}, h=1.6\text{mm}$ and $\epsilon_r=4.4$)

The variation in reflection characteristics with the pin diode position S_L is shown in figure.4.40. Forward biased PIN diode act as a short circuit and reduces the resonating length and shifts the resonant frequency to higher frequency region. All the studies are conducted for symmetric pin diode positions.

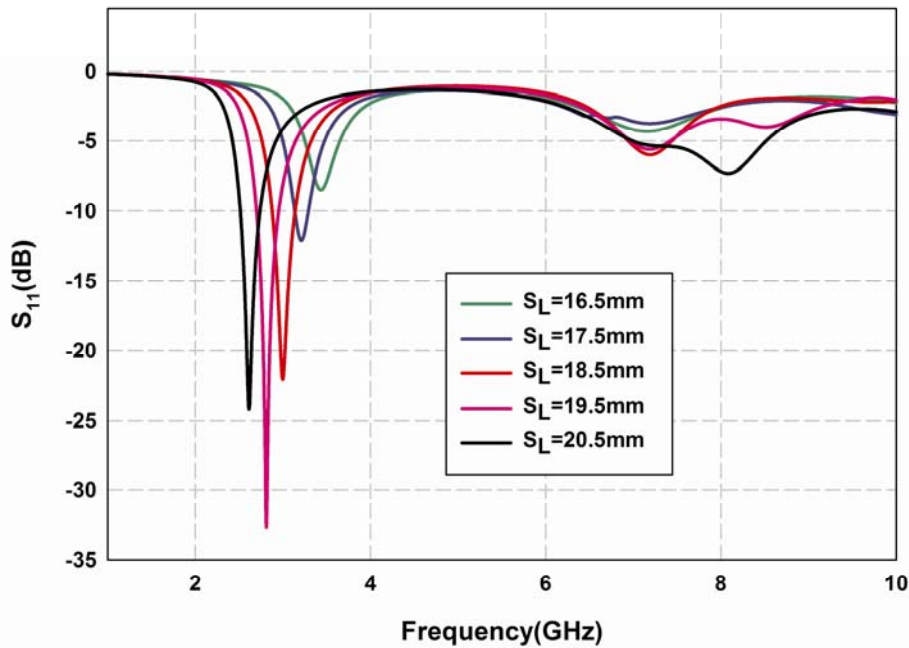


Figure 4.40 Variation in reflection characteristic of the antenna with pin diode position S_L
 ($W_g=2.5$ mm, $W_s=1$ mm, $W=3$ mm, $L_1=18$ mm, $L_g=3$ mm, $g=1$ mm, $S=0.5$ mm, $P=1$ mm, $h=1.6$ mm and $\epsilon_r=4.4$)

4.5 Conclusion of the ground optimized antenna

Thus the important conclusions arrived are

- The signal to ground plane gap 'g' plays an important role in determining the impedance characteristics of a coplanar waveguide transmission line.

- An optimum lateral ground plane width is necessary for a coplanar waveguide to behave like a normal transmission line. Further increase in ground plane will not enhance the impedance and radiation characteristics.
- The ground plane meandering can be effectively utilized to control the resonance of the antenna.
- Meandering can lower the resonance frequency.
- The resonant length is proportional to the slot perimeter.
- Since the radiating elements are purely along Y-direction, the antenna is highly linearly polarized with good cross polar isolation.
- Due to symmetry, the radiation pattern is also symmetric in nature.
- The radiation characteristics of a symmetrically ground meandered antenna is similar to that of a monopole antenna.

.....❧.....

INVESTIGATION ON SIGNAL STRIP AND GROUND PLANE MODIFIED CPW FED PLANAR ANTENNA

<i>Contents</i>	5.1 Coplanar Waveguide structure
	5.2 Asymmetrically slotted CPW fed open ended transmission line.
	5.3 CPW fed open ended antenna with Symmetrical slots
	5.4 Symmetrically slotted antenna
	5.5 Symmetrically slotted Reconfigurable antenna
	5.6 H-shaped slot antenna with Harmonic Suppression
	5.7 Conclusion

This chapter deals with the design and development of signal strip and ground plane modified coplanar waveguide (CPW) fed planar antenna. The CPW transmission line is transformed into a radiating structure by suitable modification of ground plane and signal strip. This is achieved by placing a slot on the lateral ground plane and by modifying the signal strip. A thorough parametric analysis is presented to understand the radiation characteristics and performance. This antenna has a monopole like radiation pattern and can be easily scalable to any required application band.

5.1 Coplanar Waveguide structure

Studies on Coplanar Waveguide (CPW) transmission line by varying the signal strip and ground planes are discussed in chapter 3 and chapter 4 respectively. And it is shown that the transmission line will start to radiate electromagnetic energy by creating a discontinuity. The studies were conducted by increasing the signal strip length and by meandering the ground plane. In this chapter the tendency to radiate em energy with discontinuity is initially verified by reducing the signal strip length within the overall ground plane dimension and then by creating discontinuity on both of the lateral ground planes.

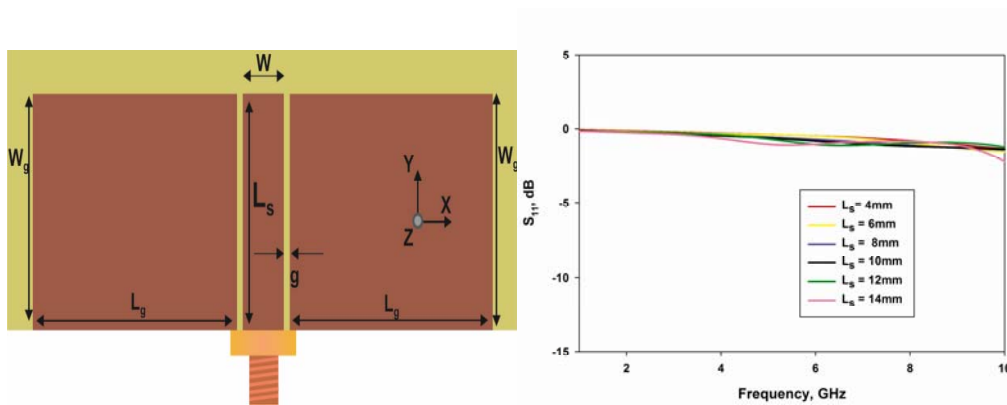
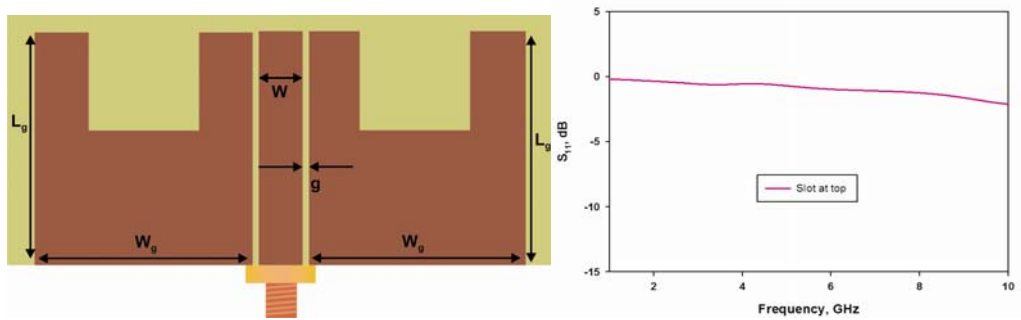


Figure 5.1 a) CPW fed transmission line b) Variation in reflection characteristics with Signal strip length L_s ($L_g=15\text{mm}$, $W_g=15\text{mm}$, $g=0.35\text{mm}$ and $W=3\text{mm}$)

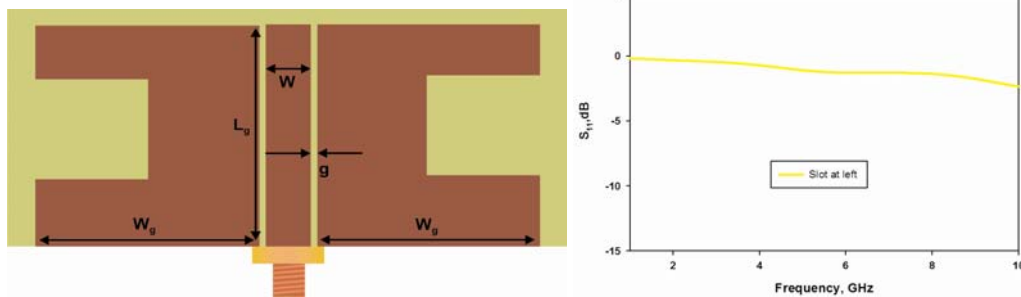
Variations in reflection characteristics for different signal strip length of a CPW fed Transmission line are shown in figure.5.1. From the figure it is clear that the total energy gets reflected back and there is no tendency of any radiation by reducing the signal strip length with 1GHz - 10GHz band. So it is not possible to create an antenna by simply reducing the signal strip length.

Without increasing the size of the above structure, how can we make a radiating element?. It is reported that using different structures like metamaterial as

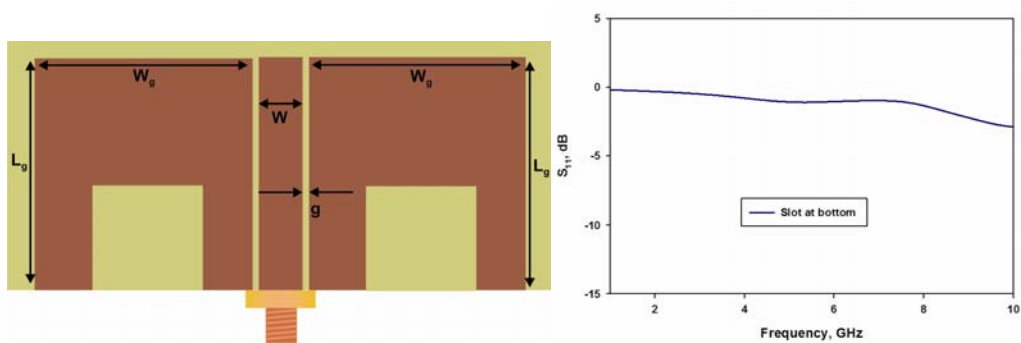
ground plane sub wavelength structure can radiate electromagnetic energy. But the structure is more complex and offers narrow bandwidth. Another possibility is to produce discontinuity on the ground plane. Some of the different possible combinations to create discontinuity in the ground plane are depicted in figure.5.2. and their corresponding reflection characteristics are also shown.



(a)



(b)



(c)

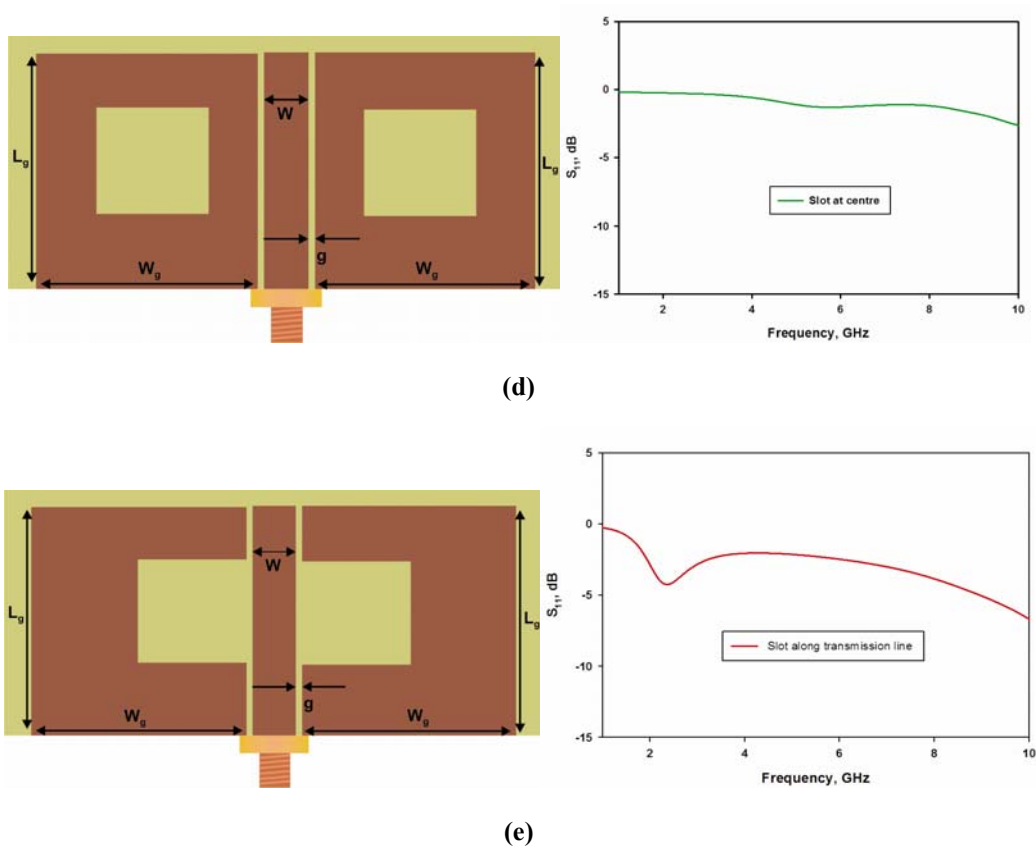
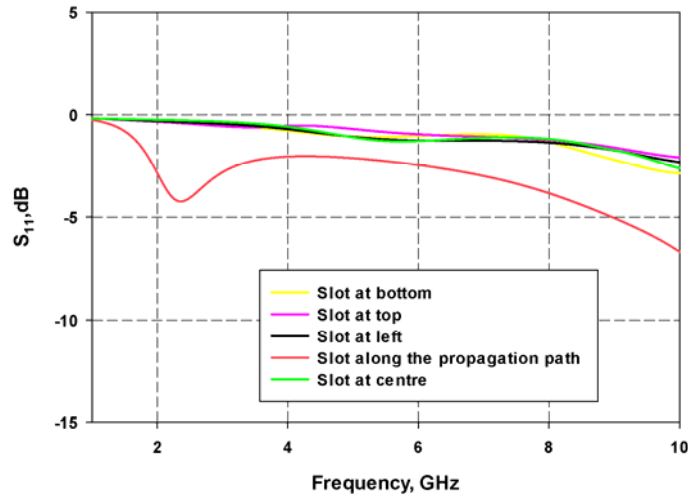


Figure 5.2 Geometry of the antenna with slot placed at different positions on a CPW structure and their corresponding reflection characteristics. ($L_g=15\text{mm}$, $W_g=15\text{mm}$, $g=0.35\text{mm}$ and $W=3\text{mm}$)

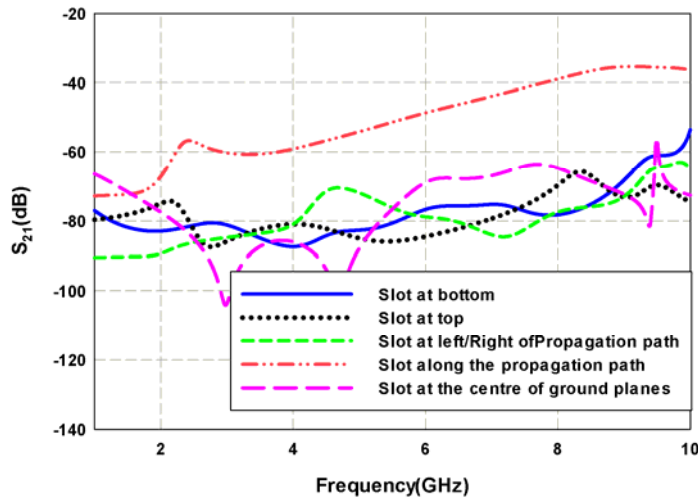
By placing the slot at the center, top, bottom and side (Fig.5.2.a-d) will not alter the fundamental mode of the Coplanar Waveguide structure; hence there is no significant radiation. There is a clear evidence (Fig.5.2.e) of radiation when the slot is placed along the propagation path of the CPW fed transmission line. Even though the structure is not satisfying the required impedance match; it may radiate electromagnetic energy.

The comparison of the total reflection and transmission characteristics of different structures are shown in the figure.5.3. It is observed that the resonance is

created if and only if the discontinuity is created along the propagation path of the transmission line. On the other hand the structure will behave as an open ended transmission line with total energy reflected back to the input port.



(a)



(b)

Figure 5.3 (a) Reflection and (b) Transmission characteristics of structures with slot at different positions ($L_g=15\text{mm}$, $W_g=15\text{mm}$, $g=0.35\text{mm}$ and $W=3\text{mm}$)

5.2 Asymmetrically slotted CPW fed open ended transmission line.

From the above section it is clear that the discontinuity should be introduced along the propagation path of the transmission line to radiate electromagnetic energy. To understand the complete effect of the discontinuity, it is good to start with an asymmetrically slotted CPW fed open ended transmission line as shown in figure.5.4. The gap width 'g' and signal strip width 'w' are chosen for 50 Ω impedance match using standard design equations.

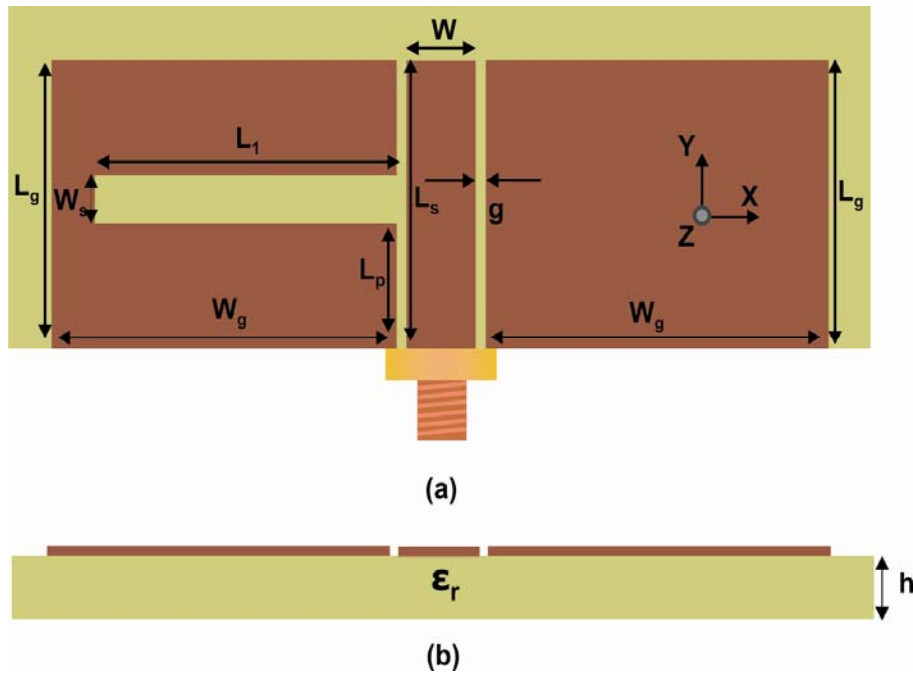


Figure 5.4 Geometry of the asymmetrically slotted antenna (a) Front view
(b) Side view
($L_g=15\text{mm}$, $W_g=15\text{mm}$, $L_1=10\text{mm}$, $W_s=2\text{mm}$, $L_p=5\text{mm}$, $L_s=15\text{mm}$
 $g=0.35\text{mm}$ and $W=3\text{mm}$)

A slot of dimension $L_1=10\text{mm}$, $W_s=2\text{mm}$ is inserted on any of the lateral ground plane of CPW to create a discontinuity as shown in figure.5.4. The slot is placed at $L_p=4\text{mm}$. The two lateral ground plane of length $L_g=15\text{mm}$ and width $W_g=15\text{mm}$ are used in the present analysis. The structure is fabricated on a substrate of dielectric constant 4.4 and height 1.6mm. The reflection and transmission characteristic of the structure is shown in figure.5.5. The structure behaves as an antenna resonating at 3.85GHz and 7GHz with poor matching. Thus the transmission line started to radiate electromagnetic energy. The position of the slot together with other parameters should be optimized for achieving good impedance matching.

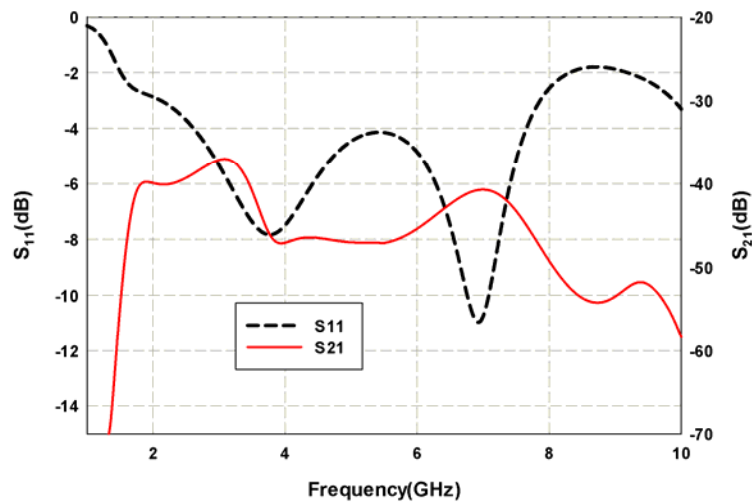


Figure 4.5 Reflection and transmission characteristics of asymmetrically slotted antenna
($L_g=15\text{mm}$, $W_g=15\text{mm}$, $L_1=10\text{mm}$, $W_s=2\text{mm}$, $L_p=5\text{mm}$, $L_s=15\text{mm}$, $g=0.35\text{mm}$ and $W=3\text{mm}$)

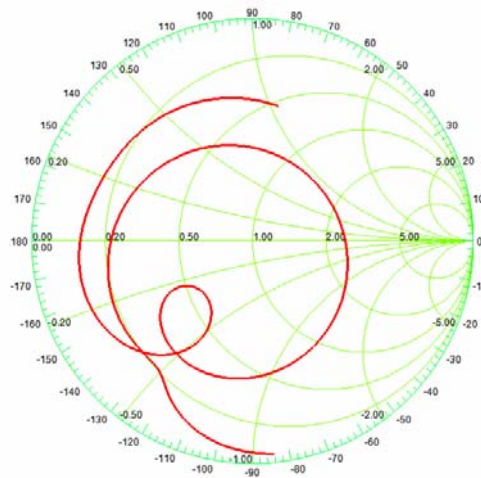


Figure 5.6 Impedance characteristics of asymmetrically slotted antenna
 ($L_g=15\text{mm}$, $W_g=15\text{mm}$, $L_1=10\text{mm}$, $W_s=2\text{mm}$, $L_p=5\text{mm}$, $L_s=15\text{mm}$
 $g=0.35\text{mm}$ and $W=3\text{mm}$)

The smith chart shown in figure.5.6. indicates the presence two resonances one at 3.85GHz and the other at 7GHz. The impedances are far away from 50Ω and it should be brought downwards to 50 ohm to have a good impedance matching.

The current distribution of the antenna at 3.85GHz and 7GHz are shown in figure.5.7 (a) and figure.5.7 (b) respectively. By modifying the ground plane the normal CPW mode is not disturbed. The signal strip together with the unslotted ground contributes the resonance at lower frequency (3.85GHz). Maximum intensity of current is found around the slot at 7GHz. Since the slot is mainly contributing for radiation its characteristics towards the impedance matching should be analyzed by varying the slot parameters. The radiation pattern corresponding to the resonant frequency is shown in figure.5.7(c) and (d). The pattern is found to be disturbed in both the frequency bands. This tilt in radiation pattern is due to the asymmetry in slot position on the lateral ground plane of CPW transmission line. The tilt should be surmounted in coming sections.

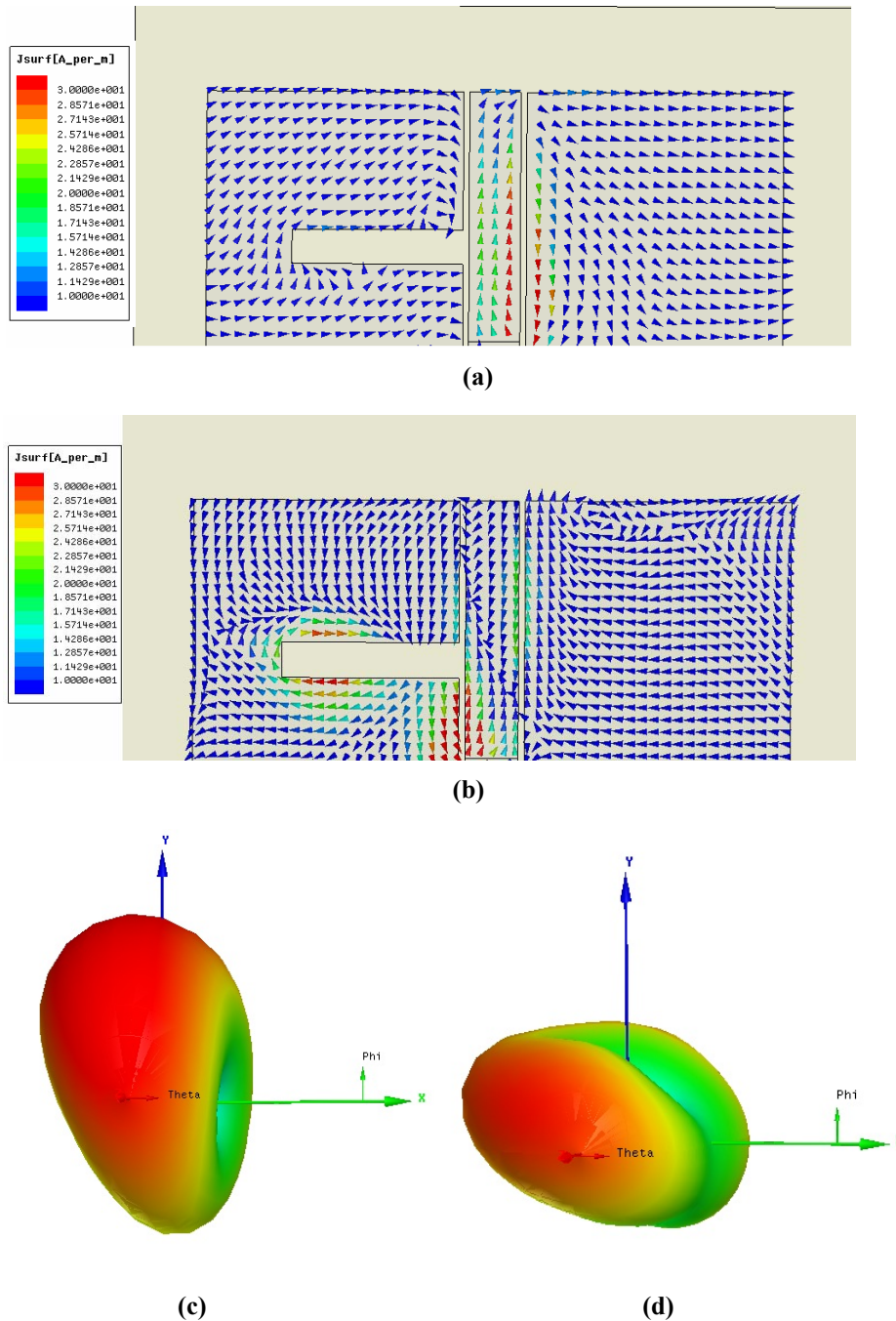


Figure 5.7 Current distribution at (a) 3.85GHz (b) 7GHz and radiation pattern at (c) 3.85GHz (d) 7GHz of asymmetrically slotted antenna ($L_g=15\text{mm}$, $W_g=15\text{mm}$, $L_1=10\text{mm}$, $W_s=2\text{mm}$, $L_p=5\text{mm}$, $L_s=15\text{mm}$ $g=0.35\text{mm}$ and $W=3\text{mm}$)

5.3 CPW fed open ended antenna with Symmetrical slots

An asymmetric slot may produce tilted radiation pattern. In order to avoid the asymmetry, symmetrical slots are introduced along the transmission line.

The fundamental geometry of the symmetrical structure along with reflection characteristics is shown in figure.5.8. The coplanar waveguide fed antenna with ground plane dimension $W_g \times L_g$ is designed for 50Ω input impedance with signal strip width W and gap 'g'. Two symmetrical slots of dimension $L_1 \times W_s$ is etched on both the lateral ground plane at a position of L_p from the feed. The geometry is etched on a substrate of dielectric constant 4.4 and thickness 1.6mm.

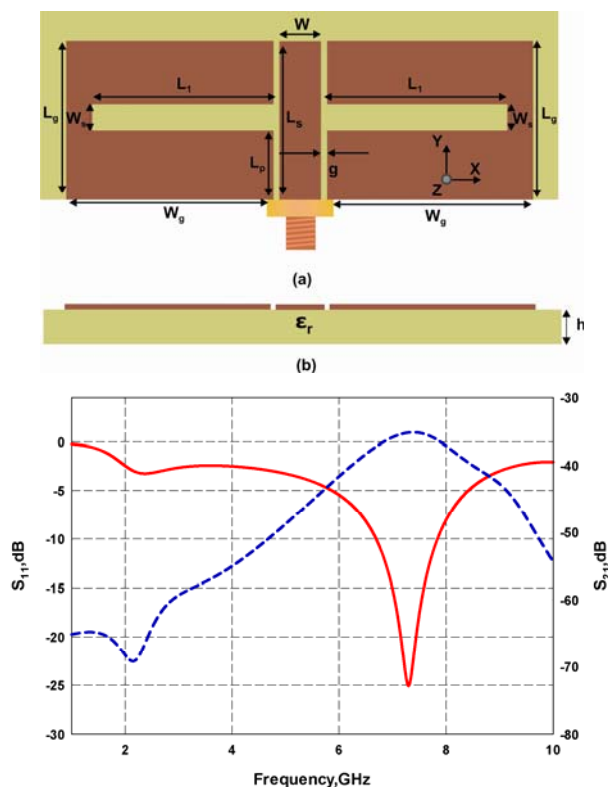


Figure 5.8 Geometrically of symmetrically slotted antenna (a) Front view (b) sideview c) Reflection and transmission characteristics ($L_g=15\text{mm}$, $W_g=15\text{mm}$, $L_1=10\text{mm}$, $W_s=2\text{mm}$, $L_p=5\text{mm}$, $L_s=15\text{mm}$, $g=0.35\text{mm}$ and $W=3\text{mm}$)

Like a asymmetrically slotted structure, this one has poor impedance matching on the fundamental resonance at 2.2GHz. But the matching at higher frequency is improved. Thus in addition to ground plane the signal strip should be modified in such a way to launch the signal into the slot effectively. Three different ways are introduced to achieve impedance matching and are described in this session,

- 1) Offset fed slot
- 2) Top loading the signal strip
- 3) Reduced signal strip length

5.3.1 Offset fed slot

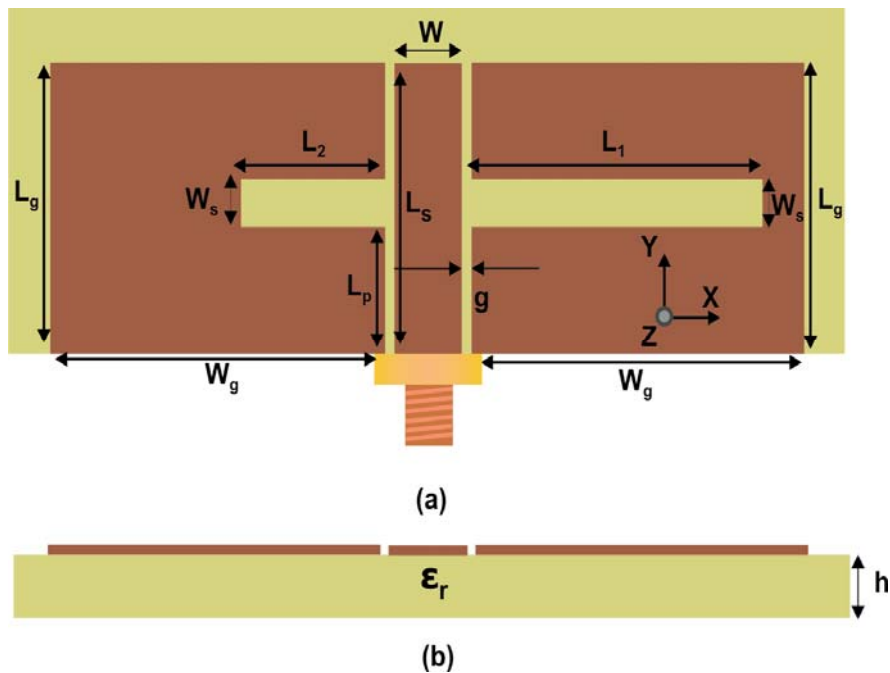


Figure 5.9 Geometry of the offset fed slot antenna (a) Front view (b) Side view
($L_g=15\text{mm}$, $W_g=15\text{mm}$, $L_2=2\text{mm}$, $L_1=14\text{mm}$, $W_s=2\text{mm}$, $L_p=7\text{mm}$,
 $L_s=15\text{mm}$, $W=3\text{mm}$, $g=0.35\text{mm}$, $h=1.6\text{mm}$ and $\epsilon_r=4.4$)

Since the terminal resistance at the centre of a resonant $\lambda/2$ slot in a large sheet is about 500Ω , an off center feed is used normally to provide the impedance match in slot antennas [1]. The same technique is adapter here also. In this section the high input impedance of the center fed slot antenna is lowered by changing the ratio of slot arm lengths. For that the feed is off centered by making the slot asymmetrical as shown in figure.5.9. The symmetrical slots (L_s) on the lateral ground plane is made unsymmetrical by decreasing one slot L_2 to 2mm and increasing other slot L_1 in to 14mm. The width of the slot remained unaffected as $W_s=2\text{mm}$.

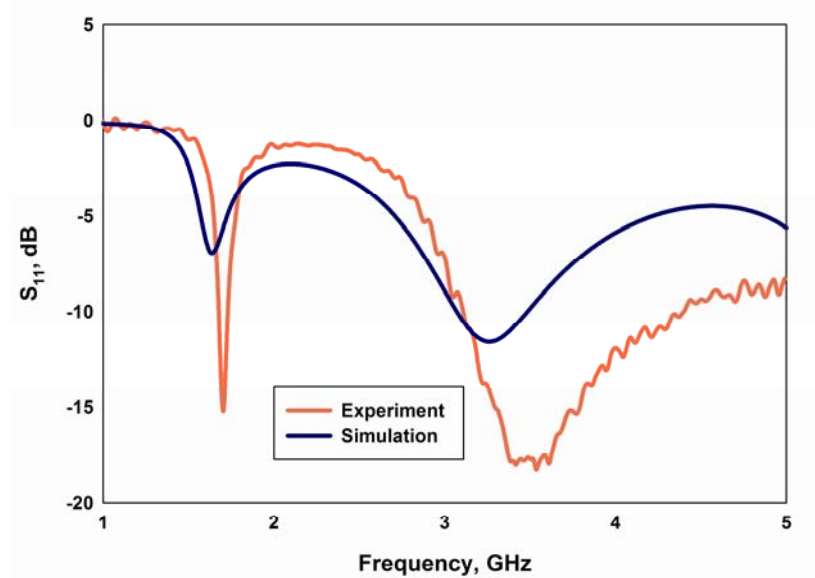


Figure 5.10 Reflection characteristics of the offset fed slot antenna ($L_g=15\text{mm}$, $W_g=15\text{mm}$, $L_2=2\text{mm}$, $L_1=14\text{mm}$, $W_s=2\text{mm}$, $L_p=7\text{mm}$, $L_s=15\text{mm}$, $W=3\text{mm}$, $g=0.35\text{mm}$, $h=1.6\text{mm}$ and $\epsilon_r=4.4$)

The experimental and simulated reflection characteristics of the optimized off centre fed antenna is shown in figure.5.10. This dual band antenna has a 2:1 VSWR bandwidth from 1.66GHz-1.73GHz and 3.10GHz-4.39GHz. The frequency can be tuned by changing the slot arm length or the slot arm ratio

(L_1/L_2). The lower resonance is due to the higher slot arm (L_1) and the higher resonance is due to the smaller slot (L_2). The slot width is mainly affecting the reactance and is kept same as 2mm. It is shown that the antenna is matched to 50Ω by properly offsetting the feed position.

The measured variation in the return loss characteristics of the off centre fed antenna with respect to the slot arm length ratio ($L_2:L_1$) is shown in figure.5.11. While offsetting the feed the reactance corresponding to the first resonance shift from highly capacitive to less capacitive and that of the second resonance from high inductance to low inductance. The real part of the impedance gets reduced from high impedance value to give proper matching [1].

The VSWR impedance bandwidths in the fundamental as well as harmonic frequencies are determined by the position of the feed point.

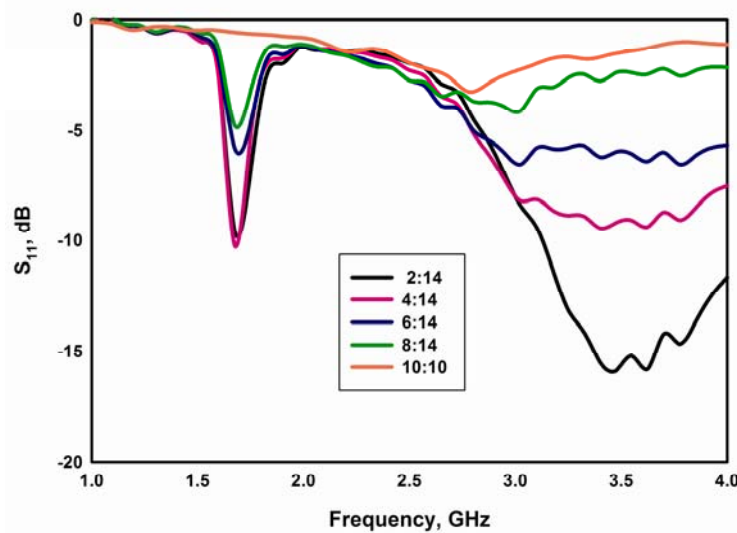


Figure 5.11 Variation in reflection characteristics with slot arm length ratio $L_1:L_2$ ($L_g=15\text{mm}$, $W_g=15\text{mm}$, $W_s=2\text{mm}$, $L_p=7\text{mm}$, $L_s=15\text{mm}$, $W=3\text{mm}$, $g=0.35\text{mm}$, $h=1.6\text{mm}$ and $\epsilon_r=4.4$)

The measured polarization of the antenna is along positive x-direction for both the bands. The measured radiation pattern of the optimized off centre fed dipole antenna is shown in the figure.5.12 (a) and (b). Like a dipole antenna there are two nulls in the positive and negative x-axis resulting a figure of eight radiation pattern along the E-plane (XZ plane). A omnidirectional pattern is obtained with good polarization purity along the H-plane (YZ plane). A better cross Polarization level of 15dB is obtained along the bore sight direction with Half Power Beam Width (HPBW) of more than 80° at 1.7GHz. A cross polar level nearer to 10dB is also obtained for 3.5GHz, but the pattern is found to be distorted as compared to the radiation pattern at 1.7GHz. The measured gain of antenna at 1.7GHz and 3.5GHz are 1.3dBi and 2.7dBi respectively.

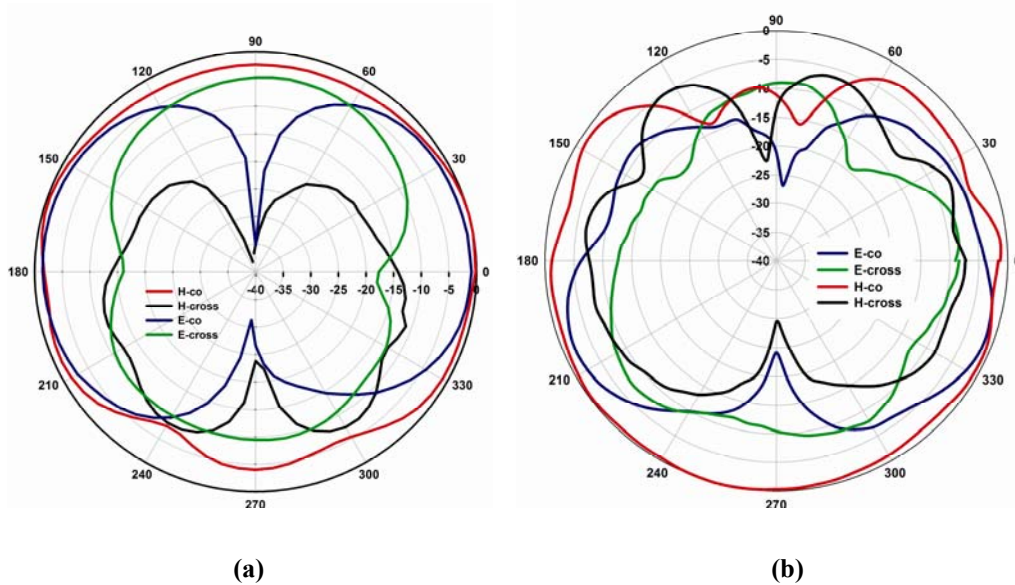


Figure 5.12 Measured Radiation Pattern at 1.7GHz and 3.5GHz of the off centre fed slot antenna
 $(L_g=15\text{mm}, W_g=15\text{mm}, W_s=2\text{mm}, L_p=7\text{mm}, L_s=15\text{mm}, W=3\text{mm}, g=0.35\text{mm}, h=1.6\text{mm}$ and $\epsilon_r=4.4$)

5.3.2 Top loading the signal strip

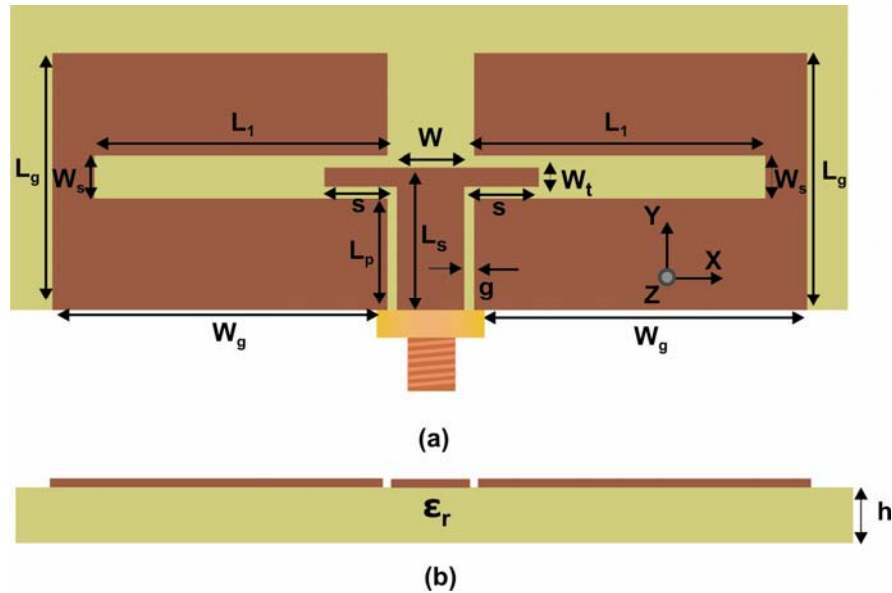


Figure 5.13 Geometry of the antenna with top loading the signal strip (a) Front View (b) Side view
 $(L_g=15\text{mm}, W_g=15\text{mm}, L_1=10\text{mm}, L_s=8.5\text{mm}, L_p=7\text{mm}, W_s=2\text{mm}, W_t=1\text{mm}, W=3\text{mm}, g=0.35\text{mm}, h=1.6\text{mm}$ and $\epsilon_r=4.4$)

In this section another feeding method is introduced to enhance the matching. The signal strip is top loaded with an additional strip S to form a T-shaped feed. The feed will launch electromagnetic energy effectively into the slot resulting in a centre fed slot antenna. The geometry is shown in figure.5.13. in which the strips of length S and width W_t are used to top load the signal strip. The width of the strip is chosen as 1mm. All other parameters of this antenna remain same as that of the earlier antenna. The antenna is resonating at 3.7GHz with good agreement between simulation and measurement. The proposed antenna has an impedance bandwidth of 200MHz and can be easily integrated with MIC's. The variation in reflection characteristics of the antenna with top loading length 'S' is shown in figure.5.14

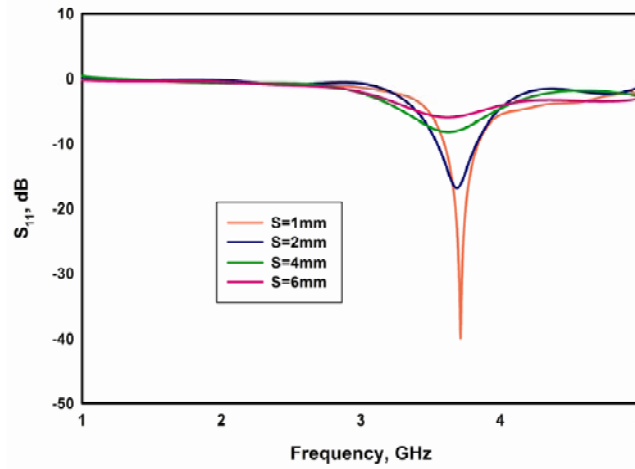


Figure 5.14 Variation in reflection characteristics of the top loaded antenna with top loading strip length S
 $(L_g=15\text{mm}, L_s=15\text{mm}, L_l=10\text{mm}, L_s=8.5\text{mm}, L_p=7\text{mm}, W_s=2\text{mm}, W_t=1\text{mm}, W=3\text{mm}, g=0.35\text{mm}, h=1.6\text{mm}$ and $\epsilon_r=4.4$)

The antenna is polarized along the y-direction. The E-plane and H-plane radiation patterns of the antenna at resonant frequency are shown in figure 5.15. A cross polar level of 10dB is obtained along the bore sight direction but lower polarization discrimination is observed along other directions which should be improved. The antenna is offering a gain of 1.1dBi.

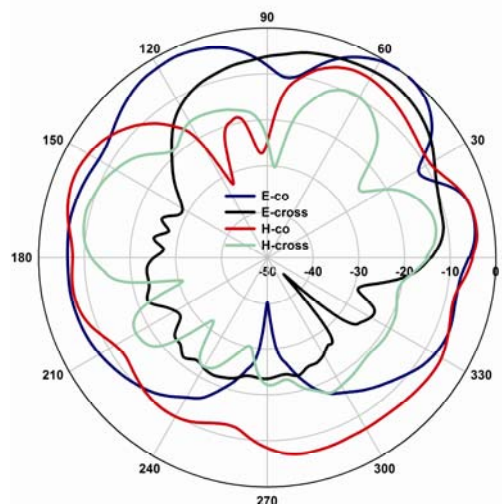


Figure 5.15 Measured Radiation pattern of the top loaded antenna
 $(L_g=15\text{mm}, L_s=15\text{mm}, L_l=10\text{mm}, L_s=8.5\text{mm}, L_p=7\text{mm}, W_s=2\text{mm}, W_t=1\text{mm}, W=3\text{mm}, g=0.35\text{mm}, h=1.6\text{mm}$ and $\epsilon_r=4.4$)

5.3.3 Signal strip reduced coplanar waveguide feed

The other type of feed that effectively exciting the slot is signal strip reduced coplanar waveguide. The effect of signal strip length on reflection characteristics of asymmetrical slotted structure (figure5.17.a) is conducted in this section. The signal strip length (L_s) is varied by keeping the slot length (L_1) and slot position (L_p) as constant. Figure.5.16 shows the reflection characteristics by varying the signal strip length for a given slot position. It is found that the resonance frequency is varying significantly with some combination of slot position and signal strip length. In all cases to attain impedance matching the strip lengths should be greater than slot positions (L_p).

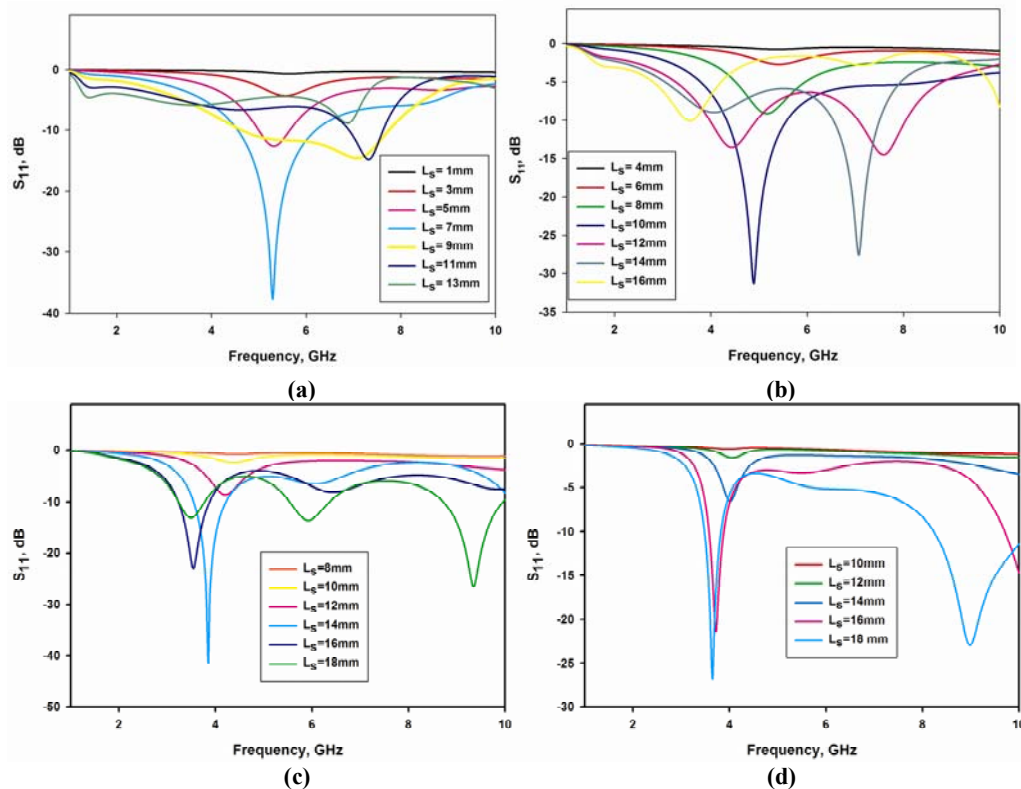


Figure 5.16 Variation of reflection characteristics of asymmetrical slotted antenna with signal strip length (L_s) for different slot positions L_p (a) $L_p=1\text{mm}$ (b) $L_p=5\text{mm}$ (c) $L_p=9\text{mm}$ (d) $L_p=12\text{mm}$ ($L_g=15\text{mm}$, $W_g=15\text{mm}$, $L_1=10\text{mm}$, $W_s=2\text{mm}$, $L_p=5\text{mm}$, $L_s=15\text{mm}$ $g=0.35\text{mm}$ and $W=3\text{mm}$)

Thus the position of the slot is an important factor in determining the impedance matching. Along with the position the signal strip length is also an important factor. From the figures it is shown that the position of slot together with the signal strip length are affecting the resonant behavior of the asymmetrically slotted CPW fed structure. For a given slot position and slot length, the signal strip length is chosen as 11mm for good impedance matching in this case.

As mentioned earlier the structure shows high impedance for signal strip length of $L_s=15\text{mm}$. The impedance is tuned by reducing the signal strip length and achieved a good impedance matching ($L_s=10\text{mm}$) as shown in figure.5.17.

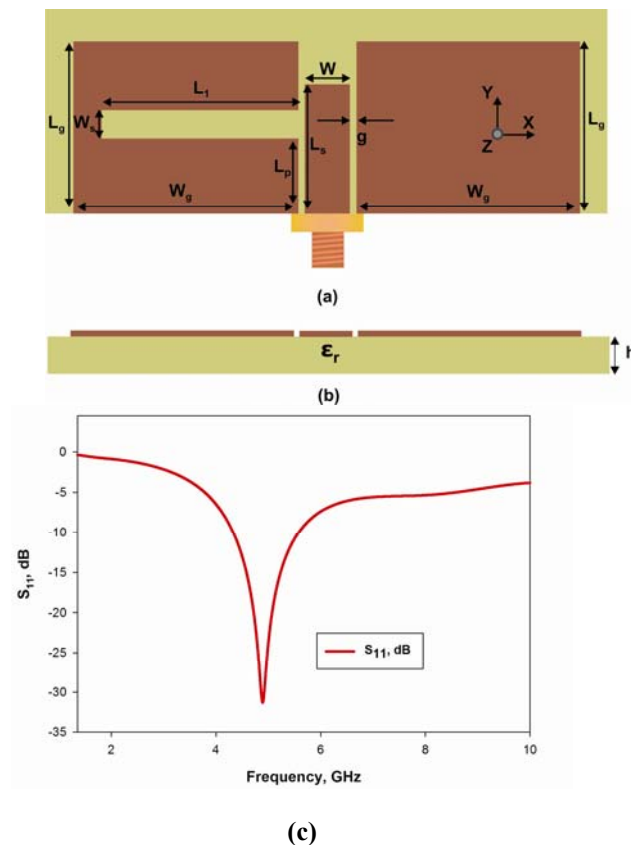


Figure 5.17 Geometry of the structure with reduced signal strip length
 (a) Front view (b) Side view (c) Reflection characteristics
 ($L_g=15\text{mm}$, $W_g=15\text{mm}$, $L_1=10\text{mm}$, $W_s=2\text{mm}$, $L_p=5\text{mm}$, $L_s=10\text{mm}$
 $g=0.35\text{mm}$ and $W=3\text{mm}$)

Variation of input impedance with signal strip length is shown in figure.5.18. As the length of the signal strip increases the real part of impedance increases. The reactance varies from high capacitance to low. This is clearly demonstrated in the smith chart shown in figure. For a signal strip length of 6mm the resonance is highly capacitive. For $L_s=8\text{mm}$ the resonant band become prominent as a loop in the figure, and the real part approaches 50Ω with negligible reactance for a signal strip length of 10mm. Further increase in signal strip length causes corresponding increase in impedance with depreciation in the impedance matching as clearly visible in the figure. Thus by trimming the signal strip dimension the impedance can be easily controlled.

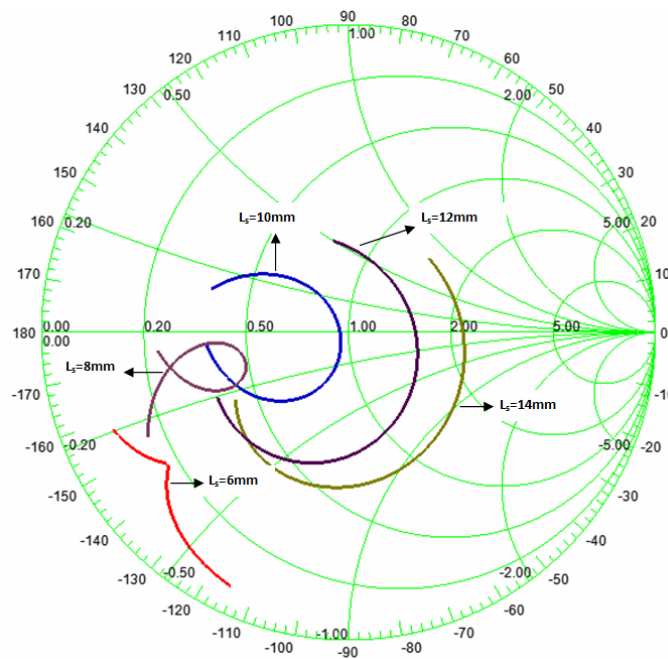


Figure 5.18 Smith chart showing the impedance characteristics of the asymmetrically slotted antenna with variation in signal strip length (L_s)
($L_g=15\text{mm}$, $W_g=15\text{mm}$, $L_1=10\text{mm}$, $W_s=2\text{mm}$, $L_p=5\text{mm}$, $L_s=10\text{mm}$ $g=0.35\text{mm}$ and $W=3\text{mm}$)

The effect of resonant frequency and matching with slot length is shown in the figure.5.19. The slot length is varied from 8mm to 12mm. As the length increases, the resonant frequency decreases as expected. A very good impedance match of -32dB is obtained for the optimized length of 10mm. The Coplanar waveguide guide the feed up to the discontinuity like a transmission line and excites the slot. The slot resonates at this frequency and reradiates electromagnetic energy.

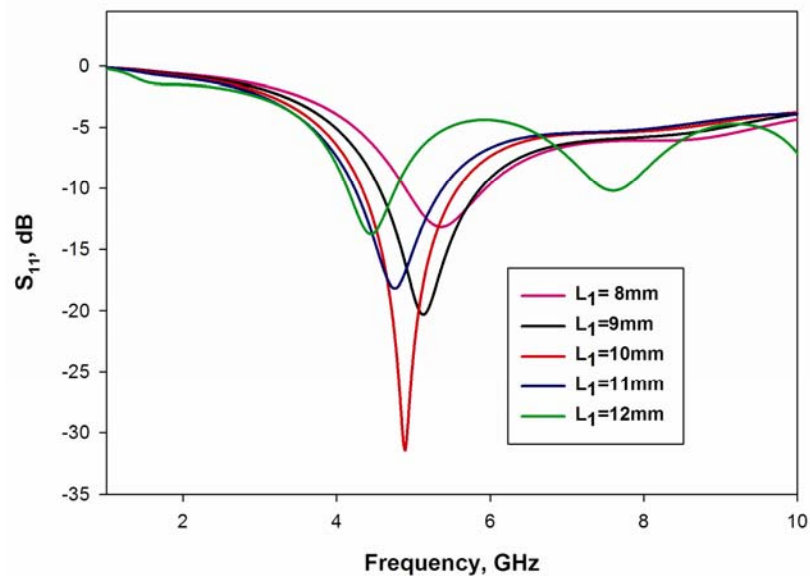


Figure 5.19 Variation in reflection characteristics with slot length L_1 of the asymmetrically slotted antenna ($L_g=15$ mm, $W_g=15$ mm, $W_s=2$ mm, $L_p=5$ mm, $L_s=10$ mm, $g=0.35$ mm and $W=3$ mm)

The above discussed structure is physically assymetrical along the y-axis by placing the slot on any of the lateral ground planes. This asymmetry can affect the radiation characteristics of the antenna. The radiation patterns of the antenna together with slot position on one of lateral ground plane are shown in figure.5.20 and figure.5.21. It is found to be tilted and the tilt in

radiation pattern is towards the slot side. If the slot is on the left ground as in figure.5.20 (a) the pattern is tilted by -30° as shown in fig.5.20 (b). Otherwise if the slot is on the right ground the pattern is tilted by 30° as shown in the figure.5.21 (b).

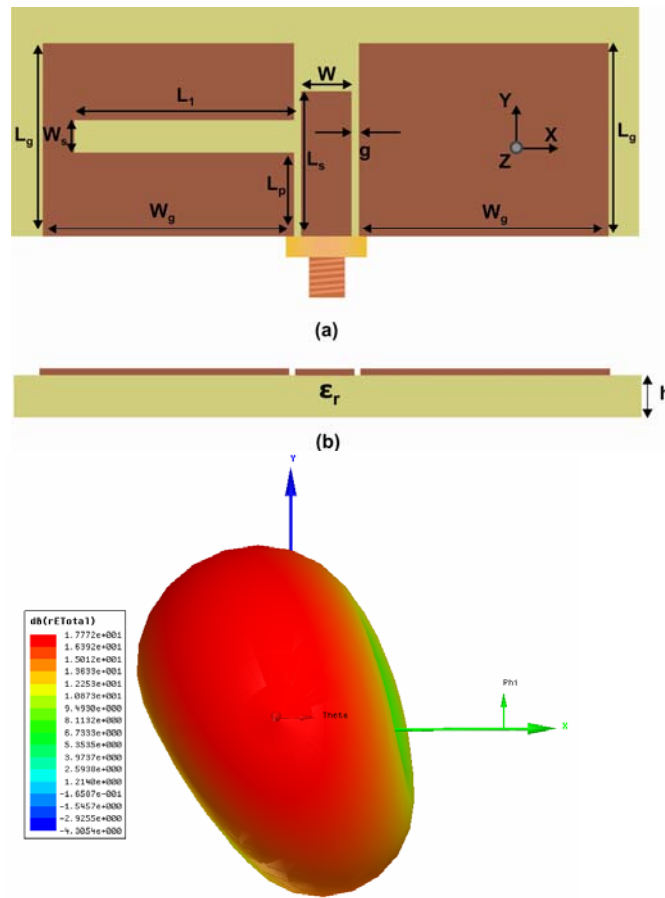


Figure 5.20 Geometry of the asymmetrically slotted antenna with corresponding radiation pattern
($L_g=15\text{mm}$, $W_g=15\text{mm}$, $L_1=10\text{mm}$, $W_s=2\text{mm}$, $L_p=5\text{mm}$, $L_s=10\text{mm}$, $g=0.35\text{mm}$ and $W=3\text{mm}$)

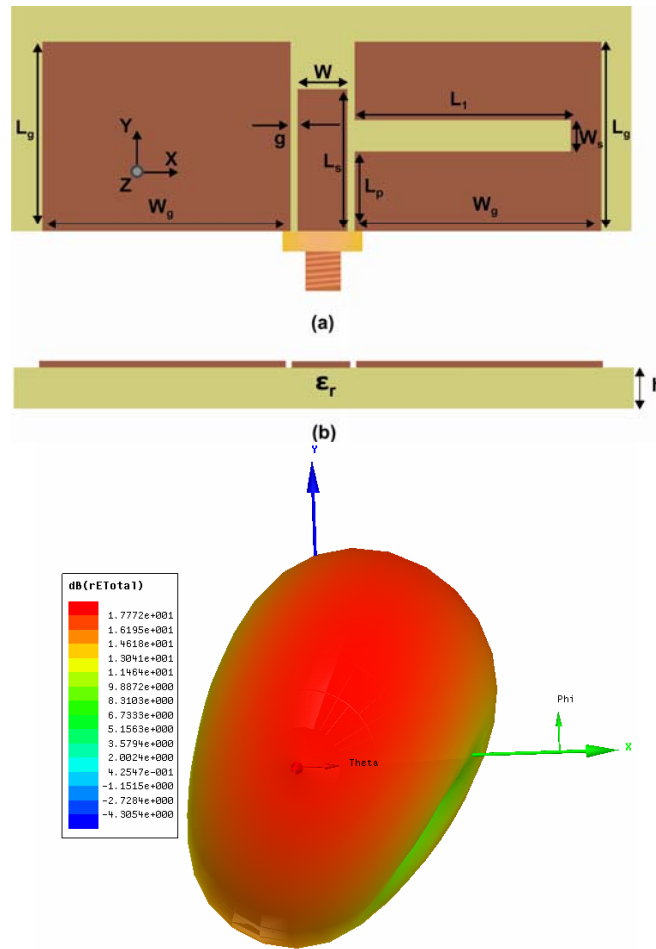


Figure 5.21 Geometry of the asymmetrically slotted antenna with corresponding radiation pattern
 ($L_g=15\text{mm}$, $W_g=15\text{mm}$, $L_1=10\text{mm}$, $W_s=2\text{mm}$, $L_p=5\text{mm}$, $L_s=10\text{mm}$
 $g=0.35\text{mm}$ and $W=3\text{mm}$)

The above observations are summarized and illustrated in table.5.1. The table describes the variation in resonant frequency and matching with signal strip length keeping all other parameters constant. From the table it is found that the combination of signal strip length and slot position is an important factor in determining the impedance matching. The length of the signal strip should be chosen in such a way that it should be higher than the slot position.

Table 5.1 Variation in resonant frequency and reflection characteristics of antenna1 with slot position and signal strip

Slot position → (L _p)	1mm (GHz,dB)	3mm (GHz,dB)	5mm (GHz,dB)	7mm (GHz,dB)	9mm (GHz,dB)	11mm (GHz,dB)
Signal strip length ↓ (L _s)						
3mm(GHz,dB)	5.47, -4.45	5.65, -1.4	-----	-----	-----	-----
5mm(GHz,dB)	5.25, -12.56	5.47, -5.1	5.47, -1.46	-----	-----	-----
7mm(GHz,dB)	5.29, -37.7	5.29, -14.79	5.27, -5.04	4.87, -1.32	-----	-----
9mm(GHz,dB)	7.03, -14.64	5.16, -19.32	5.05,-15.01	4.73,- 4.55	4.46, -1.32	-----
11mm(GHz,dB)	7.32, -14.89	4.64, -10.61	4.80,-20.74	4.53,-12.98	4.28, -4.61	4.15, -1.43
13mm(GHz,dB)	6.85, -8.86	7.21,- 8.75	4.19,-13.24	4.15, -23.7	4.015,-13.71	4.01, -5.63
15mm(GHz,dB)	-----	-----	3.85, -8.7	3.83,-13.27	3.72, -31.51	3.65,-18.80

5.4 Symmetrically slotted antenna

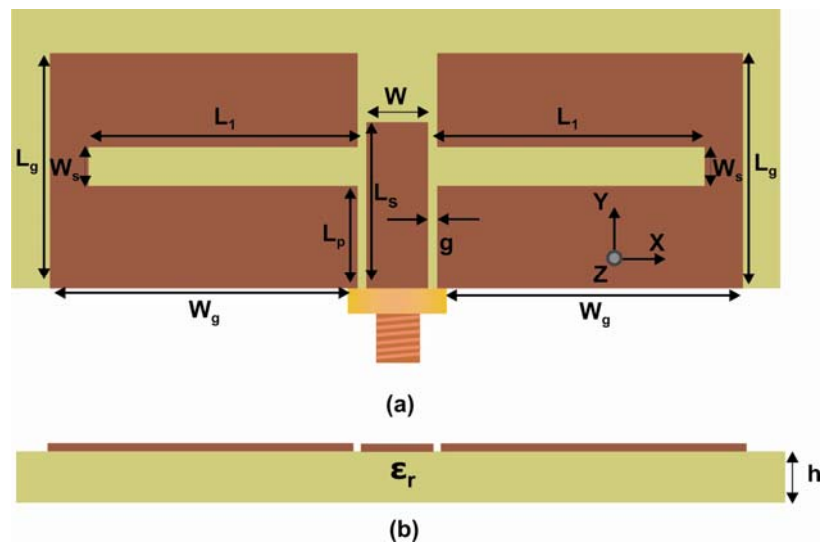


Figure 5.22 Geometry of the reduced impedance coplanar waveguide fed antenna (a) Front view (b) Side view
 ($L_g=15\text{mm}$, $L_g=15\text{mm}$, $L_1=10\text{mm}$, $L_s=11\text{mm}$, $L_p=7\text{mm}$, $W_s=2\text{mm}$, $W=3\text{mm}$, $g=0.35\text{mm}$, $h=1.6\text{mm}$ and $\epsilon_r=4.4$)

From the studies conducted in the previous session, it is shown that the length of the centre signal strip is mainly contributing the real part of impedance. Reducing the signal strip length will decrease the series resistance proportionally without affecting any other parameters of the conventional antenna. Thus the impedance matching of the structure can be improved by reducing the signal strip length. But the radiation pattern is tilted which should be avoided. This is achieved by introducing symmetry in the structure by creating slots on both the lateral ground planes. The resonance and radiation mechanism of this antenna is elaborately discussed in this section.

In this section the signal strip length of a symmetrically slotted antenna is reduced to L_s resulting in the proposed geometry shown in figure.5.22. The width W_s and length L_1 of the slot are kept unchanged. The reflection characteristics of the antenna with a single slot and symmetrical slot are compared with slot less antenna as in figure.5.23. The symmetrical slotted antenna is giving resonance at a lower frequency compared to a asymmetrical slotted antenna and hence more compact. Moreover it is found that the quality factor of symmetrical slot antenna is very high compared to a single slot antenna.

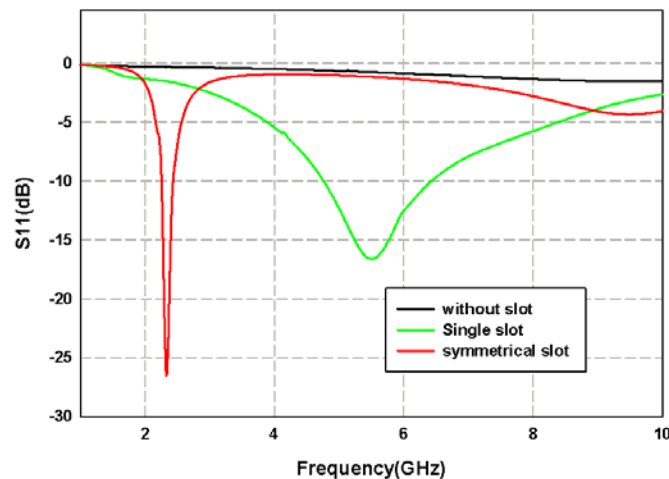


Figure 5.23. Reflection characteristics of the antenna in different cases

The antenna is matched at 2.4GHz, which is half wavelength corresponding to the total slot length. Thus by trimming the signal strip length the total input impedance of the antenna can be reduced to 50Ω to provide better matching. This method of feeding is very simple and will provide good radiation characteristics when compared to other two types of feeding. The resonance of this antenna can be tuned primarily by varying the slot dimension. The extended signal strip above the slot is also affecting the resonance which is used for fine tuning.

The polarization of the antenna is along y-direction with low cross polar level. The measured 2D radiation pattern and simulated 3D pattern of the antenna are shown in figure.5.24. The tilt in radiation pattern can be easily removed by creating symmetry in the structure. This symmetric slotted antenna provides a polarization discrimination of 12dB and 16dB along E and H planes. The greatest advantage of this antenna is the internal strip (L_s) which is associated with it to tune the resonance frequency.

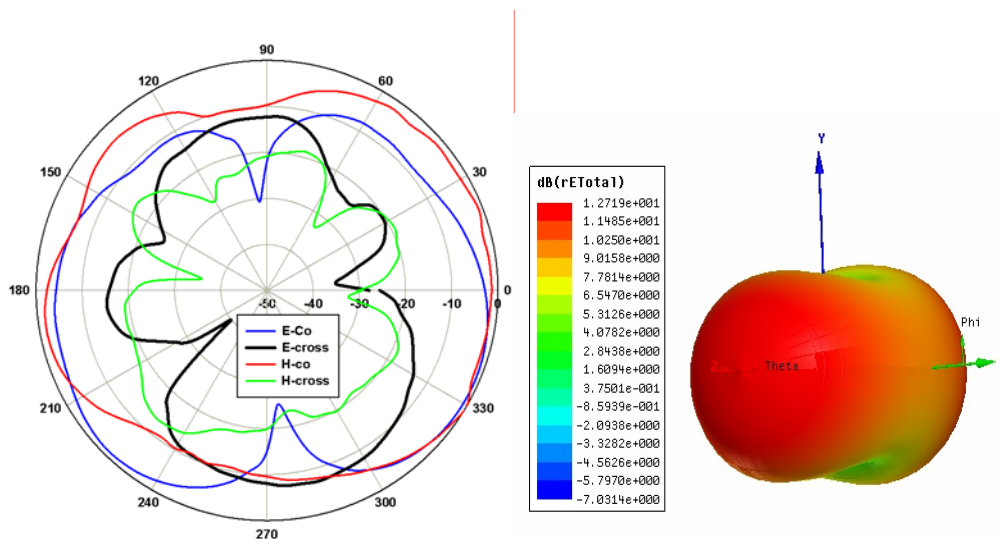


Figure 5.24. a) 2D b) 3D Radiation pattern of symmetrically slot single band antenna at 2.4GHz
 ($L_g=15\text{mm}$, $L_g=15\text{mm}$, $L_1=10\text{mm}$, $L_s=8.5\text{mm}$, $L_p=7\text{mm}$, $W_s=2\text{mm}$, $W_t=1\text{mm}$, $W=3\text{mm}$, $g=0.35\text{mm}$, $h=1.6\text{mm}$ and $\epsilon_r=4.4$)

Due to the symmetrical and simple structure of the signal strip reduced slot antenna it is considered as the better method to match the CPW structures among the feeding techniques mentioned in this section. The possibility of tuning the above structures using varactors and pin diodes are illustrated in the next sections. Rigorous parametric analysis on the impedance characteristics are also performed and explained. The observations are summarized and illustrated in table.5.2. From the table it is found that the position of the slot should be placed below the signal strip length.

Table 5.2 Variation in resonant frequency and reflection characteristics of signal strip reduced antenna with slot position and signal strip

Slot position → (Lp)	1mm (GHz, dB)	3mm (GHz, dB)	5mm (GHz, dB)	7mm (GHz, dB)	9mm (GHz, dB)	11mm (GHz, dB)
Signal strip length ↓ (Ls)						
2mm(GHz, dB)	3.83, -5.6	----	---	----	----	----
3mm(GHz, dB)	3.56, -14.99	3.94, -1.9	----	----	----	----
4mm(GHz, dB)	3.27, -16.32	3.79, -4.18	----	----	----	----
5mm(GHz, dB)	3.02, -8.68	3.58, -8.89	3.94, -1.92	----	----	----
6mm(GHz, dB)	2.82, -5.98	3.34, -23.52	3.76, -3.73	----	----	----
7mm(GHz, dB)	2.64, -4.4	3.11, -15.98	3.56, -7.44	----	----	----
8mm(GHz, dB)	2.44, -3.2	2.91, -9.74	3.31, -16.31	3.76, -3.6	----	----
9mm(GHz, dB)	2.32, -2.63	2.78, -6.89	3.11, -29.35	3.56, -7.18	3.94, -2.04	----
10mm(GHz, dB)	----	2.59, -5.00	2.93, -12.63	3.34, -14.05	3.83, -3.89	3.97, -1.32
11mm(GHz, dB)	----	2.50, -3.99	2.75, -8.77	3.11, -30.85	3.61, -7.74	3.99, -2.41
12mm(GHz, dB)	----	2.39, -3.27	2.62, -5.94	2.91, -13.26	3.36, -17.62	3.88, -4.64
13mm(GHz, dB)	----	----	----	2.77, -8.54	3.11, -21.4	3.67, -9.62
14mm(GHz, dB)	----	----	----	2.64, -6.24	2.89, -15.3	3.4, -18.47

5.5 Symmetrically slotted Reconfigurable antenna

The possibility of reconfigurability of the antenna is explored in this section. The geometry of the reconfigurable antenna is shown in figure.5.25. In this study a varactor diode is placed symmetrically at a distance of L_1 on both the lateral ground planes of the optimized CPW fed antenna. DC biasing is applied as shown in the geometry which is connected through chip inductors for achieving RF isolation.

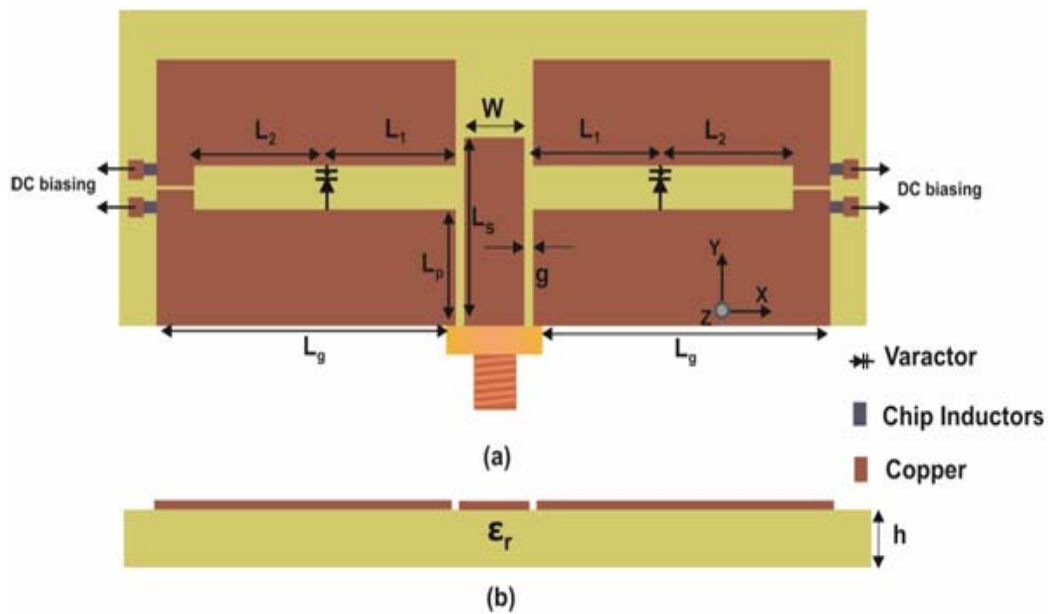


Figure 5.25 Geometry of the reconfigurable antenna
 ($L_g=15\text{mm}$, $L_1=10\text{mm}$, $L_s=11\text{mm}$, $L_p=7\text{mm}$, $W_s=2\text{mm}$, $W=3\text{mm}$,
 $g=0.35\text{mm}$, $h=1.6\text{mm}$ and $\epsilon_r=4.4$)

The variation in reflection characteristics of the antenna with the applied voltage is measured and shown in figure.5.26. When the voltage varies from 0 to 16V the resonant frequency shift from 1.9GHz to 2.1GHz as in the figure. It is interesting to note that the impedance matching is not much affected with the applied voltage. Thus the resonant frequency can be tuned effectively with the

applied voltage with the present design. Moreover, it is possible to reconfigure the antenna in frequency without modifying any physical parameters of the antenna.

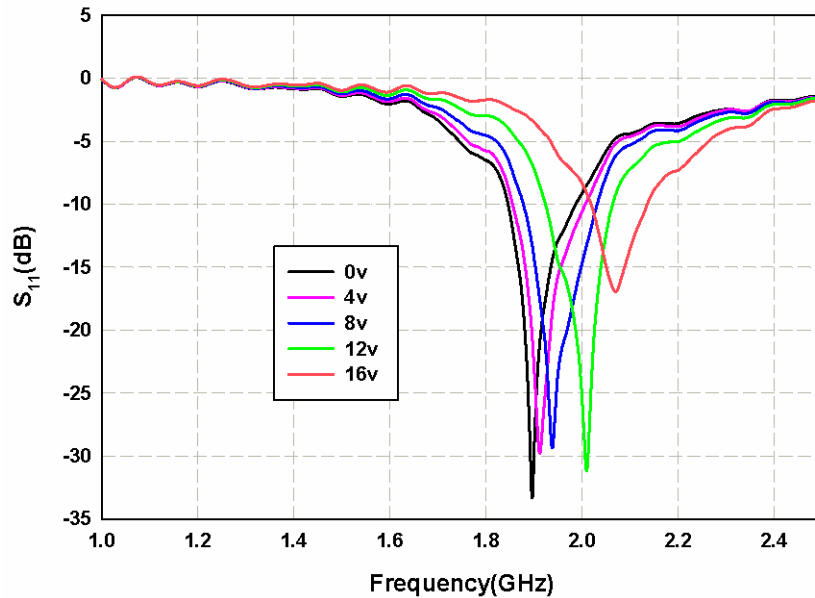


Figure 5.26 Return loss with varactor tuning
 $(L_g=15\text{mm}, W_g=15\text{mm}, L_1=10\text{mm}, L_s=11\text{mm}, L_p=7\text{mm},$
 $W_s=2\text{mm}, W=3\text{mm}, g=0.35\text{mm}, h=1.6\text{mm}$ and $\epsilon_r=4.4)$

The radiation pattern of the antenna for different applied voltage is verified. The E-plane radiation pattern of the antenna shown in figure.5.27 is found to be independent of voltage. Similarly H-plane radiation pattern shown in figure 5.28 is also found to be independent of voltage except a small change found for 16v. Thus the reconfigurable antenna presented here is a good candidate for tunable wireless application whose radiation characteristics is independent of applied voltage.

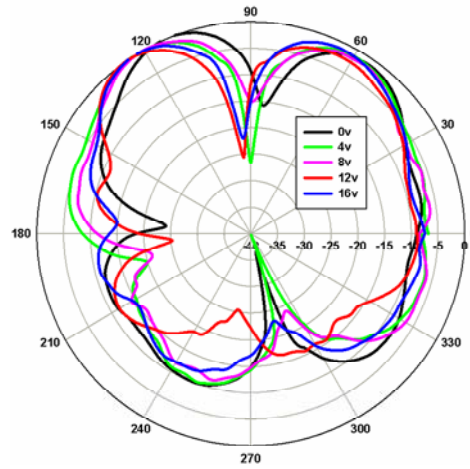


Figure 5.27 E-plane Radiation pattern with different voltage for tuning ($L_g=15\text{mm}$, $W_g=15\text{mm}$, $L_1=10\text{mm}$, $L_s=11\text{mm}$, $L_p=7\text{mm}$, $W_s=2\text{mm}$, $W=3\text{mm}$, $g=0.35\text{mm}$, $h=1.6\text{mm}$ and $\epsilon_r=4.4$)

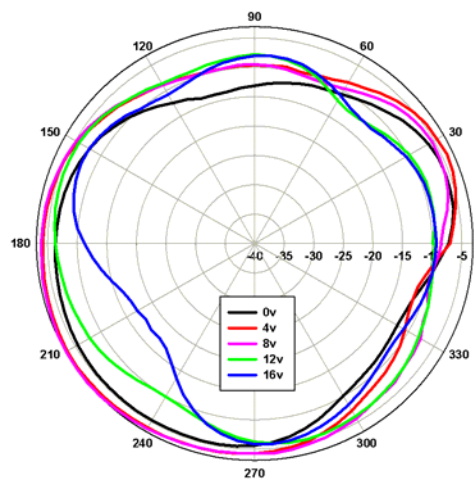


Figure 5.28 H-plane Radiation pattern with different voltage for tuning ($L_g=15\text{mm}$, $W_g=15\text{mm}$, $L_1=10\text{mm}$, $L_s=11\text{mm}$, $L_p=7\text{mm}$, $W_s=2\text{mm}$, $W=3\text{mm}$, $g=0.35\text{mm}$, $h=1.6\text{mm}$ and $\epsilon_r=4.4$)

5.6 H-shaped slot antenna with Harmonic Suppression

It is established in the earlier section that the symmetrical slot on the ground plane excites resonance corresponding to the slot dimension with stable radiation characteristics. Meandering this symmetrical slot into L-shaped slot will improve the compactness of antenna resulting in geometry as shown in figure.5.29.

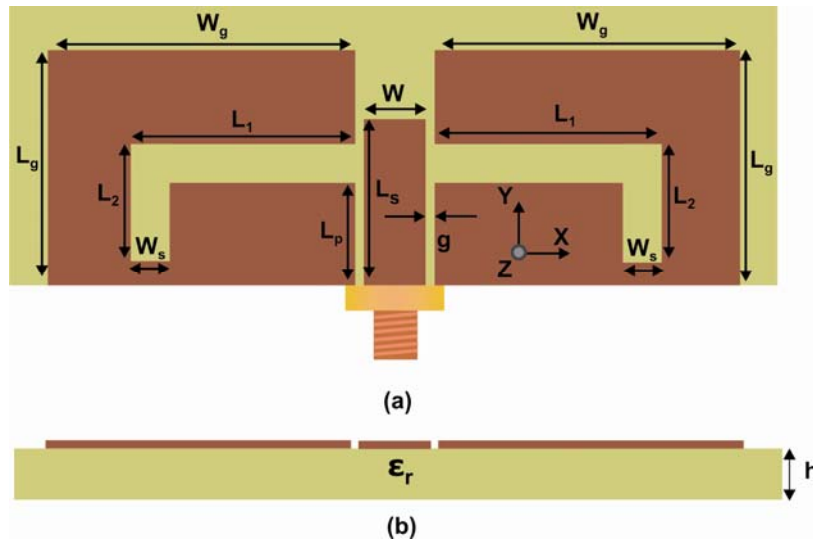


Figure 5.29 Geometry of the L-shaped slot antenna
 ($L_g=15\text{mm}$, $W_g=15\text{mm}$, $L_1=12\text{mm}$, $L_2=7\text{mm}$, $L_s=11\text{mm}$, $L_p=7\text{mm}$,
 $W_s=2\text{mm}$, $W=3\text{mm}$, $g=0.35\text{mm}$, $h=1.6\text{mm}$ and $\epsilon_r=4.4$)

The simulated and measured reflection characteristics of L-slot antenna resonating at 2.4GHz are shown in figure.5.30. The antenna exhibits a 2:1 VSWR bandwidth from 2.39GHz-2.51GHz covering the 2.4GHz WLAN band.

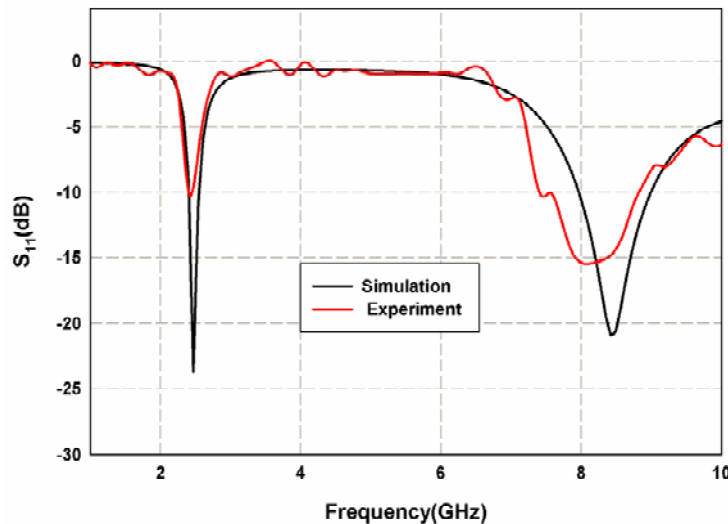


Figure 5.30 Reflection characteristics of the L-slot antenna
 ($L_g=15\text{mm}$, $W_g=15\text{mm}$, $L_1=12\text{mm}$, $L_2=7\text{mm}$, $L_s=11\text{mm}$, $L_p=7\text{mm}$,
 $W_s=2\text{mm}$, $W=3\text{mm}$, $g=0.35\text{mm}$, $h=1.6\text{mm}$ and $\epsilon_r=4.4$)

The total perimeter of the L-shaped slot is about one wavelength in the substrate (slot length = half wavelength) at the resonant frequency. The electric field distribution of the antenna in the X-directed slot is along Y-direction and that of the Y-directed slot is along X-direction. This is responsible for an effective tilt of 45° in the polarization of the antenna. The antenna has a cross polarization level of about 10dB in both the planes.

The measured peak gain in the 2.4GHz band is about 1dBi with small gain variation across the band. Meandering the slots improves the compactness, but generates higher harmonics, which should be removed for better antenna performance. This antenna exhibits second resonance at 8.5GHz as observed in figure.5.30. The first mode at 2.4GHz is matched ($59\Omega - j3\Omega$) while the second mode is suppressed due to high capacitive reactance ($55\Omega - j240\Omega$) but the third mode is excited ($79\Omega + j56\Omega$). So meandering should be done in such a way that along with the compactness the radiation characteristics should also improve.

Without increasing the overall size of the antenna, the radiating area can be effectively utilized to create further reduction in resonance frequency. The L-shaped slot of the above presented antenna is modified as H-shaped slot by adding an additional strip of length L_2 towards the upper direction. The geometry of the proposed structure is shown in figure.5.31. By meandering the structure the total resonating length will increase without increasing the overall area of the antenna.

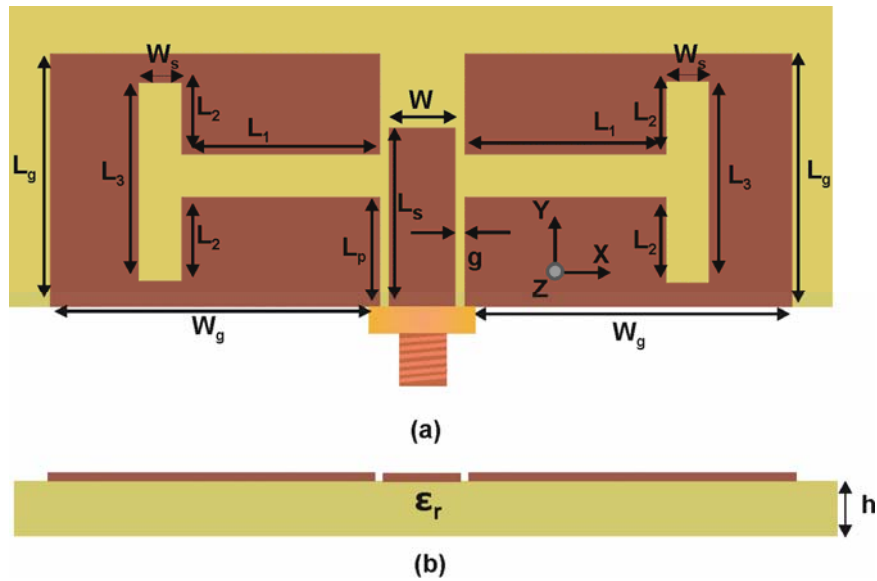


Figure 5.31 Geometry of the H-slot antenna

($W_g=11.25\text{mm}$, $L_g=15\text{mm}$, $L_1=7.5\text{mm}$, $L_2=4.5\text{mm}$, $L_3=10.5\text{mm}$, $L_s=9.37\text{mm}$, $L_p=6.25\text{mm}$, $W_s=2\text{mm}$, $W=3\text{mm}$, $g=0.35\text{mm}$, $h=1.6\text{mm}$ and $\epsilon_r=4.4$)

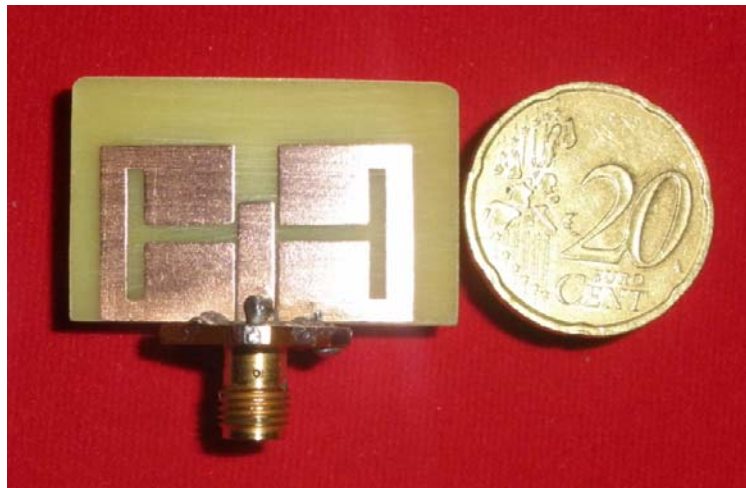


Figure 5.32 Radiation pattern of the antenna at resonance and higher harmonics (a) H-Plane (b) E-Plane

($W_g=11.25\text{mm}$, $L_g=15\text{mm}$, $L_1=7.5\text{mm}$, $L_2=4.5\text{mm}$, $L_3=10.5\text{mm}$, $L_s=9.37\text{mm}$, $L_p=6.25\text{mm}$, $W_s=2\text{mm}$, $W=3\text{mm}$, $g=0.35\text{mm}$, $h=1.6\text{mm}$ and $\epsilon_r=4.4$)

The photograph of the proposed compact antenna is shown in figure.5.32. The return loss characteristic of the antenna is shown in figure.5.33. The antenna exhibits a 2:1 VSWR bandwidth from 2.29GHz-2.49GHz covering the 2.4GHz WLAN band.

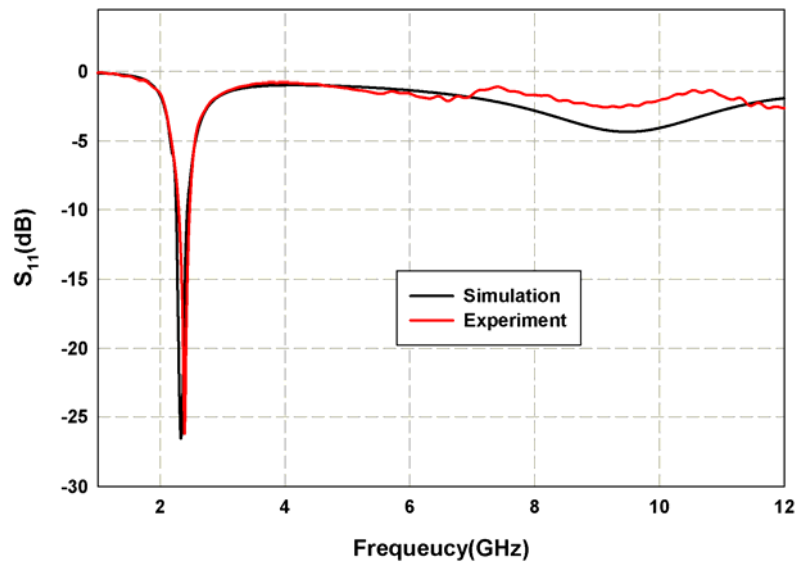


Figure 5.33 Reflection characteristics of the Proposed H-slot antenna
($W_g=11.25\text{mm}$, $L_g=15\text{mm}$, $L_1=7.5\text{mm}$, $L_2=4.5\text{mm}$, $L_3=10.5\text{mm}$,
 $L_s=9.37\text{mm}$, $L_p=6.25\text{mm}$, $W_s=2\text{mm}$, $W=3\text{mm}$, $g=0.35\text{mm}$, $h=1.6\text{mm}$ and
 $\epsilon_r=4.4$)

The third harmonics of L-slot antenna is found to be suppressed in the present antenna as evident from the reflection characteristics. This is achieved by making a H-slot to provide very low impedance ($8\Omega+j3\Omega$) at the third harmonics. The slots (L_2 - towards upper and lower part) will act as two parallel LCR circuits with equal inductance (L), capacitance (C) and resistance in each slot. Therefore the effective resistance decreases drastically and the resonance is suppressed.

The current distribution of the antenna at resonant frequency (2.4GHz) is shown in figure.5.34. The transmission line guides the wave towards the slot and then launches the wave into the slot as in the figure. A full wavelength variation along the perimeter of the slot is observed. The slot insertion is not making any change in the fundamental mode distribution of the coplanar wave guide transmission line. The X directed electric field get cancelled at the far field resulting an effective polarization along the Y-direction.

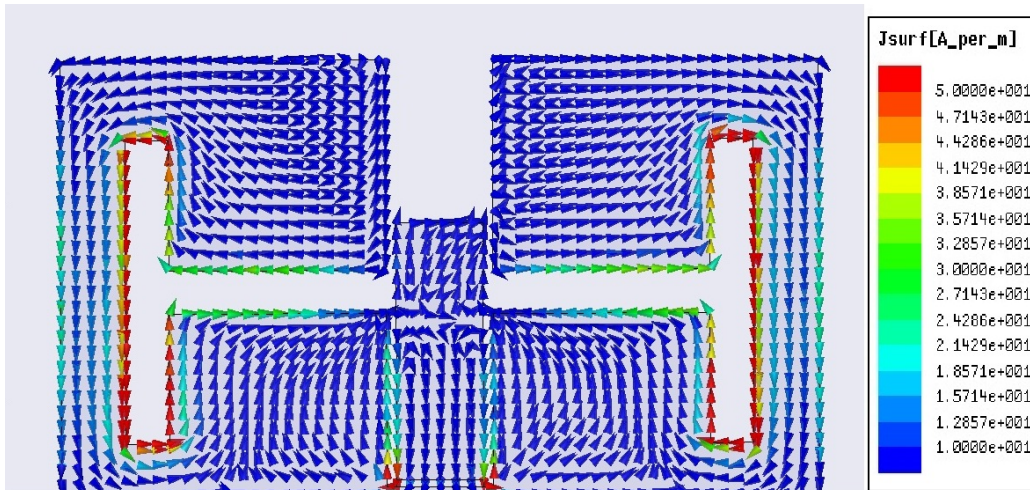


Figure 5.34 Current distribution of the H-slot antenna at the resonant frequency ($W_g=11.25\text{mm}$, $L_g=15\text{mm}$, $L_1=7.5\text{mm}$, $L_2=4.5\text{mm}$, $L_3=10.5\text{mm}$, $L_s=9.37\text{mm}$, $L_p=6.25\text{mm}$, $W_s=2\text{mm}$, $W=3\text{mm}$, $g=0.35\text{mm}$, $h=1.6\text{mm}$ and $\epsilon_r=4.4$)

The variation of input impedance with signal strip (L_s) is shown in Figure.5.35. The reactive part of impedance varies cyclically from highly capacitive to less capacitive as L_s increases. For a given slot the impedance is highly capacitive for small signal strip length. By increasing the strip length the inductance increases and the imaginary part of impedance reaches zero for an optimum length. So it is very interesting to note that the capacitance can be easily tuned by trimming the slot dimension. Similarly the inductance and real

part of impedance can be adjusted by trimming the strip length. At the optimized length, the impedance locus is around 50Ω with affordable reactance at the resonant frequency. For all other frequencies, the structure acts as an open ended CPW fed transmission line.

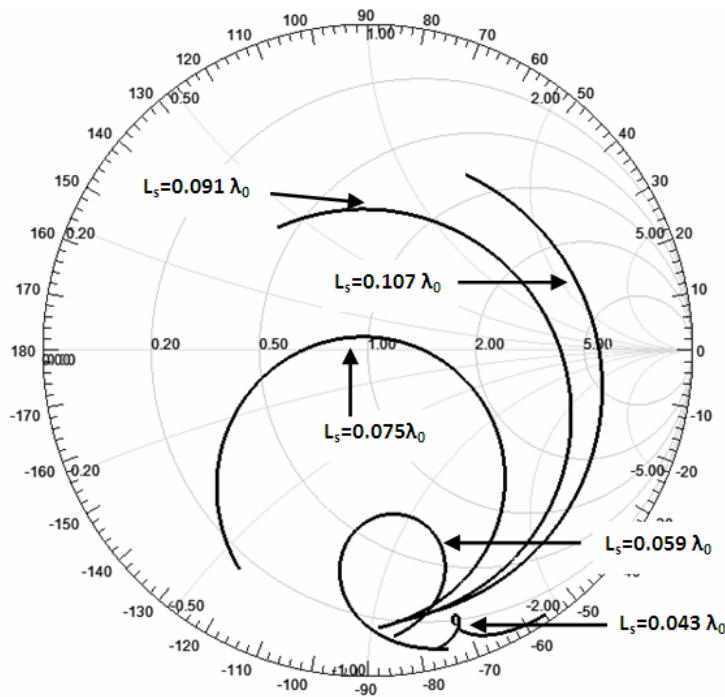


Figure 5.35 Input impedance on Smith Chart for various Strip length L_s ($W_g=11.25\text{mm}$, $L_g=15\text{mm}$, $L_1=7.5\text{mm}$, $L_2=4.5\text{mm}$, $L_3=10.5\text{mm}$, $L_s=9.37\text{mm}$, $L_p=6.25\text{mm}$, $W_s=2\text{mm}$, $W=3\text{mm}$, $g=0.35\text{mm}$, $h=1.6\text{mm}$ and $\epsilon_r=4.4$)

In communication gadgets, the antenna should be used in conjunction with lumped elements and circuit components. So their interaction on antenna performance should be analysed. Thus the antenna is tested with a conducting sheet placed at the backside as shown in figure.5.36. The surface area of the conducting sheet is much larger than that of the antenna. The performance is analyzed by varying the separation distance Z . By placing the conducting sheet at $Z=0\text{mm}$ the effective dielectric constant increases. Thus the resonant

frequency decreases to lower together with the excitation of higher harmonics as shown in figure.5.37. It is obvious that the input impedance of a CPW line will change by making it a conductor backed CPW. It is found that when Z is greater than 1mm the resonant frequency is independent of ground plane. This ensures that placing the conducting sheet at an optimized distance and incorporating the lumped elements will not produce much difference in the reflection characteristics of the antenna.

The power transmitted by the antenna is measured using a horn antenna placed at a distance of 40cm. The received power on the bore sight direction by placing the conductor at different distances is plotted in figure.5.38. The distance at which the conductor is placed depends on the required radiation pattern and radiated power. By keeping the conductor at $\lambda/4$ the total power gets reflected with same phase contributing an enhancement in power (Gain) along the boresight direction as in the figure. Similarly at $2*\lambda/4$ the wave get reflected with a phase difference of 180° contributing a null along the bore sight direction. This property repeats for multiples of quarter wavelength as in the figure.

Thus we can choose the distance of conducting sheet for a particular radiation pattern as per the application. The gain is also enhanced by an amount of 5dBi making the antenna suitable for directive application by properly placing the conducting sheet at the optimized distance.

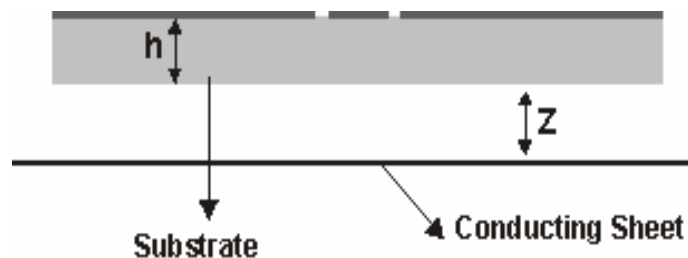


Figure 5.36 Side view of antenna with conducting sheet placed on the back side

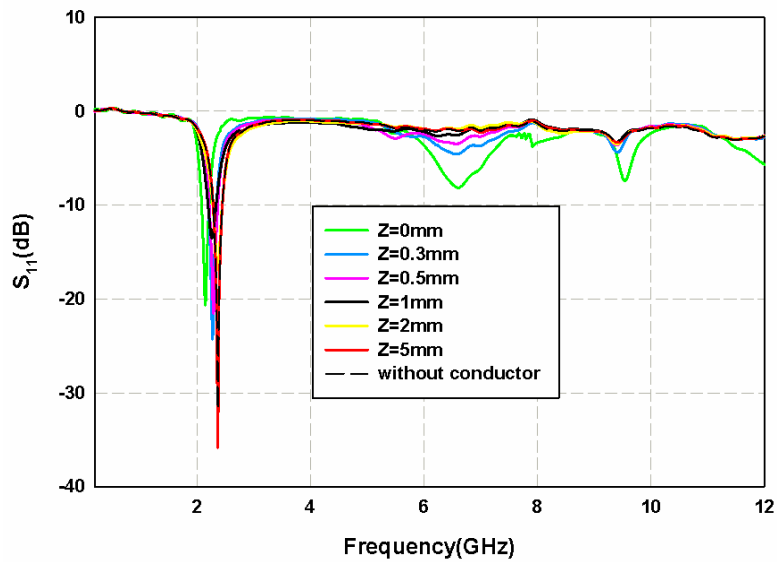


Figure 5.37 Effect of infinite conductor on Antenna performance (Measured)

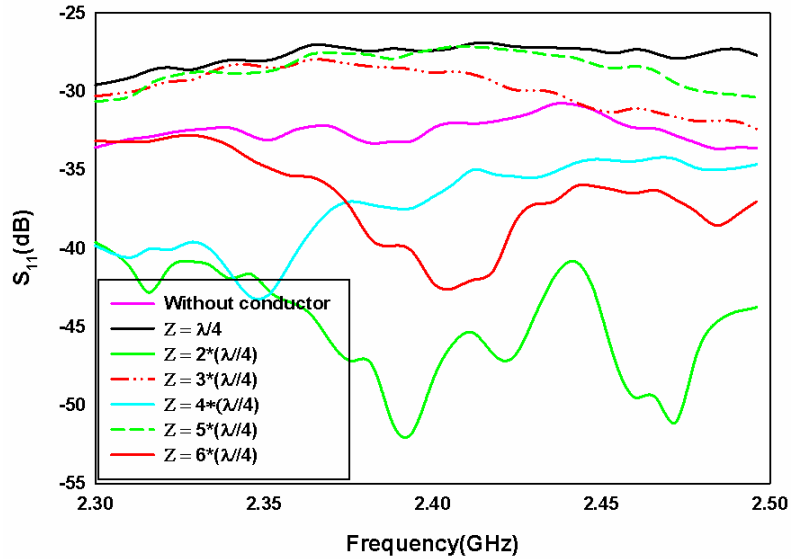


Figure 5.38 Measured Power transmitted by the antenna with conducting sheet at various distances

The H-shaped slot can be considered as a centre-fed slot dipole with each arm of length $\lambda_g/4$, where λ_g is the guided wavelength in the resonant frequency. Top loading the dipole arm (L_3) with L_4 will increase the effective electrical length like a top loaded monopole. The measured radiation patterns of Antenna at resonant frequency and higher harmonics are shown in Figure 5.39. The pattern is uniform in the H-plane and bidirectional in E-Plane as like a centre fed slot antenna. From the figure it is clear that the radiations from the higher harmonics are negligible. Without any additional filters and external circuits the antenna successfully suppresses radiation from higher harmonics up to 12GHz. The measured peak gain in the 2.4GHz band is about 1dBi with small gain variation in the band. The gain of the antenna is small compared to a conventional dipole because the antenna is electrically very small. The efficiency of the antenna measured using wheeler cap method is 79%.

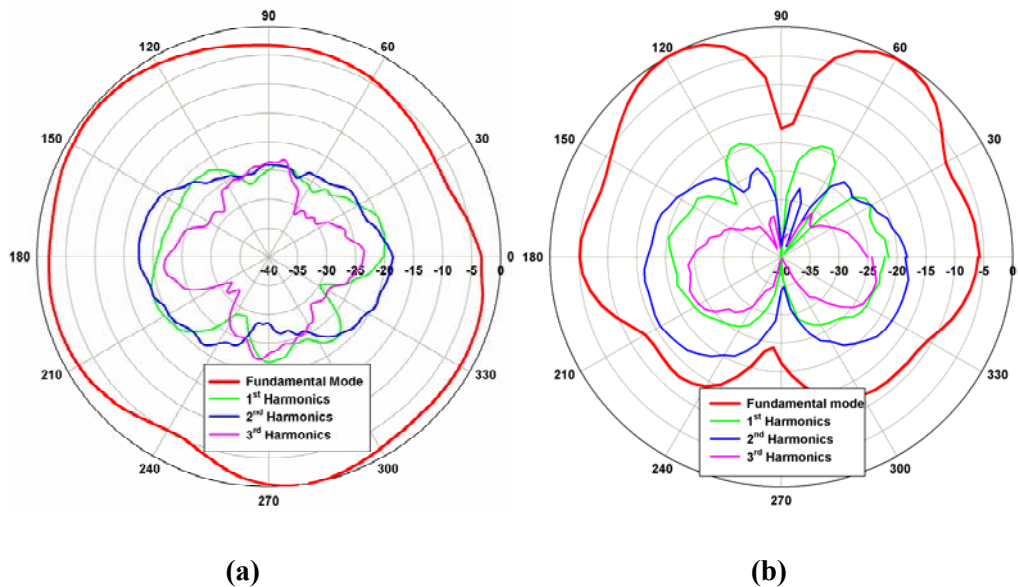


Figure 5.39 Radiation pattern of the antenna at resonance and higher harmonics (a). H-Plane (b). E-Plane
 ($L_g=11.25\text{mm}$, $W_g=15\text{mm}$, $L_1=7.5\text{mm}$, $L_2=4.5\text{mm}$, $L_3=10.5\text{mm}$,
 $L_s=9.37\text{mm}$, $L_p=6.25\text{mm}$, $W_s=2\text{mm}$, $W=3\text{mm}$, $g=0.35\text{mm}$, $h=1.6\text{mm}$
 and $\epsilon_r=4.4$)

5.7 Conclusion

- Introduction of slot along the transmission line of a Coplanar Waveguide can excite a resonance and the tilt in radiation pattern can be overcome by using a symmetrical slot.
- Three different feeding mechanisms (offset feed, Feed penetration and signal strip reduced) to excite the slots are discussed and presented.
- Reconfigurable antennas are designed and developed.
- Meandering the slot can produce additional resonating length and hence can contribute compactness.
- Harmonic suppressed H-slot antenna with suppression upto 3rd harmonics is presented.

References

- [1] John D Kraus and Ronald J Marhefka, Antennas and Wave propagation, Tata McGraw hill,2010

.....✂.....

CONCLUSION AND FUTURE PERSPECTIVE

Contents	6.1 Thesis Highlights
	6.2 Inferences from the investigations on signal strip modified Coplanar Waveguide antennas
	6.3 Inferences from the investigation on ground plane modified antenna
	6.4 Inferences from both ground and signal strip modified antenna
	6.5 Suggestions for future work

This chapter highlights the conclusion drawn from the investigations of signal and ground plane modified Coplanar Waveguide fed antennas. Thus a compact, planar antenna with good radiation characteristics is derived out of a normal coplanar transmission line structure. Suggestions for future work in the fields are also provided.

6.1 Thesis Highlights

This chapter brings the thesis to a close by presenting the conclusions drawn from the outcome of the radiation characteristics of a Coplanar Waveguide transmission line. The main objective of the thesis was to develop antennas by modifying the normal coplanar waveguide transmission line. The experimental and simulation investigations on the possibility of resonance by creating discontinuity on the signal strip and ground plane of a coplanar waveguide transmission line are extensively explained.

Chapter one provides an introduction on antenna research, state of the art antenna technologies, planar antenna research, facilities and techniques for antenna measurements. Some over view on the significant work in related areas, provided in chapter two gives real picture about the importance of the present work. The literature review clearly indicates that the antennas developed are novel concepts. Chapter three described the characteristics features of the signal strip modified coplanar waveguide fed antenna. A quad band antenna is developed by modifying the signal strip of the antenna. Chapter four describes the radiation characteristics of a ground plane modified compact antenna. This single band antenna operates with good omnidirectional radiation pattern. An harmonic suppressed antenna with good radiation properties is presented in chapter five. This harmonic suppressed antenna suppresses up to third harmonics. Appendix A of the thesis presents a planar dual band antenna.

6.2 Inferences from the investigations on signal strip modified Coplanar Waveguide antennas

Coplanar waveguide fed multiband antennas by modifying the signal strip of a Coplanar Waveguide transmission line is discussed in this chapter. Possibility of creating a resonance by folding, top loading and by introducing a

slit on the antenna without affecting the overall size is analyzed. The important inferences from the studies are as follows.

- A resonance in a CPW fed monopole antenna can be generated by suitably top loading and by introducing the folding technique.
- Folding technique can be effectively used to make the antenna more compact.
- Asymmetric loaded CPW antenna can be used for triple band operation.
- The introduction of slit will generate an additional lower resonance without increasing the overall compactness of the antenna.
- The presented quad band antenna is providing good impedance matching with independent control on resonances.
- Design equations are developed and are validated on different dielectric substrates.

6.3 Inferences from the investigation on ground plane modified antenna

A ground meandered single band antenna with high cross polar isolation and good symmetrical radiation pattern is also developed and discussed in chapter 4. Thus the important conclusions arrived are

- The signal to ground plane gap 'g' plays an important role in determining the impedance characteristics of a coplanar waveguide transmission line.
- An optimum lateral ground plane width is necessary for a coplanar waveguide to behave like a normal transmission line. Further increase in ground plane will not enhance the impedance and radiation characteristics.

- The ground plane meandering can be effectively utilized to control the resonance of the antenna.
- Meandering can lower the resonance frequency.
- The resonant frequency is proportional to the slot perimeter.
- Since the radiating elements are purely along Y-direction, the antenna is highly linearly polarized with good cross polar isolation.
- Due to symmetry, the radiation pattern is also symmetric in nature.
- The radiation characteristics of a symmetrically ground meandered antenna is similar to that of a monopole antenna.

6.4 Inferences from both ground and signal strip modified antenna

Experimental investigations have been carried out on the slot antenna by modifying both the signal and ground planes of a CPW fed compact antenna. An harmonic suppressed slot antenna with suppression up to 3rd harmonics is developed. The important conclusions arrived are

- Introduction of slot along the transmission line of a Coplanar Waveguide can excite a resonance.
- Three different feeding mechanisms (offset feed, Feed penetration and signal strip reduced) to excite the slots are discussed and presented.
- Reconfigurable antennas are designed and developed.
- Meandering the slot can produce additional resonating length and hence can contribute compactness.
- Harmonic suppressed H-slot antenna with suppression upto 3rd harmonics is presented.

6.5 Suggestions for future work

The studies on the radiation phenomenon of coplanar waveguide have resulted in a new type of antenna geometries suitable for compact wireless applications. Meandering the resonant path of the ground meandered antenna can be investigated in future for generating additional resonance. Thus the ground plane modified antenna can be easily adapted for dual band and multiband applications. The position of the slot and separation between slots can be adjusted for single and multiband antenna. Printed array can be created by placing the slot of ground and signal strip modified antenna periodically. By suitable array design the radiation pattern can be modified in such a way that it can be used for highly directive applications. The ground and signal strip modified antennas can be used as a feed for Dielectric Resonator Antennas (DRA) and other patch antenna elements. Design and development of reconfigurable antennas using various devices and RFMEMS for tunable wireless applications are a good area of research. By placing parasitic slot on the lateral ground planes the radiation pattern can be made directive. Thus beam steering can be achieved by using reconfigurable slots on any of the lateral ground planes.

.....✂.....

COPLANAR WAVEGUIDE FED ASYMMETRICALLY SLOTTED DUAL BAND ANTENNA

Contents	1. Introduction
	2. Antenna geometry
	3. Result and discussion
	4. Conclusion
	5. References

A multiband antenna developed by perturbing the ground of a Coplanar Waveguide (CPW-Fed) transmission line is studied and presented. The Antenna comprises of two asymmetrical slits on either side of a CPW transmission line. The real and imaginary part of impedance can be independently tuned by adjusting the central strip and the slot parameters to achieve the required impedance matching at resonant frequency. The experimental and simulation studies are presented and discussed in detail.

1. Introduction

Present day communication gadgets demand the requirement of very compact components. The coplanar waveguide lines are nowadays used as feed due to its excellent properties like low dispersion and easy integration with Monolithic Microwave Integrated Circuit (MMIC) devices. Various CPW-Fed antennas with capacitive [1-2] and inductive [3-4] slots have been presented earlier. The dimension of the capacitive H-shaped slot in [1] determine the resonant frequency, while that in [2] uses a asymmetrical slots on either side of transmission line to produce circular polarization. The inductive slot antenna presented in [4] uses an inductor with optimum value at one end of the inductive slot in order to achieve compactness as well as broadband. Since the electric field distribution in the slot significantly affect the value of the input impedance and the radiation pattern, the resonant modes can be easily selected by varying the slot parameters. In this paper an alternative method to easily achieve the impedance matching of CPW fed antenna is illustrated.

2. Antenna Geometry

The geometry of the proposed antenna is shown in figure.A.1. The antenna is very compact with an overall dimension of 34mm x 15mm when printed on a substrate of dielectric constant 4.4 and thickness 1.6mm. The width (w) of signal strip and gap (g) of the CPW are selected for 50 Ω impedance matching. The width (Ws) of the slot is constant and is same for both the slots. The position of the slits L_{p1} and L_{p2} are not equal as in the symmetrical structures discussed before. One of the slot in the lateral ground plane is meandered to achieve a higher resonating length by using the unutilized metallic area. The detailed characteristics of the asymmetric systems are presented.

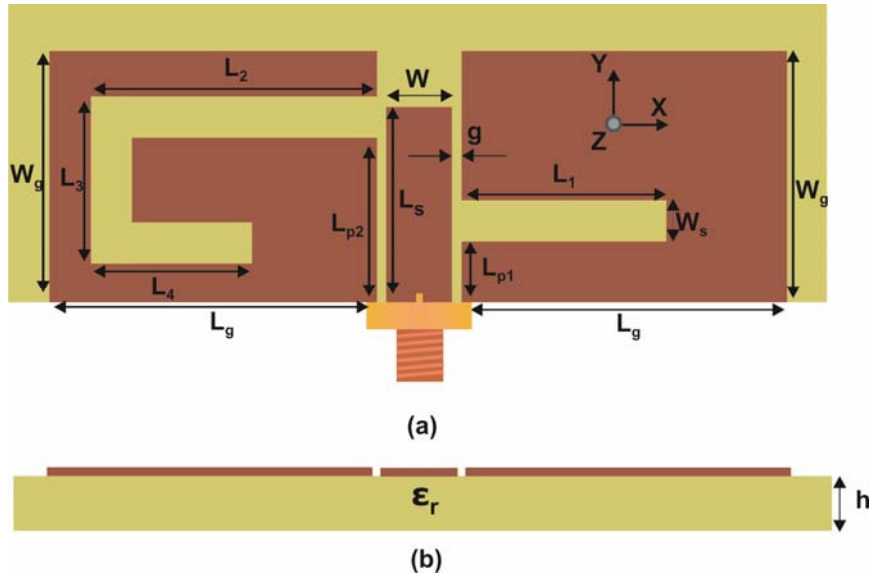


Figure A.1 Geometry of the Proposed dual band antenna
 ($L_g=15\text{mm}$, $W_g=15\text{mm}$, $L_1=10\text{mm}$, $L_2=12\text{mm}$, $L_3=8\text{mm}$,
 $L_4=6.5\text{mm}$, $L_{p2}=8.5\text{mm}$, $L_{p1}=4\text{mm}$, $L_s=10\text{mm}$ $w_s=2\text{mm}$,
 $w=3\text{mm}$, $g=0.35\text{mm}$ $h=1.6$, $\epsilon_r=4.4$)

3. Result and Discussion

The simulated and experimental return loss characteristics of unsymmetrical slotted antenna are shown in figure.A.2. The antenna is exhibiting a 2:1 VSWR band width from 2.35GHz-2.49GHz and 5.003GHz-5.47GHz covering 2.4/5.2 GHz WLAN bands. The simulation of the antenna is carried out using Ansoft High Frequency Structure Simulator (HFSS) and experiment using HP8510C Vector Network Analyser.

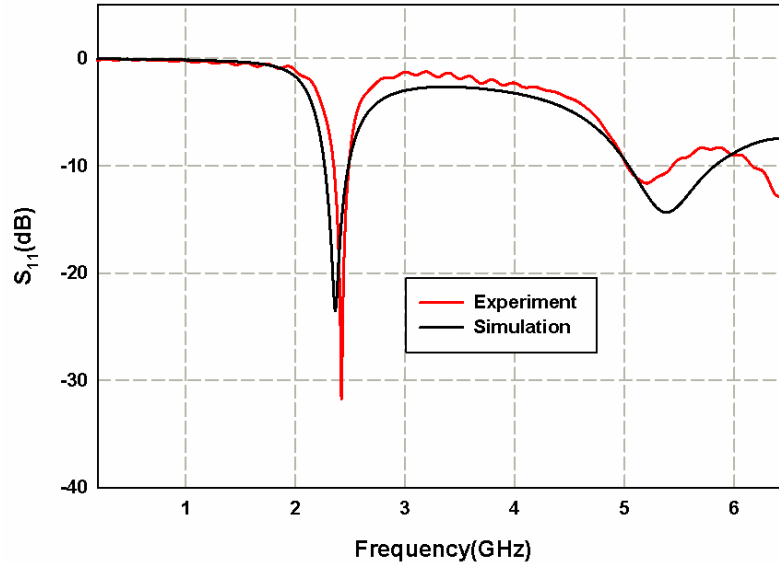


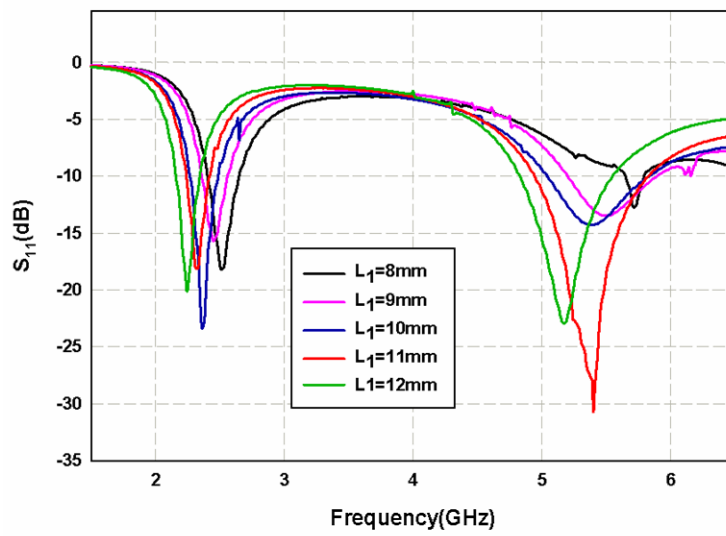
Figure.A.2 Reflection characteristics of the dual band antenna
 $(L_g=15\text{mm}, W_g=15\text{mm}, L_1=10\text{mm}, L_2=12\text{mm}, L_3=8\text{mm},$
 $L_4=6.5\text{mm}, L_{p2}=8.5\text{mm}, L_{p1}=4\text{mm}, L_s=10\text{mm}, w_s=2\text{mm},$
 $w=3\text{mm}, g=0.35\text{mm}, h=1.6, \epsilon_r=4.4)$

As already described in the previous chapter that the reflection characteristic without any slot is like that of an open ended transmission line and by introducing a slot on either ground will generate a poorly matched resonance. The radiation pattern of such an asymmetric slot antenna is found to be tilted. Here the introduction of symmetrical slots on ground can overrule this to give the single resonance having radiation pattern without any tilt. Moreover, three different feeding methods to get good impedance matching is also described. These resonances are found to be depending on the slot length. This type of antenna is very attractive for modern wireless communication gadgets. Symmetrical horizontal slots will provide polarization on vertical direction(y-directed).

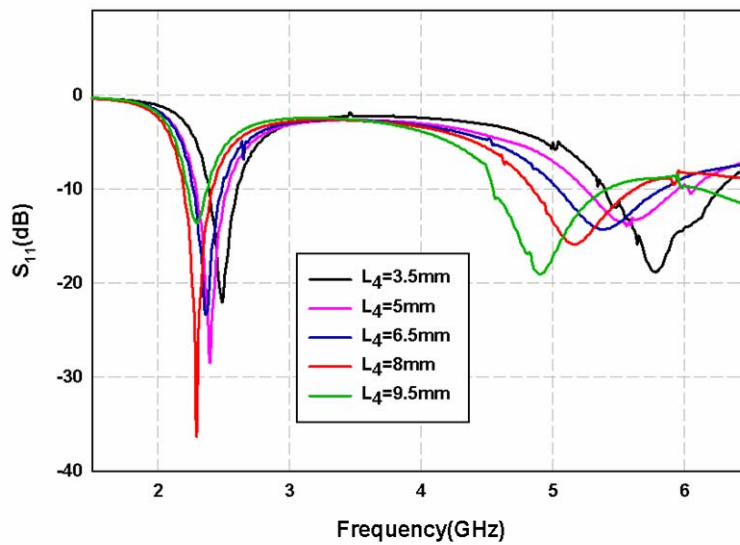
By properly selecting the asymmetrical dimensions for both the slots the user can produce different resonances. This methodology is effectively utilized for the design of presented multiband antenna. The experiment and simulation of CPW fed ground perturbed dual band antenna have been designed and successfully implemented for 2.4/5.2 GHz WLAN bands. This type of antenna is highly compact in nature and hence can be easily integrated on small electronic gadgets

The optimized slot dimension are $L_1=10\text{mm}$, $L_2=12\text{mm}$, $L_3=8\text{mm}$, $L_4=6.5\text{mm}$ and $W_s=2\text{mm}$. This antenna is resonating at 2.4GHz (2.35GHz- 2.49GHz) and 5.2GHz (5.003GHz- 5.47GHz). It is very interesting to note that when the slots are symmetric the antenna is resonating only at its fundamental mode. When the slots are asymmetric it can allow higher harmonics also. The optimization of the antenna for different slot parameters has been done and is explained in the forthcoming section.

The variations of the antenna performance with the slot dimensions are performed. The slot lengths (L_1 & L_4) are varied and their return loss characteristics are shown in figure.A.3 (a) & figure.A.3 (b). From the figures it is evident that both the resonances are varying with the slot lengths. As the slot length increases the resonance shift to lower region and vice versa. It is noted that the impedance matching is not at all affecting with the change in slot length and hence offering an affordable mechanical tuning range. Thus by considering the required impedance bandwidth at the resonant frequency, slot lengths are optimized at 6.5mm and 10mm respectively.



(a)



(b)

FigureA.3 Variation in Reflection characteristics of the dual band antenna with slot length (a) L1 (b) L4
 $(L_g=15\text{mm}, W_g=15\text{mm}, L_2=12\text{mm}, L_3=8\text{mm}, L_{p2}=8.5\text{mm}, L_{p1}=4\text{mm}, L_s=10\text{mm}, w_s=2\text{mm}, w=3\text{mm}, g=0.35\text{mm}, h=1.6, \epsilon_r=4.4)$

As explained in the earlier designs that the signal strip is the major factor in determining the impedance matching is also verified in this dual band antenna. Variation in reflection characteristics of the dual band antenna with signal strip length is shown in figure.A.4. The impedance matching together with the frequency of the antenna is varied with respect to the variation in signal strip length.

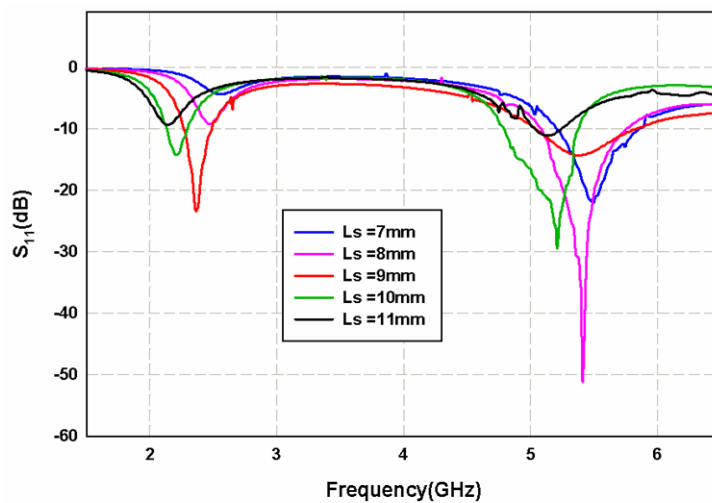


Figure A.4 Variation in Reflection characteristics of the dual band antenna with signal strip length L_s
 $(L_g=15\text{mm}, W_g=15\text{mm}, L_1=10\text{mm}, L_2=12\text{mm}, L_3=8\text{mm}, L_4=6.5\text{mm}, L_{p2}=8.5\text{mm}, L_{p1}=4\text{mm}, L_s=10\text{mm}, w_s=2\text{mm}, w=3\text{mm}, g=0.35\text{mm}, h=1.6, \epsilon_r=4.4)$

By suitably changing the slot width the imaginary part of characteristic impedance of the antenna can be adjusted for obtaining the required impedance bandwidth. The return loss variation of the antenna with the slot width W_s of the smaller and larger slots are shown in figure.A.5. and figure.A.6. Even though there is not much variation in resonance it significantly affects the impedance bandwidth. For the design presented here the slot width (W_s) for both the lower and higher slots are optimized at 2mm.

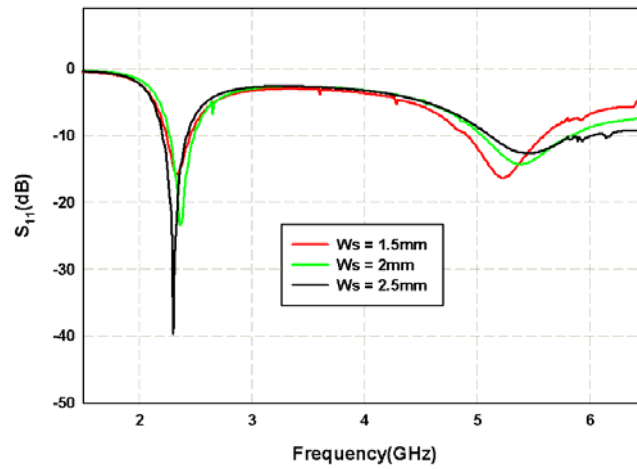


Figure A.5 Variation in Reflection characteristics of the dual band antenna with slot width W_s of strip L_1 ($L_g=15\text{mm}$, $W_g=15\text{mm}$, $L_2=12\text{mm}$, $L_3=8\text{mm}$, $L_4=6.5\text{mm}$, $L_{p2}=8.5\text{mm}$, $L_{p1}=4\text{mm}$, $L_s=10\text{mm}$, $w=3\text{mm}$, $g=0.35\text{mm}$ $h=1.6$, $\epsilon_r=4.4$)

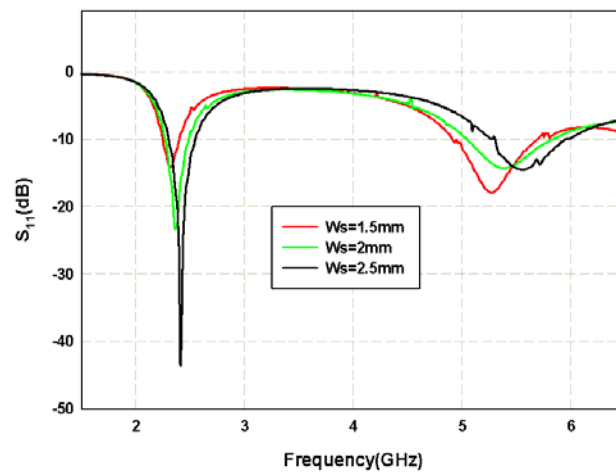


Figure A.6 Variation in Reflection characteristics of the dual band antenna with slot width of strip L_2 , L_3 and L_4 ($L_g=15\text{mm}$, $W_g=15\text{mm}$, $L_2=12\text{mm}$, $L_3=8\text{mm}$, $L_4=6.5\text{mm}$, $L_{p2}=8.5\text{mm}$, $L_{p1}=4\text{mm}$, $L_s=10\text{mm}$, $w=3\text{mm}$, $g=0.35\text{mm}$ $h=1.6$, $\epsilon_r=4.4$)

The position of the slot is also very important while designing the dual band antenna and need to be optimized. The slot position L_{p1} is affecting both the resonances in a different manner that is as the slot position increases the

lower resonances shift to higher frequency region and the higher resonance shift to lower frequency region. Thus the resonant length corresponding to first resonance increases with the slot position and that of the second resonance decreases with the slot position. The variations in reflection characteristics with respect to the slot positions are shown in figure.A.7 (a) and (b).

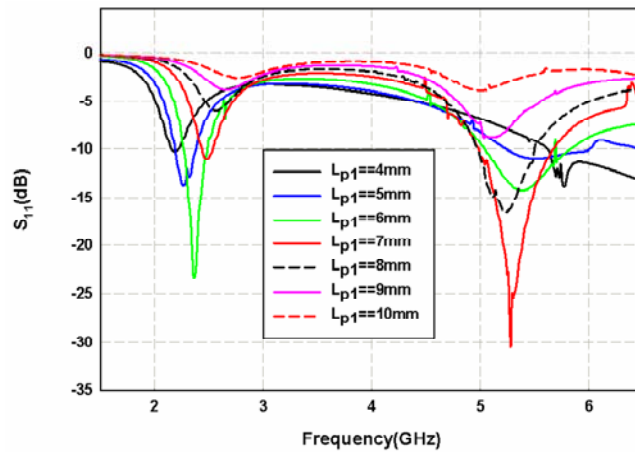


Figure A.7(a) Variation in Reflection characteristics of the dual band antenna with slot position L_{p1}
 ($L_g=15\text{mm}$, $W_g=15\text{mm}$, $L_2=12\text{mm}$, $L_3=8\text{mm}$, $L_4=6.5\text{mm}$, $L_{p2}=8.5\text{mm}$, $L_s=10\text{mm}$, $w=3\text{mm}$, $w_s=2\text{mm}$, $g=0.35\text{mm}$ $h=1.6$, $\epsilon_r=4.4$)

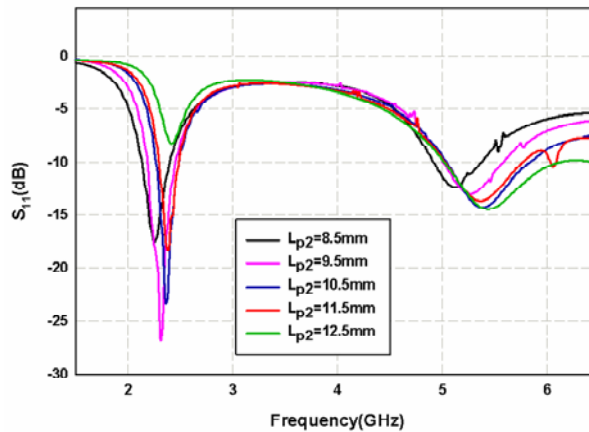


Figure A.7 (b) Variation in Reflection characteristics of the dual band antenna with slot position L_{p2}
 ($L_g=15\text{mm}$, $W_g=15\text{mm}$, $L_2=12\text{mm}$, $L_3=8\text{mm}$, $L_4=6.5\text{mm}$, $L_{p2}=8.5\text{mm}$, $L_s=10\text{mm}$, $w=3\text{mm}$, $w_s=2\text{mm}$, $g=0.35\text{mm}$ $h=1.6$, $\epsilon_r=4.4$)

The current distribution of the antenna at 2.4GHz and 5.2GHz band are shown in Figure.A.8 (a) and Figure.A.8 (b) respectively.

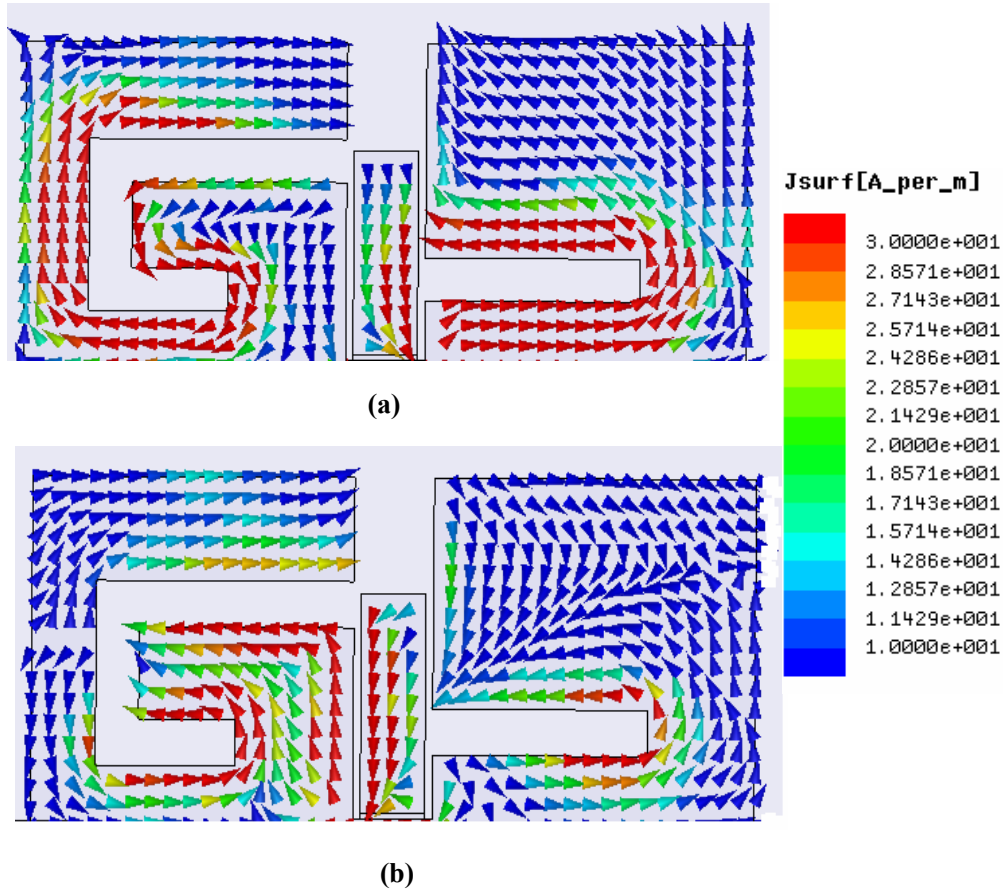


Figure A.8 Current distribution of the dual band antenna at (a) 2.4GHz (b) 5.2GHz
 ($L_g=15\text{mm}$, $W_g=15\text{mm}$, $L_2=12\text{mm}$, $L_3=8\text{mm}$, $L_4=6.5\text{mm}$, $L_{p2}=8.5\text{mm}$,
 $L_{p1}=4\text{mm}$, $L_s=10\text{mm}$, $w=3\text{mm}$, $w_s=2\text{mm}$, $g=0.35\text{mm}$ $h=1.6$, $\epsilon_r=4.4$)

A half wavelength variation along the meandered slot is contributing for the first resonance centered at 2.4GHz which is clearly visible from the current distribution. Significant current is found to be there on the signal strip along the smaller slot side.

A full wave variation along the meandered strip is occurring for the higher resonance centered at 5.2GHz. A half wave variation along the smaller slot is also contributing for the resonance. Moreover a current variation along the signal strip on the meandered slot side is convincing its effect on the resonance and impedance matching.

The electric fields along the horizontal slots will be in vertical direction(y-direction) and hence the polarization is along Y-direction. Since the horizontal slot length dominates the vertical slot, the polarization is along Y-direction. It is also noted that the asymmetrical slots can degrade the polarization discrimination. The radiation pattern of the antenna at two resonant frequencies is shown in Figure.A.9. The pattern is found to be non directional in the H-plane on both the bands. But due to the asymmetry in structure the pattern is found to be disturbed in the E-plane. Even then the antenna is showing good radiation characteristics suitable for portable wireless communication gadgets.

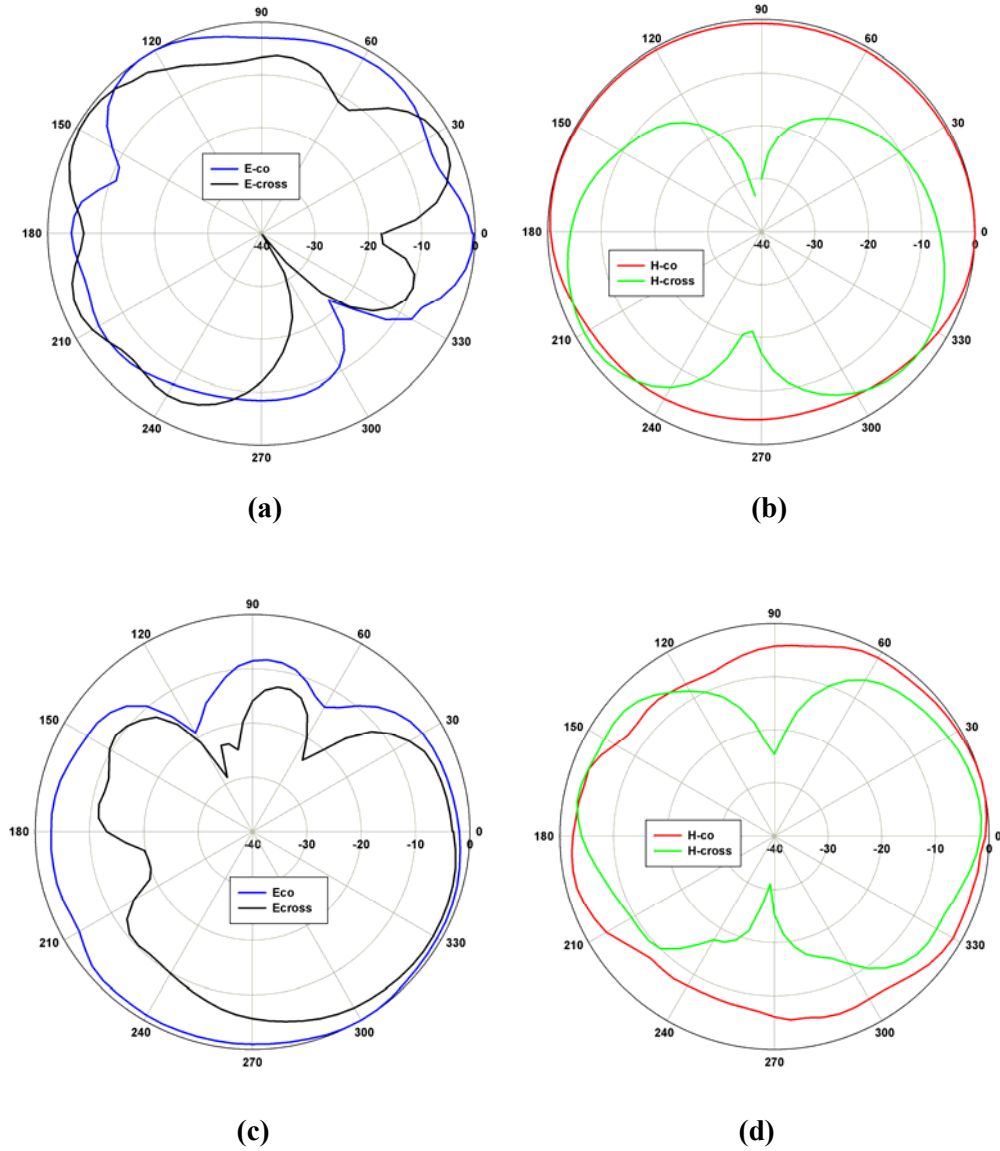


Figure A.9 Radiation pattern of the dual band antenna at 2.4GHz (a) E-plane (b) H-plane and 5.2GHz (c) E-plane (d) H-plane ($L_g=15\text{mm}$, $W_g=15\text{mm}$, $L_2=12\text{mm}$, $L_3=8\text{mm}$, $L_4=6.5\text{mm}$, $L_{p2}=8.5\text{mm}$, $L_{p1}=4\text{mm}$, $L_s=10\text{mm}$, $w=3\text{mm}$, $w_s=2\text{mm}$, $g=0.35\text{mm}$ $h=1.6$, $\epsilon_r=4.4$)

The gains of the antenna on two bands are measured using gain transfer method and are shown in figure.A.10. The antenna has a peak gain of 1.4dBi and 3.2dBi in the 2.4GHz and 5.2GHz bands.

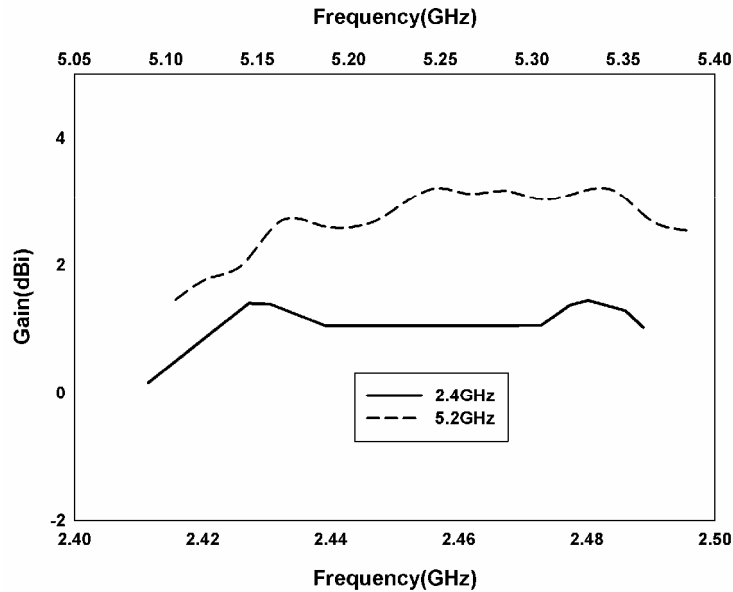


Figure A.10 Gain of the dual band antenna
 $(L_g=15\text{mm}, W_g=15\text{mm}, L_2=12\text{mm}, L_3=8\text{mm}, L_4=6.5\text{mm}, L_{p2}=8.5\text{mm},$
 $L_{p1}=4\text{mm}, L_s=10\text{mm}, w=3\text{mm}, w_s=2\text{mm}, g=0.35\text{mm}, h=1.6, \epsilon_r=4.4)$

4. Conclusion

A Novel CPW fed ground perturbed antenna for dual band application have been designed and successfully implemented. The experiment and simulation are in good agreement. This compact antenna with asymmetric slots on either side of transmission line is suitable for 2.4/5.2 GHz WLAN bands.

5. References

- [1] Y-F. Lin, P-C. Liao, P-S. Cheng, H-M. Chen, C.T.P. Song and P.S. Hall, "CPW-fed capacitive H-shaped narrow slot antenna", IEE Elect. Letters, Vol. 41, No. 17, pp 940-942, August 2005.

- [2] Chien-Jen Wang and Chih-Hsing Chen, "CPW-Fed Stair-Shaped Slot Antennas With Circular Polarization", *IEEE Trans on Antennas and Propagation*, Vol.57, pp.2483-2486, August 2009.
- [3] Alpesh U.Bhode, Christopher L.Holloway, Melinda Picket-May, Richard Hall, "Wide-Band Slot Antennas With CPW Feed Lines: Hybrid and Log Periodic Designs", *IEEE Trans on Antennas and Propagation*, Vol.52, pp.2545-2554, October 2004.
- [4] Cheng-Cieh Yu and Xian-Chang Lin, "A Wideband Single Chip Inductor-Loaded CPW-Fed Inductive Slot Antenna" ", *IEEE Trans on Antennas and Propagation*, Vol.56, No. 5, pp.1498-1501, May 2008.

.....❧.....



International Journals

1. **R Sujith**,Deepu.V,Laila D,C.K.Aanandan,K.Vasudevan and P.Mohanana, "A Compact Dual-Band Modified T-shaped CPW-Fed Monopole Antenna", Microwave and Optical Technology Letters, Vol. 51, No. 4, April 2009.
2. **R. Sujith**, S. Mridula, P. Binu, D. Laila, R. Dinesh and P. Mohanana, "Compact CPW-fed ground defected H-shaped slot antenna with harmonic suppression and stable radiation characteristics" **Electronics letters** 10th June 2010 Vol. 46 No. 12.
3. **R. Sujith**, V. Deepu, S. Mridula, Binu Paul, D. Laila, P. Mohanana "Compact CPW-fed uniplanar antenna for multiband wireless applications" AEU - International Journal of Electronics and Communications, In Press, Available online 10 October 2010.
4. **R Sujith**, Mridula S, Laila D, C K Aanandan, K Vasudevan and P Mohanana, " Compact CPW-Fed Slot Antenna with harmonic suppression", Accepted in International journal of RF and Microwave computer-Aided Engineering.
5. Sumesh George, Mailadil Thomas Sebastian, **Sujith Raman** and Pezholil Mohanana, "Novel Low Loss, Low Permittivity Glass–Ceramic Composites for LTCC Applications" International Journal of Applied Ceramic Technology, August 2009.
6. J. Chameswary , K. Jithesh , S. George , **S. Raman** , P. Mohanana , M.T. Sebastian "PTFE–SWNT composite for microwave absorption application ",Materials letters,2010
7. Laila D, ,Deepu.V, **Sujith R**, P.Mohanana,C.K.Aanandan, and K.Vasudevan "Compact asymmetric coplanar strip fed antenna for wide band applications" Microwave and Optical Technology Letters, May 2009.
8. Deepu V, S Mridula,**R Sujith** and P Mohanana, ACS fed printed F shaped uniplanar antenna for Dual band WLAN applications, Microwave and Optical Technology Letters, May 2009.

9. Deepu.V, S.Mridula, **Sujith R** and P.Mohanan, "Slot line fed dipole antenna for wide band applications", Microwave and Optical Technology Letters, Vol. 51, No. 3, March 2009.
10. Sherin Thomas, **Sujith Raman**, P. Mohanan, M.T. Sebastian "Effect of coupling agent on the thermal and dielectric properties of PTFE/Sm₂Si₂O₇ composites",Composites,Volume 41A, Issue 9, September 2010.
11. T. S. Sasikala , **S. Raman** , P. Mohanan , C. Pavithran and M. T. Sebastian "Effect of silane coupling agent on the dielectric and thermal properties of polymer-ceramic composites, Journal of polymer research,July 2010.
12. D. Laila, **R. Sujith**, M. N. Sreejith, C. K. Aanandan, K Vasudevan and P. Mohanan "Mobile antenna with reduced radiation hazards towards human head" Progress In Electromagnetics Research Letters, Vol. 17, 39-46, 2010.
13. Vishnu, Nithyaja, Pradeep, **Sujith R**, V.P.N Nampoothiri and P Mohanan, " Studies on the effect of mobile phone radiation on DNA using laser induced fluorescence technique", Accepted for publication in Laser Physics.
14. Laila.D,**Sujith.R**, Shameena V.A,Deepak.U,Nijas.C.M and P.Mohanan"CPW fed antenna for mobile handset with metal wire mesh", Accepted for publication, International Journal of Computer Applications.

Conferences

1. Deepu.V, **Sujith.R** , Binu paul and P. Mohanan "Compact asymmetric coplanar strip fed Dual Band Antenna for WLAN applications" URSI GA 2008 ,USA
2. **Sujith Raman**, Deepu V, K vasudevan, C.K Aanandan and P. Mohanan "Compact CPW fed antenna for multiband applications" Antennas and propagation Symposium(APSYM) 2008
3. **Sujith.R**, Deepu. V, Laila.D, S. Mridula and P.Mohanan, "CPW-fed Quad Band antenna for Compact wireless application" IEEE Applied Electromagnetic conference-2009 (AEMC-09), Kolkatta, India.
4. Deepu V, **Sujith R** and P. Mohanan "Compact Uniplanar PIFA For Multiband Applications", International conference on Aerospace Science and Technology (INCAST 2008),India.

5. Deepu, V. Mridula, S. **Sujith.R.** Mohanan P “Compact uniplanar antenna for multiband applications”, IEEE international conference on Recent advances in microwave theory and applications, 21-24 November 2008, Jaipur, India
6. Laila, D.; Deepu, V.; **Sujith, R.**; Mohanan, P.; Anandan, C.K.; Vasudevan, K. “Asymmetric Coplanar Strip fed wide band antenna “IEEE international conference on Recent advances in microwave theory and applications, 21-24 November 2008, Jaipur, India
7. Nisha mol M.S, Sarin V.P, Deepu V, **Sujith R**, C.K Aanandan, P. Mohanan and K. Vasudevan “ Cross patch antenna with an X-slot for polarisation switching”, Proc. of the National Symposium on antennas and propagation(APSVM-2008), 29-31 Dec. 2008, pp.217-221, Cochin University of Science and Technology, Kochi, India.
8. Sarin V.P, Nisha mol M.S, Deepu V, **Sujith R**, C.K Aanandan, P. Mohanan and K. Vasudevan “Broadband microstrip antenna for wireless applicatins”, , Proc. of the National Symposium on antennas and propagation(APSVM-2008), 29-31 Dec. 2008, pp.238-240, Cochin University of Science and Technology, Kochi, India.
9. Laila D, **Sujith R**, Deepu V, K. vasudevan, C.K Aanandan and P.Mohanan “Compact uniplannar antenna for wide band applications” Antennas and propagation Symposium (APSVM) 2008
10. S. George, **S. Raman**, P. Mohanan and M. T. Sebastian,” Polymer ceramic composites for microwave substrate and antenna applications” Indian antenna week , workshop on advanced antenna technology, June-2010, puri-India.
11. Laila D, **Sujith.R**, Deepu.V, C.K. aanandan, K.Vasudevan,”Compact CSRR based patch antenna for wireless application”Applied Electromagnetic conference-2009 (AEMC-09), Kolkatta, India.
12. **R. Sujith**,Mridula S, Binu Paul, D. Laila, C.K. Aanandan, K. Vasudevan and P. Mohanan “Compact CPW-FED Defected Ground Antenna”, EUCAP2010, Barcelona,Spain 2010
13. Laila D, **Sujith Raman**, Sreejith M Nair, Aanandan C.K, Vasudevan K. and Mohanan P “Modified CPW fed monopole antenna with a radiation pattern suitable for mobile handset”, 2011 International Conference on Communications and Signal Processing(ICCSP 2011), Calicut, India.

14. Laila.D, **Sujith.R**, Shameena V.A, Deepak.U, Nijas.C.M and P.Mohanan”CPW fed antenna for mobile handset with metal wire mesh” ICVCI-2011, St.Gits, Kottayam.
15. **Sujith R**, Mridula S, BinuPaul and P Mohanan “Stripline fed slot coupled Dielectric Resonator Antenna for low radiation hazard from mobile handset” The 9th International meeting of PACific RIM Ceramic societies (PACRIM9), Cairns, Queensland- 10th-14th, July-2011.
16. **Sujith.R**, Mridula S, C.K. Aanandan, K Vasudevan and P. Mohanan, “Compact Coplanar Waveguide Fed Ground Meandered Antenna for Wireless Application”, URSI GASS(13-20 August 2011), Istanbul, Turkey.

.....✂.....

Citations

- A. R Sujith,Deepu.V,Laila D,C.K.Aanandan,K.Vasudevan and P.Mohanan, “**A Compact Dual-Band Modified T-shaped CPW-Fed Monopole Antenna**”, Microwave and Optical Technology Letters, Vol. 51, No. 4, April 2009.
1. Chen J, Fu G, Wu G.-D, Gong, S.-X., Compact Graded Central Feeder Line CPW-fed Broadband Antenna Journal of Electromagnetic Waves and Applications, Volume 23, 2009 , pp. 2089-2097
 2. Joseph Manoj, Microstrip-fed compact dual band planar antenna, Ph.D thesis, Cochin University of Science and Technology.
 3. Shu Chang, Xiaodong Yang, Yingsong Li, Ming Li, ” A dual and wide band antenna for WLAN/WiMAX/UWB applications “2011 International Conference on Consumer Electronics, Communications and Networks (CECNet), April 2011, pp 958 – 961
 4. Hattan F. AbuTarboush, R. Nilavalan, Thomas Peter, and S. W. Cheung, “Multiband Inverted-F Antenna With Independent Bands for Small and Slim Cellular Mobile Handsets, IEEE trans. on antennas and propag, vol. 59, No. 7, July 2011, pp 2636-2645.
 5. R. Sujith, V. Deepu, S. Mridula, Binu Paul, D. Laila, P. Mohanan “Compact CPW-fed uniplanar antenna for multiband wireless applications” AEU - International Journal of Electronics and Communications Volume 65, Issue 6, June 2011, pp 553-559
 6. Hattan F. Abutarboush, R. Nilavalan, S. W. Cheung, K. M. Nasr, T. Peter, D. Budimir, and H. Al-Raweshidy “A Reconfigurable Wideband and Multiband Antenna Using Dual Patch Elements for Compact Wireless Devices, IEEE Transactions on Antennas and Propagation, PP Issue:99
 7. Chen J, Fu G, Wu G.D, Gong S.-X, Chen, X ” Combinational Structure Open Sleeve Antenna for Multiband Applications “Journal of Electromagnetic Waves and Applications, Volume 24, Numbers 11-12, 2010 , pp. 1439-1447(9)
 8. Kyunghaeng Lee, Yong Jee, “Multiresonance coplanar waveguide-fed monopole antennas with meander strips for GSM/GPS/PCS/DCS/WCDMA applications” Microwave and Optical Technology Letters, Volume 53, Issue 10, pp 2438–2441, October 2011

9. Chang shu Liying Song Yang Xiaodong, An apply WLAN / WiMAX dual-band antenna, “Harbin Engineering University, Information and Communication Engineering
- B.**
- R. Sujith, S. Mridula, P. Binu, D. Laila, R. Dinesh and P. Mohanan, “**Compact CPW-fed ground defected H-shaped slot antenna with harmonic suppression and stable radiation characteristics**” Electronics letters 10th June 2010 Vol. 46 No. 12
1. Yongle Wu, Cuiping Yu, Yuanan Liu and Shulan Li , “A Generalized 90° Impedance Transformer with Improved Spurious Suppression for Arbitrary Real Terminated Impedances” Electromagnetics ,Volume 31, Issue 7, 2011.
 2. Mohammad Saeid Ghaffarian and Gholamreza Moradi, “A Novel Harmonic Suppressed Coplanar Waveguide (CPW)-Fed Slot Antenna “, Ieee antennas and wireless propagation letters, vol. 10, 2011.
 3. Sujith, S. Mridula, D. Laila, C. K. Aanandan, K. Vasudevan, P. Mohanan “Compact CPW-Fed slot antenna with harmonic suppression “International Journal of RF and Microwave Computer-Aided Engineering Volume 21, Issue 5, September 2011, pp 543–550.
 4. Sujith, R. Mridula, S.; Aanandan, C.K.; Vasudevan, K.; Mohanan. P ,” Compact coplanar waveguide fed ground meandered antenna for wireless application”, General Assembly and Scientific Symposium, 2011 XXXth URSI, pp 1-4.
 5. Alireza Mallahzadeh, Ali Foudazi, Sajad Mohammad Ali Nezhad , “A small-size pentaband hand-shaped coplanar waveguide-fed monopole antenna, Microwave and Optical Technology Letters Volume 53, Issue 7, July 2011, pp 1576–1579.
 6. Xiao Dong Yang, A. Rahman, Qammer H. Abbasi, Y. Hao “Electrically coupled tapered slot ultra wideband antenna with tunable notch”, Microwave and Optical Technology Letters, Volume 53, Issue 7, July 2011, pp 1558–1561.

Curriculum Vitae

SUJITH R

Senior Research Fellow,
Centre for Research in Electromagnetics and Antennas(CREMA)
Department of Electronics, Cochin University of Science and Technology,
Cochin 682 022, Kerala, India
Phone: 91-484-2576418 Mobile: 91-9895680620 Fax: 91-484-2575800
E-mail: sujithrpkd@gmail.com.

OBJECTIVE

To get a challenging position in an organization to pursue research activities in the field of Electromagnetics and antennas.

SUMMARY

- **4 years of** research experience in Microwave communication, especially in Antennas, Electromagnetics and Dielectric measurements.
- **Publications – 30; International journal – 14; Conferences – 16**
- **Citations - 15**
- Proficiency in Design and Development of various types of antennas
- Proficiency in Microwave material characterization of dielectric substrates

HONORS, AWARDS & ACHIEVEMENTS

- **Young Scientist Award** by International Union of Radio Science (URSI) 2011.
- Awarded with **Research Fellowship in Sciences for Meritorious students** by University Grants Commission (UGC), Govt.of India in 2011.

AREAS OF INTEREST

Planar Antennas, Microwave communication, Metamaterial Antennas, Electromagnetics, Biological effects of Microwaves, Dielectric resonator antennas, Ferroelectric tunable devices, Microwave material characterisation etc.

TECHNICAL SKILLS

- Experienced in using **HP 8510C** Vector Network Analyzer, **PNA E8362B** Network Analyzer, **R&S ZVB20**, Anritsu Spectrum Analyzer, Anechoic chamber measurements etc.
- Experience in Antenna and RF/Microwave circuit design tools like **Ansoft HFSS** , **CST MWS** and **IE3D**.

- Experience in design and testing of compact low frequency antennas, **uniplanar antennas**, and printed monopole antennas.
- Successfully developed a **Measurement Set Up** for Radar Cross section Studies.
- Experience in **Microwave material characterisation** measurements.
- Involved in the designing of various ultra compact wide band uniplanar antennas for multiband applications highly suitable for compact mobile phones.
- Involved in the design of **radiation hazardless antenna** suitable for mobile handset.
- Experience in the measurement of microwave absorption studies and **cavity perturbation method**.
- Designed various Uniplanar antennas for applications compatible for use in Laptops and similar wireless devices.
- Designed **Tunable microwave devices** based on ferroelectric thin films.
- Experience in the fabrication of microwave devices using **clean room** facility
- Hands-on experience in **building of antenna prototypes** using photolithography and antenna experimental work.
- Experienced in working both industry and Government project.

SCIENTIFIC PROGRAMMES ATTENDED

Date (Year)	Organising Body	Title and Purpose of Events
16-18, November SYMPOL 2011	Department of Electronics, Cochin University of Science and Technology	International conference on Ocean Electronics- SYMPOL-2011 Organizing committee member
13-20 August 2011	International Union of Radio Science(URSI)	URSIGASS-2011,Istanbul, Turkey. To receive young scientist Award and to present a research paper.
4-5 March, 2011	University Grants Commission(UGC) and Cochin University of Science and Technology	National Seminar on Frontier Technologies in RF Engineering. As a Participant
14-16 December, APSYM 2010	Department of Electronics, Cochin University of Science and Technology	Antennas and Propagation Symposium -2010 Organizing committee member
14-16 December, 2009	AP-MTT Joint Chapter IEEE Calcutta section in association with the Institute of Radio Physics and Electronics, University of Calcutta and Webel, India.	Applied Electromagnetic Conferece -09 (AEMC-09) To present a research paper
18-20, November SYMPOL2009	Department of Electronics, Cochin University of Science and Technology	International conference on Ocean Electronics- SYMPOL-09 Organizing committee member
10-12, December, APSYM 2008	Department of Electronics, Cochin University of Science and Technology	Antennas and Propagation Symposium -2008 Organizing committee member and Presented a research paper
21-24 November 2008	IEEE, MTT and University of Rajasthan.	IEEE international conference on Recent advances in microwave theory and applications, Jaipur, India To Present two research papers

RESEARCH EXPERIENCE INCLUDING RESEARCH PROJECTS

Research Fellow at Centre for Research in Electromagnetics and Antennas (CREMA), Department of Electronics, Cochin University of Science and Technology, Cochin, from January 2008 onwards.

Successfully developed a automated measurement set up for Radar Cross Section Studies using R&S ZVB20 network analyser and controllers.

Worked in Department of Science and Technology granted (DST, Govt. of India) project for the development of Tunable microwave devices using ferroelectric thin films.

EDUCATION

Course	Year of Passing	University	Institution	Class
M.Sc Electronics	2005-2007	Cochin University of Science and Technology(CUSAT), Cochin, Kerala, India	Department of Electronics, CUSAT, Kerala, India	First class with Distinction CGPA 8.19
B.Sc Physics	2000-2003	Calicut University Kerala, India	Govt. Victoria College, Palakkad.	First class (80.9%)

PERSONAL

Date of birth : 16th May 1983
Sex : Male
Nationality : Indian
Marital status : Unmarried
Passport Number : G-4635846

Permanent Address : Puthukuzhy house
Pirayiri post,
Palakkad – 678019.
Kerala, India

Phone : 91-491-2508757
Cell : 91-9895680620
E-mail : sujithrpkd@gmail.com

.....*SR*.....

Index

2

2D radiation patterns, 137
2G, 5, 6

3

3G, 5, 7

A

Agilent E8362B, 65
Amplifier, 14
Anechoic Chamber, 66,68,87
Ansoft, 70,74,87
asymmetric, 192,199,225

B

Bandwidth, 47,60,61,68,69
bidirectional, 56,220

C

calibration, 66,67,68,69
Cavity perturbation, 61,66
Cellular, 6,8
characteristic impedance, 25,38,39,40,
42,45,90
communication, 2, 4, 5, 6, 7, 8, 9, 15, 17,
19, 28, 30, 39, 40, 58, 60, 62, 91, 99,
150, 238, 252, 254, 262
Coplanar, 12, 13, 15, 27, 28, 29, 31, 32,
35, 38, 39, 41, 42, 44, 45, 46, 47, 51,
80, 81, 82, 83, 84, 85, 86, 87, 88, 89,
90, 91, 92, 93, 97, 99, 100, 102, 103,
156, 201, 202, 205, 221, 242, 244,
245, 246, 248, 251
coplanar waveguide, 27, 28, 39, 42, 43,
44, 45, 46, 47, 48, 49, 50, 51, 52, 53,
54, 55, 56, 57, 58, 60, 61, 63, 64, 65,
81, 82, 83, 84, 85, 86, 87, 88, 99, 103,
107, 151, 154, 155, 167, 184, 187,
198, 201, 210, 218, 226, 245, 247,
248, 252
CPW, 12,13,14,27
CREMA SOFT, 63,65,67,68,69
cross polar level, 131,196,198,207

D

DCS, 7,52,103,120,122,137
Deschamps, 37
Dielectric Resonator, 15,52,227
Dielectric substrate, 8,10,12,36,39,60,130
Dipole, 3,4,7,24,50,197
Dual band, 27,55,101,224

E

efficiency, 10,15,17,18,60,69,71,115,153,177,
Electromagnetic, 1,7,15,18,55,70,90,140,188
electronic gadgets, 176
experimental, 28, 73, 75

F

far field, 13,19,68,103,131,152,216
FDTD, 20,21,23,24,49,81
Feed penetration, 221,226

G

gain, 12,61,66,69,112,114,136,196,213,218
GPS, 7
GSM, 7

H

harmonics, 18,38,115,213,215,218
HFSS, 70,174
HP8510C, 63,64,174
H-slot antenna, 215,221,226
HTS, 14

I

ISM, 7

L

LTCC, 18,19

M

meandered, 25,52,89,98,139,144,148,
151,154,176,184,211,227,
MEMS, 14
metamaterials, 17

microstrip, 38,46,52
MIMO, 17
MMIC, 25,36,42,50,90
Monolithic, 11,25,40,51,90
monopole, 4,25,36,52,55,89,93,99,136,
163, 177,181,183,220
multiband, 16,27,36,55,224

O

Odd mode, 13,43,52,151
offset feed, 221
omnidirectional, 36,58,89,112,133,136,
152,177,196,224

P

parasitic, 42,55,227
PBG, 18,25,53
PCS, 7,103
Photolithography, 62
PIFA, 16
PILA, 16
Planar Antennas, 1,4,8,35,48
polarization, 11,18,22,27,38,53,112,
130,162,196,207,213

Q

quad band, 26,89,103,115,120,130,224
Quality factor, 41,61,94,173,206
quasi-TEM, 12,54,90

R

Reconfigurable antennas, 221,226
RF isolation, 179,209
RFID, 7,55

S

Smith chart, 91,97,142,146,190,201,217
surface current, 21,97,142,151,161,176
symmetrical slots, 183,192

T

THRU calibration, 69
TLM, 20
triple band, 58,116,120,137,225

U

Uniplanar, 11,13,25,38,54,60,90,172

V

Vivaldi, 25,50,57
VSWR, 43,52,68,120,156,174,194,212

W

wideband, 48,51,57
wireless gadgets, 11,16,27
WLAN, 2,54,103,120,137,156,174,
212,215

Y

YIG, 65